Structural Test Design with Value of Information

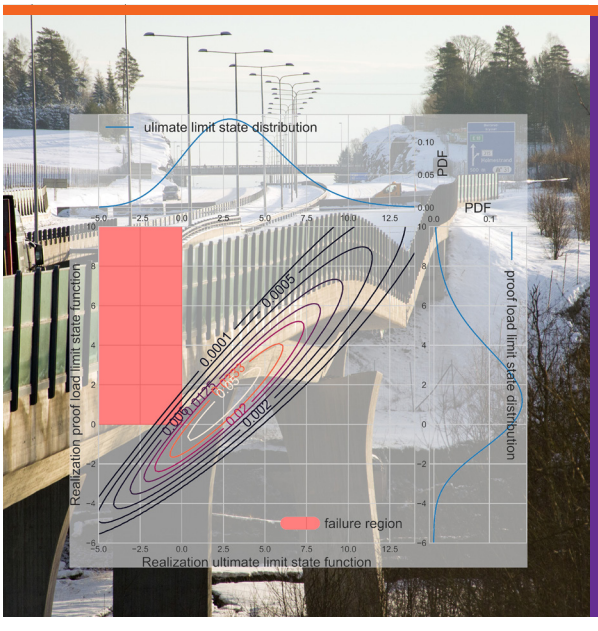

Henning Brüske

PhD Thesis

Department of Civil Engineering
2018

DTU Civil Engineering Report 401

DTU Civil Engineering
Department of Civil Engineering

Ph.D. Thesis
Doctor of Philosophy

DTU Civil Engineering
Department of Civil Engineering

Structural Test Design with Value of Information

Henning Brüske

Kongens Lyngby 2018

DTU

DTU Byg
Department of Civil Engineering
Technical University of Denmark

Brovej
Building 118
2800 Kongens Lyngby, Denmark
Phone +45 4525 1700
byg@byg.dtu.dk
https://www.byg.dtu.dk

Abstract

In order to assess the value of information of an experiment through a pre-posterior decision analysis for a specific structure, detailed analyses of the structural system performance and all relevant costs and benefits associated to the decisions through the entire life-cycle of the structure are carried out. These analyses result in expected utilities for all modeled decision options. Considered in the life-cycle analyses are: design, operation and maintenance, repair, replacement, monitoring, test costs, and finally the benefit of operating the structure. These contributions to the life-cycle benefits and costs are weighted against their probability of occurrence. With the probabilities of damage and failure computed by structural models, the direct and indirect risks along-side the expected benefit are quantified. The damage and failure probabilities are computed in structural reliability analyses that utilize structural models. The prior reliability of the structural models is updated with (pre-) posterior knowledge from experiments.

Probabilistic models for the information acquisition strategies (1) pre-construction proof load testing, (2) hybrid simulation, and (3) recorded service experience are introduced accounting for the type of the information, their precision and costs.

Owners, operators, and designers of structures face the same issue to find optimal decisions related to design, operation and maintenance, retrofitting, inspection and monitoring, or replacement. These decisions influence the structural safety and economic benefit provided by the structure. One of the main challenges in this complex environment is to spend limited resources in the optimal way for the previously listed decision options. These decisions influence each other and may be relevant at vastly different points in time. The design of the structure is at the very beginning, even be-fore the service-life begins, and retrofitting or replacement will be issues arising later. Examples of modeling such interactions of structural design and decision making at various stages of the service-life are shown. Value of information (VoI) constitutes a theory that indicates if a test or experiment is expected to provide a higher utility through increased expected benefits due to subsequent informed decisions or by the reduction of risks, the required resources and monetary expenditures. By applying the VoI theory and the concept of expected value of sample information (EVSI) based on the Bayesian decision theory by Raiffa & Schlaifer (1964) to measurement information about the condition of structures, a decision maker is able to assess information and actions in an objective manner before information acquisition and action are performed. This thesis discusses methods to acquire knowledge about the condition of structures through the means of proof load

testing in conjunction with structural health monitoring (SHM), recorded service life data about the structure, and experiments not directly conducted on the structure in question. Such off-structure experiments analyzed herein are hybrid simulations that interactively combine physical and numerical models in order to capture the influence of interactions of structural elements.

The new concepts of pre-construction proof load testing and hybrid simulation as substitute to proof load testing are demonstrated in case studies. Pre-construction proof load tests may be advantageous if applied to structures that are usually not considered for conventional proof load tests. Reasons that can prohibit a conventional proof load test can be difficulties or the impossibility to artificially load the structure with a sufficiently high proof load, or the risk arising from such a test. Both reasons can apply to offshore structures. The conceptual application of proof load testing sub-groups from the structural system in conjunction with a suitable system model is demonstrated. One can obtain such information similar to a proof load test of an existing structure. Another concept that may help to acquire structural health information is the use of hybrid simulations in order to substitute proof load tests or long term SHM. The feedback-coupled combination of physical and numerical model of hybrid simulations can help to gather knowledge about a structure that cannot be obtained with other methods. Because the experiment is not conducted with the actual structure, no information about the strength realizations of load carrying components is acquired. However, the advantage of not directly testing the structure is that no damage can be inflicted to it, is a relevant factor in the hybrid simulation value of information. The concepts of pre-construction proof load testing, hybrid simulation as a substitute for proof load testing, and the new analysis concept 'expected value of sample information and action analysis' (EVSIA) are demonstrated with case studies. EVSIA is an extension to EVSI by including actions that are only possible with posterior knowledge. The case studies consider hypothetical decisions about the optimal test strategy in order to obtain information about the structural health for an improved reliability assessment, and decisions regarding action on structural design or use of the structure. Results of the case studies indicate that:

- Higher VoI in an EVSI analysis is achieved through higher proof loads and larger tested fractions of the structure. By using the (pre-) posterior information for design improvements, the EVSIA analysis shows that the value of information and action becomes insensitive or almost independent of the proof load and can yield even higher value than an EVSI analysis.
- Structural testing before construction requires system models that account for the separated elements.
- Proof load tests usually provide high VoI to systems of high complexity i.e. constituted by many components spreading out and lowering the risk of damage.

Resumé

For at kunne vurdere et eksperiments informationsværdi ved en pre-posterior beslutningsanalyse for en bestemt konstruktion, udføres detaljerede analyser af konstruktionen selv, samt alle omkostninger og gevinster ved forskellige beslutninger gennem hele konstruktionens livscyklus. Disse analyser resulterer i forventede nytteværdier for alle modellerede beslutningsmuligheder. I livscyklusanalyserne betragtes følgende: Design, drift og vedligeholdelse, reparation, udskiftning, overvågning, testomkostninger og endelig fordelene ved at drive konstruktionen. De enkelte gevinster og omkostninger vægtes mod deres sandsynlighed for at forekomme, hvor sandsynlighederne for skade og svigt estimeres ved hjælp af strukturelle modeller. Dette muliggør at de direkte og indirekte risici kvantificeres samtidig med den forventede nytteværdi. Skades- og svigtsandsynlighederne beregnes ved hjælp af strukturel pålidelighedsanalyse, som anvender de tilhørende strukturelle modeller. Prior pålideligheden for de strukturelle modeller opdateres med information fra eksperimenter ved anvendelse af (pre-)posterior analyse. De probabiliske modeller for informationsanskaffelsesstrategierne (1) præ-konstruktion prøvebelastningstest, (2) hybrid simulering, og (3) registreret brugserfaringer introduceres ved hensyntagen til informationstype, samt deres præcision og omkostninger. Ejere, operatører og designere af konstruktioner konfronteres med de samme problemer når de optimale beslutninger søges for design, drift og vedligeholdelse, eftermontering, inspektion og monitorering, eller udskiftning. Disse beslutninger influerer på den strukturelle sikkerhed og de økonomiske gevinster som affødes af konstruktionen. En af de største udfordringer i dette komplekse miljø er at anvende begrænsede ressourcer på en optimal måde i relation til de nævnte beslutningsmuligheder. Disse beslutninger influerer hinanden og kan være relevante på forskellige tidspunkter. Designet påbegyndes allerede før konstruktionen levetid påbegyndes, og eftermontering og udskiftes er problemer der opstår senere. Eksempler på modellering af sådanne interaktioner i strukturelt design og beslutningsanalyse på forskellige stadier af levetiden betragtes.

Informationsværdi (IV) er en måleenhed, der angiver, om en test eller et forsøg forventes at give øget værdi gennem efterfølgende velinformeret beslutning, eller risikoreduktion, reduktion af ressourceforbrug, og monetære udgifter. Ved at anvende IV-teorien, samt konceptet forventet værdi af stikprøveinformation (FVSI), fra den Bayesiansk beslutningsteori (Raiffa & Schlaifer, 1964) til at repræsentere tilstanden af konstruktioner, er en beslutningstager i stand til at vurdere muligheder og alternativer på en objektiv måde før informationsindsamling påbegyndes og beslutninger tages. Denne afhandling

diskuterer metoder til at erhverve viden om tilstanden af konstruktioner ved hjælp af prøvebelastningsforsøg i forbindelse med tilstandsovervågning af konstruktioner (TOK), erfaring om konstruktionen fra målinger eller endvidere eksperimenter, der ikke udføres direkte på den pågældende konstruktion. Sådanne eksperimenter, der udføres andetsteds, er hybrid simuleringer, der interaktivt kombinerer fysiske og numeriske modeller med henblik på også at beskrive indflydelsen af interaktioner mellem konstruktionens elementer.

De nye former for før-opførelses-prøvebelastningsforsøg og hybrid simulering som erstatning for prøvebelastningsforsøg er demonstreret i case-studier. Før-opførelses-prøvebelastningsforsøg kan være fordelagtige, hvis de anvendes på konstruktioner, der normalt ikke overvejes til konventionelle prøvebelastningsforsøg. Årsager, der kan forhindre et konventionelt prøvebelastningsforsøg, kan være vanskeligheder eller umuligheden for at belaste konstruktionen med en tilstrækkelig høj prøvebelastning eller risikoen ved en sådan test. Begge problemstillinger kan være tilfældet for offshore konstruktion. Den konceptuelle anvendelse af prøvebelastningsundergrupper af konstruktioner sammen med en passende systemmodel er demonstreret. Viden tilsvarende denne, kan anskaffes ved prøvebelastningsforsøg af en opført konstruktion. Et andet koncept, som kan bidrage til at indhente oplysninger om konstruktionens tilstand, der i øjeblikket er vanskeligt at få adgang til, er hybrid simuleringer, som kan erstatte prøvebelastningsforsøg eller langsigtet TOK. Denne feedback-koblede kombination af en fysisk og numerisk model, som hybrid simuleringer bidrager med, kan bidrage til at indsamle viden om en konstruktion, hvor det ikke er muligt at få informationen ved brug af andre metoder. Da eksperimentet ikke udføres på den egentlige konstruktion, er der ikke erhvervet nogen information om styrkeegenskaber af lastbærende komponenter. Dog er fordelen ved ikke at teste konstruktionen direkte, at ingen skade kan påføres, hvilket er en relevant faktor for informationsværdien af en hybrid simulering. Koncepterne før-opførelses-prøvebelastningsforsøg og hybrid simulering kan erstatte kontroversielle prøvebelastningsforsøg, og den nye analyse 'forventet værdi af stikprøveinformation og handlinger' (FVSIH) er demonstreret med casestudier. FVSIH udvider den eksisterende FVSI-teori ved yderligere at inddrage handlinger som alene muliggøres af posterior viden. Casestudierne betragter hypotetiske beslutninger om den optimale teststrategi til at indhente oplysninger om konstruktionens tilstand for en forbedret pålidelighedsvurdering, samt beslutninger vedrørende konstruktionens design eller brug. Resultaterne fra casestudierne viser at:

- Højere IV i en FVSI-analyse opnås gennem højere prøvebelastningsniveauer og en større andel testede dele af konstruktionen. Ved at anvende den (pre-) posterior information til designforbedringerne, viser FVSIH-analysen at informationsværdien og handlingen bliver ufølsomme overfor, eller næsten uafhængig af, prøvebelastningsniveauet og kan føre til endnu større værdi end en FVSI-analyse.
- Konstruktionsprøvning før opførelse kræver systemmodeller der kan tage højde for de separate elementer.

Preface

This thesis is submitted as a partial fulfillment of the requirements for the Danish Ph.D. degree. The thesis is based on numerical investigations carried out as part of the Ph.D. project "Structural Health Monitoring Systems Design", undertaken at the Department of Civil Engineering at the Technical University of Denmark (DTU Byg), Kgs. Lyngby, Denmark between November 2014 and January 2018.
The thesis was defended on 21. September 2018. The assessment committee was formed by:

- Associate Professor Jacob Wittrup Schmidt, Technical University of Denmark (committee chair)
- Professor John Dalsgaard Sørensen, Aalborg University
- Professor Dagang Lu, Harbin Institute of Technology

The project included an external research stay with Professor Dimitri Val at the Harriot Watt University, Scotland.

The principal supervisor of the Ph.D. project was Associate Professor Sebastian Thöns from DTU Byg.

The project was financed by DTU Byg.

Henning Brüske
Kongens Lyngby, November 15, 2018

Acknowledgements

My supervisor Associate Professor Sebastian Thöns is the first person I want to thank. He have been in contact about a PhD project abput two years before he could finally offer me this great opportunity. I am very grateful for this opportunity, your support and guidance for my research. I gained deep insight and understanding in a field that was very new to me.

Another important colaborator and mentor is Profressor Dimitri Val. I appreciate his patience and help he extended to me during my research stay in Endinbrough and beyond. He helped me to widen my horizon of civil engineering and helped me to understand design processes much better.

For their patience in answering often very basic engineering questions and sharing their experience I want to say thank you to the Assitant Professors Evangelos Katsanos and Simona Miraglia. Your help has often been fundamental to learning progress.

Kathrine Nunn and Jamie Magee receive my gratitude for proof reading the thesis and turning my English into comprehensible English.

At last I want to thank my family and friends for keeping up my morals in times where I felt lost in the huge ocean of things I did not understand at that time but eventually navigated successfully.

Contents

CHAPTER 1

Introduction

Structures are usually tested to: (1) identify if a structure complies with current codes and regulations considering its current utilization; (2) gain knowledge about its condition to infer the information to similar structures or components; or (3) approve a change of utilization e.g. approving a bridge for a higher load rating in order to facilitate new load demands. Application field (1) is covered extensively in the literature and is normal practice in engineering. This thesis will focus firstly on (2), the inference of information to other structures or structural components, and secondly on (3), the value of information in testing for utilization changes.

The knowledge transfer from tested to untested components or structures may be of value for the offshore wind energy industry. Hobohm et al. [Hob+13] state that currently a cost reduction of offshore wind turbines only considers scale effects for substructures e.g. a 6 MW turbine has a cheaper substructure per MW than a 4 MW turbine. Cost reduction through improved designs thanks to posterior knowledge is not considered to date.

Case (3), the testing for fitness of a changed purpose, will be addressed with classic methods like proof load testing and with a hypothesis involving hybrid simulations. Hybrid simulations combine physical tests and numerical modeling.

A large part of this thesis deals with proof load testing. Structural health monitoring (SHM) and proof load testing are inextricably related. Proof load testing has the potential to damage or destroy the tested structure. In order to avoid this, the load progression has to be stopped before the demand exceeds the load carrying capacity of the structure. The ability to monitor for indications of imminent damage turns the potentially destructive testing method into a non-destructive test.

All experiments considered in this thesis are assessed by the value of information they provide. Simply put, the value of information is an increase of a utility that is achieved by obtaining additional knowledge about a system that provides the utility. It is assumed that an experiment comes at a cost. Only when the experiment delivers information that enables a decision that increases the utility beyond what the experiment costs, is a positive value of information is achieved. With this concept, a decision maker can evaluate the usefulness of obtaining additional information before the experiment is

carried out.

The thesis presents an extension to the value of information concept by introducing a method to also analyze the value of actions made possible through additional information. The concept could be called value of information and action analysis.

1.1 Thesis outline

Chapter one explains the motivation for the research, and sketches the connections between proof load testing, structural health monitoring (SHM), and value of information (VoI). Furthermore, the motivational introduction links the applied structural models to actual structure types.

Chapter two introduces foundational works in fields of proof load testing and accompanying structural health monitoring. The literature review provides a state of art overview of proof load testing and adjacent fields that support proof load testing. In connection to the review, the additional insight to proof load testing and decision analysis through this thesis is presented. Various types of proof load testing suitable for specific civil engineered structures are reviewed. Because proof load testing always comes with the possibility of damaging the tested structure, monitoring methods that can help to avoid damage are discussed.

Chapter three explains the applied models and presents several possibilities for the utilization of information acquired through proof load testing. The model explanation also includes the deterioration models used, in addition to structural interdependence modeling.

Chapter four introduces the economic consequence and utility modeling. The model is generic and can be applied to any kind of structure. The lifetime economy of an offshore wind turbine serves as a concrete example.

Chapter five extends the utility modeling of chapter four to Bayesian decision analysis and explains the concept of value of information (VoI). VoI is the basis of the objective assessment of proof load testing decision concepts modeled in this thesis.

The first paper follows in chapter six. It explains the VoI dependent on the structural model, component interdependence, and the number of components that constitute the proof load tested structure.

Chapter seven is the second paper on decision analysis about proof loading demonstrating the inference to proof load test results to untested components in the same structure. The information is used to update the structure's reliability estimation and to compute expected benefits with the new information in a pre-posterior decision analysis.

Chapter eight introduces the concept of expected value of information and action analysis. This analysis includes additionally to action options that are available with prior and posterior information also new actions that are only possible with further information. This extension to value of information analysis is demonstrated in case study pertaining to offshore wind energy turbines.

An analysis framework that helps a decision maker select the optimal combination of several structure testing and usage choices is presented in chapter nine. The evaluated testing options are service proofing, proof loading testing, and hybrid simulations. Subsequent actions regarding the usage are e.g. building a new structure or using the old one with potential modifications. The framework is demonstrated in a case study with a structure used with higher loads than it was designed for.

The conclusion in chapter 10 summarizes the PhD project's results compiled in this thesis. The results are put in context with previous related research, and an outlook on potential extensions and improvements is given.

1.2 Structures considered in the thesis

The structural models used in this thesis are no accurate representations of real structures. They do however, capture some important mechanical features of real structures, which would be for example characteristics of the dominant failure mode or redundancy of structural elements. This section introduces actual structure types that find resemblance in the structural system models herein. The system models used for structural reliability analysis are introduces in chapter 3.

1.2.1 Offshore structures

Offshore sub-structures usually carry a super-structure that serves various purposes. It may be a wind energy converter, electrical substation, drilling and production equipment, crew dwellings, or helicopter landing pads.

Two fundamentally different sub-structure types used for offshore installations are consider in this thesis. Firstly, structures that use multiple structural elements to distribute loads and use this redundancy is case of structural damage. Secondly, a sub-structure type that has no redundant load carrying elements.

Rigid sub-structures with redundant elements

Structures of the first type may be compliant towers [WEK99], tension leg platforms [BM12], or jackets [MCV11]. Jackets are usually built with tubular joints connected

to legs and strengthened with cross-tubular joints in a lattice structure. The tubing is usually air-filled. The level of redundancy in the jacket depends on the type of bracing (K, X or diamond) [SS06]. The jacket is anchored to the seabed through piles. A compliant tower is fixed through a base jacket to the sea floor.

Jackets and compliant towers are structures that can bear a derrick, and therefore support any operation involved in the exploitation of hydrocarbon fields. Jackets are used in hydrocarbon production up to 300 m water depth and are common sub-structures. Figure 1.1 shows photographs of a jacket sub-structure that is ready to be moved on a barge, located on the Norwegian continental shelf today in order to exploit the Ivor Aasen natural gas field.

Figure 1.1: Jacket sub-structure for the Norwegian Ivar Aasen field on a barge. Photos by Kess Torn, cc-by-sa-2.0

Jackets are also utilized today in the offshore wind energy industry in water depths between 30 m and 60 m [DDS16]. Compliant towers are not used in the wind energy sector. Greater depths are approached with buoyant structures like tension leg platforms or free floating moored platforms [MMN11].

Compliant sub-structures with redundant elements

Compliant structures are designed to deflect or translate from their neutral position under environmental load. Examples are compliant or guyed towers, semi-submersible platforms and tension led platforms.

Compliant towers are like jackets also space frame structures. They can be used in water depths exceeding 300 m but are rarely employed [Ron02]. Compliant towers are more

flexible than jackets and designed to move with environmental forces. However, their base on the seabed is usually a rigid jacket.

Tension leg platforms (TLP) are anchored to the seabed by tendons under tension caused by buoyancy. This reduces yaw, pitch, and heave motions [Kib+94]. TLPs are more common in deep water oil production, operating in seas deeper than 1000 m [Ron02]. TLPs are also considered for offshore wind energy farms for water depth between 70 m and 200 m [BM12]. An artist rendition of tension leg platforms is shown in Figure 1.2.

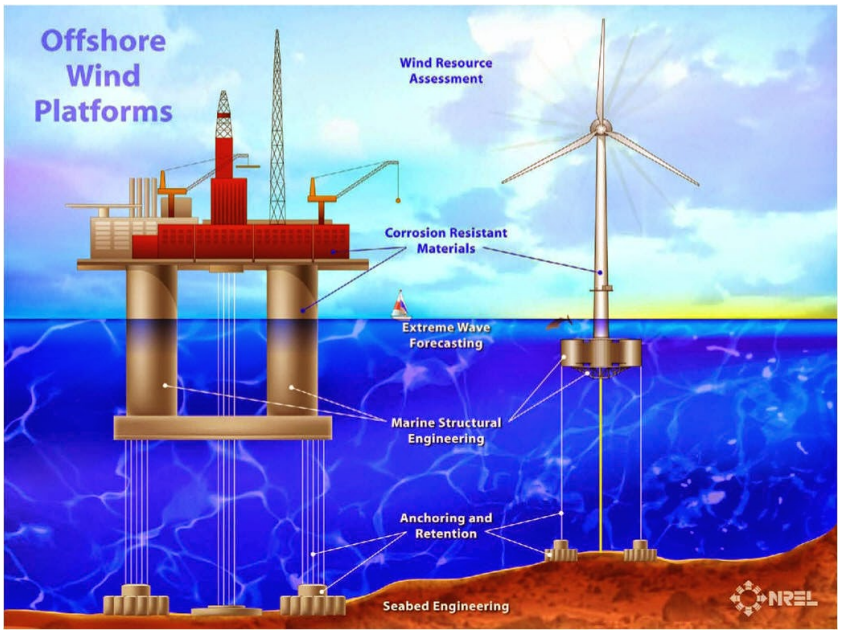

Figure 1.2: Examples of tension leg platforms. A hydrocarbon production platform on the left-hand side and a wind energy converter on the right-hand side. Adapted from the National Renewable Energy Laboratory

Semi-submersibles are also buoyant platforms moored to the seabed. The mooring lines are only tensioned by their self-weight and natural forces.

Due to their redundant designs, the thesis will look at such structures as types of parallel systems. Depending on their dominant failure mode, they may be modeled as brittle or ductile Daniels systems. A classic parallel system has no relevance in the modeling of mechanical systems.

Sub-structures with singular elements

The second general sub-structure considered in the thesis are monopiles or gravity base foundations from which only one pillar extends to the super-structure. A monopile is a cylindrical tube usually made out of steel that is driven into the seabed. See Figure 1.4b

for a schematic drawing of a monopile sub-structure. The monopile is lowered into the ground usually by hydraulic hammers or vibrations. The lowering can be supported by excavation from the inside [Bur+11; SW13]. This type of sub-structure is usually applied in water depth up to 30 m. However, large diameter monopiles can also be used in deeper waters [DDS16].

The dimensions of a monopile vary depending on the soil and loading conditions. In Adhikari and Bhattacharya [AB12] three design cases are discussed with monopile diameters ranging from 3.5 m to 4 m, pile penetration depths of 19 m to 33 m, and wall thickness from 28 mm to 70 mm. The wind turbine considered in Adhikari's and Bhattacharya's study has a power rating of 3 MW. The monopile dimensions for current turbine ratings of over 5 MW are necessarily greater.

Because it is difficult to position the monopile vertical with sufficient accuracy during the pile driving operation, it is common to add a cylindrical connection tube between the monopile and the base of the tower. The connection tube is usually called a transition piece to which the tower base is connected. The transition piece is usually sleeved over the monopile. The bonding of monopile and transition piece is generally achieved by grouting. There are three fundamental methods in application. (1) The original grouting method for connection cylindrical tubes is no longer recommended due to reduced interface shear capacity with increasing monopile diameters. Wear between the grout and steel reduces the bonding capacity [Lot+12]. This issue can be overcome to a large degree by either using (2) shear keys with a cylindrical connection of transition piece and monopile or (3) with a conical interface with angles of 1° to 3° [Lot+12]. Such a conical transition is shown in Figure 1.3. In this study the combination of monopile and transpiration piece is jointly modeled by a series system because no redundant elements are present.

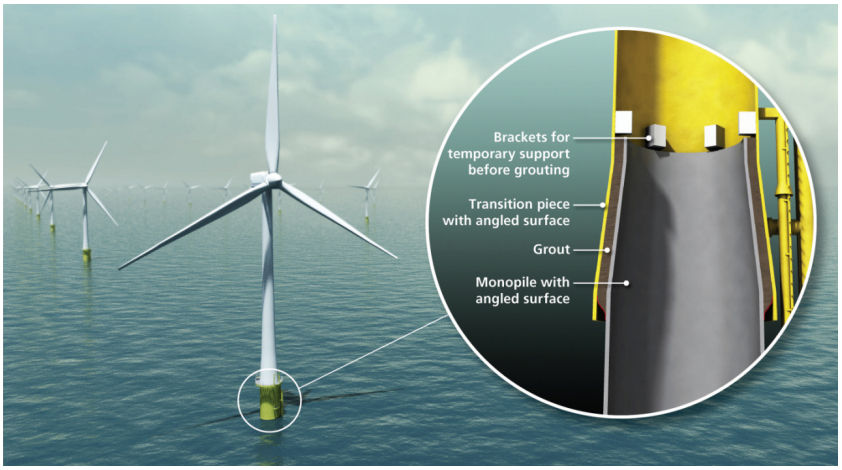

Figure 1.3: Example of a conical grouted connection of monopile and transition piece. Adapted from DNV-GL

The Draugen platform (Figure 1.4a) has a gravity base foundation from which a single large diameter concrete pillar extents to the surface and carries the super-structure [GWS93]. The design with large diameter concrete pillars is chosen in order to provide great strength against ice loads in polar regions [OWM15].

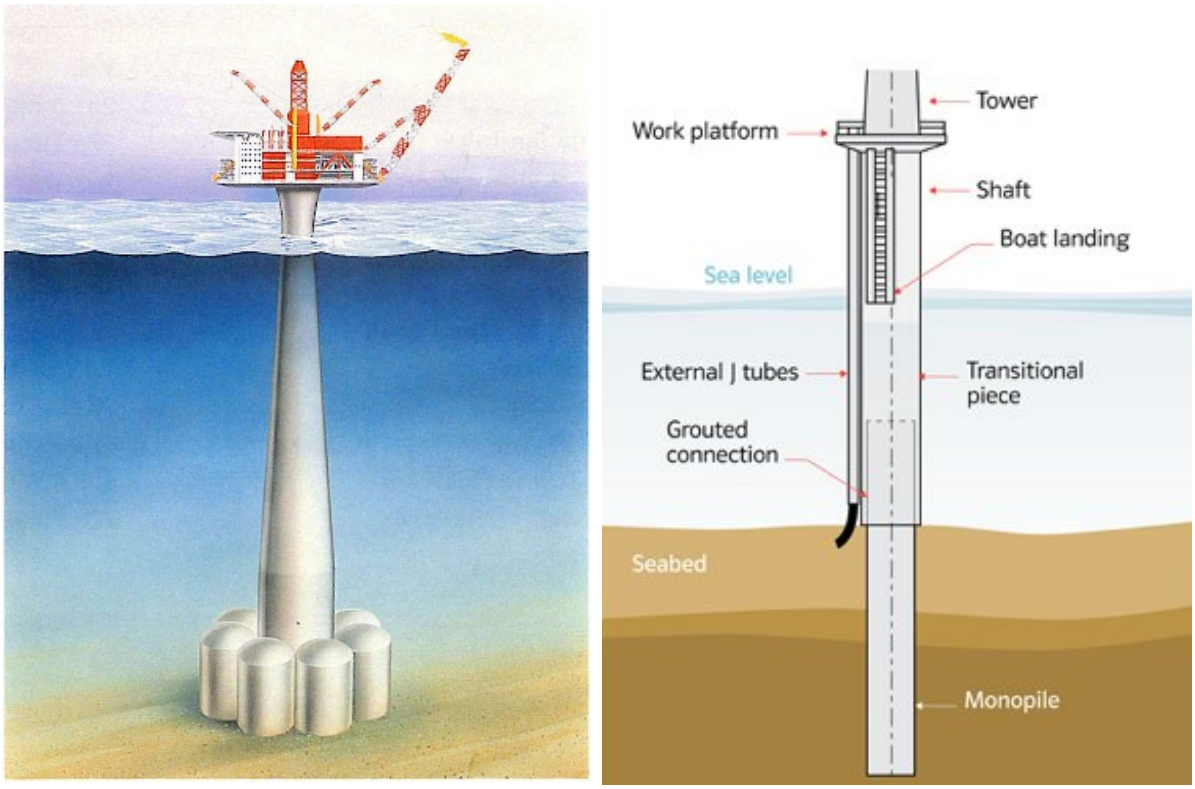

(a) The Draugen gravity base platform. Courtesy of Norwegian Contractors

(b) Schematic of a monopile. Adapted from 4C Off-shore

Figure 1.4: Examples of offshore foundation types

1.2.2 Bridges

Bridges provide a fast and safe way to pass obstacles in the landscape like canyons or bodies of water. Bridge design codes e.g. Eurocode 8 [Eur05] demand that the structures behave ductile and have redundant structural elements in order to achieve a sufficient safety level. Over millennia several bridge types have been developed. Among these are beam, truss, cantilever, arch, suspension and cable-stayed bridges. Redundancy can be present at many levels and its importance is stressed by Ghosn et al. [GMF10].

A beam bridge will probably have multiple girders. Those girders may be braced to exchange / distribute forces and the bracing can be made with several elements in the

bracing providing additional redundancy on a lower level [HH12].

Redundant elements are directly visible in suspension, cable-stayed, and truss bridges. Multiple stay cables or suspender cables constitute a high level of redundancy and multiple wires constitute another level in the load carrying cables. Photos of a suspension cable bridge and a cross-section of its suspension cables are shown in Figure 1.5a and Figure 1.5b.

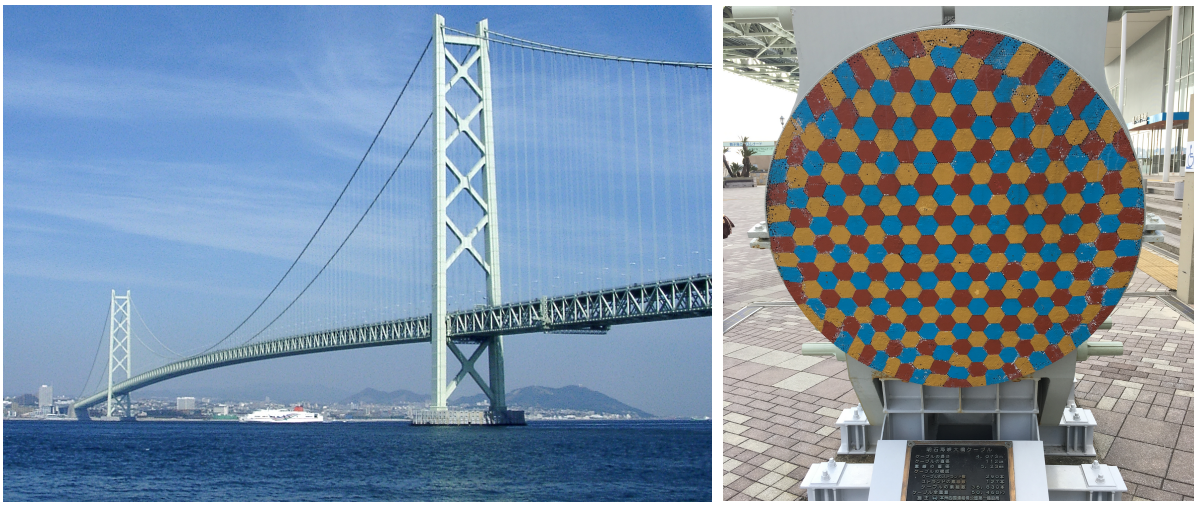

(a) Bridge panorama (b) Suspension cable cross-section

Figure 1.5: Akashi Kaikyo Ohashi bridge, cc-by-sa-2.0

Like jackets used for offshore structures, trusses are used in bridges. In this type of bridge structure, it is relatively easy to recognize how other structural elements can share loads. A sketch of a truss bridge is shown in Figure 1.6.

For example, Yang et al. [YFN04] consider logical systems for the service-life prediction of bridges. Because a bridge should exhibit a ductile failure behavior, a combination of ductile Daniels systems may be considered as a simple structural model for bridges.

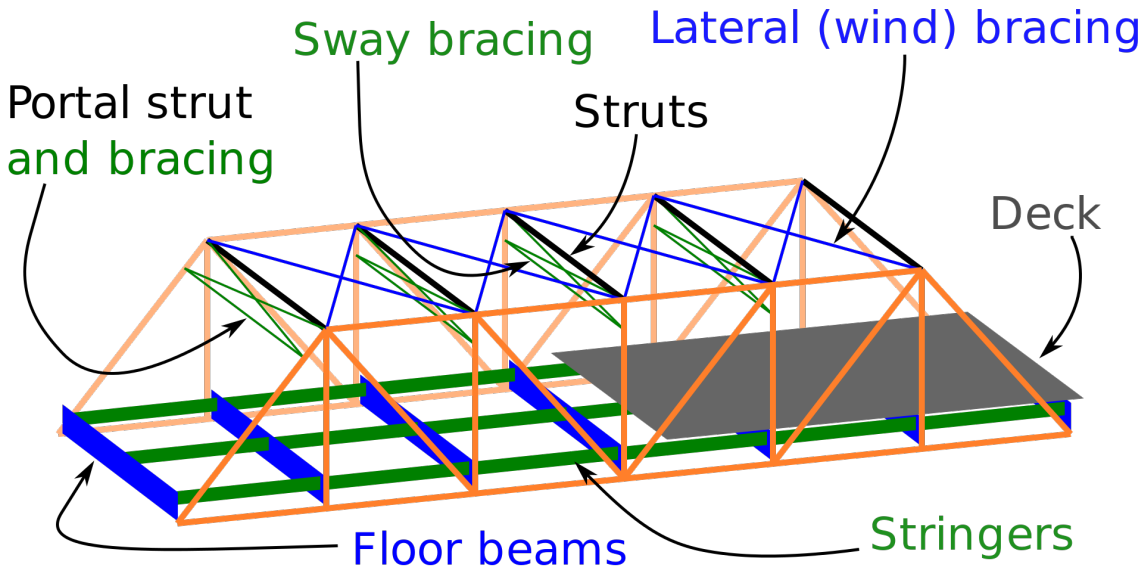

Figure 1.6: Schematic example of a truss bridge with denoted structural elements. Adapted from Wikimedia

CHAPTER 2

Literature Review

2.1 The development of fundamental proof load testing approaches and connected decision analysis

Proof load testing is relevant in many engineering fields. Rackwitz and Schrupp [RS85] clearly define and distinguish three testing paradigms: prototype testing, proof load testing, and statistical quality control. Prototype testing is defined by its main purpose of gaining knowledge about uncertain parameters. The most common way to utilize this new information is Bayesian updating of the distribution functions. The second testing paradigm is proof load testing. It does not address distribution parameters but the resistance variables or realizations. The main purpose is to eliminate weak structures or elements. The authors suggest Bayesian updating of the failure probability with survival events. The third testing paradigm is statistical quality control (SQC). Unlike proof load testing, which only deals with positive control decision, SQC randomly samples a subset from the entire production. From this subset, all observed states $y = (y_1, \ldots, y_m)$ are evaluated by an acceptance function $z(y)$. The acceptance function indicates whether the tested lot is acceptable.

Lin and Nowak [LN84] introduced two probabilistic concepts of proof load testing to the field of structural reliability engineering: (1) truncation of the resistance distribution at the most likely point of failure, and (2) Bayesian updating of the resistance PDF (prior distribution) with the proof load PDF (likelihood). Lin and Nowak stress that the resistance often dominates the limit state function in practical cases. Therefore, gaining knowledge about the resistance is an effective way to increase a structure's reliability. Truncation is commonly used to this day for updating bridge resistances [Lan+17]. Like civil engineered structures, aviation requires a high level of reliability. Yang [Yan76] presents a concept of periodic proof load testing of airplanes. He considers fatigue damage due to service loads that degraded the resistance of an aviation structure. His numerical examples deal with a transport-type and a fighter aircraft. Both types benefit in terms of structural reliability from proof load tests, and continue to benefit with periodic repetitions of the tests. The author considers proof load testing only for structures made of brittle material because yielding damage may not be noticed. However, with

appropriate monitoring techniques employed during loading and unloading, yielding can be identified – as shown four years earlier by Pollock and Smith [PS72]. Yang acknowledges that there is a trade-off between safety and the costs of proof loading and potential replacements. This indicates that the need for value of information analyses in a proof load testing context is recognized early on. Thöns et al. [TFR11] propose to explicitly consider measurement uncertainties by extending the truncation approach to a mixture distribution of proof load measurement and resistance. They assume the proof load is Gaussian distributed, an assumption supported by the guide to the expression of uncertainty in measurement (GUM) by Joint Committee for Guides in Metrology [JCG08]. GUM has been a de facto standard for handling measurement uncertainty since 1993. Diamantidis [Dia87] demonstrates that Bayesian updating leads to a higher increase of the reliability than the resistance distribution truncation for increasing proof load levels.

Ditlevsen [Dit86] provides motivation to use service loads as proof load, but points out that service loads are often not large enough to gain information. Rather, inspections and destructive tests on parts of the structure are more effective. Faber et al. [FVS00] used reliability methods to propose target proof loads either to verify the existing load limits or to assess a bridge for a higher load limit. They took into consideration the ideal load level in terms of reliability of the test and updated resistance that can be achieved. According to Val and Stewart [VS02], the successful service-life history does not provide enough information to influence the resistance factor of a structure, but it can reduce its failure probability estimate. The authors suggest a method to incorporate posterior knowledge in new codes, because current structural codes are not efficient for the assessment of existing structures. They consider proof load testing a suitable source for posterior information. However, their results indicate that the proof load has to be high in order to gain information about the structure's resistance. This also leads to a high test-failure probability.

A combination of SQC and proof loading as defined by Rackwitz and Schrupp [RS85] is called proof sampling by Grigoriu and Hall [GH84]. Their concept is based on proof load testing a few samples from a lot. The gained information is used to create a posterior resistance model for untested components of the same batch. In their example of batch-produced roof trusses with moderately high correlation, proof loading of just two trusses can replace other costly tests. Their model assumes normally distributed life-loads. Grigoriu and Hall concluded that with high correlation, proof sampling is almost as good as testing each component. Should the correlation be low, extensive sampling is required. Three years earlier, Madsen and Lind [ML82] developed a similar approach in order to reduce the uncertainty in the strength distribution of series-produced structures. Their aim was to address modeling errors and dispersion in material properties. They provide examples with wooden roof elements and steel trusses. These let them conclude that correlation has a significant influence on the strength estimate and random sampling may not be necessary if the sampling accounts for the correlation appropriately.

Nishijima and Faber [NF07] present a Bayesian approach to proof loading quasi-identical

multi-component structural systems, which would be characterized according to Rackwitz and Schrupp [RS85] as a combination of prototype testing and proof load testing as the system behavior is not explicitly modelled.

2.1.1 Decision analysis with proof loading information

Pre-posterior decision analysis modeling in conjunction with proof loading is found in Nishijima and Faber [NF07]. They present a Bayesian pre-posterior decision optimization approach to determine if proof loading is beneficial, and its optimal proof load parameters in the context of costs and separate components outside of system interaction. Brüske and Thöns demonstrate the inference of a single tested component to other components in Brüske and Thöns [BT17]. Bounds of the value of information (VoI) of various simple structural models are presented in Brüske and Thöns [BT16].

2.2 Application Areas

Proof load testing can be applied to virtually any kind of structure. These can be mobile structures as found in space travel, aviation, marine vessels, or ground vehicles. Typical civil engineered structures are fixed in their location. Examples for three different fields concerning civil engineering are given in this section.

2.2.1 Bridges

Laboratory scale

Proof load testing can be applied in order to answer wide range of questions regarding bridges. One such question pertains the actual strength of the structure, in order to assess whether the bridge is compliant with current codes or if it is even able to bear higher load than designed. Laboratory scale tests were conducted by Nilimaa et al. [Nil+12] to assess if a 1950's design railway bridge may have the bearing capacity to handle increased traffic and dead loads. An assessment of the old design with current codes predict 5% to 11% higher capacity, although visual inspections discovered flexural cracks. The laboratory scale tests an even higher capacity. Lantsoght et al. [Lan+16] evaluate current proof loading stop criteria experimentally with concrete slabs. They suggest improvements to codes in order to prevent damage, while at the same time gaining more information through higher proof loads. The beams she tested stem from an old bridge. Such laboratory tests cannot acquire information about the strength of materials used in the actual structure they intend to simulate. The data collected in labs may, however, improve models.

Full-scale until destruction

Full-scale tests until destruction are present in the literature, although the vast majority of proof load tests are conducted with the intention to not damage the structure. Such ultimate load tests are conducted on a variety of bridge types and ages. Bagge and Blanksvärd [BB14a] test a 55-year-old post-tensioned bridge until the girders and the slab fail. They aim to test and calibrate strengthening and assessment methods. The obtained data is used to update finite element models and the authors concluded that detailed knowledge of the bridge conditions can save the bridge owner money. Häggström et al. [Häg+17] discuss the result of static tests of a steel truss railway bridge. The loading was conducted with multiple load steps, which resulted in structural failure. The bridge could withstand a peak load equivalent to a load effect approximately six-fold the permitted axle load.

Full-scale with damage prevention

Full-scale tests without destruction are often carried out with the goal to preserve the bridge for longer service or even increase the maximum allowed traffic load. An overview of application examples for bridges is given in Gutermann and Schröder [GS15] using specialized loading equipment. Moses et al. [MLB94] state that the proof load level is usually around 80% to 85% of the code serviceability load. This is much higher than the expected maximum service loads over the structures entire life-time. Three simply supported, over 60-years-old steel girder bridges are proof load tested by Saraf and Nowak [SN98] using two tanks. The test load is predetermined depending on the legal maximum. Stresses and deflections in girders are monitored. The measured small stresses and linear deflection response are interpreted as indicative of capacity reserves. The observed load responses are smaller than analytical models predicted. In situ strengthening was conducted on the Haparanda bridge by Nilimaa et al. [Nil+14] and proof load tests were conducted before and after the implementation. The proof load tests indicate a larger shear capacity than predicted by EuroCode. A reinforced concrete double-trough bride is proof loaded with trains by Nilimaa and Blanksva [NB15]. Reinforcement strain and curvature deformation of the troughs are monitored. The proof loading showed that troughs interact significantly, although the design did not intend for this. Previous calculations assumed independent loading of these elements. The authors conclude that with the posterior knowledge, the load rating of the bridge can be increased without strengthening. An early application of structural health monitoring (SHM) for bridge proof loading is provided by Pollock and Smith [PS72]. They proof load test a transportable tank bridge and use acoustic emission monitoring in order to locate sources of energy released during all phases of the loading test. The acoustic emission results correlate with strain gauge and displacement measurements. Saraf et al. [SSN96] conduct proof load testing on two highway bridges. For the first one, no design details are known, and the second one has heavily corroded steel girder flanges. The applied proof load level is twice as high as maximum allowable bridge load. The bridge

capacities are found to be significantly higher than analytically assessed. Bridge number two is stronger thanks to composite action, although it was not designed for it. Proof load requirements in a load and resistance format are proposed by Fu and Tang [FT95]. These factors support the determination of target proof loads and their consequential load ratings. They consider two cases: (1) the analytical assessment yields an unsatisfactory load rating and (2) no reliable analytical load rating is obtainable. The authors conduct a sensitivity analysis in order to ensure the suggested loading requirements are not sensitive to the type of distribution family or their input parameters. Recent works focus on the optimal preparation and safe execution of the tests, see Lantsoght et al. [Lan+17]. An example of a pre-stressed, pre-cast concrete highway bridge is given by Olaszek et al. [OSC10]. They discuss several monitoring methods that may be used in order to stop the load increase before significant damage is inflicted to the bridge.

Stewart et al. [SRV01] include decision making processes in the determination of ideal load levels. Authors exemplify decision-making supported by information obtained through various reliability-based assessment methods. Their risk ranking decision process incorporates time dependent reliability estimates. A practical illustration of the assessment is given for a bridge affected by age, increasing traffic frequency, loads, and deterioration. Their risked-based approach allows for the prioritization of structural safety measures. Casas and Gómez [CG13] demonstrate the application of weigh-in-motion for the purpose of calibration of the target proof load, especially for old bridges without documentation.

None of the listed studies considers the system behavior of the structure in their analytical or numerical assessments. Several articles showed that significant difference in the structures' resistance is demonstrated through proof load testing. Recent works regarding the proof load testing of bridges rely on the simple truncation method without explicit consideration of load uncertainties.

2.2.2 Offshore structures

Diamantidis [Dia87] transfers the proof loading concepts to offshore structures. In his two cases studies, Diamantidis evaluates the air gap of a truss structure and a subsea oil storage tank. For the air gap assessment, the proof load information is the observed sea state after 15 years of service. The oil tank is assessed for its resistance to horizontal sliding in a wave storm. Moses and Stahl [MS79] consider proof load testing as an information source for offshore platform re-design. Proof load testing of offshore platforms based on experience waves is investigated by Ersdal et al. [ESL03]. They consider a jacket structure that is subjected to wave loads, the load model distribution is fitted to observed sea states. Ersdal et al. consider two fundamental cases in regards to the structures' quality, (1) no gross errors and (2) with gross errors in the construction or other damage. They found that the platform reliability in the case of no gross errors was only updated if waves with significant wave heights corresponding to annual proba-

bilities of 10^3 to 10^4 are observed. In case of gross errors, the return period lies between 100 and 1000 years. Proof load testing may also service in the probabilistic design of wind turbines as Sørensen and Toft [ST10] describe. They discuss an operational failure rather than a structural failure through e.g. the failure of turbine blades. Their approach considers an observed damage level as an indicator of a system modelled by a combination of series and parallel systems. Degenkamp and Ruinen [DR01] present a new installation method for deep-water moorings in greater depth than done previously. They conduct a full-scale proof load test in approximately 1000 m depth on vertically loaded anchors.

2.2.3 Proof load testing of pressure vessels

Pipelines

A common application of proof load testing in pipelines is the so-called hydrostatic testing. The test determines the pressure carrying capacity of the pipeline. The pipeline or single pipes are pressurized until a pre-defined limit that will be higher than the maximum operation pressure, but lower than the specified yield strength of the pipe(s).

It is usually conducted on pipes in the mill, as well as after the field installation, before the pipeline is put into service. It is also applied in cases where the pipeline cannot be inspected with in-line inspection techniques as described in e.g. Bauer and Brüske [BB14b] and Patterson [Pat+13]. Linear flaws likes cracks are especially difficult to detect with in-line inspection methods, and their elimination may be approached with hydrostatic testing [KG10]. Hydrostatic testing may also be used on aged pipelines if it is required due to circumstances such as a change of utilization, e.g. the reuse of an old liquid pipeline to transport gas. A major concern with proof load / hydrostatic testing of pipelines is the ductile growth of flaws. The ductile growth of defects due to test pressures is dealt with by Leis et al. [LBS91] and Leis and Brust [LB92] where they discuss the determination of target pressures that help to eliminate critical flaws and simultaneously minimize the growths of undetected flaws. Brongers et al. [Bro+00] focus on ductile tearing of high-strength steel affected by stress corrosion cracking. Their findings are inconclusive on the possibility to assess ductile tearing because some flaws fail under pressure tests, while others stop growing due to fracture tip blunting. Hydrostatic tests are often destructive because there is no monitoring method available that detects critical flaws before failure [KC00]. Furthermore, the large quantities of water, that will often be contaminated, cause issues in logistic, waste treatment, and pipeline drying [KG10; KC00].

Nuclear reactor containment chambers

Proof load tests of nuclear reactor pressure vessels are carried out similarly to the hydrostatic tests of pipelines. Pressure tests on small concrete prototypes are conducted by Green [Gre69] in order to determine how stress wave emission sensors can monitor the progression of damages in the concrete cover. Pressure tests until destruction are conducted by Bryan et al. [Bry+75] on full-scale reactor chambers with 6-inch-thick steel walls. Proof testing on pressure chambers is carried out by McD. Eadie [McD67] in order to confirm the vessel's pressure capacity and to calibrate sonic strain gauges for monitoring purposes. More recently, Hirama et al. [Hir+07] proof load tested close to full-scale models of reinforced concrete containment vessels for an advanced boiling water reactor. The vessel was pressure tested in combination with seismic excitations from a large-scale shaking table.

2.3 Proof load testing in conjunction with other testing methods

Proof load testing can be considered a destructive method as Bagge and Blanksvärd [BB14a] and Häggström et al. [Häg+17] demonstrate. In general, it is far more often applied to structures that are intended for continued use. In this case, the proof load test must be stopped before significantly damaging loads are applied. This load limitation is turning it effectively into a non-destructive testing method. Lantsoght et al. [Lan+16] propose stop criteria to avoid damage. Various SHM technologies are effective in detecting damages that can occur during proof loading and allow for a non-destructive application of proof load testing. Following is a brief overview of a selection of techniques and a summary of their applicability to proof load testing.

2.3.1 Local sensing

Local sensing requires the presence of measuring devices on the tested structure. Data storage and interpretation can take place in another location.

Visual inspection

Visual inspection can be carried out with the aided or unaided eye. The vicinity of humans to a proof load tested structure can result in intolerable risk to life and limb. However, visual inspection may also rely on digital image acquisition and processing. Automatic surface crack detection and characterization in road decks is demonstrated by Oliveira and Correia [OC13]. Eleven different digital image processing methods are reviewed for the purpose of crack identification by Wang and Huang [WH10]. They

outline the performance of each method in various areas, e.g. processing time, parameter sensitivity, and crack size sensitivity. Automatic data evaluation is often preferable over human evaluation because it eliminates factors like mental fatigue, skill level, and experience as Fujita and Hamamoto [FH11] state. For the inspection of railway tunnels Zhan et al. [Zha+15] use structured light emitted from LASERs to measure deformations in the structure.

Visual inspection is not a method well applicable to proof load tests. Once damage becomes visible, the damage may already be significant, and visual observations are difficult to match to indicators obtained from models. It may, however, be used to confirm indications given by other monitoring methods [OSC10].

Ultrasonic testing

Subsurface flaws and wall thickness can be measured with ultrasonic testing (UT) methods. A common method for permanent or extensive time period monitoring is guided wave UT [MG16]. Ultrasonic waves passing a flaw in the guiding medium will cause reflections and diffraction signals, which indicate location and size. Inspections can be carried with a variety of UT methods. Wall thickness is usually determined by measuring the time of flight between reflected signals with probes exciting the sample perpendicular to its surface [Kra59]. Linear flaws e.g. cracks are detectable by time of flight diffraction, synthetic aperture focusing [Spi+12], or reflection amplitude based as Bauer and Brüske [BB14b] describe.

The described ultrasonic testing methods actively emit ultrasonic waves to record this signal and its alterations due to reflection or diffraction. Therefore, this method can only be applied to monitoring when the locations that are to be monitored are known precisely. The volume of the monitored specimen that can be observed per measurement transducer is relatively small, even for guided wave applications. It is more suited for inspections than for monitoring.

Acoustic emission

Acoustic emission (AE) or stress wave emission measurements are widely used to monitor the initiation and progression of defects in various structures. AE is in principle a passive measurement technique that senses sound when energy is released during a load change of the observed element.

Jiang et al. [Jia+14] demonstrate a new algorithm for the source localization of defects in three dimensions in concrete specimens with complicated geometry. Their new algorithm significantly reduces the relative error in the source location.

In order to assess the shear strength degradation of fiber-reinforced composites, Philip-

pidis and Assimakopoulou [PA08] use AE sensors. They developed a residual strength model based on two acoustic emission descriptors. The first, most accurate scheme applies well defined proof loads. The second scheme uses operational loads of which no knowledge is required for an acceptable estimate of the remaining strength.

AE for civil structures

AE is a common monitoring technique for wind turbine blades in order to capture fatigue damage [Tso+14]. They show the development of the technology in last two decades with its increasing capabilities.

Improvements to proof load and fatigue testing methods of wire ropes utilizing AE is discussed by Drummond et al. [DWA07]. The authors test a selection of fatigue-damaged ropes and show the recorded signals allow the assessment of the rope's condition when subjected to periodic proof load tests. They conclude that permanent AE monitoring is not required for condition assessment, but proof loading can suffice.

Carmi et al. [Car+14] present a combined evaluation of acoustic emission monitoring and digital image correlation. Both data combined are used to characterize mechanical and damage behavior of a composite specimen. Digital image correlation (DIC) identified critical damage of a proof load tested masonry wall, AE identified the source locations.

Wu et al. [Wu+14] employ AE and metal magnetic memory technology in a proof load test of a crane beam until failure. AE is capable of locating the developing defects over time, and estimating their severity. The metal magnetic memory technology is only capable of estimating defect severity with similar accuracy, but does not provide an accurate location nor can it record the defects severity development over time. The prototype of a transportable tank bridge is proof load tested and monitored by Pollock and Smith [PS72] with AE sensors. The acoustic emission monitoring technique enabled the authors to track the damage progression and distinguish between yielding and cracking of bridge details.

For the monitoring of pipelines, Paradowski et al. [Par+14] develop an AE monitoring system that may substitute for inspection methods if the usual methods are restricted due to the pipeline design. Their results prove that AE testing is capable of locating defects and monitoring their growth. Studies are carried out in the laboratory and operational environments. They conclude their methods would require one AE sensor per 50 meters for the monitoring of gas pipelines. Another application of AE to pressurized structures, namely to nuclear containment vessels, is shown by Green [Gre69] and Bryan et al. [Bry+75].

AE for Aircrafts

A large experiment involving several aircrafts carried out over 10 years by Geng and Jing [GJ14] identifies AE as the first choice for fatigue monitoring. They highlight the possibility to monitor a large physical area with only a few sensors. The sensors can operate in an aircraft from its commission to decommission.

AE in general

AE is commonly used in order to monitor deformation and displacement energy released in structures. About half of the afore mentioned AE related publications demonstrate the application to proof load tests. The frequencies and energy can be used to distinguish elastic and plastic deformations. Furthermore, the distance of the recording sensors and the sound emitting location can be relatively far apart and still allow the capture of useful data.

Weigh-in-motion / Strain gauges

Weigh-in-motion is utilized in order to measure traffic live-loads on bridges. For reliability assessment purposes the load and count of heavy vehicles is of primary interest. Two principle weigh-in-motion approaches are commonly distinguished. Traditional pavement weigh-in-motion (1) uses sensors that are either on or in the pavement. The other version (2) is bridge weigh-in-motion, which allows for a so-called 'nothing on the road' measurement.

Method (1) measures the axle weight of a passing vehicle, as well as the vehicle length and number of axles. These systems rely on single load cell scales, bending plate scale, or in-road piezoelectric sensors [BP98]. Load cells and bending plates usually rely on strain gauge measurements [HW04]. The strain gauge converts an applied load into a proportional electric signal. Another common sensor type is based on the piezoelectric effect. Piezoelectric sensors can be made out of different materials which influences their performance in terms of ease-of-use and measurement quality, e.g. temperature sensitivity [HW04].

Bridge weigh-in-motion (2) was introduced by Moses and Stahl [MS79] and employs sensors on the load carrying structure to measure deflections and strains. Axle detection can be accomplished by strain measurement fed in an free-of-axle (FAD) algorithm developed during the WAVE project O'Brien and Žnidarič [OŽ01]. The FAD method is tested by Kalhori et al. [Kal+17]. The authors point out issues with the method and suggest ways to avoid these issues. A state-of-the-art review on bridge weigh-in-motion is given by Yu et al. [YCD16]. They explain Moses' algorithm, and an alternative algorithm for orthotropic bridges [OŽ01]. Yu et al. conclude that bridge weigh-in-motion is an advantage over the traditional method because it does not interfere with traffic, is

more durable, and potentially more accurate. With an experiment on a railway bridge using four passing trains conducted by Žnidarič [Žni+16] demonstrate that Moses' bridge weigh-in-motion algorithm can deviate largely from the actual weight if the passing vehicle changes its velocity during the measurement. The authors improved the algorithm to account for velocity changes.

Strain gauges can be installed temporarily or permanently on a structure and record continuously. Their location must be chosen precisely in order to capture the strain resulting from loading. Almost all discussed literature pertaining to strain gauges demonstrates their application to measurement on structures subjected to loads. These were either operational, e.g. traffic, or test loads.

Flooded member detection

Flooded member detection (FMD) is only applicable to structures that are placed in water. Such structures can be manned or unmanned oil and gas rigs, offshore wind energy structures, or even structures that are entirely underwater, like some autonomous oil or gas production facilities. Four principle methods are presented herein. Two of these are widely used, these are (1) radiographic FMD, and (2) ultrasonic based FMD. A third method is (3) thermal profiling; and lastly a new method (4) Air FMD.

Radiographic FMD (1) uses γ-radiation in order to detect the presence of water in the steel tubing [Riz14]. If, in addition to the steel wall, water is also present, the γ-ray signal gets attenuated further through photon absorption in the water.

Method (2) is applied in ultrasonic guided wave FMD systems for permanent monitoring [MGB05b; MG13]. The authors exploit the changes to the mode transfer function of guided waves when they travel no longer through a hollow, but a water-filled cylinder. The technique is demonstrated on a bridge with a tubular truss structure [MGB05a]. In Mijarez et al. [MGB07], the authors use the steel joints to simply transmit an alarm signal through the structure when a battery activated by the contact to seawater powers a transducer.

With thermal profiling (3), a defined heat is applied in the circumference of the tested member and the resulting temperature is measured [HPS93]. The slow inspection speed and issues in automating the method make it less favored by operators [Riz14].

Air FMD (4) is a technology under development which utilizes pressurized air in the tubing in order to indicate through-wall damages [TNB15]. This method would allow for a continuous monitoring for flooded members without specialized sensors. A pressure drop indicates the existence of damage, and escaping air indicates the damage location(s).

FMD can serve as a monitoring or inspection method. It is not, however, useful in monitoring proof load tests. The minimal damages that can be detected by FMD are

already significant and usually too large to be acceptable by-products of the test.

2.3.2 Remote sensing

Remote sensing does not require sensors on the tested structure. For some methods, it may be advantageous or required to place reflectors or optical patterns on the structure for optimal accuracy of the measurements.

Visual inspection

Visual inspection as a remote sensing technique has the same issues regarding proof load testing as described in the section 'local sensing'. Considering the greater distance to the observation target, compared to local sensing, a loss in accuracy can occur due to the increasing influence of vibrations with smaller imaging angles of teleoptics [EL15]. The authors extended the use of camera-assisted total stations by using optics to determine a bridge's frequencies, which they demonstrated with a live pedestrian bridge.

Utilizing unmanned aerial vehicles (UAV) may be seen as a mix of local and remote sensing. The UAV is not permanently close to the tested structure and can adjust its distance. The use of a UAV is demonstrated by Pereira and Pereira [PP15] to acquire digital images of cracks. They use an image processing system for the automatic feature extraction and feature parameter estimation. In their case study, data acquisition takes under 9 minutes for a $200\,m^2$ area. The particle filter used for image processing runs fast enough on a single board computer, than can be installed on a UAV, to process the data in real time. Galarreta et al. [FKG15] show how UAV imagery is compiled in three-dimensional point clouds, and this data is used for crack detection in facades and measuring dislocation of roof tiles. They point out that their current software produces an unacceptably high rate of false positives and false negatives.

Visual inspection is also applied for leak detection of offshore pipelines. Depending on the fluorescence of the transported medium, a dye can be added to aid the leak detection. Specialized lighting and optics equipment is used on a remotely operated vehicle as McStay et al. [McS+05] exemplify.

For most types of structures, remote visual inspection will not be a suitable monitoring system in order to support the execution proof load tests. An exception could be the visual monitoring of hydro-static pipeline tests. Hydro-static tests indicate insufficient pipeline strength through failure by leaking.

Weigh-in-motion / strain measurements

A new, and so far not commercially established method is developed by Ojio et al. [Oji+16]. The new method works via visual observation through telelenses. The authors' contactless bridge weigh-in-motion system uses video cameras to record the traffic and bridge deflections. The system does not require attaching sensors to the bridge and can be set up within one hour. It has the "nothing on the road" advantage, like the common strain-gauge based systems have. However, it is more difficult to resolve the separate axle contributions in the load deflection.

Remote strain measurements are applicable as proof load test monitoring methods, like the established strain-gauge method. Unlike the commonly used strain-gauges, the remote measurement capabilities for such a purpose are not well established yet.

Thermography

Temperature is an always present indicator for active damage processes because some of the energy released by the defect will dissipate as heat. Infrared thermography (IRT) can be setup at a remote location, making it a candidate for proof load tests [Kyl+14]. To date, IRT is common for the monitoring of machinery [Bag+13]. Vavilov et al. [VBK15] use the remote sensing capabilities of thermography to monitor the proof loading of composite grid structures in the laboratory.

Digital image correlation

The digital image correlation (DIC) technique is used for the measurement of localized deformations in high-strength steel monostrands by Winkler et al. [WFG14]. The DIC technique enables the measurement of the individual wire strains along the length of the monostrand, and provides quantitative information on the relative movement between individual wires. It was shown that the highly-localized curvatures due to bending might cause yielding of the monostrand. DIC can provide remote information about the localized deformation of details like monostrands of bridge cables. The authors were able to detect yielding of the monostrand due to bending. In combination with AE, Carmi et al. [Car+14] used DIC in order to categorize the mechanical behavior of composites and damages introduced therein. DIC detects critical damages in the specimen and enables to severity classification.

DIC may be suitable for proof load test monitoring when the data can be analyzed in real time. Strains and other deformation information can be extracted from DIC data that can be utilized for controlling proof loading.

Robotic theodolites or robotic total stations

Psimoulis and Stiros [PS07] demonstrate the use of robotic total stations for the purpose of SHM on three different types of bridges. Technological advances enable the millimeter accurate measurement of motions up to 10 m/s and oscillation frequencies up to 4 Hz. The improvement of measurement accuracy to a level that also measuring deflections of stiff structures with short spans is documented by Merkle and Myers [MM06]. The use of robotics played an important role in the precision improvements. Merkle & Myers also demonstrate the application of robotic total stations as a monitoring technique in a proof load test campaign of five road bridges in Missouri. A total station is also used by Olaszek et al. [OŁC14] in order to increase the measurement accuracy of displacements at critical points of a proof-load-tested road bridge.

Robotic total stations have been demonstrated as a useful monitoring method in supporting proof load tests of bridges. With ongoing advances, the method may even show to be useful in dynamic tests. The method's advantage lies in its high accuracy over several hundred meters measurement distance.

Laser vibrometry

Nassif et al. [NGD05] compare deflection and vibration measurements from different sensor systems that either need or do not need contact to the structure. They used linear variable differential transducers and accelerometers (geophones), which need to be affixed to the structures. The contactless, remote measurements stem from laser Doppler vibrometers (LDV). The velocities derived from LDV and accelerometers show good correlation between both methods for various traffic excitations. An excellent match of measurements is given for the deflections.

In principle, laser vibrometry could serve the purpose of monitoring the progression of deflections or other deformations during a proof load tests. However, no literature discussing this use case has been found.

2.4 Review summary

The review includes 89 scientific articles and books published in the period from 1967 to 2017. Among these, 35% of the review sources are published after 2010. The temporal distribution of review publications is depicted in Figure 2.1. These new publications deal mostly with four different topics: (1) the application of proof load testing to structures where to date proof load testing rarely is applied; (2) consideration of decision analysis; (3) introduction of new or improved measurement techniques that can be employed in order to monitor the progress of a proof load test experiment on a structure; (4) discuss

or present improvements in the execution of proof load tests by e.g. introducing new assessment methods or guideline suggestions.

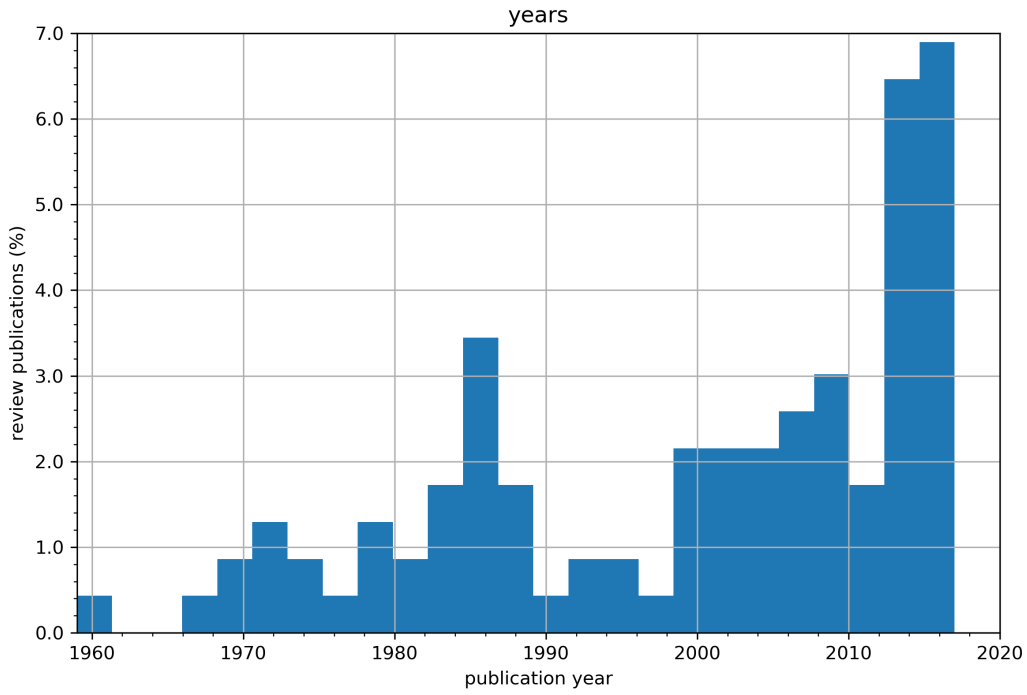

Figure 2.1: Temporal distribution of review publications

In all the literature there is at least one of two main characteristics present, allowing a total of three categories. The three categories are made up by studies that are focused on experiments, analytical or numerical modeling, or a combination of both. The dominant fractions are shown in Figure 2.2. Roughly 25% are focused on non-experimental studies, dealing with fundamental proof load testing concepts, decision analysis, or conceptual foundations for structural testing. Studies are subsumed under the experimental category when they focus on experiment and application. A numerical or analytical part is usually present therein. This analytical part is mostly data analysis or the introduction of well-established analytical background to the reader. This is the case for 61% of the sources. Only about 14% of the scientific publications have major experimental as well as analytical / numerical foci. The combinations demonstrate usually the application of an experimental technique with a new data analysis algorithm, or deal with the improvements of numerical models built for real and monitoring device equipped structures. Of those studies focusing on civil engineered structures, four types dominate the reviewed literature: nuclear reactors with 19%, offshore structure with 23.8%, and 28.6% for both, bridges and pipelines.

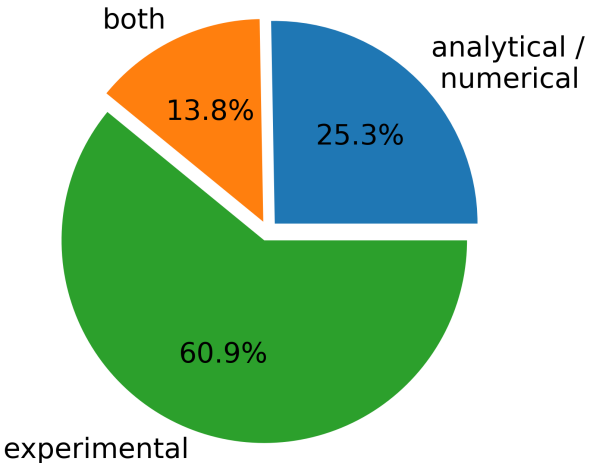

Figure 2.2: Fraction of basic study types

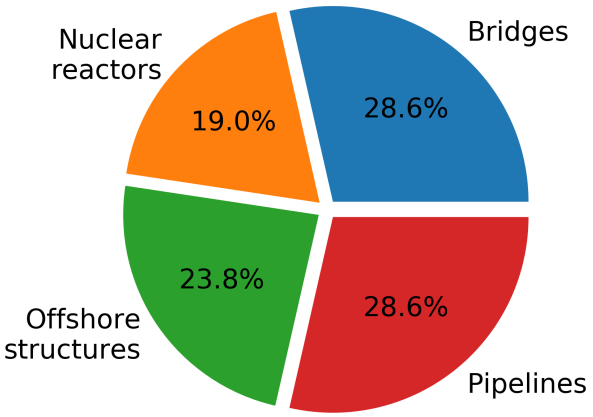

Figure 2.3: Major structure types found in the literature review

Excluding works that do not focus specifically on proof load testing, which make up the majority, just 31.2% of the publications consider decision analysis in some way combined with proof load testing. Figure 2.4 shows the ratio.

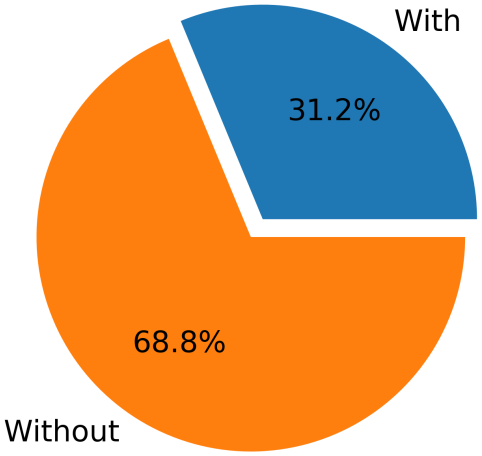

Figure 2.4: Distribution of works considering decision analysis. (Sources not specifically on proof load testing are excluded.)

2.5 Review conclusion

The reviewed research pertaining to the fundamentals of proof load testing, discuss updating structural components without considering system effects or treated the whole structure as a single component. Correlations were not included, although they may be implicitly present in structural systems reduced to one component. An investigation

that considers explicit system modeling, the influences of correlation between the failure, deterioration, and loading mechanisms on the reliability and VoI through proof load testing is not available yet. Some previous research discussed decision making but without evaluating the value of proof load testing. The thesis demonstrates the VoI derivation of proof load testing applied to structural models and examines alternatives to proof load testing that may also provide the required information.

The literature review showed that proof load testing is applied to a variety of vastly different structures. The most noticeable type would be bridges, which are visible in most people's daily lives. Bridges are of major societal relevance because they are part of the infrastructure used to generate the gross domestic product [Wan15], influence life safety, and sustainability of transport and thereon dependent factors [Tup+12]. Proof load testing is used in bridge testing mostly to verify the load bearing capacity of old bridges. It is especially useful if the structure is not sufficiently documented for assessment methods other than proof load testing. A potentially even greater role is given to proof load tests in the pipeline industry. Hydro-static tests, as proof load tests are called in this industry, are mandatory prior to commissioning in many codes around the globe. For certain pipelines, hydro-static testing is part of the usual inspection portfolio because other testing methods exhibit weakness in the detection and classification of crack-like flaws, or the pipeline design prevents such inspections. For critical structures like nuclear pressure chambers and offshore platforms, proof load testing may not be an option after operations have begun. Nonetheless, proof load tests can be used to improve the design of reactor pressure chambers and their monitoring systems. Proof load testing of offshore structures is considered by several researchers as a method to obtain valuable information on the reliability. It is not, however, common practice to proof load test large offshore structures. Instead of testing the assembled structure in its operation location, an alternative could be to test sub-systems in the factory and update the reliability estimate with advanced models. This idea is explored in Chapter 7 and Chapter 8.

Because proof load testing is usually intended to be non-destructive, the tests have to be monitored carefully to avoid damage to the structure. The review presents many monitoring or inspection techniques that can be beneficial for a safe proof load test execution. Most of these techniques to date require the installation of sensor systems directly on the structure. With the advancement in computation power, optical measurement systems, especially data analysis methods, and more remote monitoring techniques will become available. With the appropriate monitoring instruments it may be possible to acquire data that not only helps to prevent damage, but can also be used to improve the reliability estimation as demonstrated in Chapter 9 "Decision framework: structural health testing".

CHAPTER 3

Structural System Reliability and Updating

3.1 Structural System Models

The introduction lists examples of structures that can be modeled by simple models derived from logical systems. These are e.g. compliant towers, tension leg platforms, jacket structures, and monopiles.

Logical systems are simple models that are described through logical or set operations that link the elements comprising the system. Such logical operations are e.g. 'and', and 'or'. Expressed in terms of set algebra, the corresponding operations are the union '$\cup$' for 'or', and the intersection '$\cap$' for 'and'. Graphical examples in the form of Venn diagrams are given for union in Figure 3.1a and intersection in Figure 3.1b.

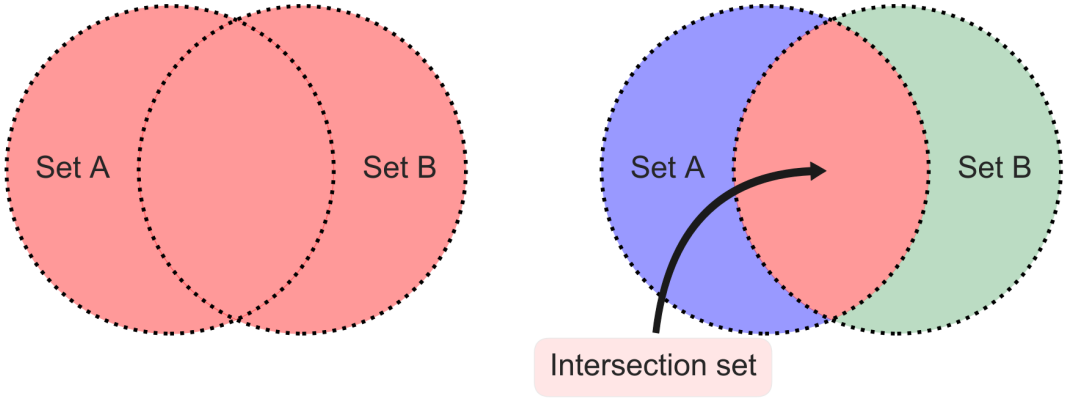

(a) Example of the union of two sets

(b) Example of two intersecting sets

Figure 3.1: Examples of two set relations

The state of the individual components shall be described through D for damaged, and $\bar{D}$ for not damaged, or F and $\bar{F}$ for failure and no failure respectively. Whether damage or failure is used in the logical operations does not influence the result, apart from its

interpretation. For brevity only failure is used in the following explanations. The failure of the i^{th} element is defined in Equation (3.1).

$$F_i = R_i \, M_{R_i} \leq S \, M_S \tag{3.1}$$

The random variables on the right-hand side are R for the resistance, M_R for the resistance model uncertainty, S for the load, and finally M_S for the model uncertainty of the load.

The two basic logical systems are the series system and the logical system. The series system failure $\underset{sys}{F^{ser}}$ is defined by the union of failure events of elements.

$$\underset{sys}{F^{ser}} = \bigcup_{i=1}^{n} F_i \tag{3.2}$$

The parallel system failure $\underset{sys}{F^{par}}$ is defined by the intersection of component failure in Equation (3.3).

$$\underset{sys}{F^{par}} = \bigcap_{i=1}^{n} F_i \tag{3.3}$$

The parallel and series systems are depicted in Figure 3.2a and Figure 3.2b respectively. In the parallel system, each component bears an individual load; load sharing between components is not possible. Furthermore, following the definition in Equation (3), the system will only fail if all components failed. Therefore, the parallel system has no relevant meaning for mechanical systems. The series system, however, can represent a structure where all elements are bearing the same external load and no load bearing redundancy is present in the structure. Such a mechanical structure could be e.g. a chain or monopile. A variation of the parallel system with relevance for the modeling of mechanical systems was introduced by Daniels [Dan45]. The now so-called Daniels system modifies the parallel system by introducing a common external load on the system that is shared among its components, as shown in Figure 3.2c.

The load distribution can be defined through the ductility of the system components. In the present thesis, the extreme cases, shown in Figure 3.3a and Figure 3.3b, of perfect ductility and perfect brittleness are considered. A perfectly brittle system or component fails the moment its load bearing capacity is reached by the load. A perfectly ductile system retains its carrying ability at the level it began yielding.

A ductile Daniels system failure $\underset{sys}{F_{dDS}}$ is defined in Equation (3.4) as the sum of the resistance terms being smaller or equal than the load term. In the ductile Daniels, all load is distributed to the elements proportional to their load bearing capacity.

$$\underset{sys}{F_{dDS}} = \sum_{i=1}^{n} R_i \, M_{R_i} \leq S \, M_S \tag{3.4}$$

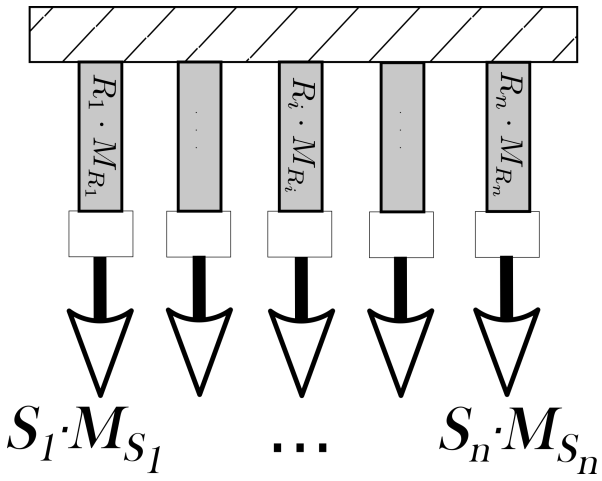

(a) Parallel system schematic

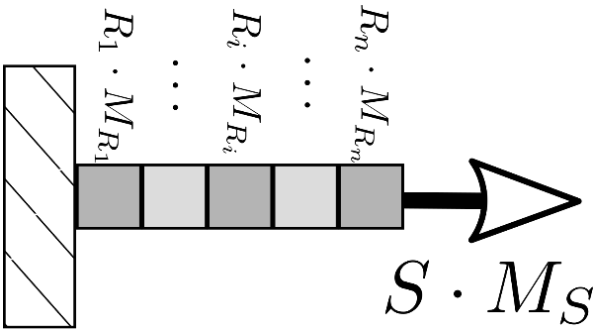

(b) Series system schematic

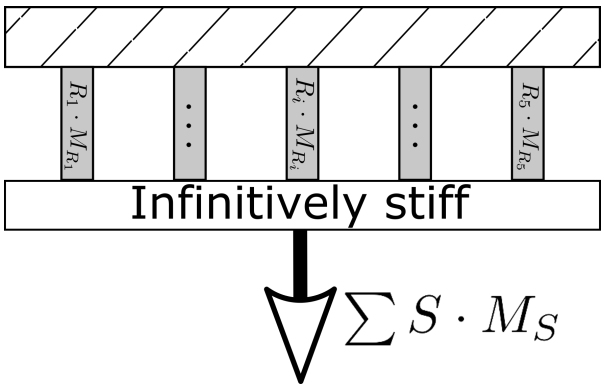

(c) Daniels system schematic

Figure 3.2: System schematics. (a) to (b) are logical systems. (c) is derived from (a) and adapted for mechanical systems

For a perfectly brittle Daniels system, the system failure event $F_{\underset{sys}{bDS}}$ is determined by Equation (5). The resistance terms $R_i\, M_{R_i}$ have to be sorted in descending order. This results in the order $\hat{R}_1\, \hat{M}_{R_1} \leq \ldots \leq \hat{R}_i\, M_{R_i} \leq \hat{R}_{i+1}\, M_{R_{i+1}} \leq \ldots \leq \hat{R}_n\, \hat{M}_{R_n}$.

$$F_{\underset{sys}{bDS}} = \bigcap_{i=1}^{n} \{(n-i+1)R_i\, M_{R_i} - S\, M_S \leq 0\} \tag{3.5}$$

A Daniels system, being a special type of parallel system, only fails when the resistance of all elements is exceeded by the attacking load. Every time the currently weakest element fails, the load is redistributed to the remaining elements until they can no longer jointly bear it. With every additional element, the redundancy in the system increases.

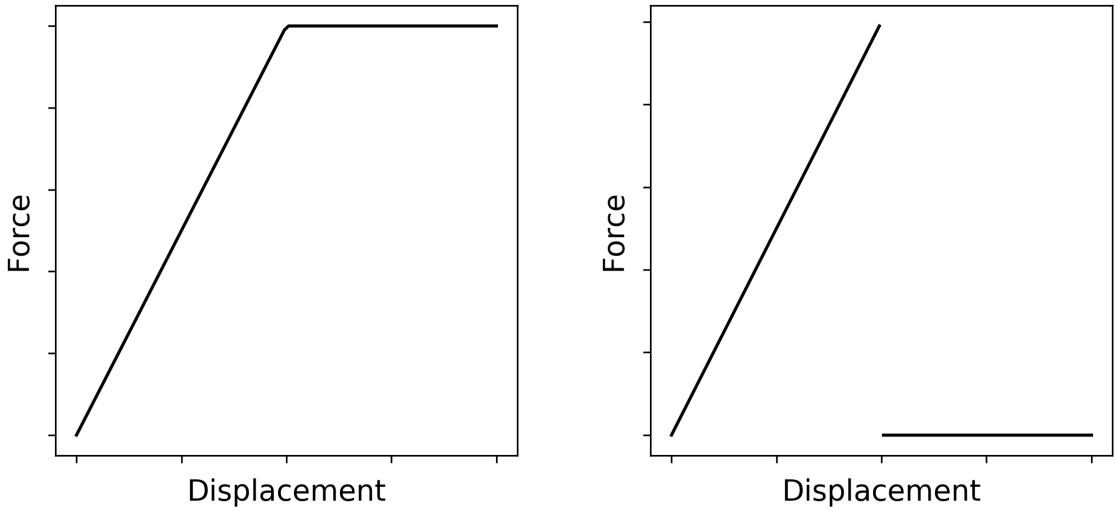

(a) Perfectly ductile (b) Perfectly brittle

Figure 3.3: Idealized behavior of force vs. displacement

3.2 Interdependence and concordance

The interdependence of random variables is an important factor in the reliability of structural systems. This is exemplified by the simple bounds of the series and the parallel system. Equation (3.6) shows the simple bound of the series system failure probability.

$$\max_{i=1,\ldots,n} \left(P(F_i)\right) \leq P\left(F_{\substack{ser \\ sys}}\right) \leq 1 - \prod_{i=1}^{n} 1 - P(F_i) \tag{3.6}$$

The lower bound (left-hand side) is the probability of failure when all components are positive, fully correlated ($\rho_{i,j} = 1$). In this case, the entire system will fail if one of the components fails, so the probability of failure equals the largest probability of failure among the system components. The upper bound (right-hand side) is the probability of failure when all components are uncorrelated ($\rho_{i,j} = 0$). Because the product of the survival probability decreases with increasing n, the failure probability increase for an increasing n.

Similarly, the simple bounds for the probability of failure of a parallel system is established by Equation (3.7). In parallel systems, failure probability decreases for increasing n if the correlation is zero (lower bound). In the case of full positive correlation, the system behaves like one component, the failure probability of which is given by the

minimum failure probability of all n components (upper bound).

$$\prod_{i=1}^{n} P(F_i) \leq P\left(F_{\substack{par \\ sys}}\right) \leq \min_{i=1,\ldots,n}(P(F_i)) \tag{3.7}$$

Interdependence can be measured in many ways. Two common measurement are presented in the following.

3.2.1 Pearson's linear correlation coefficient

The Pearson product-moment correlation coefficient measures the magnitude of linear correlation between two random variables [Pea95]. The Pearson correlation coefficient $\rho_{X,Y}$ is a dimension-less variable that is bounded between -1 and 1. Expressed through mean values $\mu(X)$ and $\mu(Y)$ the linear correlation coefficient reads as a measurement of linear association between the populations of X and Y.

$$\rho_{X,Y} = \frac{E\left[(X - \mu(X))(Y - \mu(Y))\right]}{\sigma_X \sigma_Y} \tag{3.8}$$

σ_X and σ_Y are the standard deviations of X and Y, respectively. Both must have nonzero and finite values. The expected value is written as $E[\ldots]$.

Another common formulation of the linear correlation coefficient is

$$\rho_{X,Y} = \frac{\mathrm{cov}(X,Y)}{\sigma_X \sigma_Y} \tag{3.9}$$

This is a normalized covariance. The covariance $\mathrm{cov}(X,Y)$ is also a linear measurement of correlation, and commonly used in the definition of the multivariate normal distribution. It is, however, harder to interpret covariance than the Pearson correlation coefficient, because the covariance in not bounded between -1 and 1.

3.2.2 Concordance or measure of association

A set of random variables are called concordant if they exhibit a trend in which large values for one variable are paired with large values of the other random variable, and this trend is present for small values being associated with other small values. This is a more general condition than can be measured by Pearson's correlation coefficient. Concordance of two random variables X, Y is defined as $(x_i - x_j)(y_i - y_j) > 0$ for two sets of observations (x_i, y_i) and (x_j, y_j). Discordance is given if $(x_i - x_j)(y_i - y_j) < 0$. The special concordance case of linear correlation can be produced with a random field from a multivariate random variable and affine transformations. Other random fields with more relaxed general concordance conditions cannot be generated by transforming multi-variate normal fields.

3.2.3 Generation of concordant random variables

Linear correlated random variables are often produced through the transformation of multivariate normal distribution. An alternative approach is to use copulas that represent the interdependence of random variables. The copula and marginal distributions form a joint distribution. This avoids the detour of transforming multivariate Normal distributions. Further flexibility is given by the possibility to model any interdependence that can be expressed by a distribution function [Nel13]. This allows the construction of a non-linear interdependence structure. Independence is produced with the product copula that ensures the independence of random variables X and Y as defined in Equation (3.10).

$$H(x, y) = F(x)G(y) \tag{3.10}$$

The linear correlation with Pearson's correlation coefficient as parameter is generated with the Gaussian copula.

The term correlation coefficient is used herein only for Pearson's product-moment correlation coefficient. All models used hereafter rely on copulas to generate concordant random variables. Nonetheless, the linear correlation coefficient is sufficient in all cases modeled within this thesis because no data or information about the dependency used, indicated a non-linear dependency structure.

3.3 Deterioration

The term deterioration groups processes that reduce the strength of a component or system over time. Mechanical systems can deteriorate in several ways. (1) wear of moving components that can be caused by e.g. abrasion or erosion. This type of deterioration is of minor relevance for load bearing structural components because it can usually be avoided by design. (2) fatigue and (3) corrosion are deterioration processes relevant to structural systems. This section will deal with approaches for fatigue, corrosion, and a generic deterioration model.

3.3.1 Fatigue

Fatigue is a gradual degradation, leading eventually to failure. The process occurs under repetitive / cyclic loads, which vary with time. The so-called fatigue loads are lower than the maximum load the component or structure can resist. Fatigue loads are cyclic by nature; a static load does not cause fatigue [Poo07].

Two elements are required to describe fatigue mathematically. One element has to describe the state of the test specimen / loaded component. This pertains mainly to the damage state, e.g. the presence of a material flaw that is grown by the fatigue load.

The second element in the mathematical description is the mechanical response of the specimen to the cyclic load.

3.3.1.1 Fatigue crack initiation

Cracks begin at a flaw in the material. Such a flaw can be anything that weakens the material locally on a microscopic scale. Common crack starting points are grain boundaries in material or inclusions of materials that bond weakly with their surroundings [HB12]. Under loads much lower than the tensile strength, micro cracks can form at that these initial material flaws.

3.3.1.2 Fatigue crack propagation

Fatigue crack propagation, or alternatively fatigue crack growth, are names for processes that increase the size of cracks. The propagation of cracks is usually divided into three stages. Micro crack propagation, stage (1), is often seen as the initiation phase, in which the cracks growth is parallel to the stress. Stage (2) is the macro crack propagation. The propagation direction changed and is normal to the stress. This leads to a reduction of cross section and weakening of the specimen. Stage (3) is reached once the cross section is so small that the specimen can fail in a single load cycle [Poo07].

3.3.1.3 Paris Equation

An empirical equation, the so-called Paris Equation, see Sih et al. [SPE62], is applied to describe fatigue crack growth in metals.

$$\frac{da}{dN} = C(\Delta K)^m \tag{3.11}$$

It describes the change of crack length da with change of fatigue load cycles dN in dependency of a stress range factor ΔK and two material constants C and m. ΔK is calculated from the overall stress range and shape of the crack. In experiments to derive the material parameter m and C in the Paris Equation, cyclic load with constant amplitudes is applied. For the purpose of probabilistic fatigue modeling, the amplitude can as well be represented by a random variable.

3.3.1.4 Palmgren-Miner rule

A load spectrum with variable amplitude can be analyzed with the Palmgren-Miner rule. Palmgren [Pal24] and Miner [Min45] assumed that fatigue damage accumulates linearly with the number of load cycles. Following the Palmgren-Miner rule, a specimen subjected to a stress S_1 has a life span of N_1 cycle, or for S_2 its life span is N_2 cycles. The

relation is shown in the schematic stress vs. cycle diagram in Figure 3.4. The damage accumulated at stress S_1 after n_1 cycles is n_1/N_1. For n_2 cycles at S_2 the damage will be n_2/N_2.

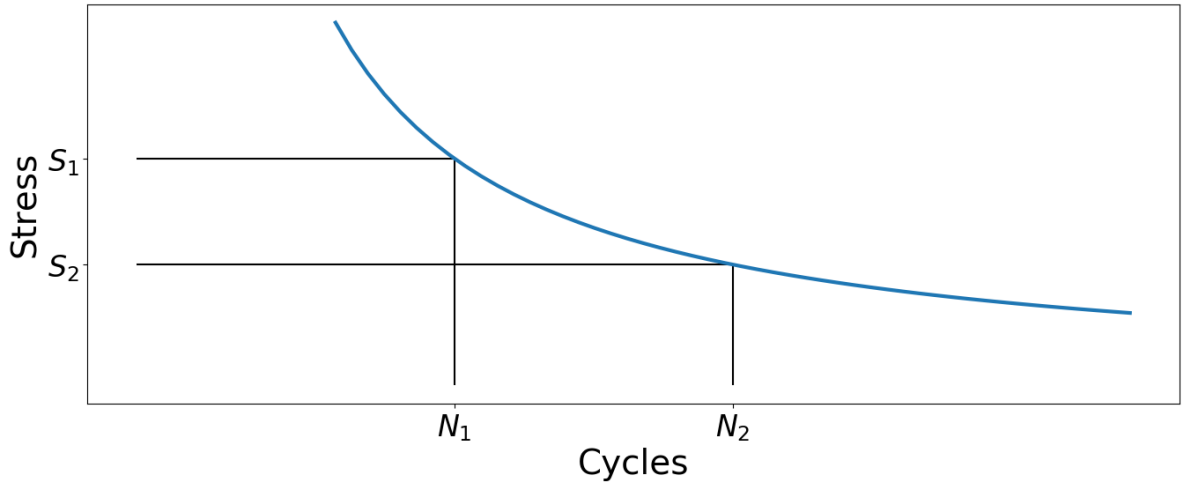

Figure 3.4: Schematic stress vs. cycle diagram for the Palmgren-Miner rule

For a spectrum of fatigue loading the partial damages sum-up to the total damage as demonstrated in Equation (3.12).

$$\sum_i \frac{n_i}{N_i} = 1 \tag{3.12}$$

This principle idea of linear accumulation of damage is also used in the generic deterioration model in Section 3.3.3.

3.3.2 Corrosion

Corrosion is an electro-chemical reaction that occurs between the surface of the deteriorating material and other materials that are in contact. For ferrous material like steel it is essentially a process of oxidation. A few common types of corrosion are uniform corrosion, pitting corrosion, galvanic corrosion, and stress-corrosion cracking.

Uniform corrosion is expected when a larger surface is not protected against corrosion, and the corrosion process attacks the entire surface in a similar rate. This type of corrosion is often found on steel structures that are directly exposed to air or water.

Pitting corrosion is usually seen when a small surface lost its protection. The corrosion may then act locally on a small area, progressing mostly inward. It is often found on pipelines with damaged protective coating.

In certain environmental conditions pitting or uniform corrosion may also be caused by bacteria [LWM92].

Galvanic corrosion is caused by a potential difference between two touching metals. This effect is also exploited to protect surfaces in corroding environments by either applying a voltage to the structure that slows the ion exchange, or by placing a galvanic anode on the surface. This method is called cathodic protection.

Stress-corrosion cracking can occur in sour, often sulfuric environments. In the tip of a corrosion crevice, stress builds up that exceeds the material's fracture toughness. This causes cracks to propagate without cyclic load.

The uniform, pitting, and galvanic corrosion can be modeled in a process depending on the corrosion rate and time. Examples are given in Equation (3.13) for the reduction of the radius of a cylinder and in Equation (3.14) for a more general reduction of cross section.

$$A_r = 2\pi(r_0 - w_r t)^2 \tag{3.13}$$

$$A_r = A_0 - w_r t \tag{3.14}$$

A_0 or r_0 is the initial area or radius, w_r is the deterioration or corrosion rate, and t is the time.

3.3.3 Generic deterioration model

The generic deterioration model by Qin et al. [QTF15] uses a random worsening / deterioration coefficient W as defined in Equation (3.15). This model is based on the Palmgren-Miner rule of linear damage accumulation over load cycles. The generic model is not specifically for fatigue damage, but could be applied to any type damage that accumulates over time.

$$W_i(t) = 1 - \sum_{k=1}^{t} \Delta_{i,k} \tag{3.15}$$

$\Delta_{i,k}$ is a conditional random variable, such that $\Delta_{i,k}|\Theta$ is conditioned with only the mean value $\Theta = \mu(M_\Delta)$ in accordance with Qin et al. [QTF15]. M_Δ is an assumed observable and provides information on the state of damage. The observable could be e.g. a crack length, corrosion depth, or any other accumulating deterioration measurement.

3.4 Updating of probability estimates with posterior information

The term updating is used herein to describe an algorithm that modifies an assumption about parameters or states in the light of new data. The assumption is called a prior belief and is either expressed by a probability density function (PDF) in case of parameters, or it is described by the probability of the state. New data that is acquired about the parameters or states is used to modify prior belief, which means updating it

to incorporate the evidence from e.g. an experiment. If the updating method used is Bayesian updating, the probability of the new information is call likelihood.

Proof load testing information can be used in different ways to update the prior believe about the tested specimen. The following paragraphs explain and critique the capabilities of several algorithms that can used in the context of proof load testing.

3.4.1 Classical truncation approach

Lin and Nowak [LN84] proposed to modify the resistance distribution by truncating at the most likely point of failure t_c formalized in Equation (3.16).

$$t_c = \min \left(R'_{\text{des}}(x) - S'_{PL}(x) \right) \tag{3.16}$$

Figure 3.5 shows the distribution R'_{des} and S'_{PL} with the most likely point of failure of the proof test t_c and the extreme load model S.

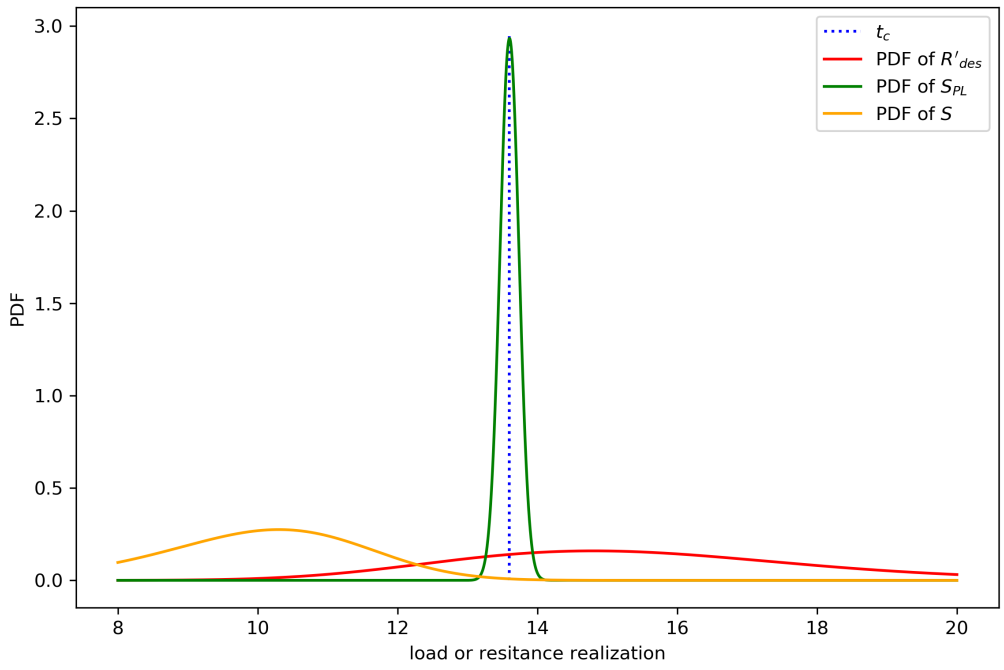

Figure 3.5: Location of truncation point t_c in relation to resistance R'_{des}, load S, and proof load S'_{PL}

With the truncation suggested by Lin and Nowak [LN84] the posterior distribution takes

on the form in Equation (3.17)

$$R'' = R'_{\text{des}}(x), x > t_c \tag{3.17}$$

Resulting in a resistance distribution R'' as shown in Figure 3.6 The updated resistance

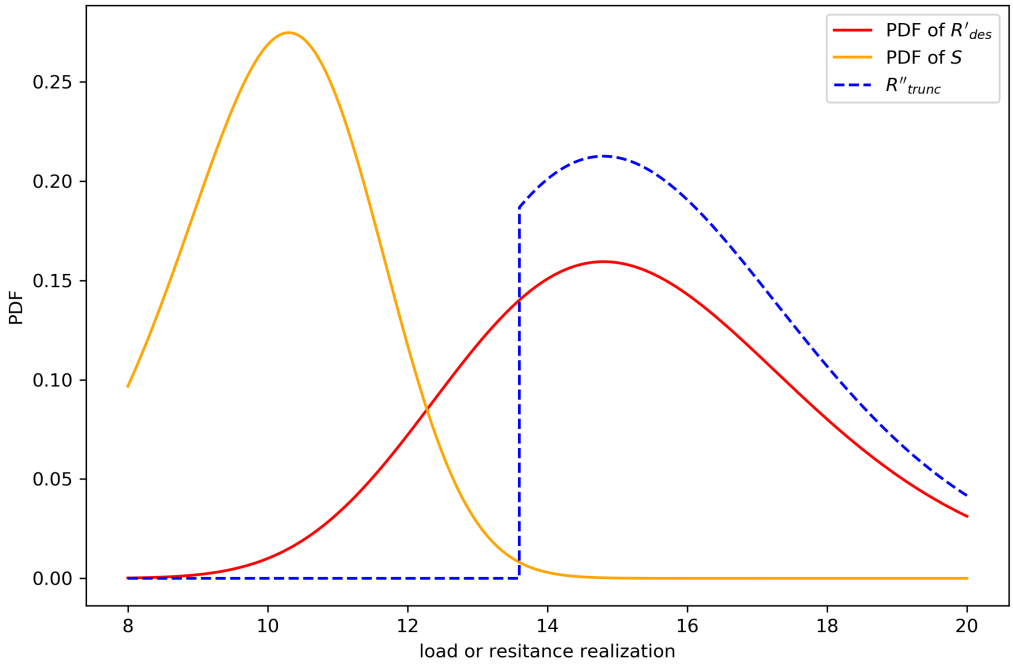

Figure 3.6: Truncation approach by Lin and Nowak. R'' (dashed line) takes on a distribution where the probability is shifted past the truncation point in comparison with R'_{des}

distribution R'' has zero probability until it reaches the truncation point t_c. By fulfilling the second axiom of probability theory, the truncation causes the probability to be shifted from the left side of the t_c to the right-hand side. As a result, the PDF of R'' is greatly reduced in the region where S has a large influence and the estimated failure probability reduces.

This approach disregards all measurement uncertainty of the proof load and shifts probability of the resistance term to higher realizations. The shifting of probability retains the shape of the distribution beyond the truncation point. No information can be obtained by proof load testing that confirms or falsifies the assumption on the distribution shape.

3.4.2 Mixture distribution considering measurement uncertainty

Thöns et al. [TFR11] suggest a mixture distribution in order to consider the measurement uncertainty of the proof load. With this method, the point of truncation $t_{i,l}$ is chosen such that it is the intersection of the lower flanks of both, R'_{des}, and S'_{PL}. The resulting mixture distribution R''_{mix} with the necessary weights is provided in Equation (3.18). The weights ensure that the $R''_{\text{mix}}(x)$ follows exactly $S'_{PL}(x)$ for $x \leq t_{i,l}$ and realizations of $R''_{\text{mix}}(x)$ for $x > t_{i,l}$ are scaled up so that the distribution integrates to 1.

$$R''_{\text{mix}} = \begin{cases} S'_{PL}(x) \dfrac{1}{S'_{PL}(t_{i,l}) - S'_{PL}(-\infty)}, x \leq t_{i,l} \\ R'_{\text{des}}(x) \dfrac{1}{S'_{PL}(-\infty) - S'_{PL}(t_{i,l})}, x > t_{i,l} \end{cases} \tag{3.18}$$

The effect on the failure probability estimation, as before in the classical approach, is due to a shifting of probability from the left-hand side of the truncation point to its right-hand side. The difference between the approaches of Lin & Nowak and Thöns is that in the mixture distribution, some probability remains on the left-hand side and therefore the estimate of the failure probability is higher with mixture distribution than with the classical truncation. The PDF of Thöns' mixture distribution in relation to the proof load distribution and the design resistance is shown in Figure 3.7. This approach considers the measurement uncertainty of the proof load but disregards the uncertainty in the resistance distribution and its model uncertainty in the region where S'_{PL} replaces R'_{des}. As before with the classical truncation approach, probability is shifted to higher realizations of the resistance term, and the PDF of the proof load remains until the truncation point.

3.4.3 Bayesian updating of design resistance distribution by proof load distribution

Bayesian updating is an inference method that allows a prior belief to be modified with additional information, the so-called likelihood. The prior belief is based on information that is at hand. It can stem from old data / observations, expert opinions, or other sources that do not consider the acquisition of new data. The likelihood is new data that may be obtained e.g. through an experiment like proof load testing.

Lin and Nowak [LN84] suggest Bayesian updating of the resistance distribution R'_{des} with the proof load distribution $S'_{PL}\left(x \mid \theta\right)$ as well. θ represents here the measured proof load. The Bayesian updating is performed according to Equation (3.19).

$$f_{R''}(\theta|x) = \frac{f_{R'_{\text{des}}}(x)\, f_{S'_{PL}}(x|\theta)}{\int_{-\infty}^{\infty} f_{R'_{\text{des}}}(x)\, f_{S'_{PL}}(x|\theta)\, d\theta} \tag{3.19}$$

This approach accounts for all uncertainties of the involved assumptions and measurements, but is usually not useful because it can result in a reduction of the posterior

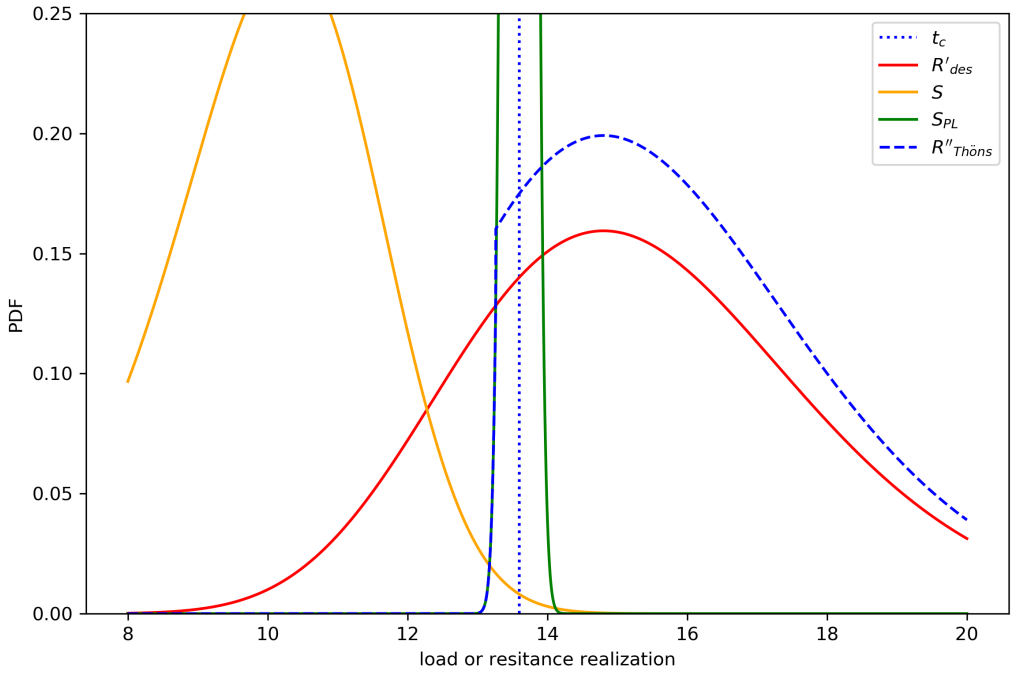

Figure 3.7: Mixture distribution approach by Thöns. R'' (dashed line) follows initially S_{PL} and after t_c is follows an upscaled R_{des}

resistance relative to the prior resistance. Figure 3.8 shows an example with an unusually high proof load mean, equal to the 0.25 quantile of the design resistance mean plotted. We observe that most of the probability in the Bayesian posterior distribution is concentrated around the most likely point of failure t_c. As later demonstrated in the comparison of the different approaches, this can result in an increase of the failure probability estimation relative to the design failure probability. According to Rackwitz and Schrupp [RS85] this is not an inference method for proof load testing, but for prototype testing.

3.4.4 Bayesian updating with proof load survival events

In the case of Bayesian updating with discrete events, the prior information is the probability of failure of the system that is solely based design assumptions. The likelihood is the probability $P(Z_{PL,\uparrow,j})$ of the indication that the proof load test was successful, $Z_{PL,\uparrow,j}$ as described in Equation (3.20). The opposite indication is $Z_{PL,\downarrow,j}$, which represents a proof test failure.

$$Z_{PL,\uparrow,j} = R_j \, M_{R,j} - S_{PL} > 0 \tag{3.20}$$

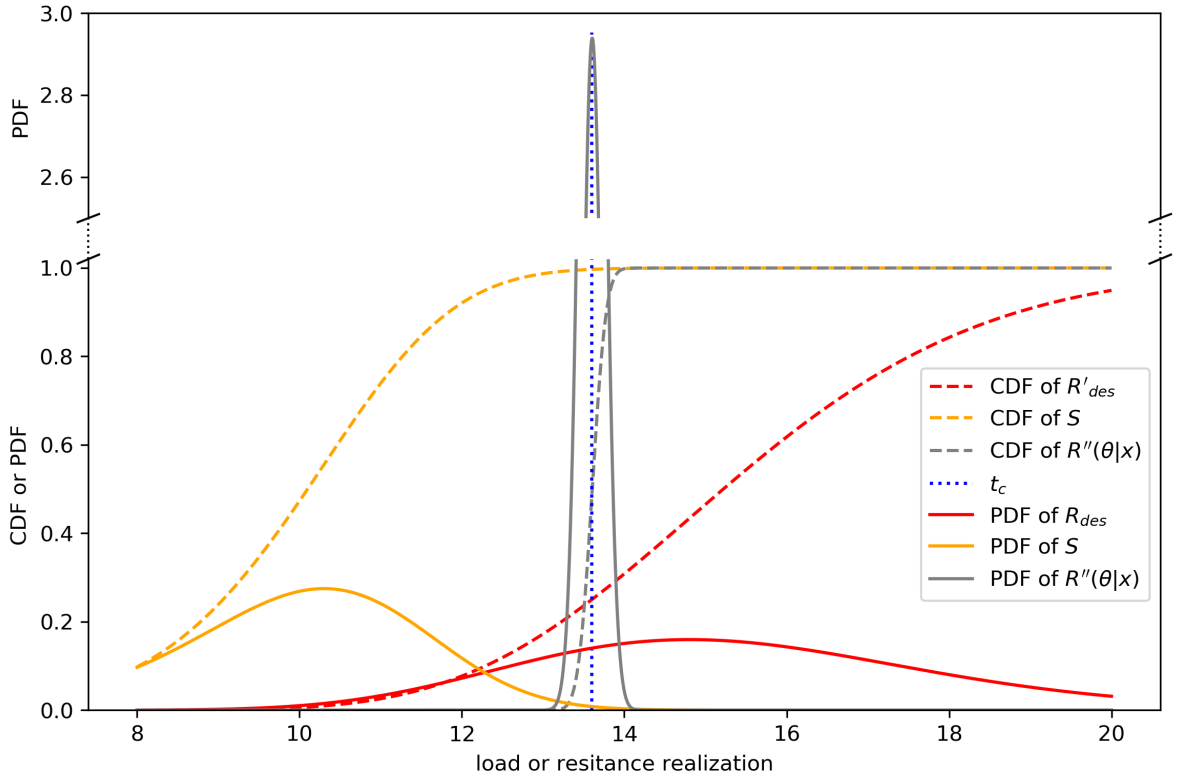

Figure 3.8: Bayesian updating of R'_{des} with S'_{PL} results in a distribution with low dispersion but potentially also smaller mean than the prior mean. Notice, the ordinate is split to leave room for a detailed figure

$$Z_{PL,\downarrow,j} = R_j \, M_{R,j} - S_{PL} \leq 0 \tag{3.21}$$

The posterior failure probability, given the indication that the proof load test succeeded $P(F|Z_{PL,\uparrow})$, is the probability of intersection of failure event with prior information and proof load success event $P(F \cap Z_{PL,\uparrow})$, normalized by the probability of proof load success (Equation (3.22)).

$$P(F|Z_{PL,\uparrow}) = \frac{P(F \cap Z_{PL,\uparrow})}{P(Z_{PL,\uparrow})} \tag{3.22}$$

A graphical example is given in Figure 3.9. The top and right-hand side graphs show the PDF of the ultimate limit state and proof load limit state, respectively. As before in Figure 3.5 to Figure 3.8, the proof load mean is the 0.25 quantile of the resistance distribution. The red area in the joint PDF graph is defined by the realizations of the ultimate limit state function that are smaller than or equal to zero, and realizations of the proof load limit state function that are greater than zero. The part of the joint distribution reaching into the red-colored failure region determines the failure probability given proof load test information.

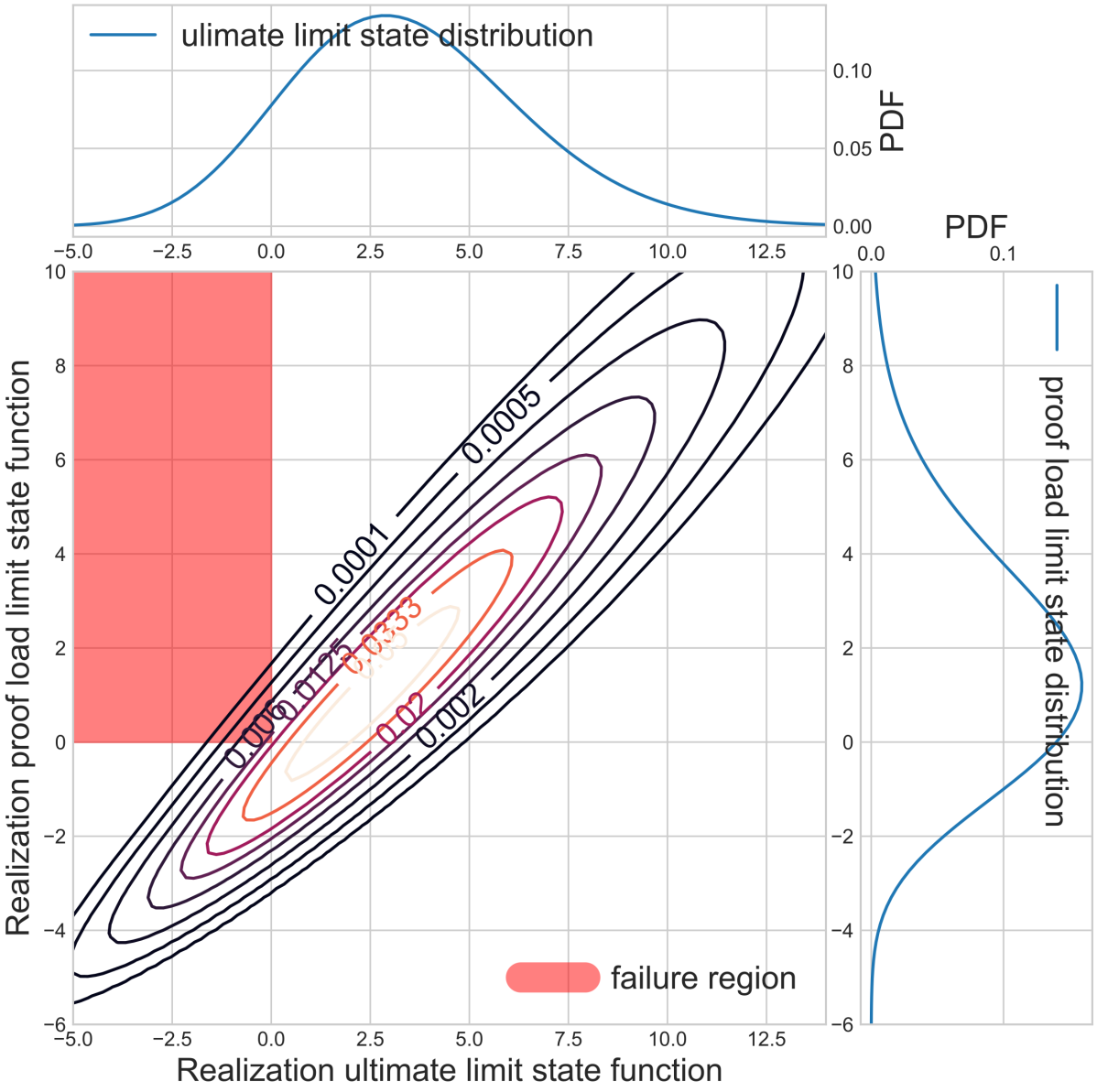

Figure 3.9: Joint distribution PDF of ultimate and proof load limit state. ULS distribution parameters match Figure 3.5 to Figure 3.8, proof load level quantile $= 0.25\,\mu(R)$

Figure 3.10 shows the effect of changing the proof load level. Two joint PDFs of ultimate limit state with two different proof load state functions are plotted. The upper contour lines visualize the joint PDF of the previously used ultimate limit state function and the proof load limit state function with a low test load of 0.001 quantile resistance. The overlap of high probability density areas of the PDF with the failure region is large. In the lower joint PDF, the proof load marginal distribution causes the mode of the joint PDF to move away from the failure region.

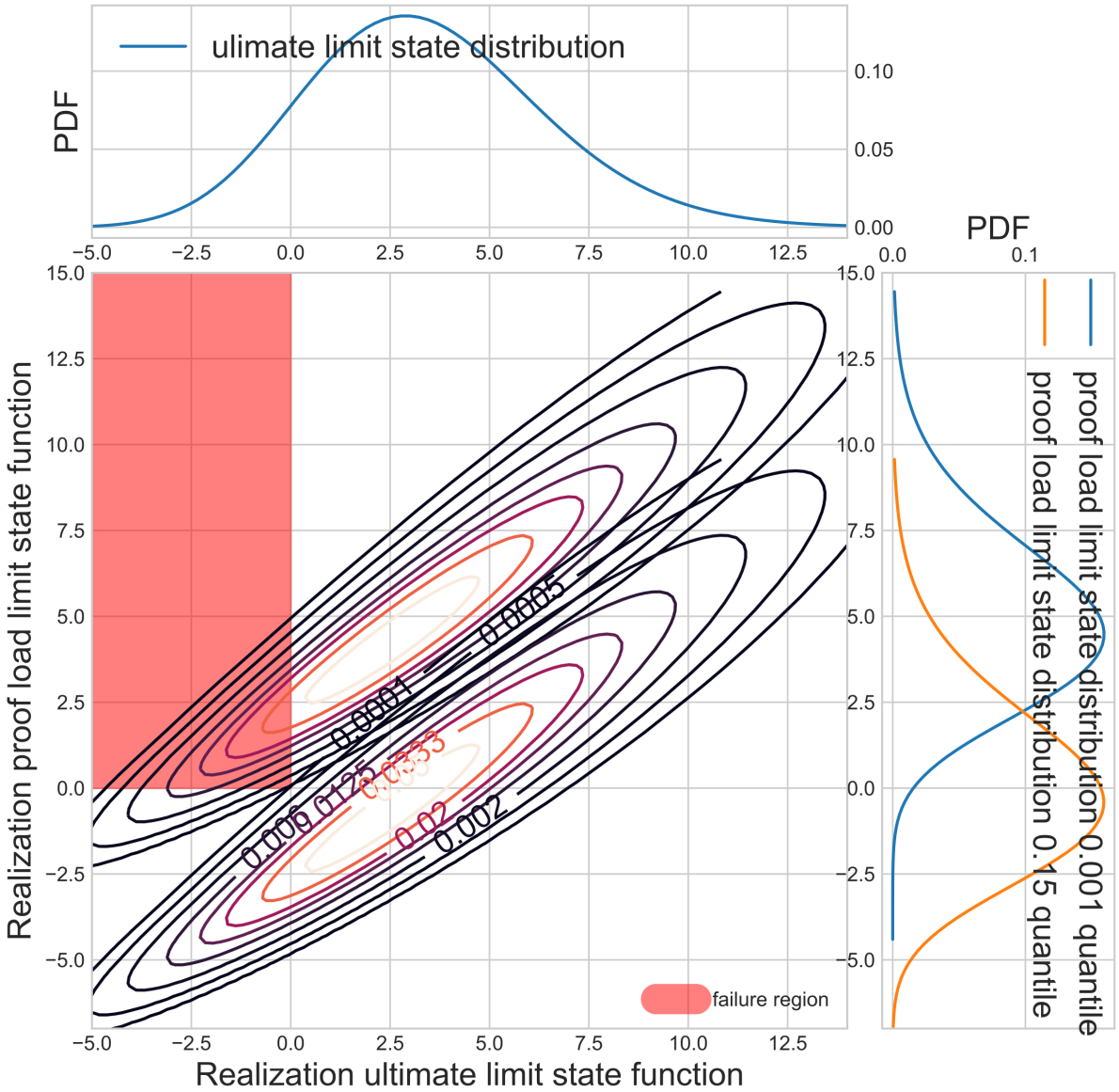

Figure 3.10: Example of proof load information inference with survival events for two different proof load levels

The four presented updating techniques listed above have different effects on the failure

probability estimate. Figure 3.11 compares the prior design probability of failure, which is 0.22 in this example, with the estimates compute for (1) the classical truncation distribution, Thöns' mixture distribution, Bayesian posterior distribution, and Bayesian updating with events. The curvature and distance between the four graphs depend on the distributions of proof load limit state and ultimate limit state. Regardless of the actual distributions involved, some features remain. Only the Bayesian posterior distribution $R''(\theta|x)$, can lead to an increase of the failure probability estate by proof load information. The classical truncation is always closed to method of Bayesian updating based on proof load survival events. Regarding the effect additional information gathered

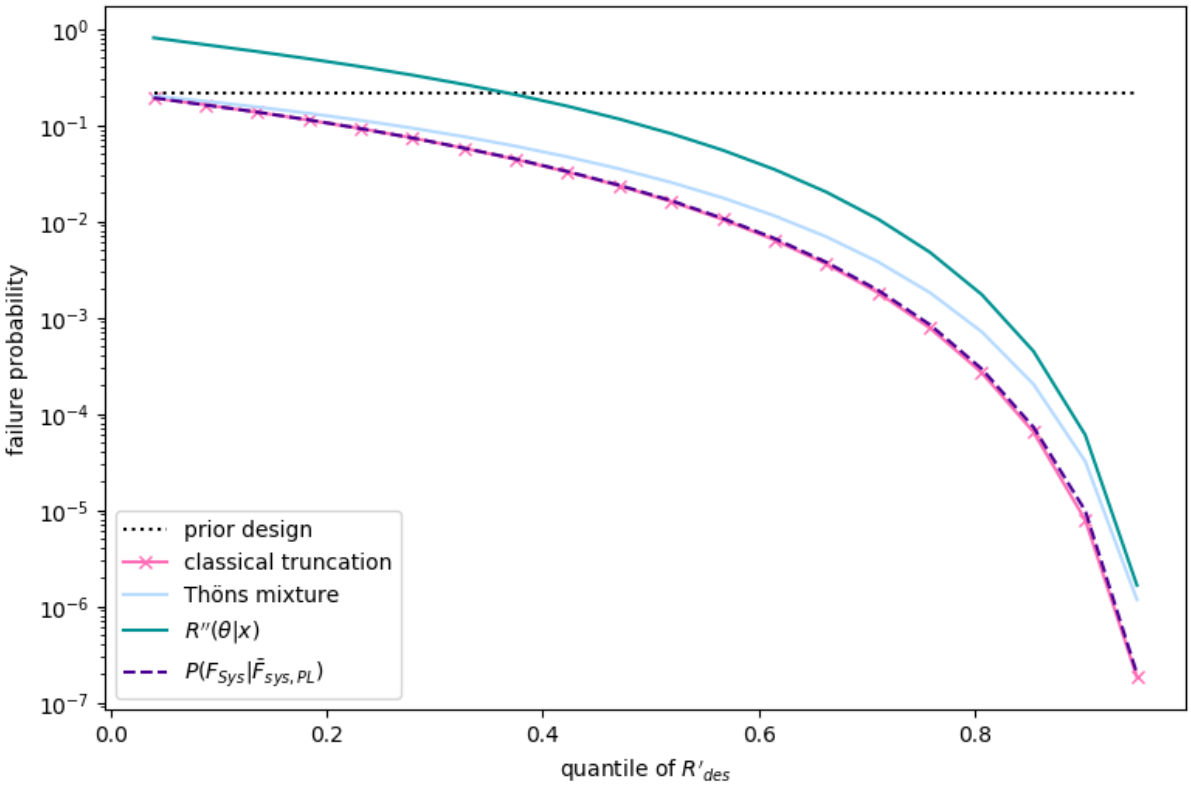

Figure 3.11: Effect of the four explained proof load information updating methods on failure probability

through an experiment has on the failure or damage probability estimation of structure, the type of structure is relevant twice. (1) the more ductile and redundant the structural components are, the lesser the impact of component damage or failure. (2) in the herein used system models based on logical systems, the internal redundancy is expressed through the intersection operator ($\cap$). This operator is present in the parallel system and the thereof derived Daniels systems, but not in the series system. Compare Equations (3.2) to (3.5). The series system, is defined with the union operator ($\cup$) instead of the intersection. The discrete Bayesian updating of Equation (3.22) applied to the parallel system does not influence the order of intersection operations. The commutative rule allows any order. With the union operation of the series system the distributive rule

has to be applied. If the series system is tested after assembly, the posterior failure probability computes as

$$P\left(F_{S,\overset{ser}{sys}}|Z_{PL,\uparrow}\right) = \frac{P\left(\bigcap\limits_{i\in Sys} F_{i,log} \cap \bigcap\limits_{i\in TC} Z_{PL,\uparrow,j}\right)}{P\left(\bigcap\limits_{j\in TC} Z_{PL,\uparrow,j}\right)} \tag{3.23}$$

Where i is the index of all load bearing system components Sys, and j is the index of all tested components TC. A three component system with two tested components is exemplified in Equation (3.24).

$$P\left(F_{S,\overset{ser}{sys}}|Z_{PL,\uparrow}\right) = \frac{P\left(F_1 \cap Z_{PL,\uparrow,1} \cap Z_{PL,\uparrow,2} \cup F_2 \cap Z_{PL,\uparrow,1} \cap Z_{PL,\uparrow,2} \cup F_3 \cap Z_{PL,\uparrow,1} \cap Z_{PL,\uparrow,2}\right)}{P\left(Z_{PL,\uparrow,1} \cap Z_{PL,\uparrow,2}\right)} \tag{3.24}$$

Testing components prior to assembly changes the calculation in the following way. The inference must exclude the interaction of the system components. Therefore, Equation (3.22) is applied component-wise and the resulting set is linked by a union operator.

$$P\left(F_{S,\overset{ser}{sys}}|Z_{PL,\uparrow}\right) = P\left(\bigcup_{i=1}^{3} F_i|Z_{PL,\uparrow,i}\right) = P\left(F_1|Z_{PL,\uparrow,1} \cup F_2|Z_{PL,\uparrow,2} \cup F_3\right) \tag{3.25}$$

CHAPTER 4

Consequence and utility modeling

Consequence and utility pertain to the economics of system throughout its life-cycle. This requires a model of all relevant costs of a system, and also an income model if it is supposed generate income. This chapter introduces the necessary economic fundamentals needed for the life-cycle analysis and demonstrates the analysis in an example based on economics of offshore wind turbines.

4.1 Interest rates and discounting

Decision making is greatly influenced by discounting. Life-cycle analyses of investments with a long life span like civil engineered structures, which also include costs for maintenance and decommission, are sensitive to discounting [JCS08]. Choosing a correct interest rate is difficult, especially for long investment periods ranging over several decades. An interest rate of 5% is often assumed in literature pertaining to engineering, although it is difficult to choose an appropriate interest rate. On the one hand, the interest in European interbank markets are currently negative [Eur17]. On the other hand, different regions have higher interest rates such as the USA [FOM17]. Interbank or national bank interest rates do not inform about the return over investment (RoI, Equation (4.4)) that a company may have achieved. For example, Andersen [And16a] claims a RoI of 6.9% from wind power without the distinction between on- and offshore. In order to establish the interest rate for discounting, each case has to be investigated individually and should be based on an interest rate that would be achieved if this considered investment was not undertaken. Establishing the discounting rate is a controversial topic as broadly presented by Donohue [Don99]. Rackwitz [Rac04] identifies the societal life quality index as a tool to derive an interest rate for public investments that takes also the value of life and health into consideration.

The discount rate r_d is used to calculate the current value CV of money earned in the future FV. The discount rate r_d in Equation (4.1) is usually defined on an annual basis.

$$r_d = (1 + i_{\%})^{-t} \tag{4.1}$$

$$CV = r_d \, FV \tag{4.2}$$

r_d is computed with the interest rate $i_{\%}$ and the time t, usually in years. Equations (4.1) and (4.2) are used for discounting in discrete steps. With Equation (4.3) one can discount the future value FV continuously.

$$CV = e^{-i_{\%} t} \, FV \tag{4.3}$$

€ 100 a person receives in a year from now has a value of € 95.24 today assuming, an interest of 5% was earned on the € 95.24. The dependence of the discount rate on the interest rate is visualized in Figure 4.1.

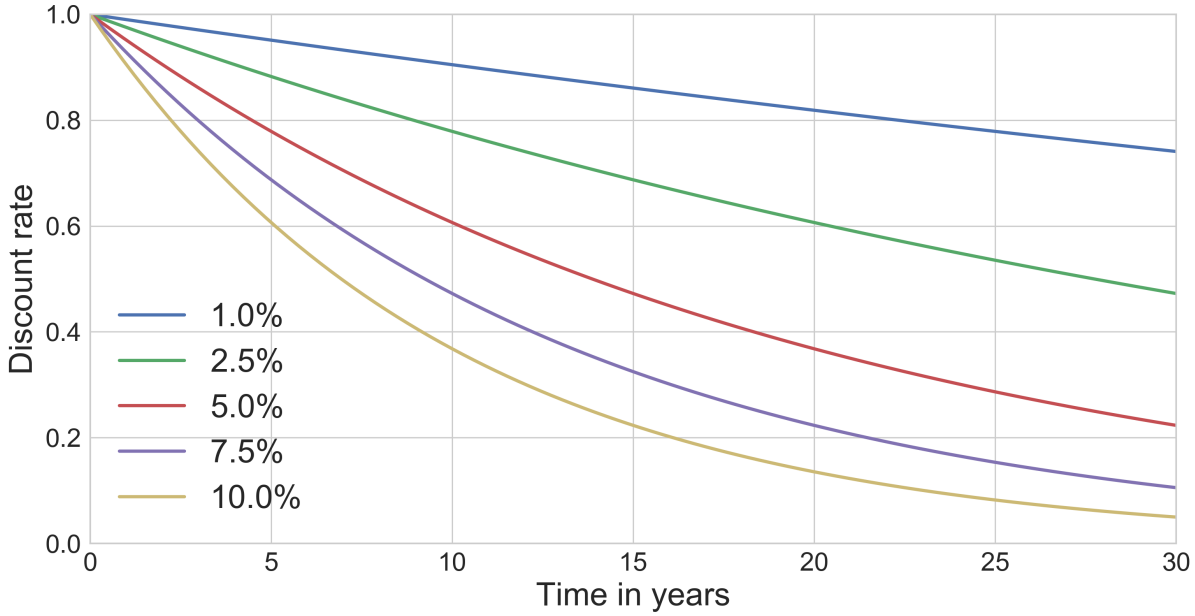

Figure 4.1: Development of discount rate over time in dependence of interest rate

4.2 Examples of cost and benefit analyses for offshore wind turbines

This section contains examples of cost / benefit analyses based in the economics of offshore wind energy turbines. Two particular examples are given based on the Danish tender model and on the German model with fixed subsidized feed in fees. The Danish tender model has been or will be adapted in a similar fashion by other countries.

Cost and benefit analysis is a prognosis method and as such it cannot forecast the result precisely. In order to achieve a rigorous and refined prognosis the input values have to be chosen carefully. Especially in a dynamic field like offshore wind energy, advances

in technology and the volatile energy market can change figures quickly. The financial support schemes are also adjusted regularly to these developments.

4.2.1 Tenders / subsidy models

Danish tendering model

The current Danish offshore wind energy subsidy model [Hed16; Nie16] is guaranteeing the feed-in tariff as tendered by the successful bidder for 50000 full load production hours. With the capacity factor from Voormolen et al. [VJS16] and availability from Ho et al. [HMC16] and Voormolen et al. [VJS16] this would correspond to the first 12.68 years of production. After the energy equivalent of 50000 full load hours has been produced, the spot markets determine the tariff.

Old German fixed subsidy model

The renewable energy act from 2014 was in place until 2017, when it was modified to a similar tender scheme as in Denmark. The pre 2017 support scheme comprises two subsidy periods as detailed by the German Federal Ministry of Economics and Technology [BMW16]. The current German system is, like the Danish system, tender based. Considering wind farms in operation until the end of 2017 the first period guarantees a high subsidy of 0.154 € / kWh for 12 years or a shorter scheme with 0.194 € / kWh over 8 years. Following the first phase a second phase follows with a subsidy of 0.039 € / kWH until year 20. The initial subsidy can be extended depending on water depth and distance to shore.

4.2.2 Cost and benefit model

The figures used in the examples are taken from Voormolen et al. [VJS16] regarding capital expenditures (CAPEX) per MW and the capacity factor. Ho et al. [HMC16] and Voormolen et al. [VJS16] provide estimates of current and near future turbine capacities. Operation costs are estimated by Barthelmie and Pryor [BP01] and Hau [Hau13]. Faulstich et al. [FHT11] determine the availability of offshore wind turbines. In the subsidy phase the feed-in tariffs are modeled as detailed in Section 4.2.1. Electricity spot market prices can be used to estimate feed-in tariffs after the subsidies phased out. The current feed-in tariffs may be derived from spot market prices available from energy exchanges e.g. European Energy Exchange [EEX16]. The findings are summarized in Table 4.1, where the three different spot market prices reflect a scenario of lower energy prices, median prices, and 0.75 quantile price from 1.1.2002 until August 2016 in current monetary value discounted with 5% interest.

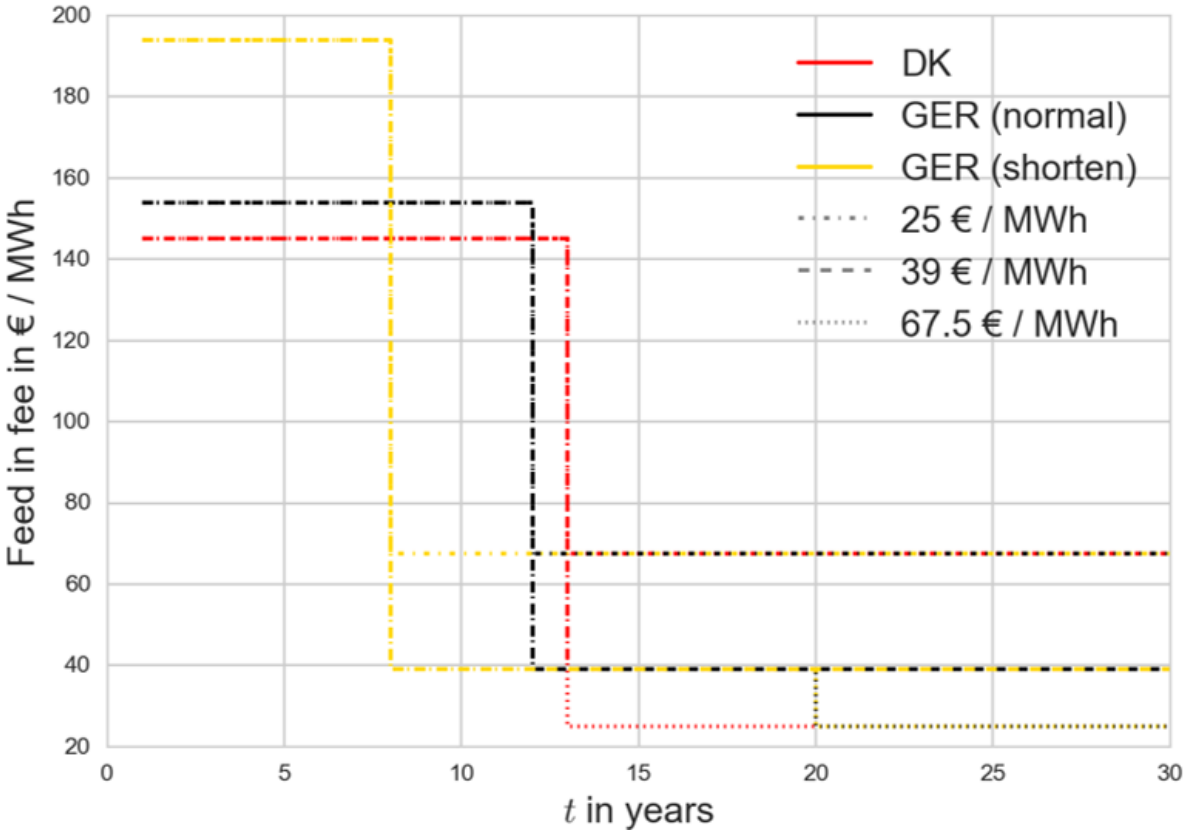

Figure 4.2: Example of feed-in tariffs

4.2.3 Example calculation

$$\text{RoI} = \frac{\text{Income}}{\text{Investment}} \tag{4.4}$$

The example cost and benefit analyses for the Danish and German subsidy models in Table C.1 to Table C.3 in Appendix C are based on the values in Table 4.1 and the respective feed-in tariffs from Section 4.2.1. In the case of the Danish example, the return over investment results in 1.134 or 1.146 after 20 or 30 years of operation, respectively. With the higher and longer subsidies applied to the German model, a RoI of 1.198 or 1.21 is achieved after the same respective operation periods. The small increase in RoI with additional 5 years of operation is due to the currently low energy prices influencing the electricity spot markets.

RoI	Denmark			Germany (pre 2017 model)		
Tariff € / MWh	25.0	39.0	67.5	25.0	39.0	67.5
20 years	1.1341	1.1754	1.2595	1.1980	1.1980	1.2967
30 years	1.1458	1.3902	1.3902	1.2098	1.2490	1.4273

Table 4.1: Return of Investment (RoI) for different schemes and market prices

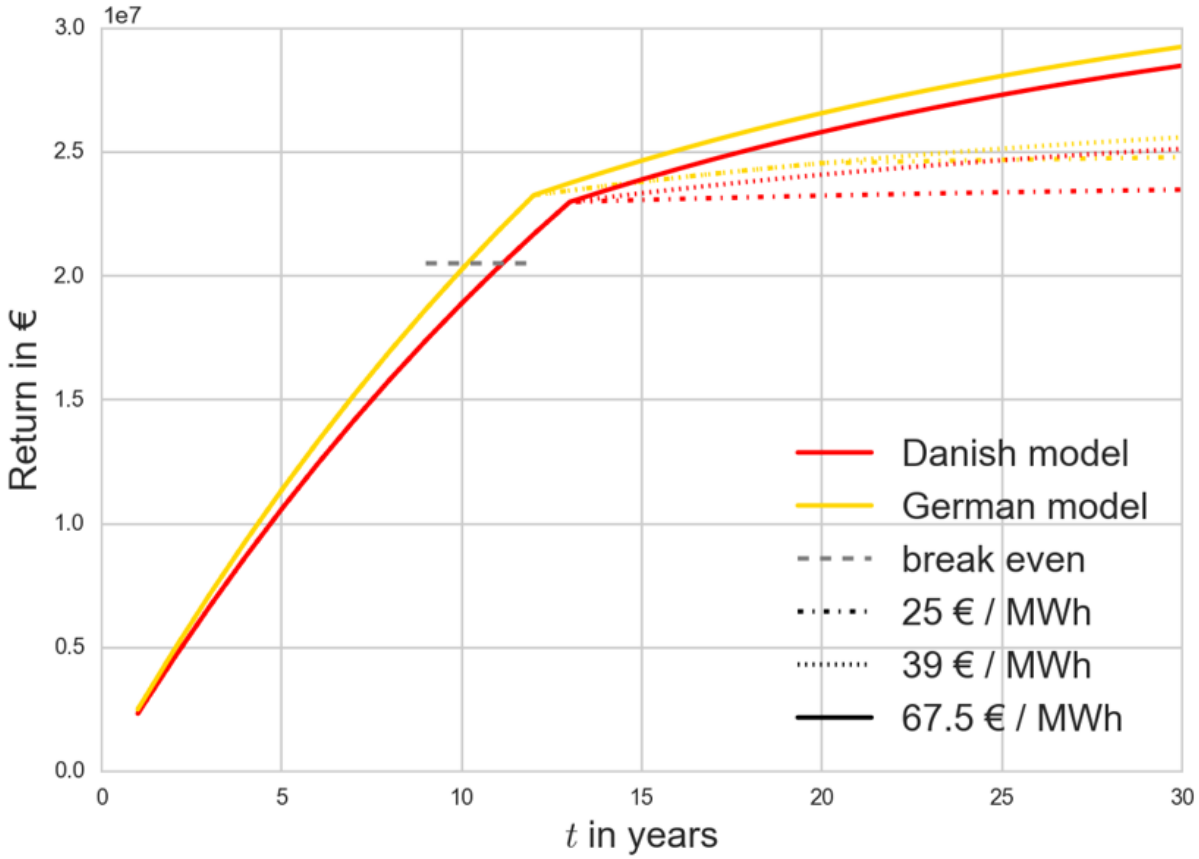

Figure 4.3: Development of profits. The kinks are due to changes in the subsidy schemes see Figure 4.1. Break even marks the time in which the investments have amortized

4.3 Utility

In the given example of offshore wind energy converters, the utility is defined by the expected lifetime benefit B that is generated by the energy sold. B considers through the described cost and benefit model the costs of investments required to generate an income in the first place. By multiplying the benefit of each year with the probability to generate it, we get an expected benefit that can be objectively compared to expected benefits generated under different conditions. In the example case, it is preferable to maximize the expected benefit B, which could also be expressed as the return over investment (RoI). However, if the utility was a cost, the optimum utility would be the minimal costs.

4.4 Other structures

A cost and benefit model for other structures, e.g. bridges or levees, can follow the general path laid out in the example for offshore wind turbines. Because the service provided by bridges or levees is very different from the electricity generation of wind turbines the model needs adjustments. Calculation of utilities may be more difficult because the indirect consequences can vary greatly and affect a larger variety of societal, economical, personal, and environmental entities through interdependencies.

CHAPTER 5

Value of information in structural health monitoring and proof load testing

5.1 Basis of value of information for SHM and proof load testing

The theory of the value of information (VoI) is part of the Bayesian decision theory developed by Raiffa and Schlaifer [RS64]. In order to obtain the VoI in the context of civil engineered structures the conditional value of sample information (CVSI) or the expected value of sample information (EVSI) must be determined. The CVSI is calculated conditionally on the state of nature when the experiment was conducted. It is the difference between expected posterior utility and the expected prior utility; thus the determination of the CVSI requires prior knowledge (no experiment) and posterior knowledge (experiment conducted). The EVSI considers experimental results before they have been obtained; it is based on the pre-posterior decision concept. In the context of proof load testing or structural health monitoring (SHM), the prior information may be retrieved from the structural design and the pre-posterior information may be obtained through modeling the experiment results probabilistically or through Bayesian updating assuming monitoring data.

An comprehensive introduction to the quantification of the value of SHM in the normal and extensive form analysis is given by Thöns [Thö18]. An explanation of the concept of VoI follows here according to Honfi and Lange, Straub, Thöns et al. [HL15; Str14; TSF15], where the value of SHM or proof load testing V_I is quantified as the difference between life-cycle benefit, B_{post}, as determined by pre-posterior decision analysis and life- cycle benefit, B_{prior}, according to a scenario without SHM utilization or proof load testing based on prior models.

$$V_I = B_{post} - B_{prior} \tag{5.1}$$

The optimal prior utility B_{prior} has to be chosen by Equation (5.2) through maximization

of the prior utilities $\vec{b}_{prior}$ depending on each of the states $\vec{X}$ and the action alternatives $\vec{a}$.

$$B_{prior} = \max_{\vec{a}} E_{\vec{X}} \left[\vec{b}_{prior}(\vec{X}, \vec{a}) \right] \tag{5.2}$$

The posterior benefit B_{post} depends on the outcome of the pre-posterior decision analysis, which depends on the choice of SHM system or proof loading parameters, structural performance, and the impact of undertaken actions, e.g. corrective measures. A proof load test influences the results by the structural relevance of the test component(s), the load, and consequently by the probability of damaging or destroying the structure. The accompanying SHM system influences the result by its capabilities (sensitivity, accuracy, monitored features) and cost. In order to choose the highest utility, the vector $\vec{b}_{post}$ must be maximized with respect to $\vec{a}$ and additionally to the choice of experiments $\vec{p}$. $\vec{Z}$ stands for the experiment outcomes.

$$V_I = \max_{\vec{p},\vec{a}} E_{\vec{Z},\vec{X}} \left[\vec{b}_{post}(\vec{Z}, \vec{X}, \vec{p}, \vec{a}) \right] - \max_{\vec{a}} E_{\vec{X}} \left[\vec{b}_{prior}(\vec{X}, \vec{a}) \right] \tag{5.3}$$

The above described VoI derivation is given in greater detail by Faber and Thöns [FT13] or Thöns et al. [TSF15]. Some examples of VoI analyses are given in Faber and Thöns, Straub, Thöns et al. [FT13; Str14; TSF15]. The value of proof load and SHM information may thus relate to increasing benefits or decreasing costs or in a wider context to increasing human safety.

The value of information V_I considers only identical action alternatives $\vec{a}$ in the prior and (pre-) posterior analysis. With new information, new action alternatives could arise that should be considered in the decision analysis. The new actions are denote $\vec{a}(I\&A)$ in Equation (5.4). This simple extension creates an expected value of information and action analysis (EVSIA).

$$V_{I\&A} = \max_{\vec{p},\vec{a}^{I\&A}} E_{\vec{Z},\vec{X}} \left[\vec{b}_{post}(\vec{Z}, \vec{X}, \vec{p}, \vec{a}^{I\&A}) \right] - \max_{\vec{a}} E_{\vec{X}} \left[\vec{b}_{prior}(\vec{X}, \vec{a}) \right] \tag{5.4}$$

Thöns [Thö18] concludes that the extensive form of the VoI analysis should be used in order to identify the optimal decision parameters because every branch of the decision tree is evaluated. The extensive form may thereafter be used to identify decision rules that cut decision branches that will not lead to optimality. Agusta et al. [ATL17] demonstrate the use of the extensive form in order to formulate decision rules that accelerate the decision analysis and only cut-off non-optimal decision options.

5.2 Potential application areas

The value of information gained through the tests may be achieved in different fields in the operation of structures, but also in the design of new structures and can relate to economic benefits and safety [FT13]. VoI is defined as a utility gain, in engineering fields this usually expressed as an increase of economic benefit. As such, VoI provides a

quantifiable basis for decision-making. The scope of VoI in an economical context can be extended to life and environmental safety through the concepts of life saving costs and life quality index [Rac04]. Economical aspects are found in construction cost reduction, operation and maintenance (O&M) costs reduction, productivity increases (potentially in connection with lifetime extension), and improved efficiency in decommissioning. The risk or safety for life and limb may also be influenced by VoI and are usage and location dependent. JCSS [JCS99] and Eurocode 0 [Eur02] distinguish different use and consequence classes; these classes may very well influence the VoI. The environmental impact may be reduced with the help of SHM, proof load testing, and VoI by reducing consumption for construction (see Chapter 8), operation [CAF16], and decommissioning through an extended service-life.

5.2.1 Operation optimization of structures and portfolios of structures

The operation of structures may be optimized by proof load test and SHM system information about a structure or many structures. The gained knowledge about the prototype structure may provide basis to adapt and improve operational, maintenance and inspections activities during the life-time of the structure [FT13]. Moreover, proof load testing and SHM systems information may provide help for the following generic scenarios during the operation of structures.

- Service life extension:
  For highly utilized structures approaching the end of their service life, an extension of the service life is often desired. Here, posterior information provides a means and help for the condition assessment and condition prognosis, which form the basis for the optimization for ensuring the structural integrity beyond the service life. Proof load testing as a testing method is especially informative in this regard. Proof load testing is the only method that provides a direct measurement of the load carrying capacity of the tested structure. Other SHM or inspection techniques can provide information about accumulated damage and life-loads for the estimation of structural performance in the extension period.

- Utilization modification:
  The utilization of structures may change throughout the service life, especially for infrastructures. Examples are bridges, which sustain a steadily increasing traffic amount, increased load rating, transformation of a gas to a liquid pipe-lines or vice versa, and the re-powering of wind energy turbines. Here, data about the past utilization of the structure, the actual condition and, if required, about the actual performance may provide some benefit for the structural integrity management. Proof load testing is a suitable tool to assess the current load bearing capacity of the structure. For a usage modification of pipelines proof load tests are often mandated in the form of hydro-static tests.

- Damage progression monitoring:
  In case that damage has been identified already, monitoring systems may identify eventual trends (i.e. opening of cracks) to monitor eventual increased accelerated deterioration. From one or few monitored locations, the damage progression at other locations maybe inferred. As progression-monitoring requires an almost permanent observation of damage (size) indicators, proof load testing is very limited in its application to this task. However, proof loading may be of help in order to estimate limit states of the damage size indicators.

- Retrofitting SHM to historical buildings:
  Monitoring and potentially proof testing historical buildings can provide information in order to help protect architectural heritage. De Stefano and Clemente [DC05] provide examples how SHM for can help to protect cultural heritage buildings. The uncertainties associated with heritage buildings are usually largely due to a lack of construction guidelines similar to today's codes. Information gathered through SHM can be used in models in order to assess the structural capacity of the historic buildings. However, one may ask whether this strategy is to be chosen over a structural retrofitting in order to increase the robustness of the building. VoI may help to identify the optimal strategy.

5.2.2 Code making and code calibration

Code making and code calibration for structure types may benefit from SHM when it is conducted systematically. The acquired information can be used to adapt the design basis in order to spare material and monetary resources while controlling safety, risk, and reliability at the desired level. This could be achieved by SHM if the model uncertainties in the design code equations are reduced by measuring the relevant magnitudes in the operational structure [FT13].

5.2.3 Early damage warning

Monitoring may indicate abnormal performance or possible damage of a structure and thus aid as indicators for remedial actions [FT13]. The indications may be derived from indicators that directly provide information about the damage state, such as e.g. flooded member detection. In this application of SHM, the value of monitoring would relate to the possibility of loss reduction by shutting down the function or reducing the loading of the structure, before human life, the structure and the environment are lost and / or damaged further. Embedded in a maintenance scheme, synergies with the structural integrity management and operation (see point (1)) can be realized. Proof load testing is not relevant for early damage warning, because permanent or at least frequent observations are required. Also, the interference with operations should be minimal. However, in case of a damage warning the alarm has to be verified. This can

either be done with inspections if suspected damage can be confirmed or falsified this way, or with a proof load test if this is appropriate.

5.2.4 Structure prototype development / design by testing

The production of larger quantities of identical structures can benefit from optimization processes supported by proof load testing or SHM. A prototype may be proof load tested or equipped with SHM systems in order to attain an optimized structural design before mass production. The proof load and SHM data may contain information to reduce uncertainties considered in the design model. Prediction of the response and performance of the prototype and mass-produced structure may become more accurate with the use of such test data. The optimized design may thus lead to an increased life-cycle benefit of the structure [FT13]. Chapter 8 demonstrates how proof load testing of components or entire structures can be utilized to improve the design.

5.2.5 SHM systems prototype development

Similar to the benefit designing structures can draw from SHM, new SHM systems may be designed and optimized using VoI concepts [FT10; HT12], The optimization parameters may be the SHM strategy including the instrumentation as well as the number and placement of sensors. With the concept of pre-construction proof loading by Brüske and Thöns [BT17] in a factory or laboratory, proof load testing may provide information that can serve as accurate prior knowledge for other SHM systems.

5.3 New research fields pertaining structural testing

5.3.1 Proof load test information for the resilience of structural systems and networks thereof

Once the recovery phase concluded after a damage event, the capacity of the structure can be established by proof load testing. With an identified resilience level (under to over resilience) the societal preparedness level described by Faber et al. [FQM17] can be optimized.

Failure of structure in network might not require replacement if one can demonstrate with proof load testing that remaining network elements can provide the destroyed ca-

pacity. The application of SHM and its provided value of information as tool to analyze and support resilience is discussed by Miraglia et al. [Mir+17] and Faber et al. [FQM17].

5.3.2 SHM information for the resilience of structural systems

In the case of a structural system disruption, SHM systems may provide valuable information to mitigate any consequences and thus support resilience by speeding up recovery. Honfi and Lange [HL15] explain how SHM and implicitly VoI may support major aspects of resilience. Proof load testing poses difficult to quantify risk to a damaged structure, therefore it seems here only relevant as a tool to obtain a reference value for the damaged structure.

An application to resilience of networks by rerouting demand based on SHM information may be very difficult. SHM cannot provide direct information about the capacity of a system unlike proof load testing. However, a capacity assessment similar to the proof load test scenario described in the previous section maybe achievable by gradually increasing the service load beyond the limits specified by design. Because this would be in an operational state the resulting risk have to be analyzed thoroughly including consequences that may be excluded during a proof load tests.

5.3.3 Seismic safety

An entire structure cannot be subjected to earthquake test loads in order to obtain proof loading information about the resistance to high amplitude ground motions. Nonetheless, critical components can be tested outside of the structure, which in turn can facilitate a better design of SHM system or structural retrofitting.

5.3.4 Structural retrofitting vs. installing SHM systems

Retrofitting vs. SHM is discussed by e.g. Pozzi and Der Kiureghian [PD12] using a bridge in an earthquake hazard region as example. The decision problem is here addressed by utilizing VoI. The issues is to weigh the value of gaining new information vs. the value of direct structural improvement. The information may also be collected though experiments like proof load testing. A concept of expected value of sample information and additional action analysis (EVSIA) may be useful to address this issue, see Chapter 8. It would allow to the analysis of the value of testing in combination with structural retrofitting.

5.3.5 Sustainability

Martinez-Luengo [MKW16] claim that SHM can improve the sustainability of off-shore wind turbines. Different aspect of this have been demonstrated by e.g. Agusta et al. or Thöns [ATL17; TSF15]. These studies focus on safety and economic aspects, which do not cover all elements that should be considered in life-cycle analysis (LCA) aiming to optimize with respect to sustainability.

Proof load test information may also contribute to a sustainable life-cycle. An idea for such a life-cycle optimization through proof load information could be based on Chapter 8. The pre-construction proof load information therein is used to assess weaker and cheaper designs. This analyze could be extended to a comprehensive LCA by including all relevant element of the production chain.

5.4 Challenges in quantifying the value of information

Whether or not the VoI is positive for a specific application or application fields has to be consistently and systematically quantified. So far, a few cases have been considered relating to e.g. fatigue monitoring of offshore wind turbines [TSF15; TF13], to ice accretion monitoring for cable stayed bridges [RGF15], to bridge monitoring [PD12], proof load testing [BT17], or to sensor placement [MP16].

The VoI is not gained by obtaining the information, but by using the information for actions and to plan actions in well-defined decision scenarios. Therefore, the benefits of using SHM systems must be identified, and the information obtained must be understood and effectively utilized for decision support (see also [BH08]). Beyond these fundamental and necessary conditions theory and practice are challenged with various issues. Faber et al. and Straub [FVT15; Str14] summarize many of the major challenges as:

- Computational effort.
- Assessment and modelling of SHM triggered actions.
- Probabilistic models relating to the overall system model, especially the monitoring and monitoring process model.
- Understanding of the decision process in the context of SHM in order to find a good representation of this process and suitable approximations.

CHAPTER 6

Value of information by updating of model uncertainties utilizing proof loading in the context of series and Daniels systems

Brüske, H. & Thöns, S. Value of information by updating of model uncertainties utilizing proof loading in the context of series and Daniels systems. *Proceedings of the International RILEM Conference Materials, Systems and Structures in Civil Engineering* 52–61 (2016).

Abstract

In this paper, an approach is presented for the determination of the value of information (VoI) in relation to models, which can represent structural systems such as e.g. towers, cables, jackets. Stochastic capacities and loads are assumed for the models studied herein. The VoI is obtained with a prior and a pre-posterior decision analysis. The prior decision analysis takes basis in the design phase of the structural system. Pre-posterior decision analysis builds upon modeling results of not yet conducted experiments. In order to perform the prior and pre-posterior Bayesian decision analysis, the expected life-cycle benefit of the considered systems are computed. The difference in the expected benefits relating to the prior and pre-posterior decision analysis leads to the VoI. The system models are probabilistically computed using the Monte Carlo / Importance sampling simulations to estimate their probability of failure. Next to the intrinsic uncertainties in loads and capacities further uncertainties accounting for the model uncertainties are included in the simulations. As an SHM strategy, proof loading is considered and modeled

as a process accompanying the construction. The costs of proof loading and probable component failures are considered explicitly. The analyses results point to high value of information for component proof loading in systems with a low reliability.

6.1 Introduction

It is currently often unclear whether experiments, e.g. proof load testing that provide data on the structural performance are beneficial. A method in order to assess this benefit is the Bayesian decision theory. The decision analysis is based on system models (Section 6.2). The discussed series system could represent a monopile and the Daniels system a jacket substructure. The system models and measurements incorporate model and measurement uncertainties, respectively. In Section 6.3 the model updating is explained and a short outline of the Bayesian decision theory is given. Section 6.4 presents the modeling results taking basis in the economics of offshore wind turbines. The paper is concluded and summarized in Section 6.5.

6.2 System models

Various typical structural systems can be represented by generic models. A series system can represent e.g. a tower or single fiber cable consisting of several components. A Daniels system can present e.g. cables, tendons with several fibers or jackets and other truss structures. The failure of the discussed systems is described by the limit state function (Equation (6.1)).

$$R\,M_R - S\,M_S \leq 0 \tag{6.1}$$

with the resistance force R, and the load S. The model uncertainties for R and S are represented by M_R and M_S respectively. All four random variables are sampled as described in Table 6.1. The limit state function in Equation (35) is used in order to determine the failure probabilities of the systems described in Section 6.2.1 and Section 6.2.2.

6.2.1 Series system

A series system fails if any of its n components fail. Equation (6.2) follows the definition in Rackwitz [Rac97]. The weakest component determines the capacity of the whole series system.

$$P_F = P\left(\bigcup_{i=1}^{n} F_i\right) \text{ with } F_i = \{R_i\,M_{R_i} \leq S\,M_S\} \tag{6.2}$$

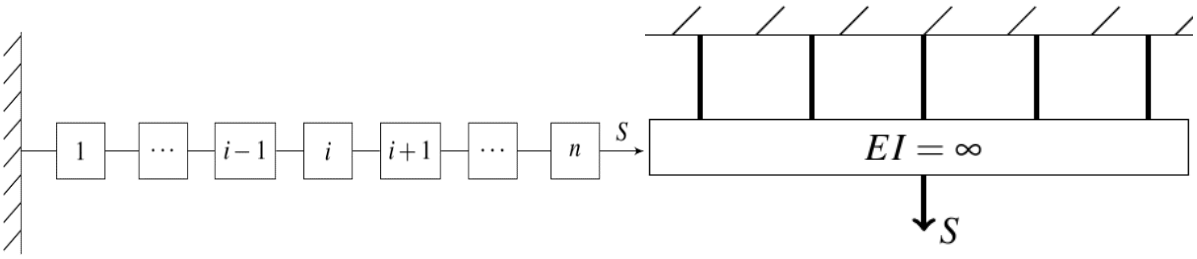

(a) Series system

(b) Daniels system with infinitively stiff bar for the instantaneous load redistribution

Figure 6.1: Schematics of used system models

6.2.2 Daniels system

The so-called Daniels system was first introduced by Daniel [Dan45], Figure 6.1b. It is a parallel system with special properties that make it meaningful in terms of mechanic systems. As described by Gollwitzer and Rackwitz, Rackwitz [GR90; Rac97] all components experience the same load, $S_i = S_{tot}/n$, which is the n^{th} fraction of the total load, S_{tot}. If the load exceeds the system's load bearing capacity the weakest component breaks first and the load is equally redistributed among the remaining intact components. The entire system fails when the remaining intact components cannot jointly carry the additional load fraction that was sustained by the last component that broke.

In the presented Daniels systems, it is distinguished whether all their components behave perfectly brittle or perfectly ductile. A structural component is called perfectly brittle if it loses its bearing capability completely at failure. A perfectly ductile component maintains its load level after failure.

The probability of failure of a perfectly ductile Daniels system is given by Equation (6.3).

$$P_F = P\left(\sum_{i=1}^{n} R_i\, M_{R_i} - S\, M_S \leq 0\right) \tag{6.3}$$

For a perfectly brittle Daniels system the failure probability is determined by Equation (6.4)

$$P_F = P\left(\bigcap_{i=1}^{n}\{(n-i+1)R_i\, M_{R_i} - S\, M_S \leq 0\}\right) \tag{6.4}$$

Where the realizations of $R_i M_{R_i}$ are ordered according to $\hat{R}_1\, \hat{M}_{R_1} \leq \ldots \leq \hat{R}_i\, \hat{M}_{R_i} \leq \hat{R}_{i+1}\, \hat{M}_{R_{i+1}} \leq \ldots \leq \hat{R}_n$
$, hat M_{R_n}$.

6.2.3 Probabilistic model simulation

The applied model parameters are described in Table 6.1. In case of the prior model the variables R_i and S are substituted by $R'_{\text{des},i}$ and S'_{des}, respectively. In the pre-posterior model R_i is substituted by the variable R''_{mix} that follows the distribution explained in Section 3.4

Model parameter	Distribution type	Mean (μ)	Standard dev. (σ)
R_i Resistance	To be substituted by either prior ($R'_{\text{des},i}$) or pre-posterior (proof loading) uncertainties. See Section 6.3.3.		
$R'_{\text{des},i}$ Design resistance	Lognormal	13.4196	1
S'_{des} Design load	Weibull	10	$\sqrt{2}$
R''_{mix} updated resistance	Mixture	Depend on distribution definition	
M_R uncertainty of R	Lognormal	1.15	0.15 mean(M_R)
M_S uncertainty of S	Lognormal	1.0	0.05 mean(M_S)

Table 6.1: Parameters of the structural probabilistic model

6.2.4 Single component reliability

This study is based on a target component reliability of $\beta_t = 2$. This is achieved by pre-defining the mean and the variance of the load, S, as well as the variance of the component strength, Var(R_i). The mean of R_i is calibrated iteratively so it matches β_t. $\beta = 2$ is approximately equal to a probability of failure = 0.02275 [Cor67].

6.2.5 Correlation

Correlation between the random variables has a strong influence on the system reliability. The random variables of the resistance R_i, are correlated in a range from 0 to 1 in the system models. This is achieved by applying a normal copula, which uses the Spearman rank as input correlation. According to Moan [Moa94] the ultimate strength of tubular joints in jacket structures are correlated in a range from 0.2 to 0.9. The wide spread maybe due to varying joint dimensions and welding craftsmanship. As the components are represented by the same models it seems reasonable to assume a correlation between their model uncertainties M_R in the discussed systems fully ($\rho_{M_R} = 1$) as well as uncorrelated ($\rho_{M_R} = 0$) model uncertainties are simulated in order to compute upper and lower bounds.

6.3 Value of information in proof load testing

6.3.1 Decision theory

The theory of the value of information is part of the Bayesian decision theory developed by Raiffa and Schlaiffa [RS64]. In order to obtain the VoI in the context of civil engineered structures with pre-posterior information, the expected value of sample information (EVSI) is to be determined. The EVSI considers experimental results before they have been obtained. In the context of proof load testing, the prior information may be retrieved from the structural design and the pre-posterior information may be obtained through modeling the proof load testing results probabilistically.

A brief explanation of the concept of VoI follows here according to Faber and Thöns, Straub, Thöns et al. [FT13; Str14; TSF15] where the value of Information V is quantified as the difference between life-cycle benefit B_{post}, as determined by pre-posterior decision analysis and life-cycle benefit B_{prior}, according to a scenario without proof load utilization based on prior models, see Equation (6.5).

$$V = B_{post} - B_{prior} \tag{6.5}$$

The life-cycle benefit B_{post}, depends on the outcome of the pre-posterior decision analysis which depends on the choice of the proof load test, structural performance and the impact of undertaken corrective measures. The proof load test influences the result by its capabilities, i.e. load type and its distribution, and cost. In order to choose the highest utility $B_{post} = E_X[B(X, s)]$, expressed as the expected value of benefits must be maximized accounting for the decision alternative s, see Equation (6.6).

$$V = \max_s E_X[\vec{b}_{post}(X, s)] - B_{prior} \tag{6.6}$$

The above described VoI derivation is given in greater detail by Faber and Thöns [FT13] or Thöns et al. [TSF15]. Some examples of VoI analyses are given by Benjamin and Cornell [BC14]. The value of proof load information may thus relate to increasing benefits or decreasing costs, or in a wider context, to increasing human safety.

6.3.2 Prior and pre-posterior knowledge

The prior model incorporates the design model uncertainties, M_S and M_R, of the load and resistance respectively. The prior model uncertainties are defined as suggested by JCSS [JCS02] in Table 6.1. In order to obtain pre-posterior knowledge proof load testing is applied to each component separately which updates the structural resistance R. Relevant for obtaining the updated knowledge is the proof loading distribution with its parameters listed in Table 6.2.

Uncertain parameter	Distribution type	Mean (μ)	Coefficient of variation
S_{PL} proof load	Normal	0.85 mean(R'_{des})	0.01

Table 6.2: Parameters of the proof load distribution

6.3.3 Updating by proof loading

Proof loading for reliability updating has been considered already in 1984 [LN84], by applying a load to a structure its capacity can be tested and the resistance distribution be updated. Thöns et al. [TFR11] suggest to update the resistance distribution by combining the proof load and resistance distribution to a posterior mixture distribution R''_{mix}, which will substitute R'_{des} in the reliability analysis, represented in Equation (6.7). R''_{mix} consists of two truncated distributions, first it follows the proof load distribution R'_{proof}, up to a threshold l, and beyond l it follows the design resistance R'_{des}. l is chosen such that it is at the intersection point of the PDFs of S_{PL} and R'_{des} on their increasing flanks. The updating is solely based on survival information, as failed components will not be used for construction.

$$R''_{\text{mix}} = \begin{cases} S_{PL}, \text{for } x \leq l \\ R'_{\text{des}}, \text{for } l < x \end{cases} \tag{6.7}$$

With the chosen distribution parameters the proof load had to be rather high in order to obtain numerically significantly different results. 85% of the mean(R'_{des}) was chosen. With increasing uncertainty in the prior distribution of the resistance model the required proof load becomes smaller in order to achieve significant differences. Such a high proof load is probably best realized by testing single components. The here-in presented models assume that each component is updated separately. The probability of failure during the proof load test estimates to approximately 0.0421. PDFs of the involved distributions are shown in Figure 6.2.

6.3.4 Computation of the value of information

In order to estimate the benefit of the presented models, assumption are made based on Voormolen et al. [VJS16] for offshore wind turbines. Capital expenditures are assumed to be 3.0 M€ / MW. The proof load tested system contributes 600 k€ / MW to the capital expenditures. The income per MWh is 45 €, and the capacity factor 50%, over a service-life of $t = 1, \ldots, 20$ years and is discounted with the rate $r_d = (1 + 0.025)^{-t}$. The component cost is assumed to be anti-proportional with the amount of components in the system. Expenses for operation & maintenance are not considered. Direct consequences arise from component failure during proof load testing, indirect consequences defined by the capital expenditures and the system failure probability. The costs for proof loading are assumed to be 1% of the system costs. On the bases of work by Moan [Moa94] the

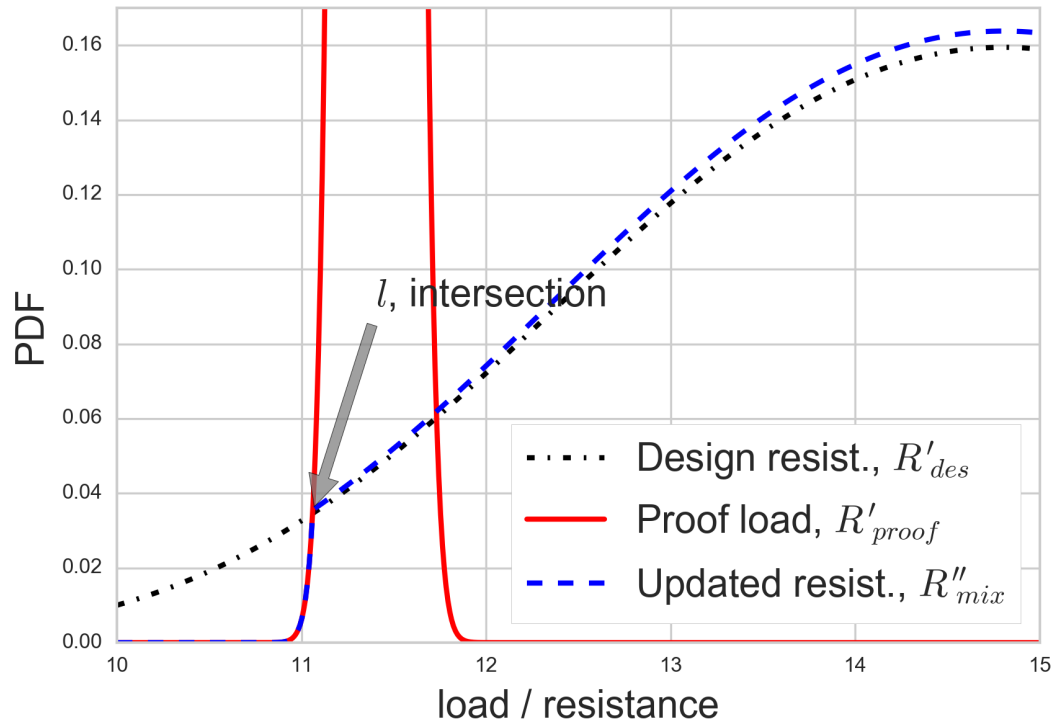

Figure 6.2: Visualization of the resistance updating process using probability density functions

distribution of the component resistance correlation, ρ_{R_i}, is chosen as shown in Figure 6.3.

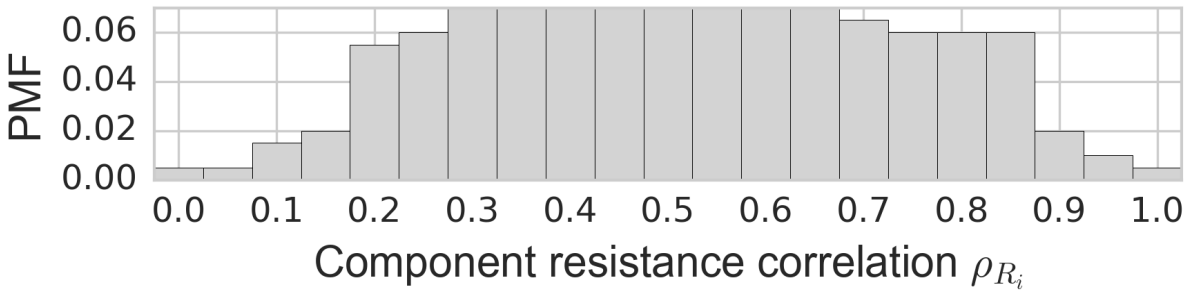

Figure 6.3: Assumed distribution of component resistance correlation

The Bayesian pre-posterior decision analysis follows the decision tree in Figure 6.4. Based on the not yet known test results a component that failed will not be used for construction; a surviving component will be used. Thus, failure is not explicitly modeled which results in the simple decision tree in Figure 6.4. The first chance nodes after the decision represent the probabilities of a certain component resistance correlation. The following chance nodes branch into system failure or survival.

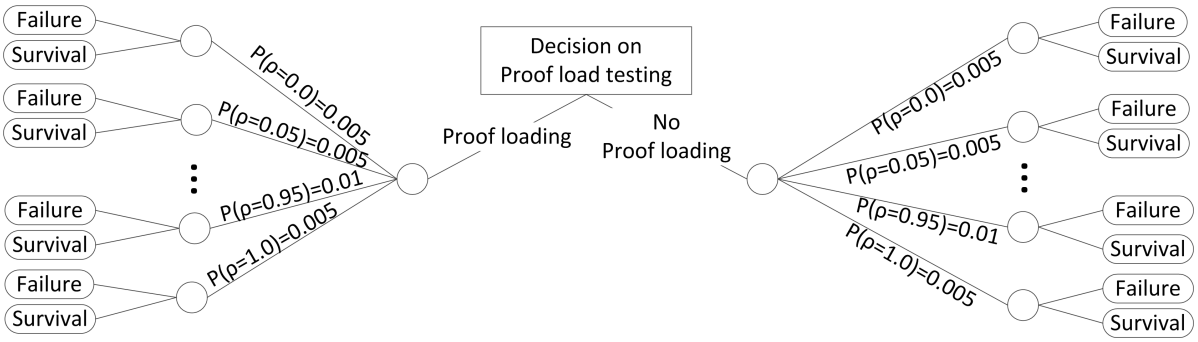

Figure 6.4: Decision tree. The resistance correlation ρ varies according to Figure 6.3

6.4 Model results

Figure 6.5 to Figure 6.7 show the relative change of the reliability index β normalized by the target index $\beta_t = 2$. Figure 6.8 to Figure 6.10 display the difference of the proof load test reliability and the design model reliability normalized by the difference in reliability one component gained. The images use bi-linear interpolation. In order to aid the graph interpretation, recognize that a dark color in the background represents a low value with a light color contour line for better contrast. A high value is thus shown by a light background color and a dark contour line.

6.4.1 Design model

For the series (Figure 6.5) and brittle Daniels (Figure 6.6) systems it can be observed how the system reliability is reduced with increasing number of components; a higher correlation counter acts on this effect. In Figure 6.7 one can observe an increase in reliability with increasing amount of components in ductile Daniels systems. In case of fully correlated model uncertainties the reliability converges faster to its maximum reliability which is only slightly higher than $\beta_t = 2$.

6.4.2 Updated structural models

In Figure 6.8 to Figure 6.10, a value larger than 0 represents a gain in reliability through proof load testing, a value larger than 1 indicates gain in the system reliability that is larger than the gain of a single updated component.

In the series system models (Figure 6.8) the proof load testing increases the reliability estimate with increasing numbers of components and a low correlation of component resistances. Thus the maxima are concentrated in the lower right corner of the graphs. Furthermore the reliability increase is stronger when the model uncertainties are correlated with $\rho_{M_{R_i}} = 1$.

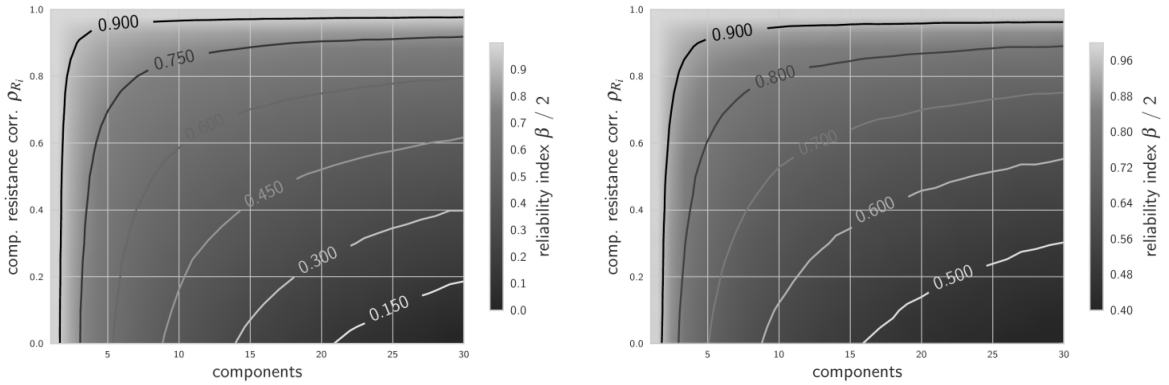

(a) $\rho_{M_R} = 0$ (b) $\rho_{M_R} = 1$

Figure 6.5: relative change of reliability index β prior series systems

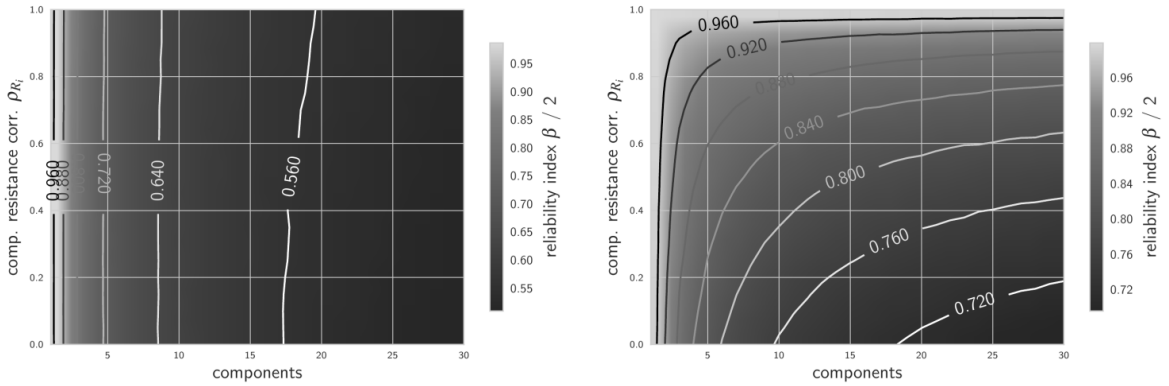

(a) $\rho_{M_R} = 0$ (b) $\rho_{M_R} = 1$

Figure 6.6: relative change of reliability index β prior brittle Daniels systems

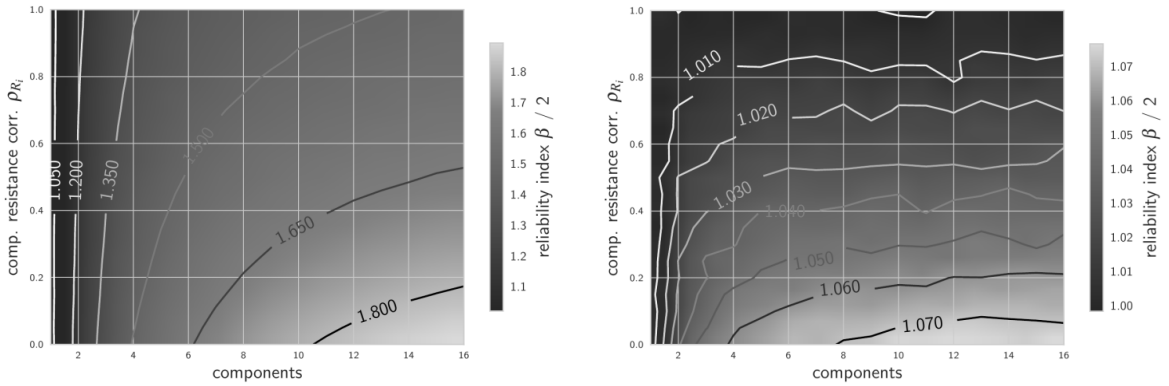

(a) $\rho_{M_R} = 0$ (b) $\rho_{M_R} = 1$

Figure 6.7: relative change of reliability index β prior ductile Daniels systems

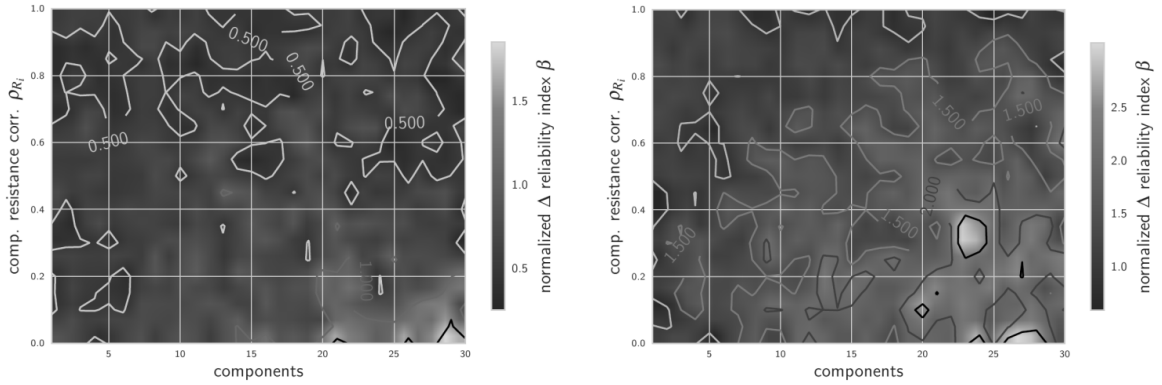

(a) $\rho_{M_R} = 0$ (b) $\rho_{M_R} = 1$

Figure 6.8: relative change of reliability index β posterior series systems

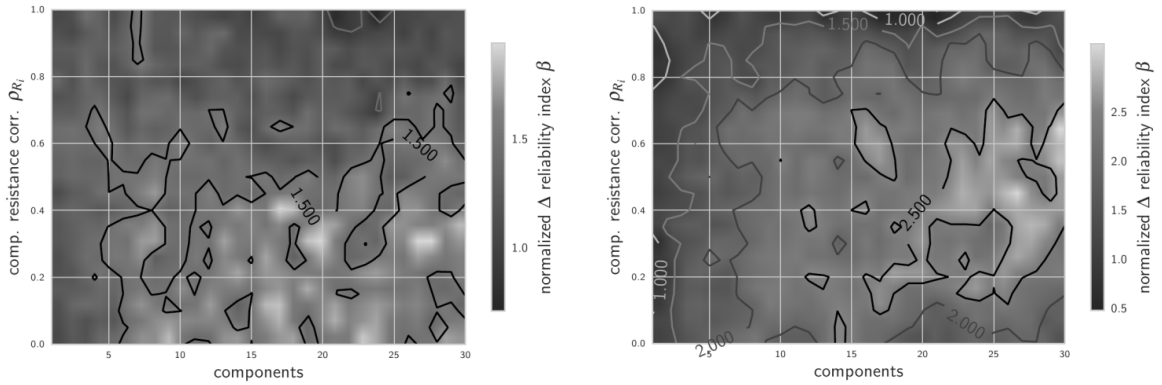

(a) $\rho_{M_R} = 0$ (b) $\rho_{M_R} = 1$

Figure 6.9: relative change of reliability index β posterior brittle Daniels systems

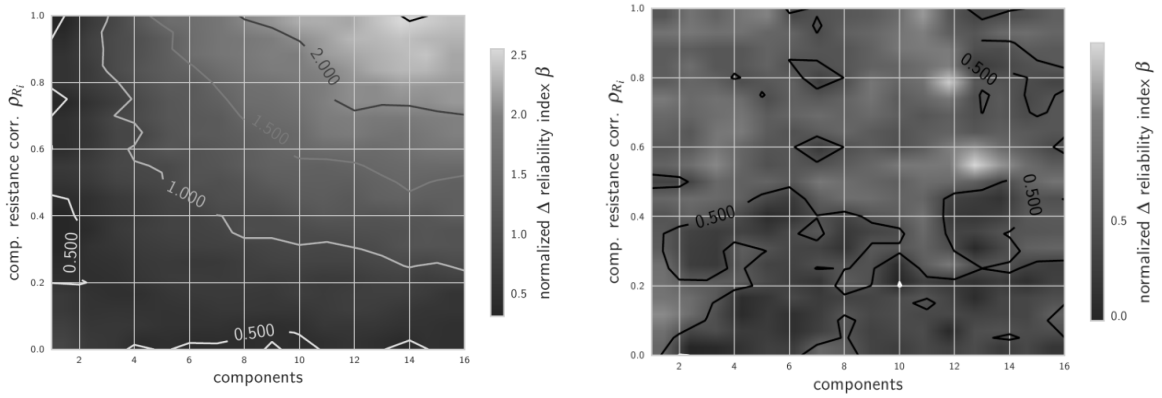

(a) $\rho_{M_R} = 0$ (b) $\rho_{M_R} = 1$

Figure 6.10: relative change of reliability index β posterior ductile Daniels systems

Brittle Daniels systems show behavior similar to that of series systems in case of $\rho_{M_{R_i}} = 0$. The peak reliability gain remains with a large amount of components but moves towards a higher correlation of component resistance.

Ductile Daniels systems gain more reliability through proof load testing with high component resistance correlation. This is especially pronounced with uncorrelated model uncertainties.

6.4.3 Decision analysis

As shown in Figure 6.11, the VoI of proof load testing for series and brittle Daniels systems become positive for larger numbers of components. The VoI = 0 is exceed between 11 and 16 components and beyond. Proof load testing of ductile Daniels system components does not provide a positive VoI in this study. The increase of the VoI with the number of components is due to lower risk associated with the failure of a component as the price per component is anti-proportional to the amount of components.

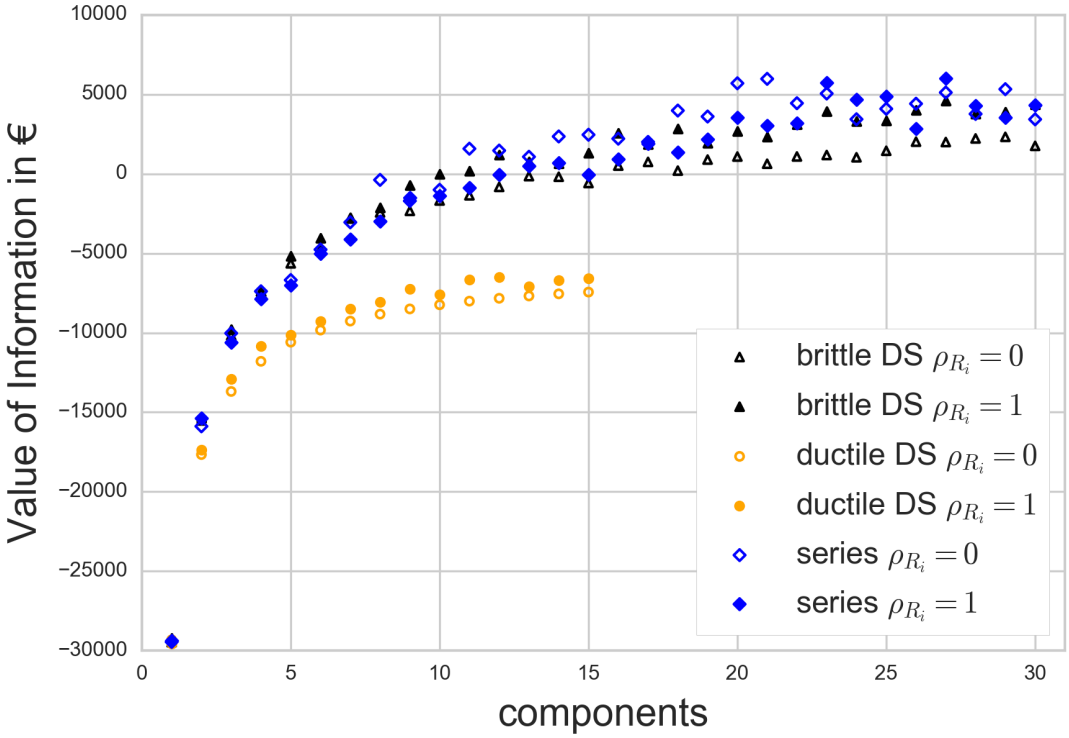

Figure 6.11: Value of information obtained by proof load testing

6.5 Summary and conclusion

The study has shown how proof load testing of individual components can be utilized in order to update the system resistance distribution and hence the system's reliability for series and Daniels system models. But for owners and operators of structural systems a more accurate estimation of the system reliability is not sufficient in itself. Before conducting an experiment such as proof load testing it is preferable to assess the value the experiment provides to the owner or operator. In this study the value of information was estimated using the Bayesian decision theory in order to assess whether or not proof load testing of single components can add value.

Considering the same type of system the value of information is mainly influenced by the risk associated with the proof load tests. The larger the amount of components, the larger is the value of information as the individual component price drops in more complex systems. Across systems the value of information is changing with the fundamental reliability of the system. From the most reliable system type in this study, the ductile Daniels system, to the least reliable system, the series system, the value of information increases. This generic approach requires an adaptation to relevant failure mechanisms for actual applications.

CHAPTER 7

On decision analysis about proof loading with inference to untested components

Brüske, H. & Thöns, S. On decision analysis about proof loading with inference to untested components. *International Conference on Structural Safety and Reliability* 3030–3039 (2017).

Abstract

In this paper, a model is presented that applies proof load testing to separate components of structural systems before construction in order to update their component and system reliability. This model may be beneficial if the structure itself is difficult to proof load test and only its components can be tested. We discuss how the information of only one or a few tested components is inferred to further components. For this, a new approach is developed which facilitates to take the correlation of the components' performance into account through the method of Bayesian updating using series and Daniels systems as models. With the proof loading information, the expected life-cycle benefits are computed within the framework of the Bayesian decision analysis. The described framework is applied to offshore wind turbines. The life cycle economy is calculated based on a detailed cost and benefit analysis with consideration of the direct risks due to component deterioration, indirect risks due to system failure and the expected costs and direct risks of the proof loading procedure in a (pre-) posterior decision analysis. Based on this case study, it is demonstrated how the optimal decision can be determined and what effect the system behavior of structural systems has.

7.1 Introduction

Proof load testing is usually applied to existing structures it is a common assessment method for bridges, for examples see [CG13; FVS00; SSN96]. Such a test is costly and runs the risk of damage to the tested structure and its surroundings. A proof load testing in an offshore environment may be even more costly due to logistics and loading technologies. Proof load test provides information about the resistance of a structure or element. If the tested object survives the loading undamaged, one may conclude that the resistance of the object is at least equal to the introduced loading. However, proof load testing may be performed prior to construction, which may circumvent high risks and costs. This paper thus addresses proof load testing in the context of wind turbines prior to construction and commissioning.

The proof loaded structural system models are introduced in Section 7.2, while in Section 7.3 the deterioration, which degrades the design state over time, is formulated. We explain in Section 7.4 how the proof loading information allows us to update a belief about the prior resistance to a posterior probability. The decision model and its assumptions are given in Section 7.5. In Section 7.6, the results are presented and the conclusions follow in Section 7.6.4.

A component, as used herein, does not necessarily describe a single girder or tube. The term component may as well refer to a structural sub-element that comprises several elements, such as two joined tubes in a monopole or a minimal number of tubes / beams in a jacket.

7.2 Structural Models

The limit state function in Equations (7.1) and (7.2) are used in order to determine the failure probabilities of the structural systems with five components. A series system fails if any of its n components fail, as in Equation (1). The weakest component determines the capacity of the whole series system

$$P_F = P\left(\bigcup_{i=1}^{n} F_i\right) \text{ with } F_i = \{R_i\, W_i\, M_{R_i} \leq S\, M_S\} \tag{7.1}$$

with the resistance force R the worsening or deterioration coefficient W, and the load S. The model uncertainties for R and S are represented by M_R and M_S respectively. S and M_S are defined on the system level and are distributed to the components according to the system model. The random variables are sampled as defined in Table 7.1, in Section 7.3 “Deterioration”. R, M_R, S, and M_S are independent from each other. Correlation among structural components is considered in R and M_R.

The so-called Daniels system is a special type of parallel system, see [GR90; Rac97]. If the load exceeds the system's load bearing capacity the weakest component breaks first and the load is equally redistributed among the remaining intact components. The entire system fails when the remaining intact components cannot jointly carry the additional load fraction that was sustained by the last component that broke.

This study considers perfectly brittle components in the Daniels system. For a perfectly brittle Daniels system the failure probability is determined by Equation (7.2).

$$P_F = P\left(\bigcap_{i=1}^{n}\{(n-i+1)R_i\,W_i\,M_{R_i} - S\,M_S \leq 0\}\right) \tag{7.2}$$

Where the realizations of $R_i\,D_i\,M_{R_i}$ are ordered according to $\hat{R}_1\,\hat{W}_1\,\hat{M}_{R_1} \leq \ldots \leq \hat{R}_n\,\hat{W}_n\,\hat{M}_{R_n}$. The system is tuned such that a single component has a reliability of $\beta = 3.1$ in accordance with JCSS [JCS99] for the case of minor failure consequences and large cost of safety measures.

7.3 Deterioration

The deterioration coefficient W is computed by randomly sampling Paris' Law. Equation (7.3) describes the crack length $a(n)$, in dependency of the stress cycles N, the stress range S_{range}, the initial crack length a_0, and two material parameters m and C.

$$a(n) = \begin{cases} \left(a_0^{\frac{2-m}{2}} + \frac{2-m}{2} C\,\pi^{\frac{m}{2}}\,S_{range}^{m}\right), m \neq 2 \\ a_0 e^{C\,\pi\,S_{range}^2\,N}, m = 2 \end{cases} \tag{7.3}$$

In order to arrive at a single random variable that represents the fatigue crack growth, Equation (7.3) was randomly sampled in increments of one year and fitted to a three-parameter lognormal distribution. The random variables S and N are described in Table 7.1 From Bïlïr [Bïl90] $m = 1.29$ and $C = 1.19 \times 10^{-6}$ were taken and the initial crack length assumed as $a_0 = 0.1$ mm. The parameters for S_{range} and N were calibrated in order to achieve a probability of failure < 1 for series systems with 25 components in 20 years.

The crack length to depth ratio is $a/c = 4$. The reduction in capacity is assumed to be directly proportional to the cracked area with the cracking beginning at the outer diameter. The remaining, load carrying area A_{lc}, is determined via Equation (7.5) for circular hollow sections, based on the conservative assumption that only the un-cracked radius of the component carries load. The initial load carrying area is calculated by Equation (7.4).

$$A_{comp} = \pi\left(r^2 - (r-t)^2\right) \tag{7.4}$$

$$A_{lc} = \pi \left((r - c(n))^2 \right) - (r - t)^2 \tag{7.5}$$

The component cross-section A_{comp}, is used to normalize and non-dimensionalize the fatigue effect. In order to simulate the fatigue degradation, the resistance term is multiplied by $W = {}^{A_{lc}(n)}/_{A_{comp}}$. Herein the radius is $r = 3$ m, and the wall thickness is $t = 0.1$ m, following Achmus et al. [AAK08] and Lesny and Wiemann [LW05].

Model parameter	**Distribution type**	**Mean**	**Standard dev.**
R_i Resistance	Substituted by either prior ($R'_{\text{des},i}$) or pre-posterior (R''_{mix})		
$R'_{\text{des},i}$ Design resistance	Lognormal	16.4404798	1.0
S'_{des} Design load	Weibull	10.0	$\sqrt{2}$
M_R uncertainty of R	Lognormal	1.15	0.15 mean(M_R)
M_S uncertainty of S	Lognormal	1.0	0.05 mean(M_S)
W_i deterioration coef.	Lognormal	Depend on time, S, N	
S stress range	Weibull	2.0	0.5
N fatigue cycles	Normal	170000	17000
S'_{PL}	Normal	**Percentile** ($R\,M_R$)	$0.01\,\mu(S'_{PL})$
		$5\hat{=}\mu(R\,M_R) = 14.319$	
		$10\hat{=}\mu(R\,M_R) = 15.182$	
		$15\hat{=}\mu(R\,M_R) = 15.794$	

Table 7.1: Model parameters

7.4 Resistance updating and information transfer

7.4.1 Transferring information to untested components via Bayesian updating

Proof load testing describes a method where a structure or component is subjected to a load close to the extreme exposures throughout the service life. This test establishes a minimum load level that the specimen can sustain. The information such test provides has been traditionally utilized by truncating the resistance distribution to exclude the proof loaded areas, see e.g. Thöns et al. [TFR11] and Brüske and Thöns [BT16]. However, this concept is of limited generality, especially when structural systems are considered. For this reason, we developed an approach to model the proof loading indication, which is then utilized to update the structural reliability.

The single component failure probability is updated via Equation (7.6).

$$P(F|I_{PL})\frac{P(z_{PL,\uparrow})\,P(F)}{P(Z_{PL,\uparrow})} = \frac{P(F \cap Z_{PL,\uparrow})}{P(Z_{PL,\uparrow})} \tag{7.6}$$

Where I_{PL} is the indication that the proof load test succeeded and F indicates failure of the tested component in operation. The gained information is transferred considering the correlation with respect to resistance. For a series system the failure probability of a set Sys of components given a set PL of proof load tested components, is given in Equation (7.7).

$$P\left(F_{S,\overset{ser}{sys}}|Z_{PL,\uparrow}\right) = P\left(\bigcup_{i\in TC} F_i|Z_{PL,\uparrow,i} \cup \bigcup_{j\in Sys\setminus TC}\right) \tag{7.7}$$

For a brittle Daniels system, the Bayesian updating is achieved according to Equation (7.8).

$$P\left(F_{S,\overset{bDS}{sys}}|Z_{PL,\uparrow}\right) = \frac{P\left(\bigcap_{i\in TC}\{(n-i+1)R_iM_{R_i}W_i - SM_S \leq 0\} \cap \bigcap_{j\in PL}\{R_jM_{R_j} - S_{PL} > 0\}\right)}{P\left(\bigcap_{j\in PL}\{R_jM_{R_j} - S_{PL} > 0\}\right)} \tag{7.8}$$

7.5 Decision model

7.5.1 Description of the decision scenario

The decision model constitutes a scenario with one offshore wind turbine structure over a time span of 10 years. The probability of structural failure and the generated benefit serves as a measurement for the structural performance. The decision model shall identify the optimal experiment parameters of the proof loading to maximize the expected benefit. The expected benefit comprises here the generated monetary value over the modeled period.

The decision (e) is modeled with the rectangular node in Figure 7.1 and comprises several proof loading strategies vs. the performance of no proof loading. The second decision (a) is modeled with the different proof loading strategies and the actions of utilizing successfully tested components and reproducing failed components. The system performance (X_2) is modeled through system failure (F) or survival ($\bar{F}$).

If the experiment outcome (X_1) is survival, the tested element group will be used in the structure. If however, the component fails, a new improved set of components will be tested. It is assumed then that this new set passes the test. The test failure probabilities in this study are $P\left(\overline{Z_{PL,\uparrow}(S_{PL,1})}\right) \approx 2.748 \times 10^{-4}$, $P\left(\overline{Z_{PL,\uparrow}(S_{PL,2})}\right) \approx 1.3671 \times 10^{-3}$, and $P\left(\overline{Z_{PL,\uparrow}(S_{PL,3})}\right) \approx 0.0150528$. In the following case study, one component of the system will be proof load tested.

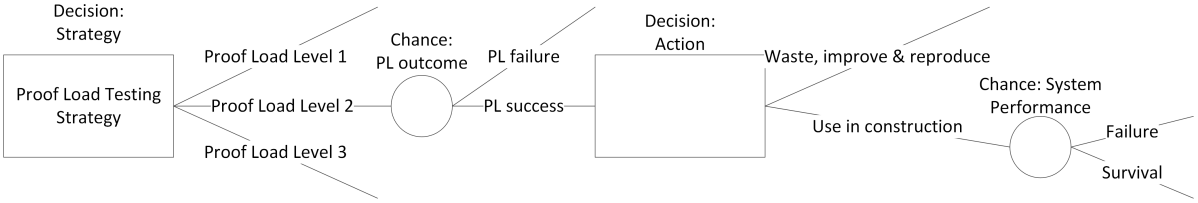

Figure 7.1: Decision tree modeling the determination of the optimal proof load test strategy. Decision nodes are represented by rectangles and chance nodes are shown as circles

7.5.1.1 Consequence model

The cost-benefit model is based on several publications concerning the economics and operation of offshore wind turbines. The basis of the benefit model is the tendering conditions of the Danish offshore wind energy park Krieger Flak [Nie16]. Technical and operations details pertaining to the benefit and cost side are taken from Barthelmie and Pryor, Faulstrich et al., Hau, Ho et al. and Voormolen et al. [BP01; FHT11; Hau13; HMC16; VJS16]. A detailed explanation of the cost-benefit model is found in Chapter 4 and in Brüske [Brü16]. The direct costs of structural failure due to deterioration are calculated with the capital expenditures of 4.1 M€ / MW. The structural system contributes 600 k€ / MW to the capital expenditures, which is to be spent again in case of proof load test failure. The indirect consequences arise from a loss of production. The production value is derived from a bid-price per kWh which is 0.15 € / kWh, followed by 0.039 € / kWh, see Chapter 4 or Brüske [Brü16] for details. The capacity factor of the Turbine is 50%, and it is operating over a service-life of $t = 1, \ldots, 10$ years. The proof load cost is 5000 €. All monetary values are discounted by 5%.

7.6 Results

7.6.1 Reduction of failure probability

Both structural system types with five components yield higher reliability indices by acquiring addition information about their capacities through proof load testing of one component. Figure 7.2 provides the time dependent failure probability P_f of the untested design models. One can see that the series system is generally more reliable with high correlations, but the Daniels system has no clear trend in its reliability with respect to the component correlation.

Figure 7.3 and Figure 7.4 show the development of the difference of annual failure probability ($\Delta P_F = P(F) - P(F|Z_{PL,\uparrow})$) over time between the prior information (no proof loading) and the (pre-) posterior information. In Figure 7.3 it is apparent that a higher

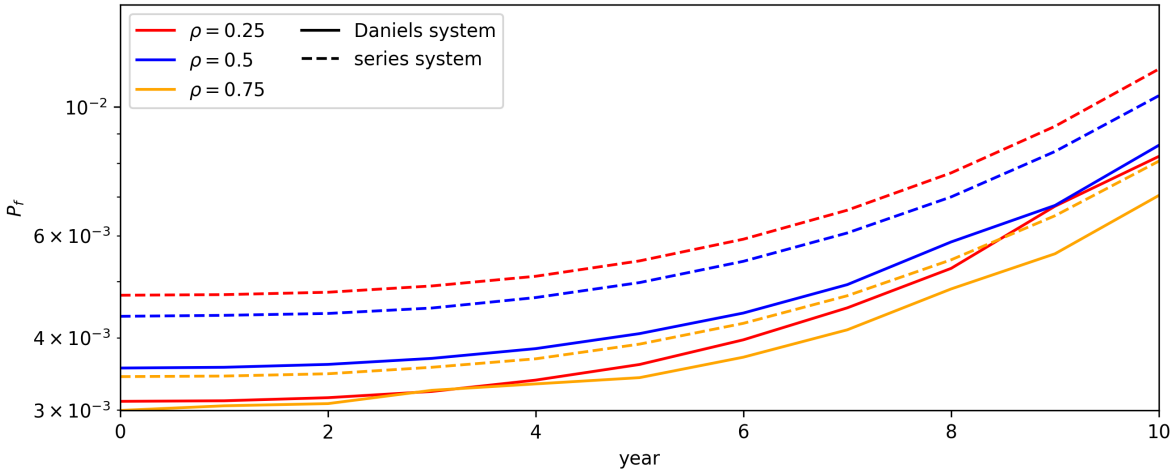

Figure 7.2: Development of annual system failure probability (P_f) over time due to deterioration

proof load level also provides better reliability information. Higher component correlation supports the increase in reliability.

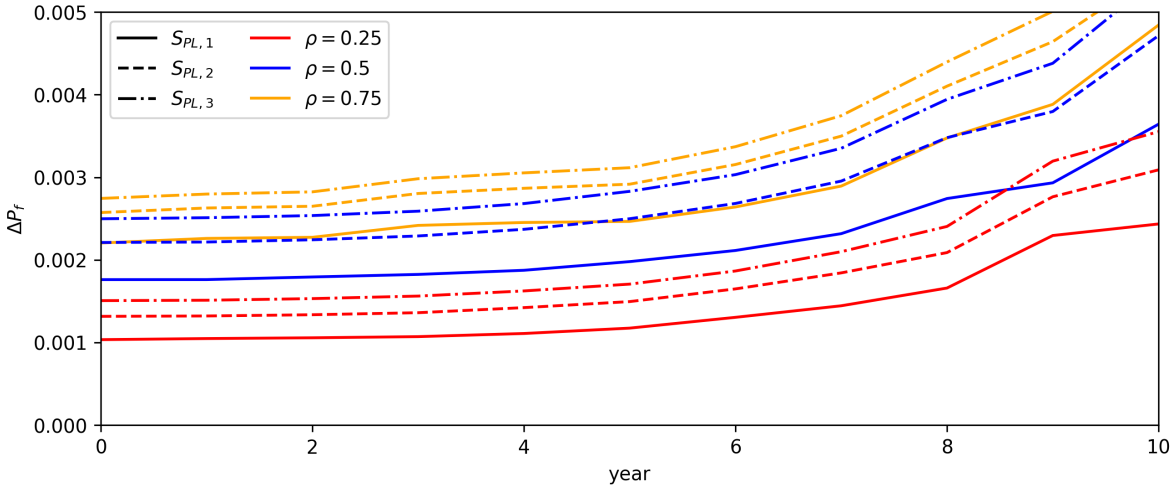

Figure 7.3: Reduction of annual failure probability (ΔP_f) of the brittle Daniels systems for different load levels and resistance related correlation

The same is the case for the series system. The increase of proof load levels does not provide as informative data in the case of the Daniels system. Thus, the series system has a lower reliability improvement. In both Figure 7.3 and Figure 7.4, a clustering of graphs with respect to the component correlation is present. This is more pronounced in the series systems.

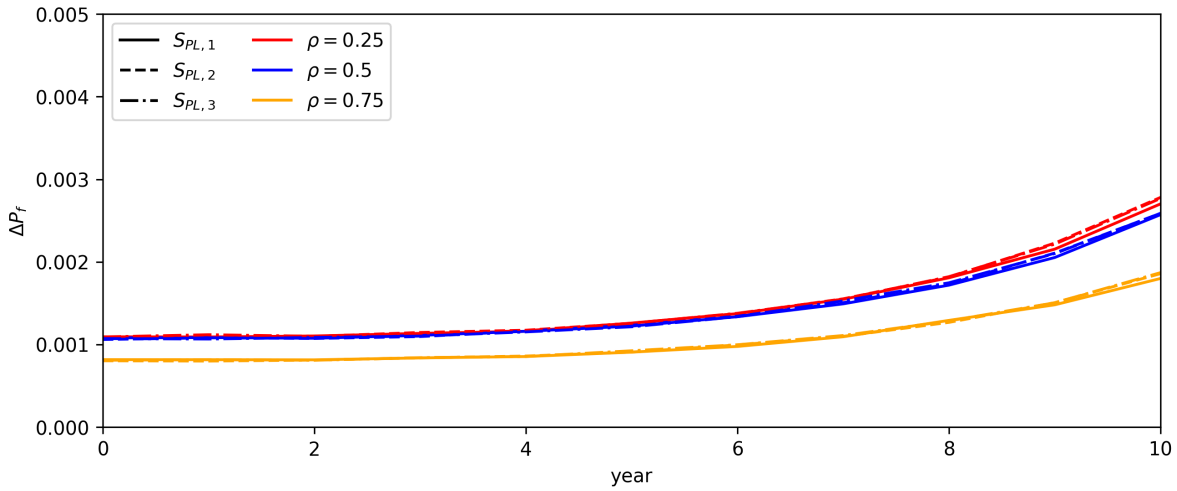

Figure 7.4: Reduction of annual failure probability (ΔP_f) of the series systems for different load levels and resistance related correlation

7.6.2 Reduction of risk

The total risk (direct and indirect) for both system models increases with the proof load as seen in a comparison of Figure 7.5 and Figure 7.6. Concerning the correlation of the five components, in R_i and as well M_{R_i} we observe a similar trend; for both systems higher component correlation means lower risk. As before, in Figure 7.3 and Figure 7.4 (reduction of failure probability) the graphs cluster, here by component correlation (series system) and by proof load level (Daniels system). As before, the different scenarios produce a clear separation of risk in the Daniels but a less pronounced separation in the series system.

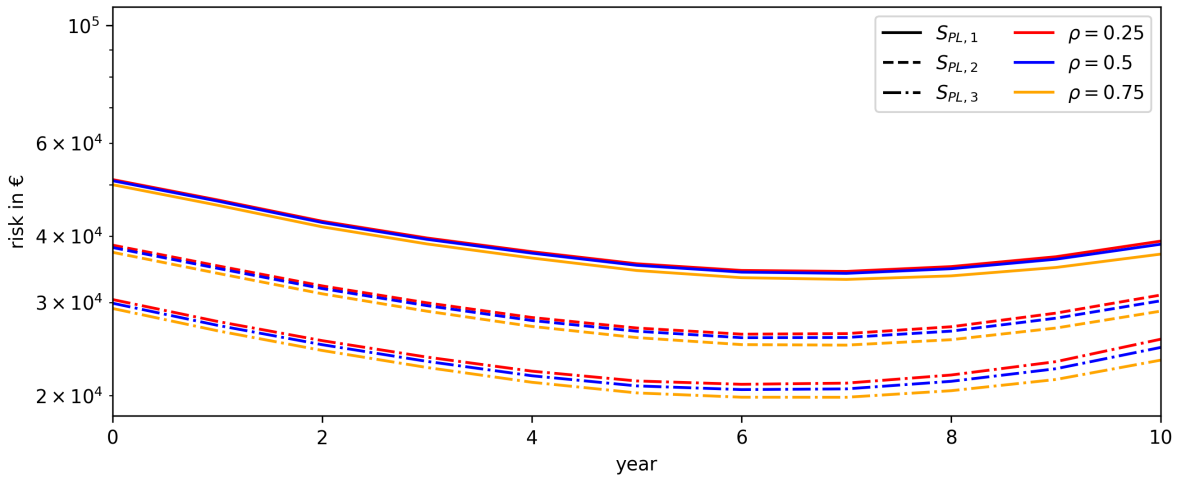

Figure 7.5: Risk over time for the proof load level for brittle Daniels system

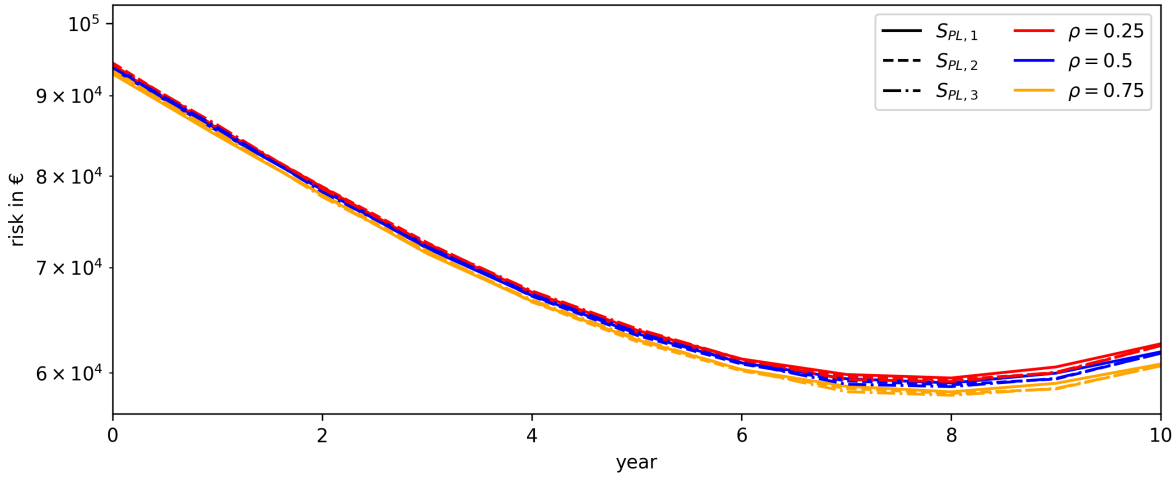

Figure 7.6: Risk over time for the series system

Figure 7.7 and Figure 7.8 show the development of direct risk, indirect risk, and expected benefit over time for an example proof load scenario in comparison to the design model. The proof load test is performed in year 0. The gained proof load information reduces the direct and indirect risk, and consequently the expected benefit increases.

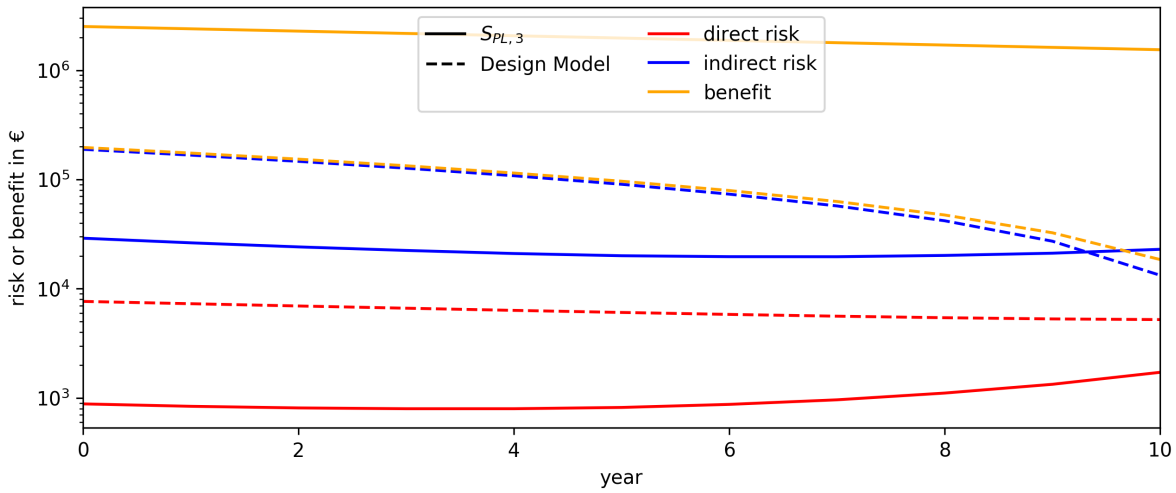

Figure 7.7: Direct risk, indirect risk and expected benefit for the design model and proof load tested brittle Daniels system

7.6.3 Optimal decision

The optimal decision is determined by the highest expected benefit. All excepted benefits of the proof load testing scenarios in this study are listed in Table 7.2. The trends of the

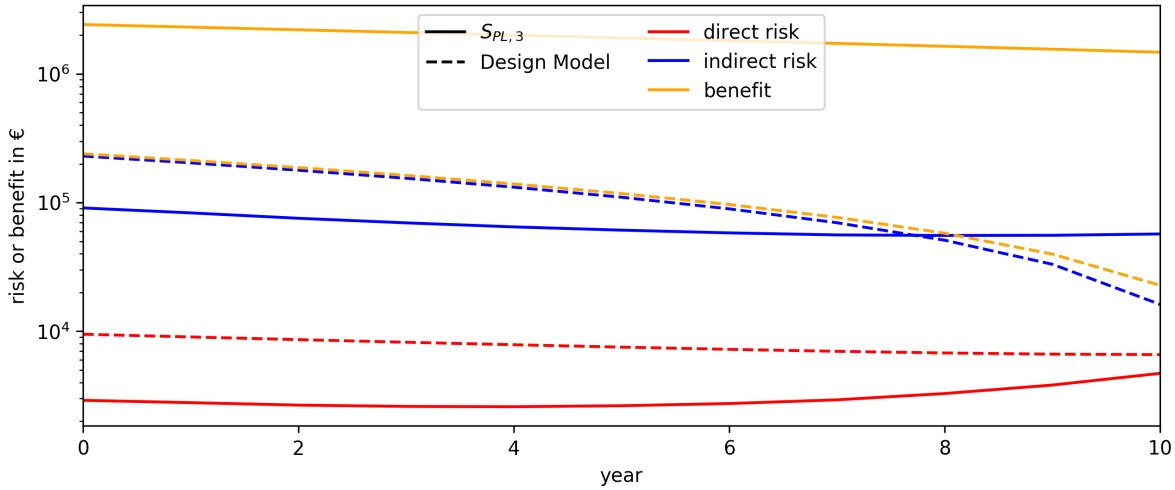

Figure 7.8: Direct risk, indirect risk, and expected benefit for the design model and proof load tested series system

optimal decisions pertaining series and Daniels system go towards higher proof loads. The effect of the three simulated proof loads on the series is rather small, and the correlation of load carrying components is more pronounced. The behavior of the brittle Daniels system is similar but the applied load is more relevant than in the series system cases.

The optimal decision for both systems is the highest load level $S_{PL,3}$, independent of the correlation.

	Load	$\rho = 0.25$	$\rho = 0.5$	$\rho = 0.75$
Series system	$S_{PL,1}$	21,017,444	21,116,289	21,291,030
	$S_{PL,2}$	21,019,193	21,116,737	21,291,121
	$S_{PL,3}$	21,019,551	21,116,874	21,292,503
Brittle Daniels system	$S_{PL,1}$	21,409,919	21,487,900	21,754,453
	$S_{PL,2}$	21,481,756	21,605,745	21,852,391
	$S_{PL,3}$	21,531,775	21,681,242	21,901,189

Table 7.2: Cumulative expected benefits in €

7.6.4 Conclusions

This generic model demonstrates the principle feasibility of proof load testing before the construction of structures where such tests would be very difficult in an operation-ready state. Furthermore, a pre-construction proof load test allows for test loads that are too risky for the completed structure. As the correlation of R_i and the correlation of

M_{R_i} are used to transfer the proof loading information, we see an increase in benefit with increasing correlation. In the case study, proof load testing is applied to only one component in order to update the reliability of the entire structural system. The Daniels system and series system react differently in terms of failure probability depending to the applied proof load. This is partially due to different system design reliabilities, i.e., the series system is weaker than the Daniels system. A second cause may be the fundamentally different system behavior of series and Daniels systems. This system behavior could be the cause of the low influence of increasing proof loads on the series system compared to the noticeably larger load level influence on the brittle Daniels system.

It should be noted that the term components as used in this study might describe a sub-system consisting out of several elements depending on how the complete structure can be divided for the testing purpose. For a monopile, the said component could be two joint tubes, or for a jacket, a small set of braces.

Future work may investigate whether the difference in response of series and brittle Daniels system is due to the different system design reliabilities or due to systematic behavior. Furthermore, various and new decision parameters, such as the number of proof load tested components, can be examined in greater detail.

CHAPTER 8

Value of information of pre-construction proof loading information for structural design improvement

8.1 Introduction

This chapter begins with an introduction to the examined structural models in this study, which were chosen as representation for monopile and jacket sub-structures with their explicitly considered deterioration process. Thereafter follows an explanation of the utilization of proof loading tests. The components are tested separately, and the proof loading information is inferred to untested components in the system models. The decision process is explained based on the value of information theory and is motivated by a decision problem on the selection of a structural system and proof load scenarios. The decision process takes basis in the economics of offshore wind turbines. Finally the modeling results are presented with the conclusions.

8.2 Reliability of structural systems

This study demonstrates the updating of reliability estimations using proof load information with series, and two types of parallel system. Furthermore, the value of proof loading information in context of series systems and brittle Daniels systems with $n = 5$ components is investigated. A series system fails if any of its n components fail, see

Equation (8.1). The system load in this study is acting equally on every component.

$$P_{F_S,ser} = P\left(F_{S,ser} = \bigcup_{i=1}^{n} F_{i,log}\right) \text{ with } F_{i,log} = R_i\, W_i(t)\, M_{R_i} \leq S\, M_S \tag{8.1}$$

With the resistance force R, the worsening / deterioration coefficient W, and the load S. The model uncertainties for R and S are represented by M_R and M_S respectively. R, M_R, W, and M_S are independent from each other. Spatial correlation among structural components is considered in each constituent of R, M_R, and W. The worsening coefficient W is defined in Equation (8.2).

$$W_i(t) = 1 - \sum_{k=1}^{t} \Delta_{i,k} \tag{8.2}$$

$\Delta_{i,k}$ is a conditional random variable, such that $\Delta_{i,k}|\theta$ is conditioned with only the mean value $\theta = \mu(M_\Delta)$ in accordance with Qin et al. [QTF15]. The distribution parameters of the introduced random variables are provided in Table 8.3.

The parallel system definition, see Equation (8.1), is similar to the series, here the union operation is replaced by the intersection operation. If any amount of components can sustain the load, the system survives.

$$P_{F_S,par} = P\left(F_{S,par} = \bigcap_{i=1}^{n} F_{i,log}\right) \text{ with } F_{i,log} = \{R_i\, W_i\, M_{R_i} \leq S\, M_S\} \tag{8.3}$$

The brittle Daniels system, Equation (8.4), is a special type of parallel system that exhibits brittle material failure behavior. Note that for the calculation, the realizations of $R_i\, W_i(t)\, M_{R_i}$ are to be sorted in ascending order, i.e. $\hat{R}_1\, \hat{W}_1(t)\, \hat{M}_{R_1} \leq \ldots \leq \hat{R}_n\, \hat{W}_n(t)\, \hat{M}_{R_n}$.

$$P_{F_{S,bDS}} = P\left(\bigcap_{i=1}^{n} F_{i,bDS}\right) \text{ with } F_{i,bDS} = \{(n-i+1)\, \hat{R}_i\, \hat{W}_i\, \hat{M}_{R_i}\} \tag{8.4}$$

Examples of a Daniels system and a series system are depicted in Figure 8.1. The remainder of this study focuses on the series system and the brittle Daniels system. The series system is used as a representation of a monopile because monopiles are statically determined and have no redundant elements. The brittle Daniels system serves as a model for jacket structures because a jacket has redundant elements, and the main failure mode is buckling, which is a brittle failure mode.

8.2.1 Design target of the structures

The JCSS probabilistic model code [JCS99] distinguishes nine cases to determine an annual target reliability on the bases of failure consequences and relative costs of safety

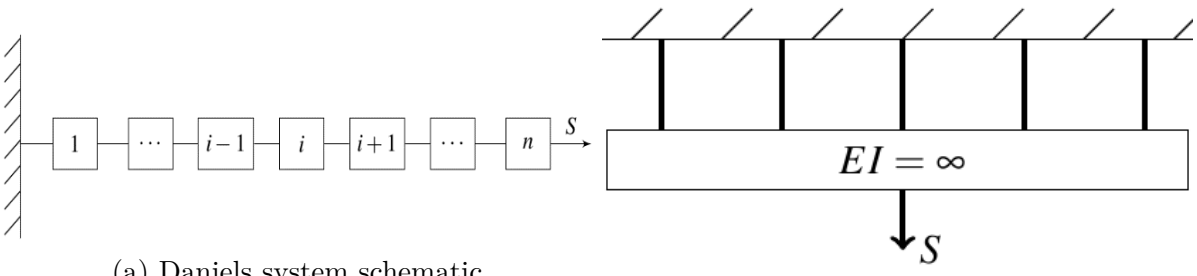

(a) Daniels system schematic

(b) Series system schematic

Figure 8.1: Illustration of the structural system modeling for the considered 5 components (gray rectangles)

measures. Sørensen and Toft [ST14] suggest for offshore wind turbines an annual target reliability index of $\beta = 3.3$. $\beta = 3.3$ corresponds to "moderate failure consequences" and "high relative costs of safety measures". Offshore wind turbines are most of the time unmanned, only inspection and maintenance can require human presence. Therefore, the consequences are almost entirely limited to the structure and of financial concern.

Two factors dominate the consequences in case of structural failure, namely the monetary loss of the wind turbine and the subsequent production loss. The production loss consequences diminish towards the end of the service life. Based on this argumentation it is suggested that at the end of the service life the consequences are classified as "minor / some" leading to an acceptable target reliability of $\beta = 3.1$ at the end of service. Therefore, two reliability levels are defined for the models, namely $\beta = 3.3$ at the beginning of operations ($t_0 = 0$) and $\beta = 3.1$ at the end of service-life.

8.3 Decision modeling

In the following section of Chapter 8 a different notation for value of information is used. The symbol V_I that is usually used in the thesis will be written with additional subscripts, for example $V_{I,\vec{a}^{pr}}$, in order to distinguish three cases of information pertaining to different action alternatives.

8.3.1 Value of information

The value of information ($V_{I,\vec{a}^{pr}}$) is defined as the difference between the optimal utility computed with (pre-) posterior information (B_{post}), minus the optimal utility obtained using only prior information (B_{prior}). The concept of introduced in Section 5.1 with Equations (5.1) to (5.3).

The life-cycle benefit B_{post} depends on the outcome of the pre-posterior decision analysis. The analysis depends on the choice of the proof load test, structural performance of the specific system type and the impact of operation adjustments. Such adjustments are for example load control or service-life extension. The proof load test influences the result by its capabilities, i.e. load type, load distribution, and cost. In order to choose the highest utility with prior knowledge, the expected value, $E_{\vec{X}}\left[\vec{b}_{prior}(\vec{X},\vec{a}^{pr})\right]$ has to be maximized with respect to the states $\vec{X}$ and decision alternatives $a^{\vec{p}r}$. $E_{\vec{Z},\vec{X}}\left[\vec{b}_{post}(\vec{Z},\vec{X},\vec{p},\vec{a}^{pr})\right]$ expresses the expected value of benefits which is maximized in the context of pre-posterior knowledge comprising the proof load strategy ($\vec{p}$ and sub-structure alternatives ($\vec{a}^{pr}$), see Equation (8.5).

$$V_{I,\vec{a}^{pr}} = \max_{\vec{p},\vec{a}^{pr}} E_{\vec{Z},\vec{X}}\left[\vec{b}_{post}(\vec{Z},\vec{X},\vec{p},\vec{a}^{pr})\right] - \max_{\vec{a}^{pr}} E_{\vec{X}}\left[\vec{b}_{prior}(\vec{X},\vec{a}^{pr})\right] \tag{8.5}$$

See Figure 8.2 for a visualization of the corresponding value of information decision tree.

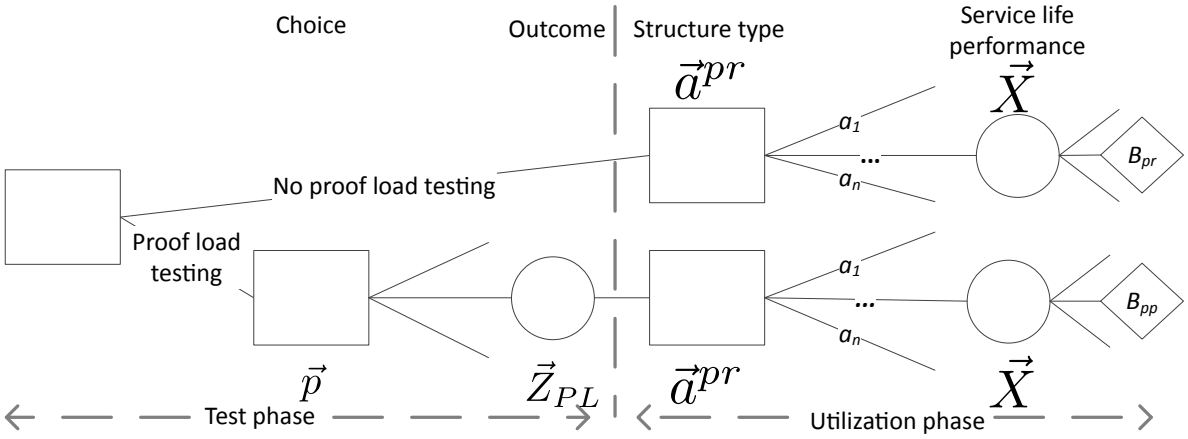

Figure 8.2: Generic VoI decision tree based on sample information

The above described VoI derivation is similar to the approach by Pozzi and Der Kiureghian [PD11], an extensive example may be found in Thöns et al. [TSF15]. The value of proof load information may thus relate to increasing expected benefits or decreasing expected costs and risks. In a wider context the value relates to increasing human safety, economic efficiency, and reducing environmental impact.

8.3.2 Value of information extended

Note that $V_{I,\vec{a}^{pr}}$ is defined as comparison of identical actions. However, the proof loading information may allow to explore further action alternatives. Next to the actions in $\vec{a}^{pr}$, which are present in both, the prior and (pre-) posterior decision analysis branches,

the pre-posterior part can be extent to a vector with new options $\vec{a}^{pr\&I}$. The new action vector $\vec{a}^{pr\&I}$ contains $\vec{a}^{pr}$, but holds additional options that become possible with new information. β_1 to β_m mark alternatives that are not possible with only prior information.

Analogous to value of information, the value of information and actions is computed as the difference of expected benefits from the optimal prior decision and the optimal decision and action combination of the pre-posterior branch. Because the example deals with sample information, $V_{I,\vec{a}^{pr\&I}}$ is the expected value of sample information and actions (EVSIA). The posterior benefit $\vec{b}_{post}$ is now defined with the new action vector $\vec{a}^{pr\&a}$.

$$V_{I,\vec{a}^{pr\&I}} = \max_{\vec{p},\vec{a}^{I\&A}} E_{\vec{Z},\vec{X}} \left[\vec{b}_{post}(\vec{Z},\vec{X},\vec{p},\vec{a}^{pr\&I})\right] - \max_{\vec{a}^{pr}} E_{\vec{X}} \left[\vec{b}_{prior}(\vec{X},\vec{a}^{pr})\right] \tag{8.6}$$

In order to consider new design alternatives that arise from the possibility to use a prior design weaker than $\beta = 3.3$ and update its reliability estimate via proof load information the decision tree from Figure 8.2 needs to be extended, as shown in Figure 8.3. With the new information dependent actions the expected value of sample information (EVSI) has to be extend in its scope.

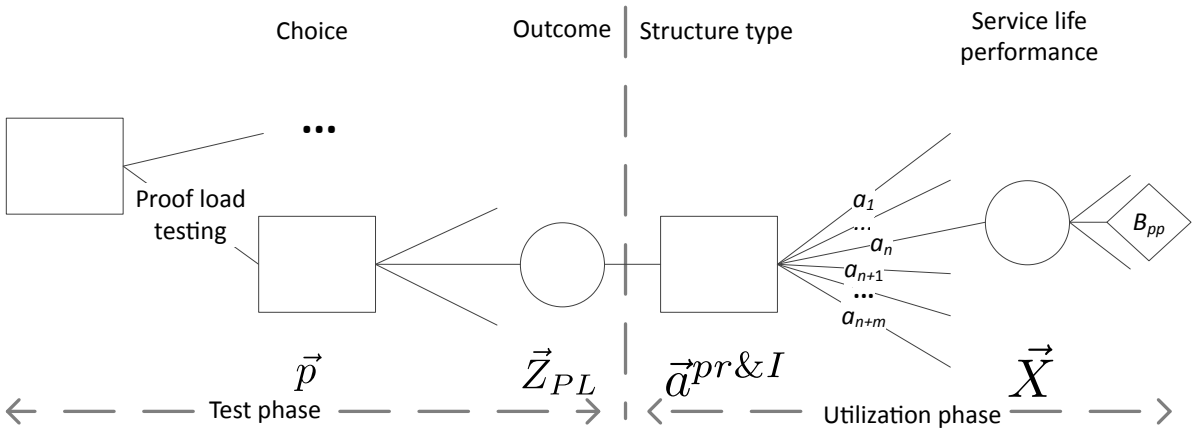

Figure 8.3: Generic decision tree based sample information and considering new action alternatives. The upper branch represented by the ellipsis is identical to the prior branch in Figure 8.2

$V_{I,\vec{a}^{pr}}$ is included in $V_{I,\vec{a}^{pr\&I}}$, thus $V_{I,\vec{a}^{pr\&I}}$ will yield at least the same value as $V_{I,\vec{a}^{pr}}$. The value of new actions can be separated from $V_{I,\vec{a}^{pr\&I}}$ to $V_{I,\vec{a}^{I}}$ that is maximized with respect to $\vec{a}^{I}$ that contains all new actions.

$$V_{I,\vec{a}^{I}} = \max_{\vec{p},\vec{a}^{I}} E_{\vec{Z},\vec{X}}[\vec{b}_{post}(\vec{Z},\vec{X},\vec{p},\vec{a}^{pr})] \tag{8.7}$$

8.3.3 The decision problem

The following two sections explain the decision problem in the context of EVSI, and the same problem with additional action option in the context of EVSIA.

The decision maker plans an offshore wind energy park. In the present scenario the capital expenditures (CAPEX) for either using monopiles or jacket support structures are equal in the prior information design. Additional information may be gathered via proof load testing of single components before construction. This allows for a pre-posterior decision analysis considering as well proof loading with the parameters load level S_{PL}, and number of testing components n_{PL}. Furthermore, the proof loading information may support a "weaker" prior design with lower CAPEX that meet the reliability constraints. In summary the decision variables are: (1) proof loading (yes / no), proof loading parameters (S_{PL}, n_{PL}), and the prior reliability calibration with posterior information. The decisions are taken in the planning and decision phase before construction. In order to make the decisions before acquiring the proof loading information and before construction of the wind park, a value of information analysis and pre-posterior decision analysis is required.

The proof loading strategies $\vec{p} = [S_{PL}, n_{PL}]$ are described with the proof loading level $S_{PL,m}$ and the number of proof loaded components n_{PL}. The proof loading results in an uncertain outcome $\vec{Z}_{PL} = [Z_{PL,\uparrow}, Z_{PL,\downarrow}]$ with $Z_{PL,\uparrow}$ denoting proof loading survival and $Z_{PL,\downarrow}$ proof loading failure of the component. The limit state functions of $\vec{Z}_{PL}$ are given in Equations (8.8) and (8.9). Survival of the proof load test ($Z_{PL,\uparrow}$) results in no further costs, failure ($Z_{PL,\downarrow}$) comes with the costs of component replacement. The test survival or failure is dealt with by a decision rule, surviving components will be used for construction, and failed components will be replaced.

The actions $\vec{a}$ are described with choosing the structural system (series or brittle Daniels system). The service life performance is described with the operational benefit (OB) and engineering / construction costs (EC) $\vec{X} = OB + EC$. OB depends of states $[\bar{F}_S, F_S, \bar{D}_S, D_S, \bar{F}_{C,n_C}, F_{C,n_C}, \bar{D}_{C,n_C}, D_{C,n_C}]$ encompassing the system and the component failure and damage states, F_S, D_S, F_{C,n_C}, and D_{C,n_C}, the bared states ($^-$) symbolize the survival or undamaged states. EC depend mainly on design, and civil engineering costs, equipment and material costs, as well as fabrication / construction time. The last four points depend also on the structures weight.

Equations (8.1), (8.3), and (8.4) describe system failure, that is when the load acting on the system is greater or equal the system resistance. If the load is smaller than the system resistance, the system will be in the state of survival F_S. Component failure is defined as $F_{C,n_C} = R_{n_C} W_{n_C} M_{R_{n_C}} - S M_S \leq 0$. All failure or damage states are super states of F_S. E.g. a structural failure is a sub state of component failures F_{C,n_C}. The ranking is $F_S \in D_S \in D_{C,n_C}$ and $F_S \in F_{C,n_C} \in D_{C,n_C}$. A system damage state D_S is

given if component D_{C,n_C} (including F_{C,n_C}) is present. D_{C,n_C} has the limit state function $D_{C,n_C} = R_{n_C} W_{n_C} M_{R_{n_C}} - S M_S \leq Crit$ with a critical value $Crit \geq 0$, much like F_{C,n_C}.

8.3.4 Description of the decision scenario using EVSI

The objective function for the quantification of decision benefits is given as EVSI in Equation (8.5), in the previous section "Value of information". The decision ($\vec{p}$) is to be taken in the testing phase and is associated with the single element proof loading. It is to be decided how the testing will be conducted in terms of load level S_{PL}, and number of tested components n_{PL} (any 1, 3 or 5 components). Action ($\vec{a}^{pr}$) is to be taken in the utilization phase. At ($\vec{a}^{pr}$) the decision maker has to choose a type of support structure, either monopiles or jackets. The action vector $\vec{a}^{pr}$ constitutes of the alternatives $\vec{a}^{pr} = [a_1, a_2]$.

The consequences of action ($\vec{p}$) are related to the costs of proof loading and its failure. These consequences are represented by the chance node $\vec{Z}$. If the test fails, new components have to be produced and tested. The consequences of action ($\vec{a}^{pr}$) arise from different benefits generated over the entire service-life at chance node $\vec{X}$. The combination of costs and benefits with their respective probabilities form the utility ($\vec{b}_{prior}$ or $\vec{b}_{post}$), that is to be maximized.

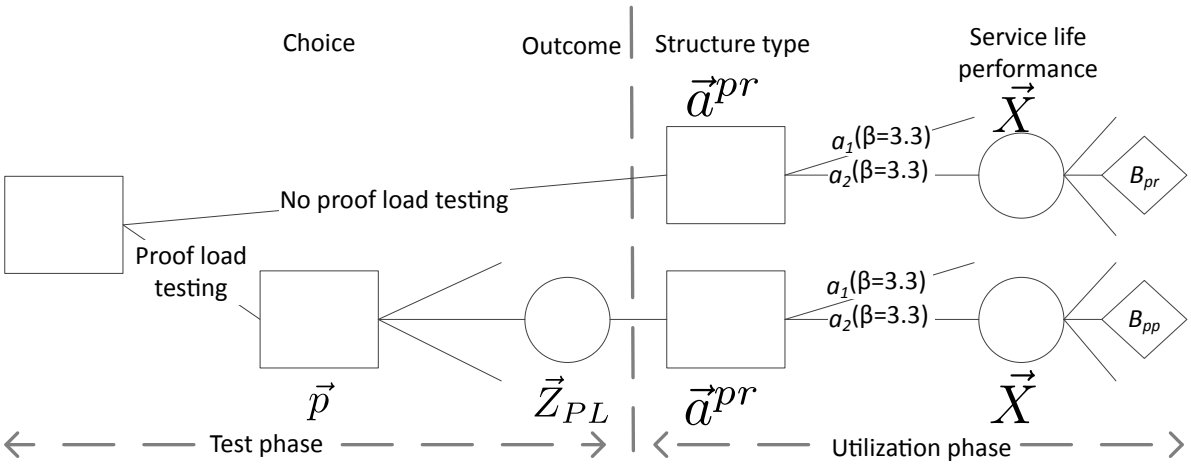

Figure 8.4: Decision tree modeling the determination of the optimal proof loading strategy ($\vec{p}$) for system type selection ($\vec{a}$). Decision nodes are represented by rectangles and chance nodes are shown as circles

In this EVSI based decision analysis the structural reliability has to comply with two constraints. At time $t_0 = 0$ the structural reliability must be at least $\beta = 3.3$, at the end of the service-life the reliability must be at least $\beta = 3.1$.

8.3.5 Description of the decision scenario using EVSIA

The decision making approach (2) uses an EVSIA based decision analysis. Herein, the prior information design that may be $\beta < 3.3$ and uses proof load testing of single structural components to gather information that is used to update the reliability in order to comply with constraints (1) and (2) as defined in Section 8.2.1.

In the context of the EVSIA decision scenario the new action alternatives have a prior $\beta < 3.3$ at $t_0 = 0$ and the action vector is extended to $\vec{a}^{pr\&I} = [a_1, a_2, a_{1,\beta_1}, a_{2,\beta_1}, \ldots, a_{1,\beta_m}, a_{2,\beta_m}]$. The prior reliability indices used in approach (2) are represented by β_1 to β_m. All other decision variables remain the same.

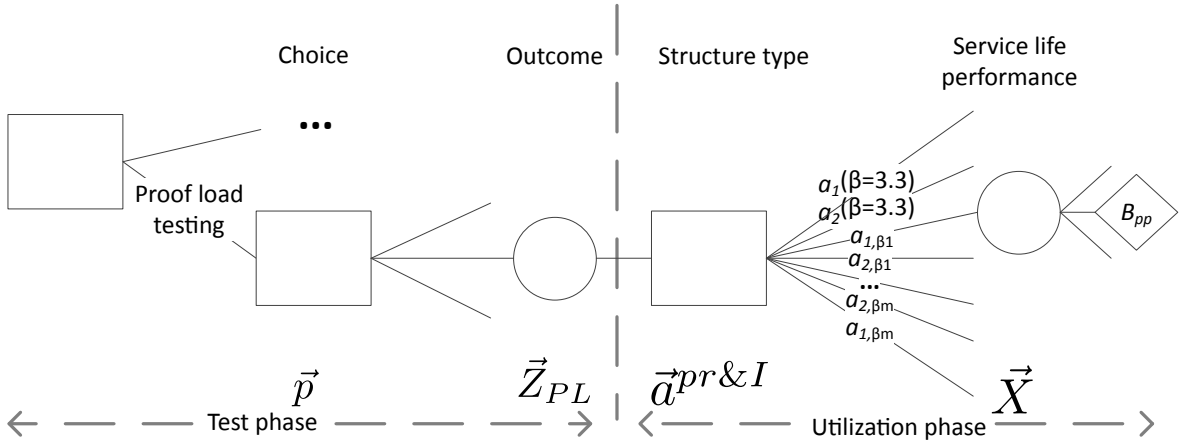

Figure 8.5: The pre-posterior branch is extended with actions possible only with new information. The ellipsis represents the prior branch

8.4 Utilization of proof load information in system models

The proof load event $Z_{i,j}$ is described by the limit state function

$$Z_{PL,\uparrow,j} = R_j \, M_{R,j} - S_{PL} > 0 \tag{8.8}$$

$$Z_{PL,\downarrow,j} = R_j \, M_{R,j} - S_{PL} \leq 0 \tag{8.9}$$

An approach is developed by which the proof loading indication $Z_{PL,j}$ is modeled, which is then utilized to update the structural reliability as used by Brüske and Thöns [BT17]. $S_{PL,j}$ will be highly correlated in a laboratory environment, therefore $\rho(S_{PL}) = 1$ is assumed and further on only S_{PL} will be used. This results in the definition on the proof load testing survival indication $Z_{PL,\uparrow,j}$ in (8.8).

Proof loading information can be used to update the failure probability using Bayesian probability theory as described in Equations (8.10) to (8.14). The derivation of system model updating begins with the general parallel system (Equation (8.11)) and applies the concept analogously to the brittle Daniels system (Equation (8.12)). The series system updating is presented in Equations (8.13) and (8.14) for the case of proof loading single elements in the assembled system and for the case of testing components outside of the system. Sys represents all system components and TC is the set of proof load tested components, thus $Sys \setminus TC$ is the set of all components without the tested components. Because the proof load and component properties are identically distributed the combination of tested components is irrelevant in this study, see Figure 8.1 for system model sketches.

In this study Bayesian updating is applied in order to utilize proof loading information. For a single failure event F_1 with associated proof loading information $Z_{PL,\uparrow,1}$ the updating equation is

$$P\left(F_1 | Z_{PL,\uparrow,1}\right) = \frac{P(F_1 \cap Z_{PL,\uparrow,1})}{P(Z_{PL,\uparrow,1})} \tag{8.10}$$

Updating a parallel system is straight forward thanks to the associativity and commutativity of the intersection operator substitution of F_1 in (8.11) with the system limit state function $F_{par} = \bigcap_{i \in Sys} F_i$, compare (8.3), and the indication $Z_{PL,\uparrow,1}$ with the indication state all tested components survived the proof loading that is $Z_{PL,\uparrow} = \bigcap_{j \in TC} Z_{PL,\uparrow,j} = \bigcap_{j \in TC} \{R_j \, M_{R,j} - S_{PL} > 0\}$.

$$P\left(F_{S,par} | Z_{PL,\uparrow}\right) = \frac{P\left(\bigcap_{i \in Sys} F_i \cap \bigcap_{j \in TC} Z_{PL,\uparrow,j}\right)}{P\left(\bigcap_{j \in TC} Z_{PL,\uparrow,j}\right)} \tag{8.11}$$

The updating algorithm is identical for the case that separate components are tested outside of the system, or if separate components are tested in the assembled system. For the scenario that components are tested before system assembly, the modeling of the system indication holds because only components, which have survived the proof loading, will be used for the system assembly. For in situ testing failed components need to be replaced or repaired.

The last step for the brittle Daniels system updating in (8.11) is to introduce the ranking of component strengths from $F_{i,bDS}$ as in (8.4)

$$P(F_{S,bDS} | Z_{PL,\uparrow}) = \frac{P\left(\bigcap_{i \in Sys} F_{i,bDS} \cap \bigcap_{j \in TC} Z_{PL,\uparrow,j}\right)}{P\left(\bigcap_{j \in TC} Z_{PL,\uparrow,j}\right)} \tag{8.12}$$

The series system updating requires a distinction between testing single components in the system and testing single components before assembly due to non-commutativity of the union operator. Testing single components in a series system follows the same approach as previously demonstrated for parallel and brittle Daniels systems.

$$P\left(F_{S,\overset{ser}{sys}}|Z_{PL,\uparrow}\right) = \frac{P\left(\bigcup_{i\in Sys} F_{i,log} \cap \bigcap_{j\in TC} Z_{PL,\uparrow}\right)}{P\left(\bigcap_{j\in TC} Z_{PL,\uparrow}\right)} \tag{8.13}$$

If however, the components are tested before assembly the approach varies. In this case the updating has to be done component wise and in the next step the system behavior has to be included.

$$P\left(F_{S,\overset{ser}{comp}}|Z_{PL,\uparrow}\right) = P\left(\bigcup_{i\in TC} F_i|Z_{PL,\uparrow,i} \cap \bigcap_{j\in Sys\setminus TC} F_j\right) \tag{8.14}$$

8.4.1 Damage and failure consequences

The consequence model encompasses the costs of the (1) proof load testing in dependency of the proof load strategy and its outcomes and (2) consequences associated to each of the system states. The consequences have to be discounted to the year they occur. The consequences are detailed in Table 8.1. The proof load test will be conducted on single

Proof load testing consequences (1)		State consequences (2)	
No test	Structure cost according to prior information design	System failure	Loss of CAPEX, loss of all future income
Proof load test	Structure cost according to posterior information design, Consequences of proof load failure	System damage	Major repair costs, loss of income due to long down time
		Component failure	Moderate repair costs, loss of income due to long down time
		Component damage	Minor repair costs, loss of income due to short down time

Table 8.1: Design / Proof load and operation consequences

components of the structure before its construction, see structure sketches in Figure 8.1b. The service-life of the deteriorating structure is $t_{25} = 25$ years where the annual reliability index shall remain above or equal $\beta = 3.1$ at the end of service-life.

8.5 Case study

8.5.1 Economical boundary conditions

The case study is used herein to demonstrate the decision process, and it takes bases in the scenarios described in the previous two sections. It is simplified by studying only ultimate limit states of the system models.

The economic model takes basis in construction and operation of offshore wind turbines and is explained and exemplified by Brüske [Brü16]. The income calculations are based on the Danish tendering model [Hed16; Nie16], which subsidies 50000 full load hours to a tendered price and subjects the electricity price afterwards to the spot market. The study considers the availability estimated by Faulstich et al. [FHT11]. Operation costs are estimated by Barthelmie and Pryor [BP01] and Hau [Hau13]. The resulting economic base figures are given in Table 8.2. The expenditure 'other' summarizes costs for cables, sub-station, certification, and permissions, which are considered weight independent. The offshore wind energy turbines shall be erected in a water depth of approximately

	Expenditures € / KW	Interest rate %	Operation costs %	Capacity factor %	Availability %
Structure	871.0	5	2	50	90
Installation	548.0				
Reserve	506.0				
Other	1,997.0				

Energy price until year 12.68 € / KW	Energy price after year 12.68 € / KW	Proof test per component €
0.10	0.0675	5,000

Table 8.2: Economic conditions adapted from Damiani et al. [DDS16] and Voormolen et al. [VJS16]

40 m where structure costs of monopiles and jackets are about equal as considered in this study [DDS16]. The planed service life is 25 years. The structural costs are taken from Hobohm et al. [Hob+13] and scenario 1 at location B for the year 2017. The resulting sub-structure cost are 871 € / KW, and the installation costs are 548 € / KW, this cost is assumed for both prior designs. The proof load based design costs are varied according to their reliability for the evaluation of CAPEX changes by adjustments in the posterior design.

The costs of a structure are a function of many variables. In case of an off-shore structure the variables may include water depth, environmental forces, water-structure-soil interaction, contingencies, equipment, and fabrication and construction time. A design with reduced design reliability may influence the structure's mass and complexity, these can influence costs such as material consumption, transport, and installation. Herein it is assumed that one 20^{th} of the sub-structure and installation costs and subsequently the reserve are proportional to the reliability. The reliability dependent costs are calculated as shown in Equation (64) and (65).

It is assumed that the risks are dominated by system failure, due to the ratio of damage to failure consequences of 1 to 100 [TFV17; TSF15]. Therefore, only system failure and survival will be considered in the case study.

8.5.2 Structural model parameters

The systems are designed with two reliability boundary conditions considering explicitly deterioration, which is reducing the system's reliability with time. The first boundary condition applies to the new structure, the second condition applies to the structure at the end of its service-life. Boundary condition (1) constraints the initial reliability to be equal or better than $\beta = 3.3$. Boundary condition (2) requires that the structure's reliability is not smaller than $\beta = 3.1$. The change in the failure consequences is justified if the failure consequences are dominated by the loss of future income, as it would be the case for energy producing facilities. This argument, which supports time dependent target reliabilities is given in the section "Design target of the structures" and is in line with [ST14].

Table 8.3 provides the model distribution parameters that are used in the limit state functions of the structural models (R, S, M_R, M_S), the deterioration W $(\Delta_{i,k}(M_\Delta))$, and the proof load indication (R, M_R, S_{PL}). Spatial interdependence is considered with correlation coefficients $\rho(R) = \rho(M_R) = 0.5$, and W via $\rho(\Delta_k) = 0.75$. The relation of W and Δ_k is given in (8.2).

Parameter	Distribution	Mean	Standard deviation
R design resistance	Lognormal	case dependent	1.0
S design load	Weibull	10.0	$\sqrt{2}$
M_R model uncertainty of R	Lognormal	1.15	$0.15\,\mu(M_R)$
M_S model uncertainty of S	Lognormal	1.0	$0.05\,\mu(M_S)$
$\Delta_{i,k}$ deter. coefficient	Normal	$\hat{M}_\Delta$	0.011
M_Δ deter. conditioning	Normal	0.00001	0.01
S_{PL} proof load	Normal	case dependent	$0.01\,\mu(S'_{PL})$

Table 8.3: Model parameters

8.6 Results

8.6.1 Reliability

The proof load information helps to reduce the failure probability estimates of both system types. Figure 8.6 shows the development of failure probabilities for the modeled proof load test cases with time. The failure probability increase with time due to deterioration. The rate of decrease depends primarily on the proof load level. One can see that the slope becomes steeper for higher proof loads and constant amount of tested components.

The amount of tested components manifests clearly through the overall reduction of failure probability. This is evident through the offset from the prior design baseline (black). Testing all components at the lowest load level has a greater effect on the reliability estimate than testing one component at the highest load level. The reliability

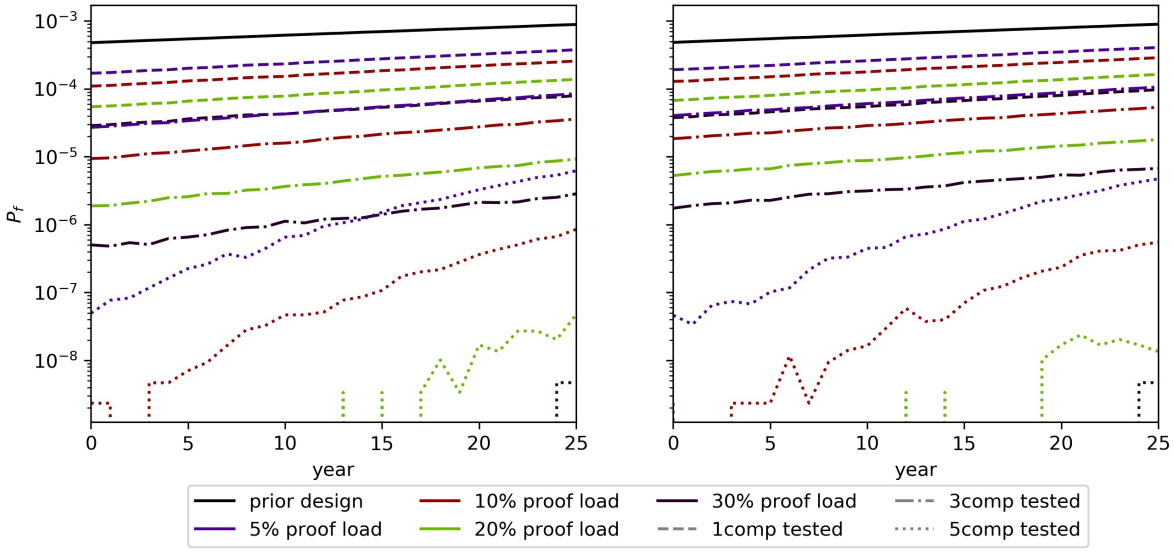

Figure 8.6: Failure probabilities of brittle Daniels system (left) and series system (right). The line style represents the number of tested components, the color represents the proof load level

indices of the prior design brittle Daniels system are $\beta = 3.302$ and $\beta = 3.124$ for service-life beginning and ending, respectively. The same values for the series system are $\beta = 3.300$ and $\beta = 3.122$. Table 8.4 and Table 8.5 list these reliability indices for the various proof load scenarios. ∞ is shown for cases where the computation has not converged. Table 8.4 and Table 8.5 demonstrate that increasing the proof load level and number of tested components is beneficial in terms of the reliability estimate and posterior reliability estimates result in values higher than required by the constraints.

#	$q = 0.05$		$q = 0.10$		$q = 0.20$		$q = 0.30$	
	t_0	t_{25}	t_0	t_{25}	t_0	t_{25}	t_0	t_{25}
1	3.583	3.368	3.695	3.472	3.869	3.635	4.023	3.778
3	4.036	3.759	4.278	3.969	4.623	4.282	4.891	4.537
5	5.329	4.369	5.858	4.786	∞	5.337	∞	5.741

Table 8.4: Service-life beginning and ending reliabilities of brittle Daniels systems in dependence of load level (q) and number of tested components (#)

#	$q = 0.05$		$q = 0.10$		$q = 0.20$		$q = 0.30$	
	t_0	t_{25}	t_0	t_{25}	t_0	t_{25}	t_0	t_{25}
1	3.551	3.347	3.654	3.442	3.817	3.592	3.958	3.724
3	3.942	3.702	4.126	3.873	4.405	4.133	4.640	4.352
5	5.341	4.429	5.858	4.873	∞	5.560	∞	5.741

Table 8.5: Service-life beginning and ending reliabilities of series systems in dependence of load level (q) and number of tested components (#)

The proof loading information can be used to cost optimize the design by using the information to produce a weaker structure that matches the reliability requirements given test data. Here one can see a similar dependence of the failure probability estimate on the amount of tested components and proof load level. The objective of the optimization is to ensure that the reliability of $\beta(t_{25}) \approx 3.1$ is achieved. Therefore all graphs in Figure 8.7 converge on approximately $P_f = 0.001$ at $t_{25} = 25$ years. Unlike before in the models with a prior design of $\beta(t_{25}) = 3.3$, the slope of the graphs depends predominantly on the amount of tested components. The load level is of less significance. Compare to Figure 8.6. The prior designs are based on mean resistance values for the series system $R_{ser} = 18.28$, and the brittle Daniels system $R_{bDS} = 18.14$. With new proof loading information, weaker designs are possible that still fulfill the reliability conditions of $\beta(t_0) = 3.3$ and $\beta(t_{25}) = 3.1$. The new values of R in dependence of the proof load scenario and system type are given in Table 8.6 and Table 8.7. The installation costs

#	$q = 0.05$			$q = 0.10$			$q = 0.20$			$q = 0.30$		
	R	t_0	t_{25}	R	t_0	t_{25}	R	t_0	t_{25}	R	t_0	t_{25}
1	18.08	3.282	3.1	17.97	3.304	3.103	17.7	3.309	3.108	17.44	3.313	3.106
3	17.62	3.312	3.1	17.25	3.316	3.1	16.72	3.337	3.105	16.25	3.326	3.1
5	15.7	3.568	3.1	15.04	3.6	3.105	14.22	3.672	3.107	13.60	3.682	3.102

Table 8.6: Resistance values for the brittle Daniels systems designed with proof load information together with the reliability indices for t_0 and t_{25}. # stands for "number of tested components"

$c_{\text{inst}}(R)$ and structure cost $c_{\text{struc}}(R)$ are calculated depending on the resistance value in Table 8.6 and Table 8.7 by Equations (8.15) and (8.16). $c_{\text{inst,prior}}$, $c_{\text{struc,prior}}$ and R_{prior}

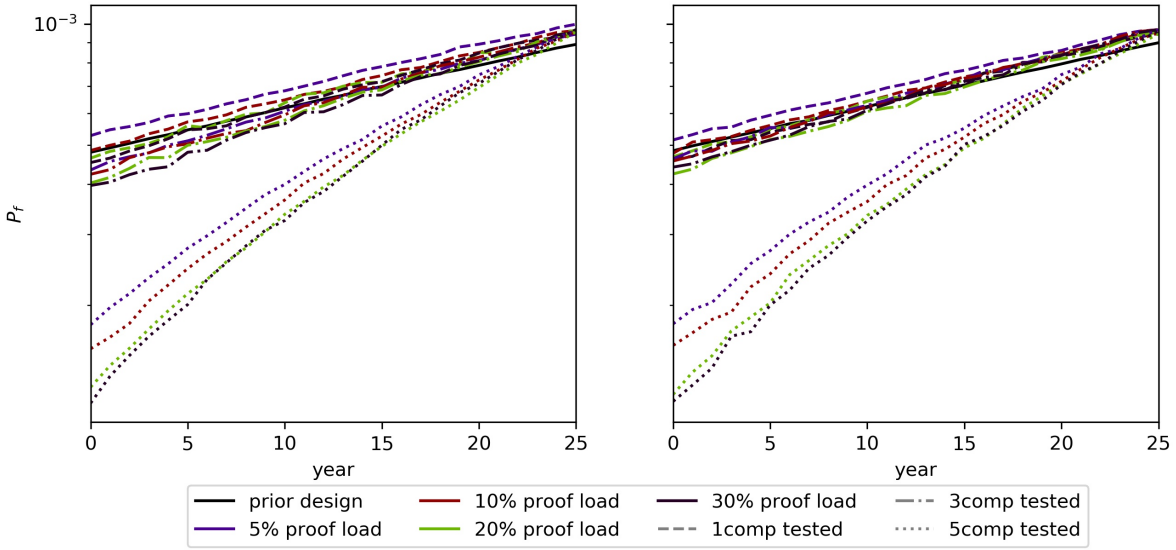

Figure 8.7: Failure probabilities of the optimized brittle Daniels system (left) and the optimized series system (right)

#	$q = 0.05$			$q = 0.10$			$q = 0.20$			$q = 0.30$		
	R	t_0	t_{25}	R	t_0	t_{25}	R	t_0	t_{25}	R	t_0	t_{25}
1	17.91	3.275	3.1	17.80	3.299	3.102	17.53	3.311	3.101	17.25	3.318	3.1
3	17.45	3.33	3.1	17.05	3.337	3.103	16.47	3.351	3.104	16.00	3.355	3.105
5	15.68	3.569	3.1	15.03	3.605	3.103	14.21	3.662	3.104	13.59	3.685	3.1

Table 8.7: Resistance values for the series systems designed with proof load information together with the reliability indices for t_0 and t_{25}. # stands for "number of tested components"

are the prior design investment or structure costs and prior reliability, respectively.

$$c_{\text{inst}}(R) = c_{\text{inst,prior}} \left(0.95 + 0.05 \frac{R}{R_{\text{prior}}}\right) \tag{8.15}$$

$$c_{\text{struc}}(R) = c_{\text{struc,prior}} \left(0.95 + 0.05 \frac{R}{R_{\text{prior}}}\right) \tag{8.16}$$

8.6.2 Value of Information

Equation (5.1) defines $V_{I,\vec{a}^{pr}}$ as the difference of the optimal decision with prior information and the optimal decision with (pre-) posterior information and is formulated for the case study decision problem in Equation (8.5). Applicable actions in the EVSI analysis are limited to actions that are also available in a prior decision analysis. In this EVSI decision scenario the objective is to achieve the highest expected benefit. This benefit is

influenced by the risk of system failure, which results in the loss of the structure. The expected benefit is also reduced by the indirect risk, which is the loss of revenue due to failed production. Figure 8.8 and Figure 8.9 show that the proof load test information reduces both risks effectively. The brittle Daniels system benefits more from the proof load information in terms of risks. The expected cumulative benefit considers next to

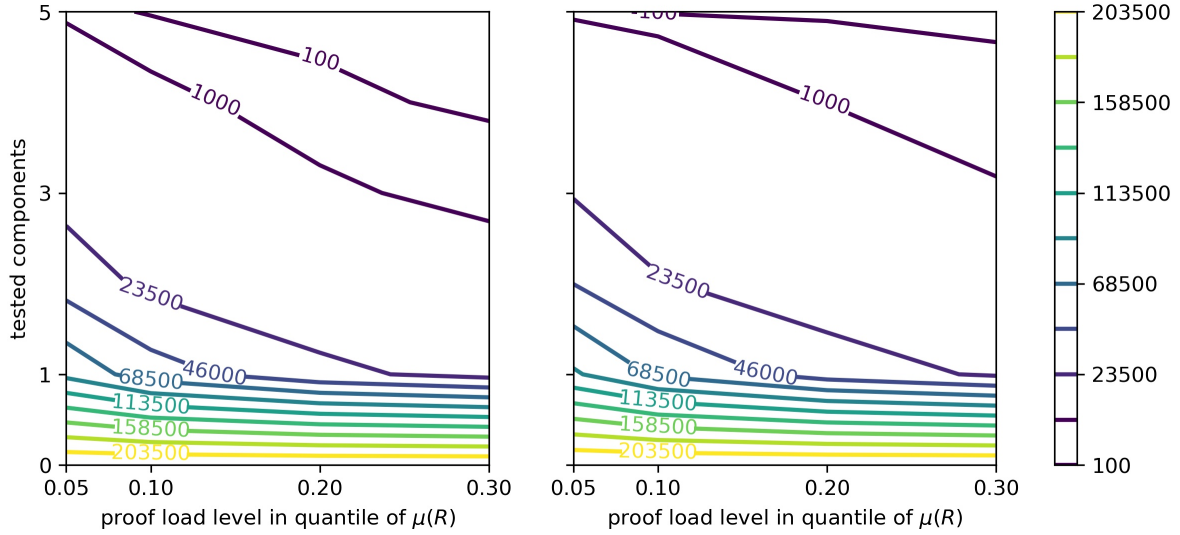

Figure 8.8: Direct risks due to structural failure. Brittle Daniels system (left), series system (right)

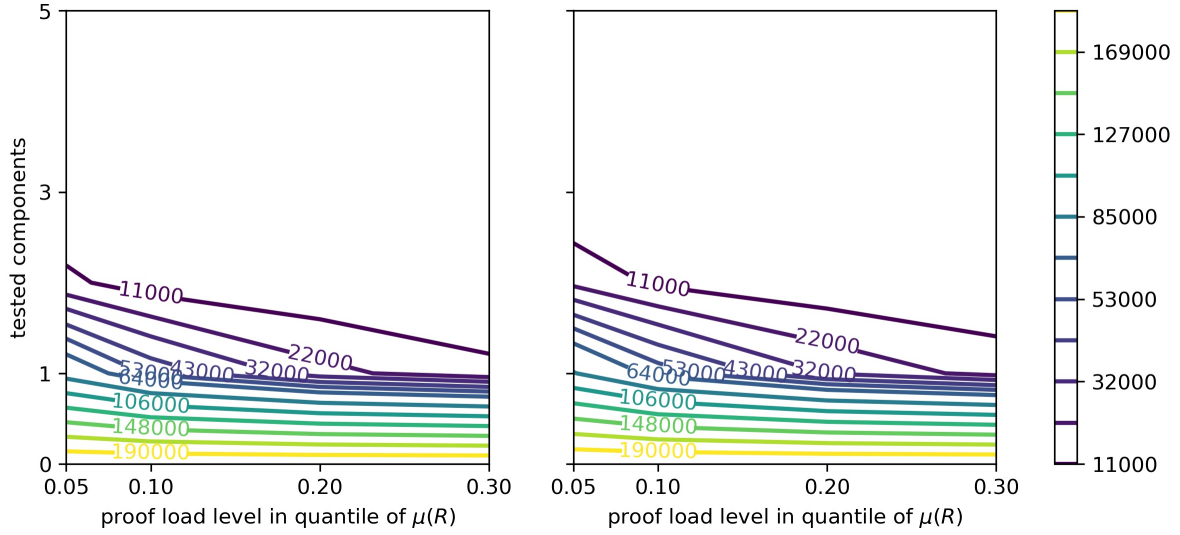

Figure 8.9: Indirect risks of failure, lost revenue due to no production. Brittle Daniels system (left), series system (right)

the risks, the expected benefit from the energy production and offsets all by the CAPEX.

Figure 8.10 shows that the proof load information results in a higher expected benefit. The maximum benefit of brittle Daniels system is € 11,631,557, and the series system yields € 11,629,894.

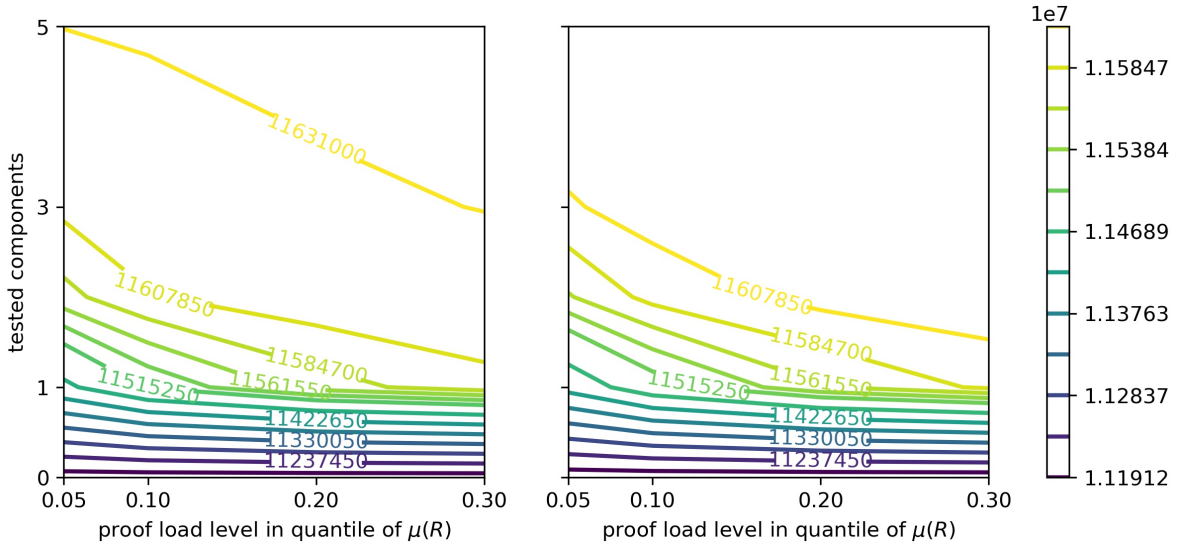

Figure 8.10: The expected cumulative benefit. Brittle Daniels system (left), series system (right)

#	$q = 0.05$	$q = 0.10$	$q = 0.20$	$q = 0.30$
1	287286	346536	402063	428353
3	442286	453386	458557	459645
5	459666	460029	460066	**460068**

Table 8.8: $V_{I,\vec{a}^{pr}}$ for the proof load scenarios of the brittle Daniels system. The optimal value is highlight in bold font. # stands for "number of tested components"

#	$q = 0.05$	$q = 0.10$	$q = 0.20$	$q = 0.30$
1	270992	331329	391608	421965
3	437804	450791	458795	461151
5	462148	462418	462437	**462438**

Table 8.9: $V_{I,\vec{a}^{pr}}$ for the proof load scenarios of the series system. The optimal value is highlight in bold font. # stands for "number of tested components"

Therefore, the optimal decision utilizing proof loading information it to choose the jacket sub-structure and apply proof load testing of all components with the highest load level of $q = 0.3$. The expected benefit obtain with the series system and the brittle Daniels system are only marginally different if all components are tested. Only if less than all

components are tested, the brittle Daniels system appears to perform significantly better than the series system.

8.6.3 Value of information and additional action options

$V_{I,\vec{a}^{pr\&I}}$ incorporates $V_{I,\vec{a}^{pr}}$, therefore only $V_{I,\vec{a}^{I}}$, the part pertaining to new actions options is discussed in the following sections.

Due to the weaker prior design of the structural systems the direct (Figure 8.11) and indirect (Figure 8.12) risks for both systems types increase. Most relevant is the amount of tested components, the more components are tested, the closer the slope of the iso-lines comes to zero. The weak slope towards proof loading all components indicates that risks are almost independent of the test load level. In Figure 8.13 it is apparent that

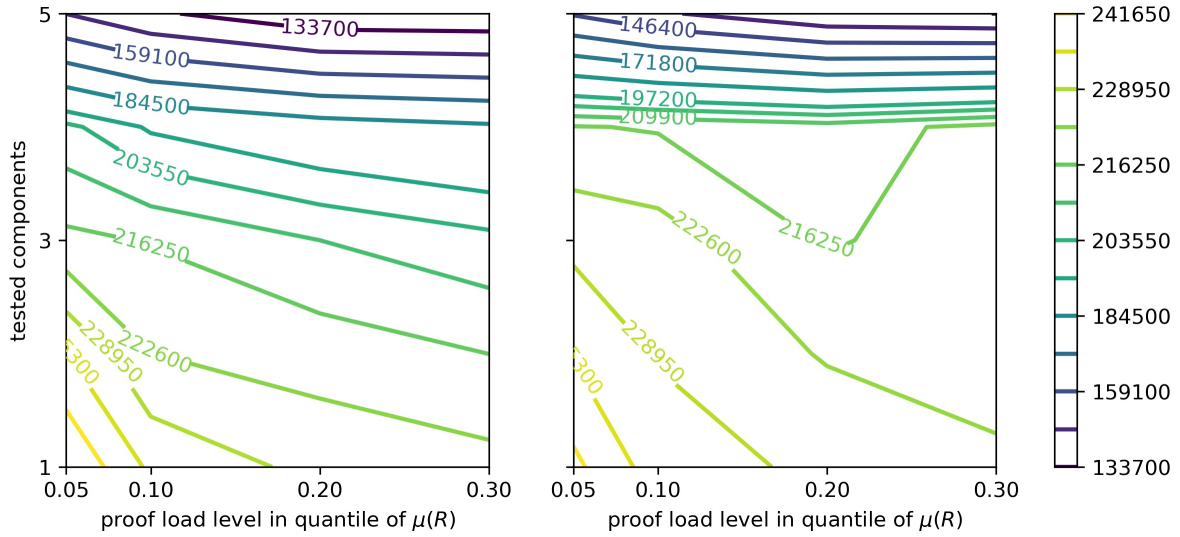

Figure 8.11: Direct risks due to structural failure of proof load information optimized structures. Brittle Daniels system (left), series system (right)

the expected benefit is also hardly sensitive to the proof load level for large fractions of tested components. The iso-lines are almost parallel to the abscissa. The highest utilities are achieved by applying the highest proof load level to all components. The differences in benefit between proof load levels become smaller the higher the load levels rise. With the series system benefit of € 11,773,406, and the brittle a benefit of € 11,780,842 is estimated for actions present in $V_{I,\vec{a}^{pr}}$. Both values are higher than those found in the EVSI analysis.

By comparing the expected benefits via the difference of the prior design with $\beta(t_{25}) =$

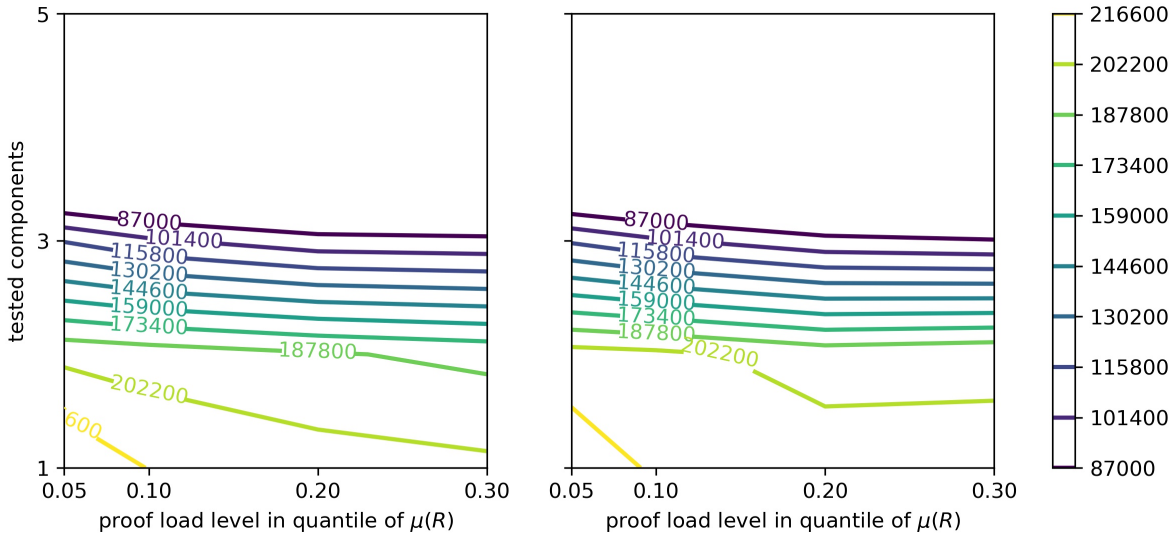

Figure 8.12: Indirect risks of failure, lost revenue due to no production of the proof load information optimized structures. Brittle Daniels system (left), series system (right)

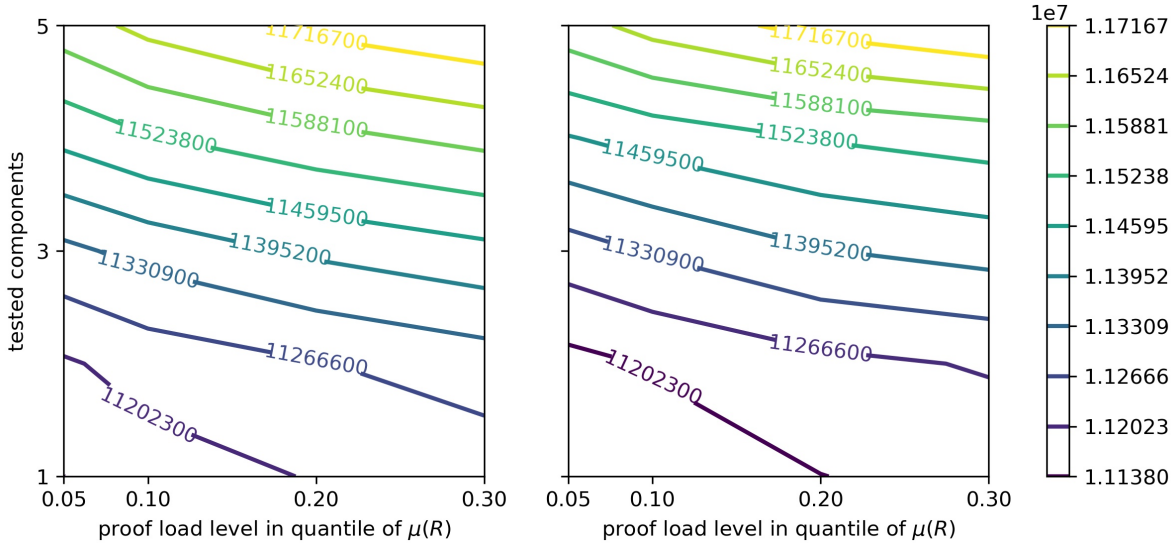

Figure 8.13: The expected cumulative benefit of the proof load information optimized systems. Brittle Daniels system (left), series system (right)

#	$q = 0.05$	$q = 0.10$	$q = 0.20$	$q = 0.30$
1	-33746	-2940	34701	58005
3	143831	181838	235416	271290
5	448535	500331	563147	**601917**

Table 8.10: $V_{I,\vec{a}^I}$ for the optimized design of the brittle Daniels system. The optimal value is highlight in bold font. # stands for "number of tested components"

#	$q = 0.05$	$q = 0.10$	$q = 0.20$	$q = 0.30$
1	-23861	-7046	-33738	56993
3	134447	169491	225151	252406
5	458073	509386	572748	**613385**

Table 8.11: $V_{I,\vec{a}^I}$ for the optimized design of the series system. The optimal value is highlight in bold font. # stands for "number of tested components"

3.3 and the optimized prior designs in Figure 8.14 one finds that the proof load tested prior designs yield higher expected benefits for all parameter combinations except those were all components are with at least load level $q = 0.1$ for the series system and load level $q = 0.2$ for the brittle Daniels system.

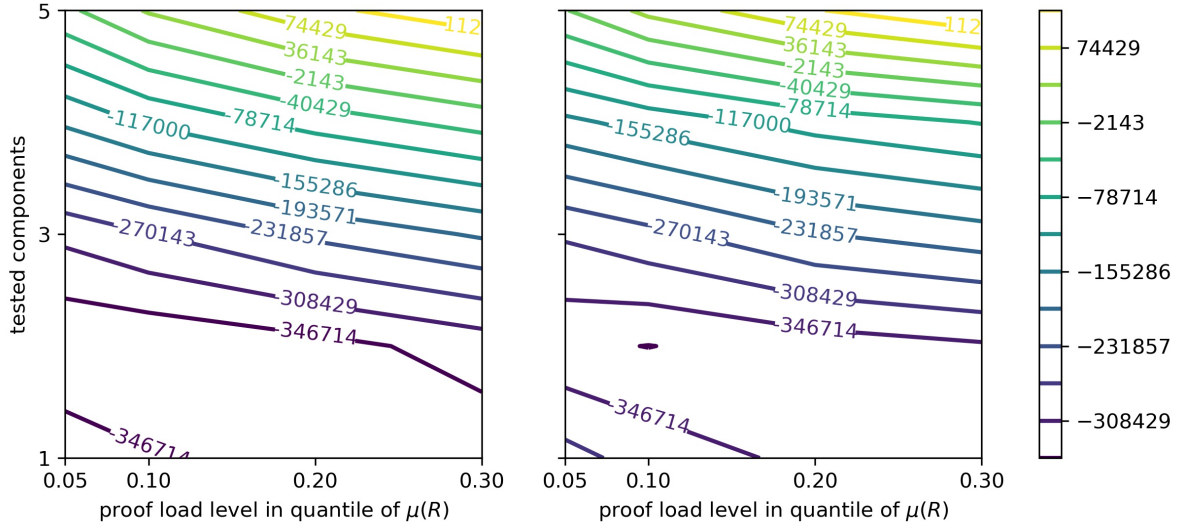

Figure 8.14: Difference of expected benefit between initial design with proof load information and designs optimized with proof load information

Figure 8.15 plots $V_{I,\vec{a}^{pr}}$ (solid) and $V_{I,\vec{a}^{pr\&I}}$ (dashed) over the test load expressed in load dimension, not load level. It is apparent that a higher value can achieved through EVISA analysis although the actual test loads are lower than those required in an EVSI analysis to yield the same value.

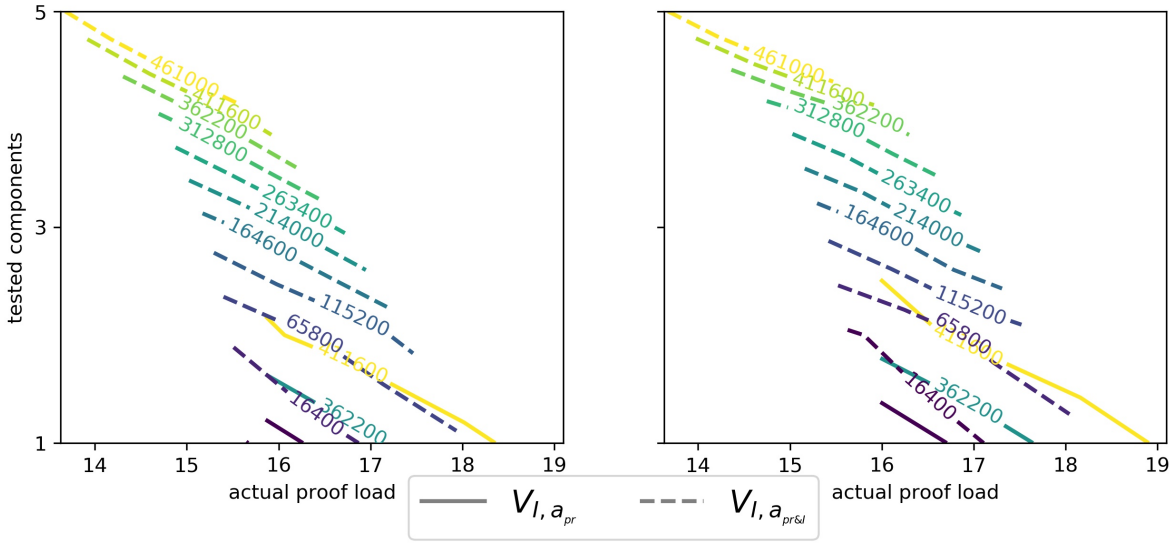

Figure 8.15: Value of information ($V_{,\vec{a}^{pr}}$) and value of information and action ($V_{I,\vec{a}^{pr\&I}}$) vs. test load

8.7 Conclusions

This study introduced the concept of expected value of sample information and additional actions (EVSIA) as a formal method in order to analyze the value of information, and further more to estimate the value of new action alternatives that become possible with the new information.

A case study demonstrates the expected value of sample information (EVSI) analysis and new EVSIA analysis utilizing proof load testing information to obtain an updated reliability estimate and the updated expected life-cycle benefit. EVSI yields the value $V_{I,\vec{a}^{pr}}$, EVSIA yields $V_{I,\vec{a}^{pr\&I}}$, which is at least equal to $V_{I,\vec{a}^{pr}}$ but is potentially greater through a contribution from information with new actions yielding $V_{I,\vec{a}^{I}}$. The case study deals with the decision between using either monopiles or jackets as offshore sub-structures. The formulated decision problem is almost insensitive to the choice of sub-structure in the EVSI analysis, the values of $V_{I,\vec{a}^{pr}}$ differs by about 0.5%. The optimal decision is to choose the monopile sub-structure, proof load test all components of the structure and apply the highest proof load. $V_{I,\vec{a}^{pr}}$ increases with increasing test load and more tested components. In the range of modeled test parameters, the number of tested components appears to be of greater than the test load.

With the EVSIA analysis choosing also the monopile sub-structure shows to be the optimal action. However, the new testing and design scenario in the EVSIA analysis do yield a about 33% higher value $V_{I,\vec{a}^{pr\&I}}$ than those already derived for $V_{I,\vec{a}^{pr}}$. Thus the EVSIA analysis does provide additional value of the EVSI analysis in the case study.

For both, the EVSI and EVSIA analysis, the optimal set of test parameters is to test all components at highest proof load. However, $V_{I,\vec{a}^{pr\&I}}$ yields higher values for several test parameter combination than the optimal test parameters for $V_{I,\vec{a}^{pr}}$. This is the case if less than all components are tested and also for low load levels with all components.

Furthermore, it is noticeable that $V_{I,\vec{a}^{pr}}$ rather insensitive to the load level. This could be of relevance if there is a practical limit to the test load that can be generated.

The structural system models are not based on actual designs and are therefore limited to assume how much the action alternatives arising through EVSIA affect the capital expenditures of the structures. Under other costing circumstances the additional action alternatives could provide the optimal decision.

CHAPTER 9

Decision support framework involving value of information analyses for structural health testing

Brüske, H. & Val D., & Thöns, S. Decision support framework involving value of information analyses for structural health testing. In review. Submitted to *Structural Safety* (2018).

Abstract

In the paper a decision support framework involving value of information (VoI) analysis is proposed for planning of structural health testing (SHT). Since the application of VoI analysis to real structures usually requires complex and computationally expensive solutions a simple structural model capable to simulate key features of the design and assessment processes, structural service performance and testing outcomes is introduced. Special attention is given to the representation of relevant uncertainties and their treatment as new data about a structure are collected from observation of its past performance and by SHT. Regarding the latter, two testing methods are considered – proof load and hybrid simulation. They are discussed in more detail in the context of risk they may pose to a tested structure and their ability to reduce different uncertainties affecting the assessment of the structure condition. The decision framework for SHT planning along with the concept of VoI analysis with an extension that considers the cost of information is then described. An example illustrating the application of the decision framework in combination with the proposed structural model is provided.

9.1 Introduction

Structures, e.g. bridges, or buildings, deteriorate over time due to applied loads and harmful environmental effects that damage their strength and serviceability. To ensure that structures are sufficiently safe and suitable for their intended use they need to be regularly checked, which can be carried out via on-site inspections, continuous/periodic monitoring and/or testing. In principle, all these methods are aimed to assess the health of an examined structure. Historically, various monitoring techniques are referred to as structural health monitoring (SHM). This paper concentrates on various testing methods such as proof load testing (e.g. [SSN96; FVS00; CG13; Lan+18]) and hybrid simulation testing (e.g. [Ben08; SS08; WMS16]), which in the following, by analogy, will be referred to as structural health testing (SHT).

In essence, the purpose of both SHM and SHT is to obtain new information about the current condition of a structure. This information is then used to assess the structure so that, subsequently, decisions can be made regarding what actions (e.g. maintenance, repair, replacement) need to be carried out to ensure that the structure remains fit for its intended use in the future. To select the most efficient course of actions a life-cycle cost-benefit analysis is usually employed to support the decision process (e.g. [Tho12]). In recent years, the owners and operators of structures have become also concerned about the cost efficiency of methods used for the information collection, i.e. SHM and SHT. This issue can be addressed through a value of information (VoI) analysis (e.g. [Str+17]). The latter is based on Bayesian statistical decision theory and requires a pre-posterior analysis, which includes decisions on both inspections (i.e. data collection) and following actions [RS64]. In the context of structural engineering applications, the required analysis is usually very complex since it involves probabilistic modeling of a structure, loads and environmental effects acting on it, relevant deterioration processes and uncertainties associated with employed models and data collection methods. Thus, so far VoI analysis has been applied to the optimisation of SHM in combination with simple structural models (e.g. [PD11; Str14; ZGA14; KSF16; TFV17]).

In this paper a decision support framework involving VoI analysis is proposed for SHT planning. As explained above, an application of VoI analysis to real structures usually requires complex and computationally expensive solutions. By that reason in the previous studies, which focused on SHM, simple idealised structural models have been employed. A similar approach is used in this paper as well. A simple structural model capable to simulate key features of the design process, structural service performance and testing outcomes is presented. Special attention is given to the representation of relevant uncertainties and their treatment as new data about the structure are collected from observation of its past performance and by SHT. Regarding the latter, two testing methods are considered – proof load and hybrid simulation. They are discussed in more detail in the context of risk they may pose to a tested structure and their ability to reduce different uncertainties affecting the assessment of the structure condition. The decision

framework for SHT planning along with the concept of VoI analysis is then described. An example illustrating the application of the decision framework in combination with the proposed structural model is provided.

9.2 Structural model and relevant uncertainties

The aim of this section is to formulate a structural model that is sufficiently simple to be used with VoI analysis but at the same time able to represent major sources of uncertainty associated with structural design and assessment. Since most structures are statically indeterminate the model is presented as a parallel system of n components, which is schematically shown in Figure 9.1a. Each component is characterised by two geometric properties: A_i – cross-sectional area and l_i – length, and its material can be modeled as either linearly elastic or brittle (Figure 9.1b) or linearly elastic perfectly plastic (Figure 9.1c); S represents the total load resisted by the system. As it becomes clear from the stress-strain diagrams shown in Figure 9.1, E_i denotes the modulus of elasticity, $f_{y,i}$ the yield stress, $\varepsilon_{y,i}$ the yield strain, $f_{u,i}$ the ultimate strength and $\varepsilon_{u,i}$ the ultimate strain of the material. If necessary, components with limited plasticity, i.e. plastic strain in the diagram in Figure 9.1c is limited by $\varepsilon_{u,i}$, can also be considered.

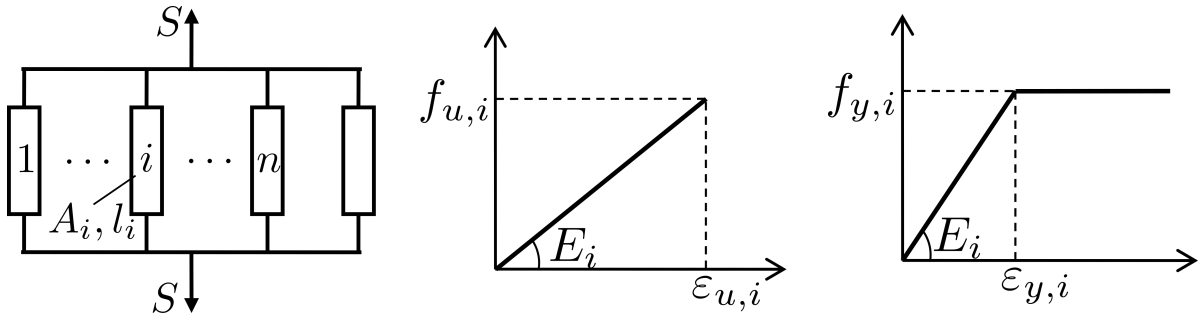

(a) (b) (c)

Figure 9.1

To account for inherent variability associated with loads acting on a structure, S is treated as a random variable. There is uncertainty related to a selected load model, which can be described by a random variable α_S so that in a probabilistic analysis the load is represented as the product of the two random variables, i.e. as $\alpha_S\, S$. Often, a combination of several loads needs to be considered. In this case, the total load can

be expressed as the sum of random variables representing the individual loads, each of them multiplied by a random variable which accounts for the corresponding model uncertainty.

In the design process load effects in each structural component are typically determined by performing a global structural analysis. For simplicity, this can be considered as a distribution of the total applied load between the components. Thus, the load effect in the i$^{\text{th}}$ component, S_i, can be expressed as

$$S_i = \eta_i \, \alpha_S \, S \tag{9.1}$$

where η_i is the fraction of the applied load resisted by the component and

$$\sum_{i=1}^{n} \eta_i = 1 \tag{9.2}$$

There is uncertainty introduced by global analysis due to inaccuracies and simplifications associated with the structural model employed in the analysis. To account for that the coefficients η_i can be treated as random variables, which are not independent since they need to satisfy Equation (9.2). It is logical to assume that these variables are non-negative and have the same type of distribution.

After load effects in components have been determined, it is necessary to verify that the components have sufficient resistance to withstand these load effects. In the context of the structural model described herein, the resistance of the i$^{\text{th}}$ component, R_i, can be expressed as $R_i = A_i \, f_{y(u),i}$ (whether it is f_y or f_u depends on the material of the component). Due to inherent variability of materials their strengths, i.e. f_y and f_u, are modeled as random variables. There is also uncertainty associated with a resistance model, which can be taken into account by introducing a random variable α_R. The limit state function for the i-th component in the context of ultimate limit state, $g_{f,i}$, can then be formulated as

$$g_{f,i} = \alpha_{R,i} \, R_i - S_i = \alpha_{R,i} \, A_i \, f_{y(u),i} - \eta_i \, \alpha_S \, S \tag{9.3}$$

The required cross-sectional area, A_i, of the component can be found from the condition that the probability of its failure $P_{f,i} = P[g_{f,i} \leq 0]$ should not exceed a target value P_{fT}. A more advanced approach, which is rarely used in practice, is to evaluate the probability of failure of a whole structural system and ensure that it is less than a target value. For a structural system with parallel components, like the system shown in Figure 9.1a, the probability of failure can be defined as

$$P_f = P\left[\bigcap_{i=1}^{n} (g_{f,i} \leq 0)\right] \tag{9.4}$$

For a parallel system with perfectly ductile components, i.e. their materials have a stress-strain diagram shown in Figure 9.1c, the calculation of the probability of the system failure can be simplified. In this case the limit state function can be written for the whole system as

$$g_f = \sum_{i=1}^{n} \alpha_{R,i}\, A_i\, f_{y,i} - \alpha_S\, S \tag{9.5}$$

and the probability of the system failure is determines as $P_{f,i} = P[g_f \leq 0]$.

A structure becomes unfit to its intended use also due to serviceability failures, which can be reversible and irreversible. In the case of irreversible serviceability failure the structure becomes permanently damaged. The limit state function for serviceability failure of the i$^{\text{th}}$ component, $g_{d,i}$, can be expressed as

$$g_{d,i} = a_{lim,i} - a_i \tag{9.6}$$

where $a_{lim,i}$ is the limit value of a certain parameter, which characterises the serviceability performance of the component (e.g. deflection, stress) and a_i the value of this parameter caused by applied load, which usually depends on the load effect S_i. If $g_{d,i}$ represents irreversible serviceability failure then the probability of the component damage is $P_{d,i} = P[g_{d,i} \leq 0]$. Since a structure is damaged when any of its components has been damaged then the probability of the structure damage is

$$P_d = P\left[\bigcup_{i=1}^{n} (g_{d,i} \leq 0)\right] \tag{9.7}$$

SHT is usually performed when a structure deteriorates over its service life. Deterioration of the i$^{\text{th}}$ component of the presented structural model can be simulated through reduction of its cross-sectional area, e.g. as linear function of time t

$$A_i(t) = A_{0,i}(1 - w_r\, t) \tag{9.8}$$

where $A_{0,i}$ is the initial cross-sectional area of the component and w_r the deterioration rate. To take into account uncertainty associated with deterioration w_r can be treated as a random variable. Of course, more complex deterioration models can also be employed. This formula for $A_i(t)$ is then substituted in Equations (9.3) (or (9.5)) so that the limit state functions $g_{f,i}$ (or g_f) and, subsequently, the probability of failure become time-dependent. Since the reduction of A_i may also affect a_i in Equation (9.6) the probability of damage may become time-dependent as well.

9.3 Testing options

Generally, relevant new information about an existing structure can be obtained based on its past performance and also by its inspection, SHM and/or SHT. However, within

the scope of this paper, only the past performance and SHT, namely proof load and hybrid simulation testing, are considered. In the following it will be discussed how data from these sources can be utilised to reduce the uncertainties affecting the structural reliability assessment, which have been defined in the previous section. In addition, a brief description of proof load and hybrid simulation testing will be provided.

9.3.1 No testing

No testing implies that no tests of a structure (or its components) are conducted before and at the time of its assessment. This does not exclude inspections (e.g. visual) of the structure, which may be required during its service life before the assessment. Some local damage to the structure can be detected at such inspections and, subsequently, repaired. However, it is assumed that any relevant data collected at the inspections have been integrated into prior information used at the time of assessment.

The only new information that is taken into account in this case is the fact that the structure has survived all loads acting on it before the assessment. Moreover, the calculation of the probability of failure of the structure before and after the assessment at any point in time must be conditional on the structure's survival up to this point. In principle, this requires computing the outcrossing rate of a stochastic process representing load through a time-dependent barrier, which represents the resistance of a deteriorating structure. In practice, the problem is often simplified by dividing time into discrete intervals. For each time interval the load is described by a distribution of its maximum value within this interval while the resistance is treated as a random variable with a constant mean value, e.g. in the middle of the interval. It is convenient to consider one-year intervals since for this period of time distributions of maximum loads, deterioration rates and target probabilities of failure are usually available/given. Using this approach, the probability of failure of the structural system presented in the previous section in year j given its survival in all previous years, $P_f(t_j|t_{j-1})$, can be expressed based on Bayes' theorem as

$$P_f(t_j|t_{j-1}) = \frac{P\left[\left(\bigcap_{i=1}^{n} g_{f,i}(t_j) \leq 0\right) \cap \bigcap_{t=t_1}^{t_{j-1}} \left(\bigcup_{i=1}^{n} (g_{f,i}(t) > 0)\right)\right]}{P\left[\bigcap_{t=t_1}^{t_{j-1}} \left(\bigcup_{i=1}^{n} (g_{f,i}(t) > 0)\right)\right]} \tag{9.9}$$

In the case of a parallel system with perfectly ductile components, (9.9) can be simplified and becomes

$$P_f(t_j|t_{j-1}) = \frac{P\left[(g_f(t_j) \leq 0) \cap \bigcap_{t=t_1}^{t_{j-1}} (g_f(t) > 0)\right]}{P\left[\bigcap_{t=t_1}^{t_{j-1}} (g_f(t) > 0)\right]} \tag{9.10}$$

The influence of the load history on the reliability of deteriorating structures was investigated in Stewart and Val [SV99], where it was also shown that $P_f(t_j|t_{j-1})$ could be relatively easily calculated by Monte Carlo simulation.

Regarding damage, it is assumed that a structure which has been damaged can be repaired and damaged again. However, in the context of Monte Carlo simulation a structure that has failed in a certain year during its considered design life is excluded from further analysis and, therefore, its possible damage in this and following years are not be counted.

9.3.2 Proof load testing

Load testing of an existing structure is performed in order to: (i) demonstrate that the structure is capable to support a certain rated load without violating prescribed safety conditions – proof load test; or (ii) collect new data about the structure for validation/calibration of its analytical/numerical model which is then to be used for the structure's assessment – diagnostic load test (e.g. [Lan+18]). In proof load tests high loads need to be applied, in some cases more than twice of the rated load [SV99; SN98], that may damage or even cause a collapse of the structure. Thus, this type of test is often carried out when the structure has failed an assessment using available analytical/numerical approaches. In diagnostic load tests applied loads are within service limits, hence, risk to damage the structure is usually negligible.

In the context of this paper, the emphasis is on data that the test can provide and how these new data can reduce uncertainty associated with prior information. At the same time, the level of applied load is not limited in terms of the probabilities of damage and failure that it can cause, although these probabilities are evaluated. Thus, in the following such load tests will be referred to as proof load tests and be distinguished in terms of the level of instrumentation used in the test, namely 'without instrumentation' and 'with instrumentation'. The former term does not mean that no instrumentation has been used in the test. It simply means the level of instrumentation is insufficient to accurately determine the distribution of applied load between the structural components; thus, uncertainty associated with the load distribution coefficients η_i's remains unchanged after the test. In the case 'with instrumentation', it is assumed that this uncertainty has been eliminated so that after the test the η_i's are treated as deterministic parameters represented by their mean values.

The main new information produced by proof load testing is that the structure has survived (or failed) the test. In the case of the structure's survival its probability of failure after that the test, $P_f(t_j|t_{PL})$, in which t_{PL} is the time of the test and $t_j > t_{PL}$,

can be expressed as

$$P_f(t_j|t_{PL}) = \frac{P\left[\bigcap_{i=1}^{n}(g_{f,i}(t_j) \leq 0) \cap \bigcup_{i=1}^{n}(g_{f,i}(t_{PL}) > 0)\right]}{P\left[\bigcup_{i=1}^{n}(g_{f,i}(t_{PL}) > 0)\right]} \tag{9.11}$$

where $g_{f,i}(t_{PL})$ denotes the limit state function given by Equation (9.3), in which S is replaced by the total load during the test, S_{PL}. The latter is usually a combination of the load applied in the test and permanent load. Of course, the effect of load history represented by Equation (9.9) should also be taken into account. In the case of a parallel system with perfectly ductile components Equation (9.11) becomes

$$P_f(t_j|t_{PL}) = \frac{P\left[(g_f(t_j) \leq 0) \cap (g_f(t_{PL} > 0))\right]}{P\left[g_f(t_{PL} > 0)\right]} \tag{9.12}$$

It is worth to note that non-survival of a proof load test by a structure does not necessarily mean that the structure physically collapses during the test. The test can be stopped earlier, when it becomes clear that the structure is incapable to sustain the load level planned for the test. However, insufficient strength of the structures is demonstrated so that the latter is decommissioned after the test.

9.3.3 Hybrid simulation testing

Hybrid simulation testing is described as a combination of physical testing of structural parts in a laboratory and numerical (e.g. finite element) modeling of the rest of the structure [Ben08; SS08]. This way the interaction of the tested structural component with modeled parts of the structure can be simulated. Loads applied to the component result in its physical responses that are measured and used as boundary conditions for the modeled part of the structure. The reaction of the model is then used to modify the applied loads and so forth, until the component fails. Typically, hybrid simulation is employed to investigate the performance of a structure and its critical components under dynamic loading. However, it can also be performed for other types of loading, e.g. quasi-static or even thermomechanical [WMS16]. This type of testing does not pose any risk to the structure, while at the same time prototypes of critical components of the structure can be tested up to failure. Such an arrangement enables to significantly reduce uncertainty associated with the resistance models of the components, i.e. $\alpha_{R,i}$. In the following, it will be assumed that this uncertainty can be fully eliminated due to the test design and with a statistically significant number of tests. In principle, hybrid simulation can also reduce uncertainty in the load distribution, i.e. η_i's, due to more sophisticated and accurate structural modeling. However, this will not be taken into account in further analysis.

9.4 Decision support framework and value of information with information-cost analysis

9.4.1 Decision-making process

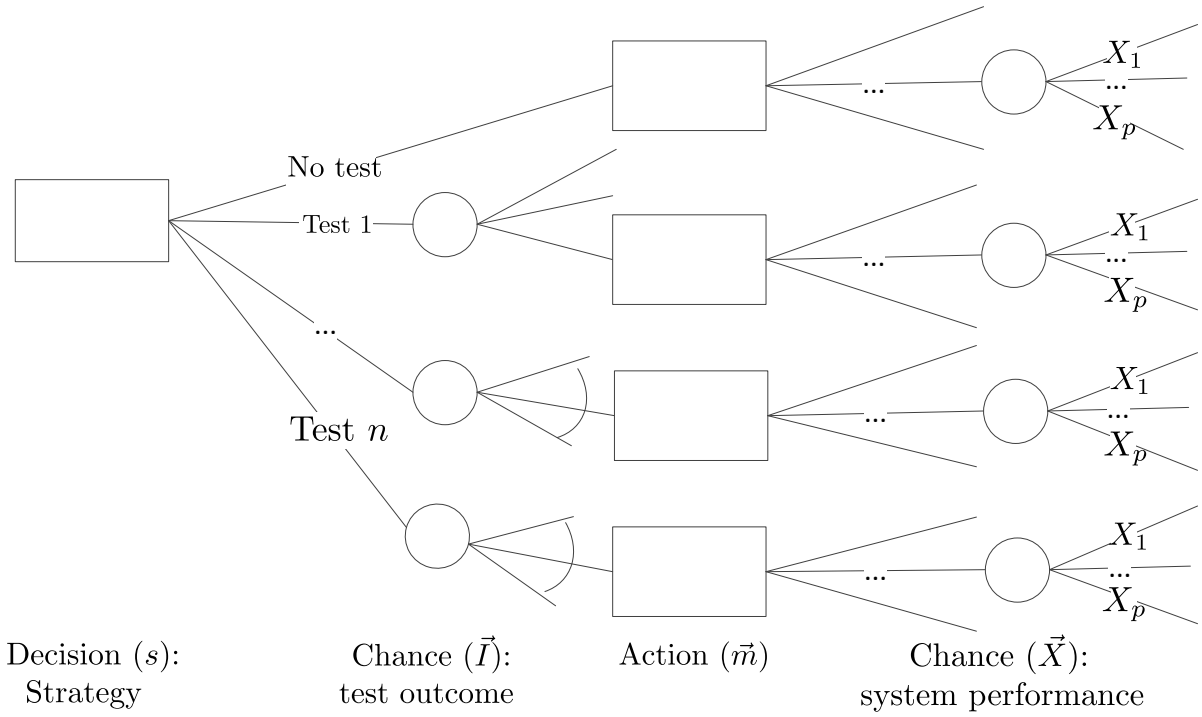

Figure 9.2: Decision tree of generic SHT decision-making framework

A decision maker (DM) may need to deal with a structure that fails the reliability assessment based only on prior information about the structure, which is usually strongly affected by epistemic uncertainty (i.e. uncertainty associated with the lack of knowledge and data). This uncertainty may be reducible with new (i.e. posterior) information acquired through SHT; two possible testing methods, including their influence on different types of uncertainty, are described in Section 9.3. In this case, in order to identify an optimal course of actions a pre-posterior decision analysis needs to be performed. In this analysis a DM can choose from a variety of possible tests, which, for generality, are now simply numbered from Test 1 to Test n (see Figure 9.2). Each test has a random outcome $\vec{I}$, which is a realisation either from a discrete (e.g. Test 1) or continuous (e.g. Test n) result space. Each test outcome $\vec{I}$ is followed by a set of possible actions, $\vec{m}$. Each action may be specific to a particular test or even its outcome, e.g. if the structure is destroyed by the test the number of choices is consequently reduced. This justifies the introduction of decision rules based on the state of nature, regulations, or DM preferences that reduce the decision tree. Finally, the random performance $\vec{X}$ of

the considered structure is determined via the probabilities of the structure's states X_1 to X_p.

9.4.2 Value of information

The utility can be defined by costs or benefits. The value of information (V_I) is determined as the difference between the optimal utility obtained using only prior information, U_{prior}, minus the optimal utility obtained computed with (pre-) posterior information, U_{post}, when the utilities are expressed in terms of costs as $V_{I,cost}$

$$V_{I,cost} = U_{prior} - U_{post} \tag{9.13}$$

and the other way around when the utilities represent benefits as $V_{I,benefit}$, see Equation (9.14).

$$V_{I,benefit} = U_{post} - U_{prior} \tag{9.14}$$

The optimization of the utility is then expressed as minimisation as shown in Equation (9.15) for costs or maximisation for benefits, see Equation (9.16)

$$V_{I,cost} = \min_{\vec{m}} E_{\vec{I},\vec{X}} \left[U_{prior}(\vec{X}, \vec{m}) \right] - \min_{s,\vec{m}} E_{\vec{I},\vec{X}} \left[U_{post}(\vec{I}, \vec{X}, s, \vec{m}) \right] \tag{9.15}$$

$$V_{I,benefit} = \max_{s,\vec{m}} E_{\vec{I},\vec{X}} \left[U_{post}(\vec{I}, \vec{X}, s, \vec{m}) \right] - \max_{\vec{m}} E_{,\vec{X}} \left[U_{prior}(\vec{X}, \vec{m}) \right] \tag{9.16}$$

Herein, the initial decision s is whether to test or not, and if 'yes' how to test. Each alternative has a time independent cost. The tests have random outcomes ($\vec{I}$) that influence the estimation of the structural performance. The next step is to choose from the action alternatives ($\vec{m}$). The set of actions $\vec{m}$ is identical for each decision s, if however, an action is no longer possible due to a certain outcome $\vec{I}$ it may be disregarded. The structure's performance ($\vec{X}$) determines the time dependent part of the expected utility via the structural model.

Since costs and benefits may occur at different times to obtain consistent results the utilities U_{post} and U_{prior} are usually discounted to present values using the following equation

$$U(t_d) = \frac{U_0}{(1+r)^{\frac{t}{d}}} \tag{9.17}$$

where $U(t_d)$ is the present value of the utility that occurs at time t_d since decision making, U_0 the value of the utility at the time of decision making (i.e. $t_d = 0$) and r the discount rate. To calculate the expected utility in Equations (9.15) and (9.16), the values from Equation (9.17) are multiplied by the corresponding probabilities of occurrence.

9.4.3 Value of information with information-costs

While it is useful to know V_I for decision making, the final decision will also depend on the costs of obtaining this information, which in the following will be referred to as 'information-costs'. Thus, value of information with information-costs, $V_{I\&C}$, is a simple extension of Equations (9.13) or (9.14) to include also the costs of prior, C_{prior}, and posterior, C_{post}, information to be obtained. Prior information is often considered without associated costs but this may not be the case if the prior information comes from certain action (e.g. analysis).

$$V_{I\&C,cost} = (U_{prior} + C_{prior}) - (U_{post} + C_{post}) \tag{9.18}$$

$$V_{I\&C,benefit} = (U_{post} + C_{post}) - (U_{prior} + C_{prior}) \tag{9.19}$$

9.5 Illustrative example

The main purpose of this example is to illustrate the decision-making framework and, therefore, a number of simplifying assumptions about the considered structure, its condition and environment, SHT strategies, and actions pertaining the structure's use will be introduced. These assumptions may be adjusted or changed in order to apply the framework to different SHT scenarios and structures, including more accurate and detailed modeling. In particular, this concerns the structural model employed herein, which has been chosen because of its ability to represent essential features associated with structural design, testing and assessment, including the treatment of uncertainties, relevant for the illustration. However, this structural model is not necessarily suitable to describe the behaviour of a specific structure.

9.5.1 Structural model and probabilistic description of associated uncertainties

The structure considered in the example is represented by the structural model described in Section 9.2. For simplicity, it consists of three parallel components (i.e. $n = 3$) made from linearly elastic perfectly plastic material. It is assumed that properties of the components are completely uncorrelated. The yield stress of the material is treated as a lognormal random variable with mean equal to 400 MPa and coefficient of variation (COV) 0.07. Since the components are uncorrelated, the material yield stress of each component is represented by an independent random variable.

The structure is subject to the combination of permanent load, S_G, and variable load, S_Q. The permanent load is a normal random variable with mean of 1.5 MN and COV of 0.1. The variable load is a cyclic load; its magnitude in one cycle follows a normal

distribution with mean of 0.5 MN and COV of 0.40. The analysis will be carried out on annual basis, therefore, the distribution of the maximum annual load is of interest. The permanent load can be treated as time-independent. It is assumed that $N = 1000$ cycles of the variable load is expected per year. Thus, the maximum annual variable load, S_{QN}, can be represented by a Gumbel distribution with the following parameters

$$\alpha_N = \frac{\sqrt{2\ln(N)}}{\sigma(S_{Q_1})} \tag{9.20}$$

$$u_N = \mu(S_{Q_1}) + \sigma(S_{Q_1})\left(\sqrt{2\ln(N)} + \frac{\ln(\ln(N)) + \ln(4\pi)}{2\sqrt{2\ln(N)}}\right) \tag{9.21}$$

where $\mu(S_{Q_1})$ and $\sigma(S_{Q_1})$ are the mean and standard deviation of load in one cycle. This variable load modeling is similar to modeling the maximum traffic load on bridges (e.g. [SCG17]). The total maximum annual load can then be expressed as the sum of the two random variables

$$S = S_G + S_{QN} \tag{9.22}$$

The random variables representing the uncertainty of the resistance model, $\alpha_{R,i}$ $(i = 1, \ldots, 3)$ are modeled as normal random variables with mean of 1 and COV 0.10. The random variable representing the uncertainty of the load model, α_S, is not taken into account since the posterior information considered in the example does not affect it. Thus, for simplicity, α_S is neglected. To account for uncertainty associated with global structural analysis, the coefficients η_i's representing the load distribution between the structural components are treated as non-negative random variables with the same type of distribution. The sum of these random variables should satisfy Equation (9.2). It can be proven that this condition is satisfied when random variables are defined as follows by Ruschendorf and Uckelmann [RU02]

$$\eta_1 = B\,\cos(X) + \mu_{\eta_1}; \eta_2 = B\,\cos\left(X + \frac{2}{3}\pi\right) + \mu_{\eta_2}; \eta_3 = B\,\cos\left(X - \frac{2}{3}\pi\right) + \mu_{\eta_3}; \tag{9.23}$$

where μ_{η_i} $(i = 1, \ldots, 3)$ are mean values of η_i with sum equal to 1, B and X independent random variables with X uniformly distributed on $(0, 2\pi)$. It is assumed that the load is equally distributed between the components so that $\mu_{\eta_i} = 1/3$. B is then represented by a Beta random variable distributed on $(-1/3, 1/3)$ with zero mean. It can then be shown that the variance of η_i equals $1/2\sigma_B^2$, where σ_B is the standard deviation of B. If to assume that the COV of η_i is 0.10 then $\sigma_B = \sqrt{2} \times 0.10 \times 1/3 = \sqrt{2}/30$.

The serviceability limit state is defined as exceedance of yield stress in any of the structural components. This means that in Equation (9.6) $a_{lim,i} = f_{y,i}$ and $a_i = S_i A_i$. To design the components, i.e. determine values of A_i, the following annual safety targets are selected: for ultimate limit state the target reliability index $\beta_T = 4.7$ ($P_{fT} = 1.3 \times 10^{-7}$), for serviceability limit state (irreversible) $\beta_T = 2.9$ ($P_{dT} = 1.865 \times 10^{-3}$) [Eur02]. Using

probabilistic analysis it has been checked that if the cross-sectional area of each component is $0.0037\,\mathrm{m}^2$ then both conditions are satisfied (annual probabilities of failure and damage are 1.1×10^{-7} and 1.71×10^{-3}, respectively); in the context of the ultimate limit state the failure of the whole structural system has been considered.

Deterioration of the structure is simulated based on Equation (9.8). It is assumed that the deterioration of the components is uncorrelated. Thus, the deterioration rates of the components are treated as independent random variables with identical lognormal distributions with mean of 0.0021 and COV 0.10. Properties of the random variables used in the example are summarised in Table 9.1.

Variable	Distribution type	Mean	Standard deviation
f_y	Lognormal	400 MPa	28 MPa
S_G	Normal	1.5 MN	0.15 MN
S_{Q1}	Normal	0.5 MN	0.2 MN
α_R	Normal	1.0	0.1
B	Beta on $(-1/3, 1/3)$	0	$\sqrt{2}/30$
X	Uniform on $(0, 2\pi)$	-	-
W_r	Lognormal	0.0021	0.00021

Table 9.1: Description of random variables

9.5.2 Conditions for decision-making

The decision maker (DM) has to deal with a structure that failed a reliability assessment based on prior information in the 51^{th} year of service within a planned 100-year service life. The decision tree in Figure 9.3 begins with four basic SHT decision strategies (s) for the reliability assessment: (i) No testing, (ii) Proof load testing with instrumentation, (iii) Proof load testing without instrumentation, and (iv) Hybrid simulation testing. The strategies (ii) to (iv) have random test outcomes $\vec{I}$ that influence the actions $\vec{m}$. $\vec{I}$ has two possible discrete outcomes (failure or success) for proof load tests, while hybrid simulation testing can, in principle, provide information in the form of continuous outcomes.

However, only one of its outcomes relevant in the context of the example is considered, namely the elimination of the resistance model uncertainty α_R, i.e. confirming that the model for predicting the component resistance is accurate when the actual material strength is known. The possible actions m depend on the chosen SHT strategy. 'No testing' can only allow a change of load rating (CLR) in order to continue operating the old structure in compliance with safety requirements, or replacing the structure with a new one. If the structure fails during a proof load test (i.e. has insufficient strength

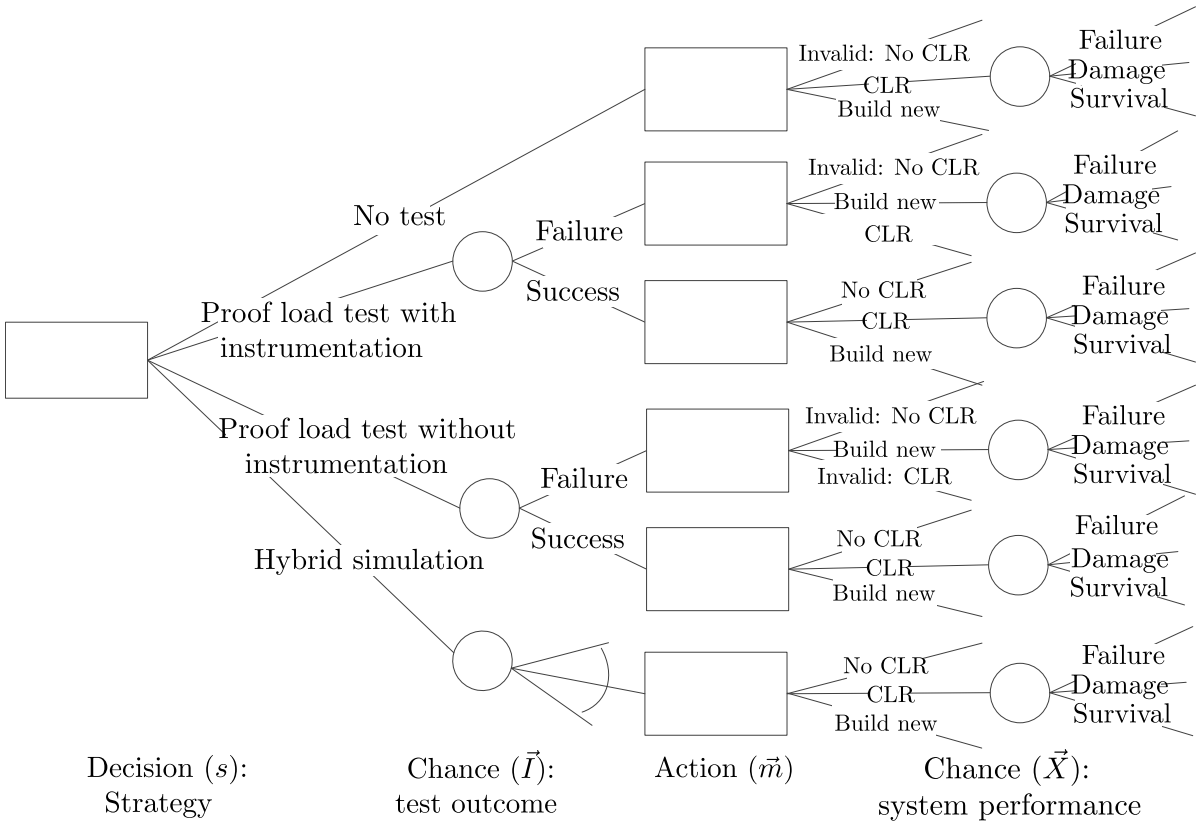

Figure 9.3: Pre-posterior decision tree for structural health testing. Decision nodes are shown as rectangles, and chance nodes as circles

to sustain the proof load) a new structure must be build. A successful proof load test or a hybrid simulation test have the following options: building a new structure, no CLR (in the case of hybrid simulation it may not be always possible, i.e. reduction of uncertainty provided by this test may not necessarily lead to an acceptable reliability assessment), or CLR. Actual values of CLR that ensure that the structure complies with safety requirements for the rest of its service life need to be determined by probabilistic analysis. All actions that are known beforehand not to be allowed because they cannot fulfill safety requirements are noted as 'invalid' in Figure 9.3 and cannot be chosen based on this decision rule.

9.5.3 Results of probabilistic analyses

The original structure being subject to deterioration has cumulative probabilities of failure of 6.80×10^{-5} and 7.48×10^{-5} at $t = 50$ and 51 years, respectively, as assessed with prior information (see Figure 9.4). This requires SHT or another actions (e.g. CLR or replacement with a new structure) in year 50 since the corresponding target probability is $P_{f,T:t=50} \approx 7.23 \times 10^{-5}$ ($\beta_{T:t=50} = 3.8$) for 50 years according to Eurocode 0

[Eur02]. If the structure is left unattended its cumulative probability of failure increases to 5.86×10^{-3} at the end of the planned 100-year long service life, while the target probability of failure for this period determined based on recommendations of Eurocode 0 [Eur02] is $P_{f,T:t=100} \approx 1.30 \times 10^{-4}$.

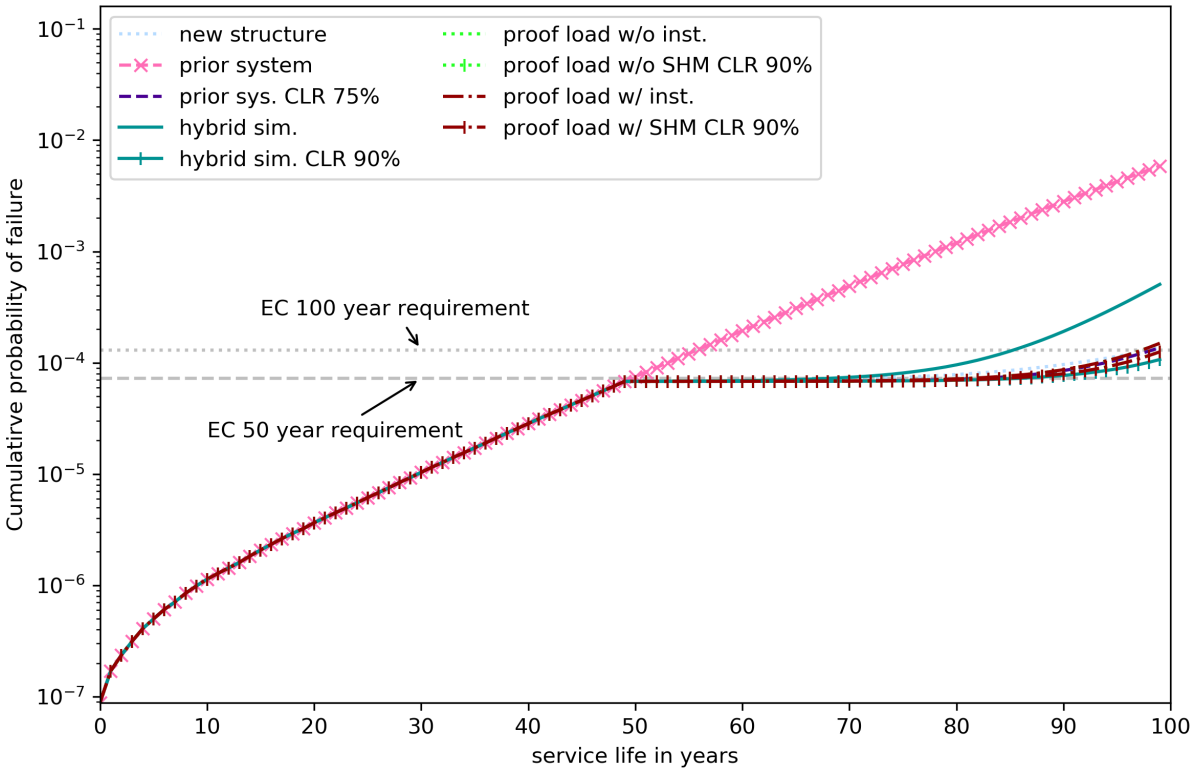

Figure 9.4: Comparison of cumulative failure probabilities for each SHT scenario

In order to satisfy the safety requirement in the case of 'no testing' the structure is either replaced with a new one (the cumulative probability of failure at t = 100 years is then $P_{f:t=100} = 1.36 \times 10^{-4}$, i.e. negligibly higher than the target value) or its load rating should be reduced to 75% of the original one, i.e. CLR 75% (once again $P_{f:t=100} = 1.36 \times 10^{-4}$) – see Figure 9.4. In the case of proof load testing, when the structure survives the proof load of 1.975 MN the cumulative probability of failure after 100 years becomes $P_{f:t=100} = 1.44 \times 10^{-4}$, i.e. just slightly higher than its target value. However, the probabilities of failure and damage during the test are $P_{f,PL} = 5.66 \times 10^{-2}$ and $P_{d,PL} = 0.4607$, respectively.

Hybrid simulation testing does not pose any risk to the real structure and enables to reduce uncertainty associated with its resistance modeling. As noted above, it is assumed in the example that this uncertainty is completely eliminated. However, it only helps to decrease the cumulative probability of failure after 100 years to 5.00×10^{-4} that is insufficient. Thus, reduction of load rating is also required in this case. It has been found

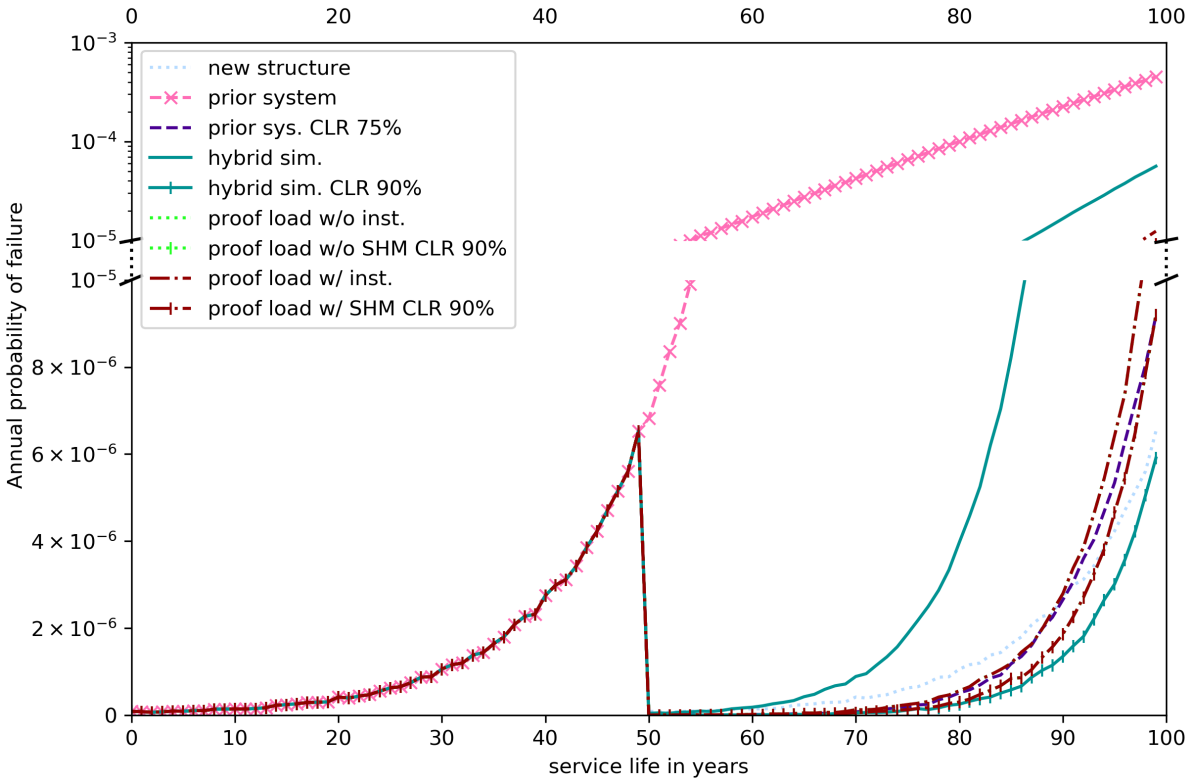

Figure 9.5: Comparison of annual failure probabilities. The figure is split in two parts using a linear y-axis (bottom) and a log y-axis (top); failure probabilities due to the proof load tests are not displayed

that reducing it to 90% of the original one, i.e. CLR 90%, leads to $P_{f:t=100} = 1.01 \times 10^{-4}$ that is smaller than its target value. In order to achieve better consistency in comparison between the different strategies, proof load testing with CLR 90% is also considered. In this case, to comply with the safety requirement the proof load of 1.75 MN needs to be applied. If the structure survives this proof load along with CLR 90% after the test results in $P_{f:t=100} = 1.19 \times 10^{-4}$ ($< 1.30 \times 10^{-4}$). The probabilities of failure and damage during the test are then $P_{f,PL} = 9.97 \times 10^{-3}$ and $P_{d,PL} = 0.2969$, respectively. The cumulative and annual probabilities of structural failure before and after SHT are shown in Figure 9.4 and Figure 9.5, respectively.

As explained previously, it is assumed in the example that damage to the structure is repaired and then may reoccur again. This means that the calculation of the cumulative probability of damage similar to that of failure does make sense. Thus, only annual probabilities of damage have been calculated and these results are shown in Figure 9.6. In this context, it is worth to note that proof load testing with instrumentation enables to eliminate uncertainty associated with the prediction of the load distribution between the structural components. This does not affect the evaluation of the probabilities of failure but leads to more accurate prediction of damage and reduction of the annual

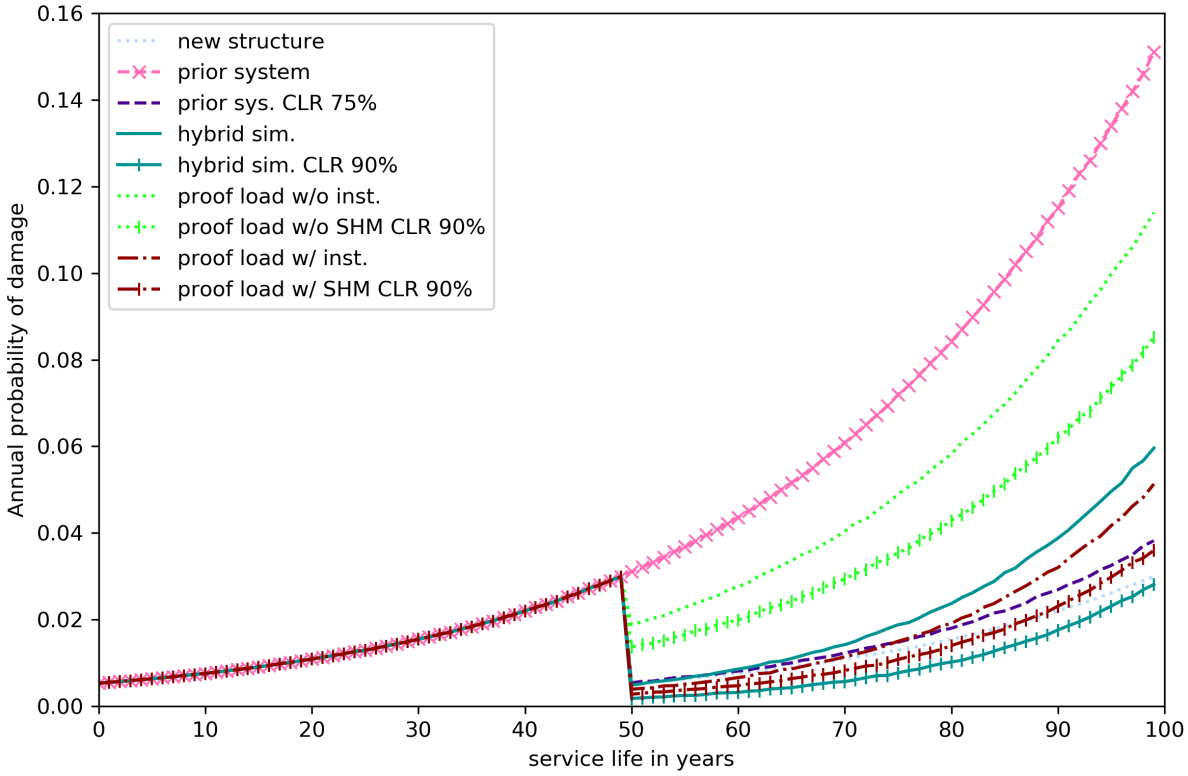

Figure 9.6: Comparison of annual damage probabilities for each SHT scenario; damage probabilities due to proof load tests are not displayed

probabilities of damage after the test as can be seen in Figure 9.6.

9.5.4 Costs associated with structural failures and tests used in the example

All costs used in the example are expressed in notional monetary units (MU). Their values are assumed to reflect major differences in the costs associated with SHT methods, structural failures, repairs and mitigation measures (i.e. CLR). It has also been intended to keep realistic relations between the different assumed costs but it may not necessarily be the case for various specific structures. In general, the costs of tests are typically much lower than the costs associated with failure and major damage of a structure. Hybrid simulation is more costly than proof load testing because prototypes of all relevant structural elements have to be built and then tested using a complex experimental setup.

The costs of SHT for different testing methods given are given in Table 9.2. The costs associated with the actions m and the states of system performance $\vec{X}$ are shown Ta-

Structural Health Test	Cost
No testing	0 MU
Proof load test w/o instrumentation	5 MU
Proof load test w/ instrumentation	10 MU
Hybrid simulation	50 MU

Table 9.2: Costs of SHT

ble 9.3. Auxiliary costs for in-service failure of the structure reflect the fact that in this case indirect consequences (e.g. loss of life, third party losses, legal fees) may be much costlier compared to the structure's failure during a proof load test. The value for these auxiliary costs is based on studies that examine the indirect consequences of attacks on civil infrastructure as a reaction to a rise of terror acts since the 9/11 attacks in New York and Washington D.C. and following attacks in Europe. The US Federal Highway Administration established the Blue Ribbon Panel on bridge and tunnel security [FHW03]. This panel estimated for the loss of a critical bridge or tunnel in the national highway network a replacement cost of US $1.75 billion and together with socioeconomic losses a total of US $10 billion. The EU project SeRoN [SeR12b; SeR12a] presents an example that considers a 2-lane, 250 m highway bridge and estimates a total loss of about €280 million in the case of the bridge collapse. This loss includes €43 million for the bridge reconstruction, €160 million for loss of life and €80 million for further losses. With the cited loss figures an indirect to direct cost ratio of 5.7 (Blue Ribbon Panel) to 9.3 (SeRoN) is indicated. In the following analysis the ratio of 9 is selected. It is assumed that the new structure has the same properties as the original one. It is also assumed that all damages not resulting in failure of the whole structure are subsequently repaired; however, these repairs do not rectify negative effects of deterioration. If the load rating is reduced (i.e. mitigation action) this incur costs in the years that follow the reduction. These costs are defined on an annual basis and depend on CLR (i.e. 75% or 90%).

Actions / consequences	Cost (MU)
Cost of structure, C_{str}	10,000
Auxiliary costs for in-service failure, C_{aux}	90,000
Repair damage, C_{rep}	1,000
Mitigation action CLR 75%, C_{m75}	125 per year
Mitigation action CLR 90%, C_{m90}	50 per year

Table 9.3: Costs of actions and their consequences

The expected cost due to in-service failure and damage in the t$^{\text{th}}$ year is calculated using

the following equation:

$$U(t) = (P_f(t)(C_{str} + C_{aux}) + P_d(t)\, C_{rep})\, \frac{1}{(1+r)^{\frac{t}{d}}} \tag{9.24}$$

where $P_f(t)$ and $P_d(t)$ are the annual probabilities of failure and damage shown in Figure 9.5 and Figure 9.6, respectively; since the decision is made in year 50 $t_d = t - 50$ (see Equation (9.17)) and $t > 50$. In the cases, when the load rating has been reduced $C_{m75(90)}(1+r)^{t_d}$ should be added to the expected annual cost. The total expected cost over the remaining service life of the structure, without the costs associated with carrying out SHT, is calculated as the sum of the annual expected costs.

9.5.5 Expected cost associated with different SHT strategies

The expected costs of the structure vary with each test or no test scenario due to risks arising during the structure's operation, which includes mitigation (i.e. CLR) costs if applicable. There are the direct and indirect risks in the operation of the structure after the tests, and the risks associated with the tests. The direct risk is the probability of structural damage times the associated consequences. One form of indirect risk is caused by structural failure plus auxiliary failure cost if the structure failed in service. Another indirect risk stems from mitigation costs if the load rating is changed. Figure 9.7 presents the total expected utility based on the estimated structural performance, this excludes test costs and test risks. All monetary values are discounted to $t = 50$, i.e. the year of the test, with a 5% interest rate.

The lowest expected cost without SHT is exhibited by the existing structure with CLR to 75%. Of all SHT scenarios that meet the 100-year reliability criterion the 'proof load test with instrumentation' performs the best in terms of the expected costs, followed by the 'proof load test without instrumentation'. Hybrid simulation without CLR fails the 100-year reliability criterion; in order to comply with the criterion the CLR to 90% is required. The CLR to 90% of the rated load reduces the failure and damage risks effectively but the corresponding mitigation costs are too high to perform better than the SHT scenarios without CLR. From all SHT scenarios with CLR to 90%, the one with hybrid simulation leads to the lowest expected costs, closely followed by the 'proof load test with instrumentation'. The accumulated expected costs at the end of the planned service-life are summarised in Table 9.4. As can be seen, the costs associated with no SHT (i.e. no testing) scenarios are significantly higher than the costs with SHT.

Based on the expected structural costs alone, the optimal decision would be to continue the operation of the existing structure after a 'proof load test with instrumentation'. This risk-based analysis does not consider the expected cost of information in the optimal choice determination. The cost of information will be examined in the next section.

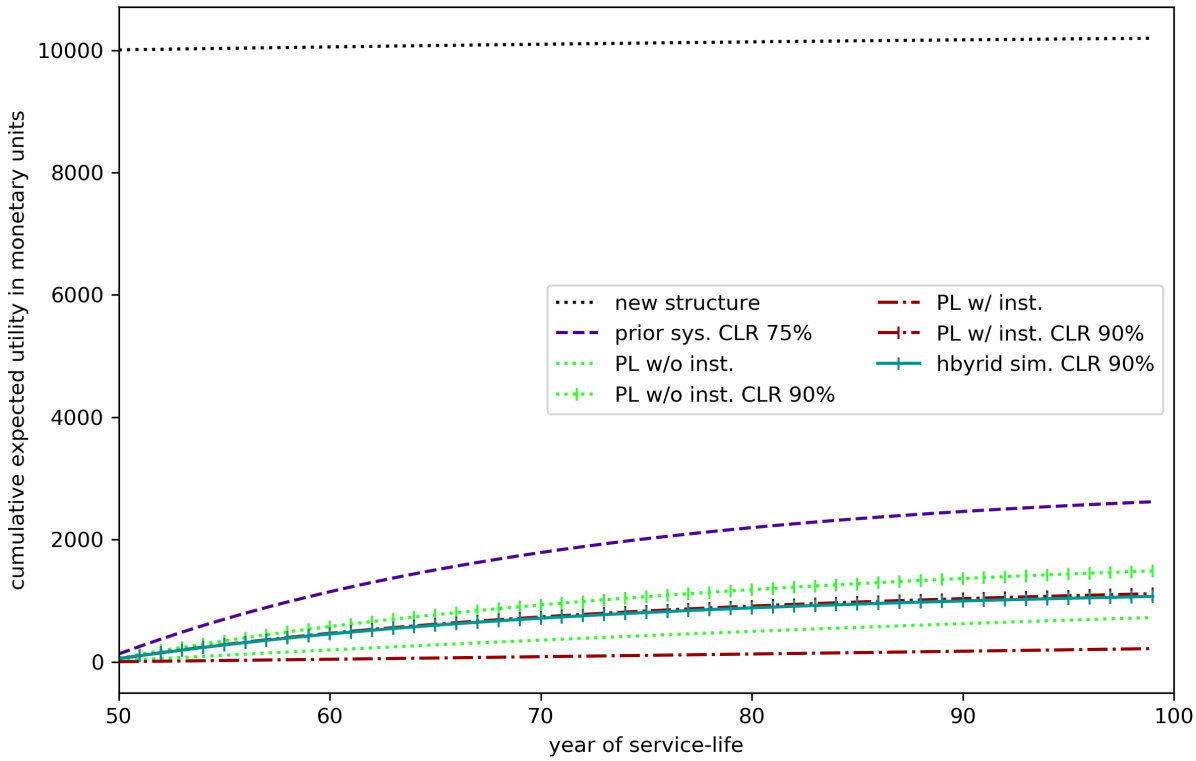

Figure 9.7: Cumulative expected utility of the structure

Strategy	Expected costs at $t = 100$	
	No CLR	No CLR
No testing, replacement	10196	-
No testing, CLR 75%	-	2619
Hybrid simulation, CLR 90%	-	1071
Proof load w/o inst.	727	1489
Proof load w/ inst.	218	1116

Table 9.4: Accumulated expected costs of considered strategies (in MU)

9.5.6 Value of information and information-cost analyses

VoI quantifies and compares decision alternatives in order to establish an acceptable cost of information that is to be paid to acquire the information. The quantification is based on Equation (9.15) because the utility is completely defined by costs. Keeping the existing structure with a reduced load rating in operation is the optimal choice identified in the prior decision analysis. Thus, its corresponding expected cost (i.e. 2619 MU – see Table 9.4) will represent U_{prior}.

Strategy	VoI	Expected information-cost	Value excess
Hybrid simulation, CLR 90%	1548	50	1498
Proof load w/o inst.	1892	1030	862
Proof load w/o inst., CLR 90%	1130	400	730
Proof load w/ inst.	2401	1039	1362
Proof load w/ inst., CLR 90%	1503	406	1097

Table 9.5: VoI, information costs and benefits of SHT strategies (in MU)

The VoI obtained through the various tests that satisfy the reliability criterion at the end of the service life of the structure are listed in Table 9.5. Therein the highest VoI is given by the proof load test with instrumentation. Figure 9.8 shows the development of the VoI over time. All considered SHT scenarios provide valuable information. However, over the life-time of the structure the VoI reduces. The more the information improves the reliability estimate, the quicker the VoI decays.

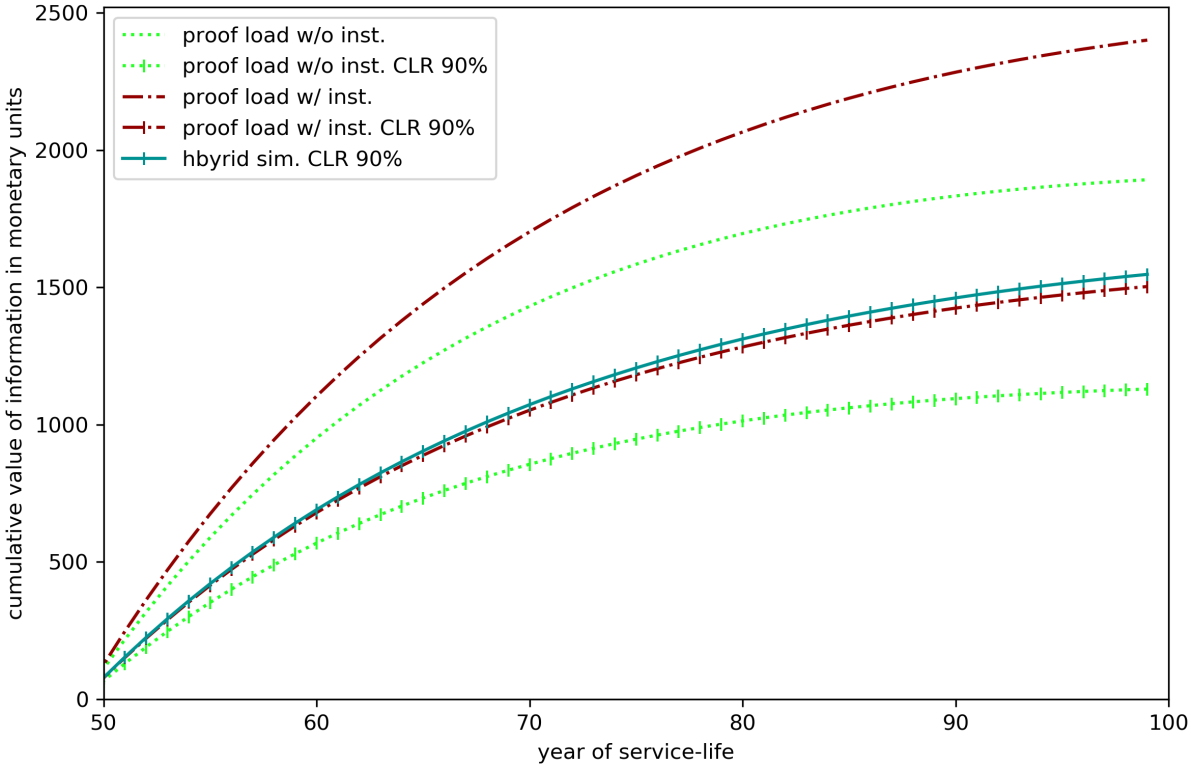

Figure 9.8: Development of the value of information over time

The limitation of a VoI analysis becomes apparent once we consider the expected costs of each test. The VoI cannot be negative by definition and excludes the costs of obtaining the posterior information Raiffa and Schlaifer [RS64]. Thus, this tool alone is not sufficient to identify the optimal decision regarding a SHT strategy. By extending

the VoI analysis through including the expected costs of the information (see Equation (9.19)) that can lead to negative values the analysis becomes more meaningful. The baseline with value 0 in Figure 9.9 is the original structure with CLR to 75% and no SHT. Negative values (i.e. below the baseline) indicate that the costs associated with the specific SHT option are too costly at this point in time. Values above the baseline indicate savings. Figure 9.9 shows that the proof load test scenarios require up to 10 years to break even with the optimal prior decision. If, for any reason, the structure is decommissioned before this 'break-even' point in time the prior decision will be cheaper. The hybrid simulation provides a positive value of information with information-costs from the start. Its advantage over the proof load tests is that it poses no risk to the actual structure.

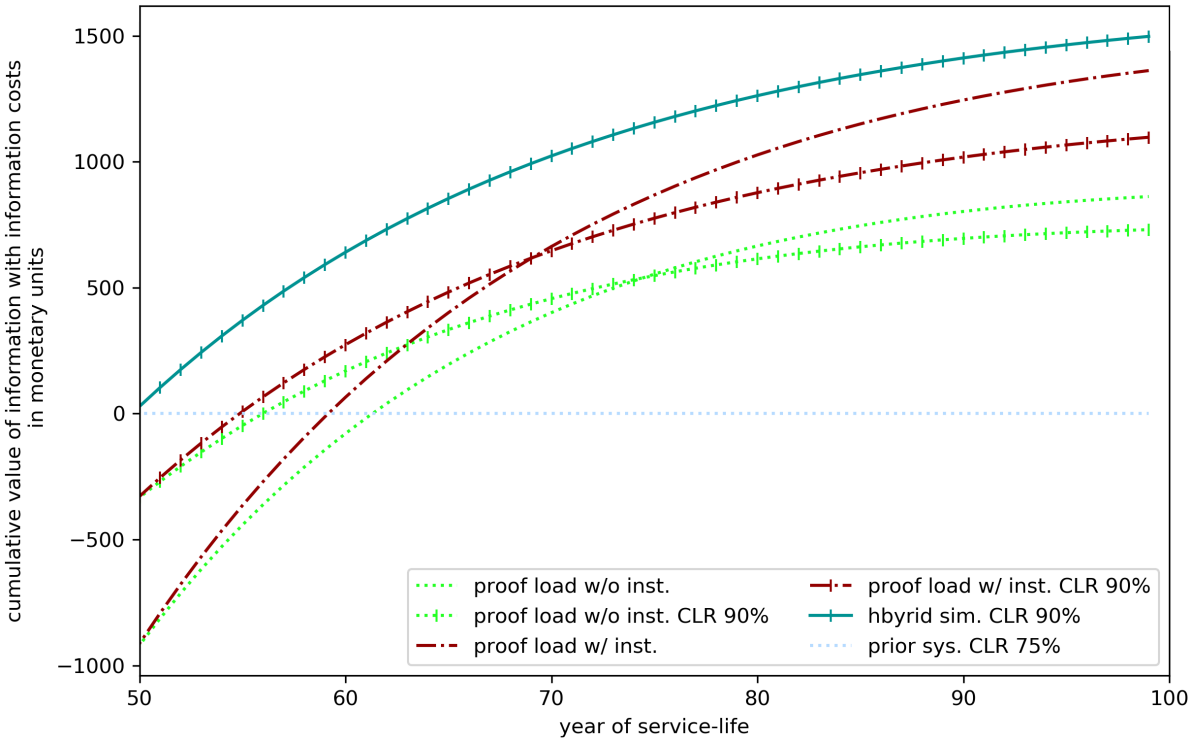

Figure 9.9: Development of the value of information with information-costs over time

A summary of all values of SHT information with information-costs (i.e. value excess) is given in Table 9.5. The highest value of information with information-costs is provided through hybrid simulation with CLR to 90%, which yields the highest value and meets the reliability criterion. The close second in terms of the eventual value excess is the proof load testing with instrumentation. The third best SHT strategy is the proof load test with instrumentation and CLR, which is significantly better than the proof load tests without instrumentation. This is the case because the expected costs after SHT are dominated by the risk of damage, which is lower after the tests with instrumentation.

9.5.7 Discussion

The example presented above is generic and comprehensive although, in order not to complicate the illustration, a number of simplifying assumptions were made. For example, specific assumptions were made regarding the information provided by SHT, both proof load and hybrid simulation testing, and its ability to reduce various types of uncertainty. In particular, it was assumed that hybrid simulation would completely eliminate uncertainty associated with structural resistance modeling. This does not necessarily occur since it may be very difficult to accurately simulate loads imposed by the rest of a structure on its critical elements; moreover, the tested elements can differ from those in the structure. At the same time, hybrid simulation may help to reduce uncertainty in the load distribution between the structural elements that was not taken into account. Possible monitoring of service loads acting on the structure that could reduce uncertainty due to load modeling was also not considered.

Obviously, results of the analysis are also sensitive to the costs allocated to various considered actions, their consequences and mitigation (i.e. CLR) options. These costs were mostly, simply assumed and although it was a clear intention to keep their relative values within realistic bounds this may not always be the case. In particular, it may concern the costs due to indirect consequences of failure, which strongly depend on the importance of the considered structure. One US [FHW03] and one EU [SeR12b; SeR12a] project have been used to establish the ratio of indirect to direct consequences of structural failure. However, it is worth to note that due to the safety requirement the probabilities of structural failure should be very low so that the influence of these costs on decision making may be minor (as happened in the example). At the same time, the expected costs calculated in the example depended significantly on the cost due to damage, which was modeled in a very simple way, i.e. as the cost of repair which took place continuously over the life of the structure as soon as damage induced by loading occurred. It was also assumed that the repair would restore the structure to its original state, except of effects of deterioration due environmental influences. The above assumptions were made to keep the illustration of the proposed decision framework simple and clear. However, it is more complicated in real life, e.g. time intervals between consecutive repairs are at least a few years, repairs usually rectify/reduce damage due to all courses, etc. More accurate modeling of damage, repairs and their effects may lead to results, in terms of the optimal SHT strategy, different from those in the example. Of course, different damage and repair options can be implemented within the presented framework.

There are some other factors that may influence the overall outcome (i.e. optimal STH strategy) but have not been addressed in the example. For instance, it has been considered that only one assessment and then SHT are carried out during the service life of the structure. In reality, this can be done more than once. It is also possible that the life of the structure is extended beyond the initial 100-year design life.

An issue that has also been omitted in the example is who bears the costs. This can be important, in particular, in the context of proof load testing. In this case, the owner usually pays a fixed sum to a contractor, who performs the test. Potential costs associated with damage (or failure) of the structure during the test are the responsibility of the contractor.

All factors mentioned above can be taken into account within the proposed decision framework. Moreover, most of them can be implemented, at least approximately, using the structural model introduced in the paper. This will enable to examine their relative importance for selecting the optimal SHT strategy by carrying out relatively simple analyses. It is worth to note that such studies may be very relevant and timely because of the current condition of the built infrastructure in Europe and North America. For example, data provided by the US Federal Highway Administration show a steady increase in the number of deficient bridges in the USA [Lub16]. The same trend is observed in Germany, where 2456 bridges (i.e. 5% of the current bridge stock) are in deficient condition [BaS17]. The proposed framework can be of great help for selecting optimal strategies to extend the service life of these deficient bridges.

9.6 Conclusions

A decision support framework for structural health testing (SHT) like proof load and hybrid simulation testing has been introduced based on Bayesian pre-posterior decision analysis. The framework is generic and can be adapted to various decision scenarios. A simple structural model has also been proposed, which can be used in combination with the framework to investigate the influence of various factors on the selection of optimal SHT strategies. The framework includes a value of information (VoI) analysis. However, it has been shown that the VoI analysis without consideration of expected information costs is insufficient for decision making.

An example illustrating the framework has been presented. Three main options – no testing, proof load testing and hybrid simulation testing have been considered. It has been shown that under the assumptions made in the example the hybrid simulation testing with a small reduction of the original load rating provides the best option in terms of the value excess. It is also important to note that in terms of the VoI, the analysis indicated the proof load testing with instrumentation as the best option. However, high probabilities of failure and damage of the structure during the test and the expected costs associated with it resulted in a significant reduction of the value excess. In this context, the issue of who bears these costs – the owner of the structure or the contractor who performs the test, becomes important.

Acknowledgement

The COST Action TU1402 on Quantifying the Value of Structural Health Monitoring is gratefully acknowledged for networking support, in particular of a short-term scientific mission of the first author.

CHAPTER 10

Conclusions and outlook

The guiding hypothesis of the work accumulated in this thesis may be phrased as: "Quantitative probabilistic models of the value of structural testing facilitate an optimized design of the testing methods before their implementation."

The following conclusions state how value of information analysis is applied to decision problems pertaining the design of structural tests with respect to design and operation of structures in order to identify the optimal test design in order to arrive at decisions that maximize the utility of the tested system.

10.1 Thesis conclusion

Owners, operators, and designers of structures face the same issue to find optimal decisions related to design, operation and maintenance, retrofitting, inspection and monitoring, or replacement. These decisions influence the structural safety and economic benefit provided by the structure. One of the main challenges in this complex environment is to spend limited resources in the optimal way. These decisions influence each other and may be relevant at vastly different points in time. The design of the structure is at the very beginning, even before the service-life begins, and retrofitting or replacement will be issues arising towards the end of the service life. First attempts to model such interactions of structural design and utilization in conjunction with transparent and consistent decision making are shown in this thesis. Thereby the hypothesis stated at the beginning of this chapter is demonstrated. The tool required in order to demonstrate the validity of the hypothesis are: (1) a value of information analysis considering content and accuracy of test information alongside a cost and benefit analysis. (2) a system model in order to infer test information to the performance of the tested structural system.

Herein, the following contributions to structural test design with value of information are accomplished:

1. A decision framework based on value of information (VoI) analysis for structural tests has been established. The framework is demonstrated with a case study that

considers various sources of posterior knowledge. VoI of proof loading has not be considered in the past, although the demand for a formal analysis has been seen already in the 1970's [Yan76].

The framework takes into account the different ways each testing method contributes to posterior knowledge by separately treating natural variability, model uncertainty and measurement uncertainty.

2. The developed pre-posterior decision and value of information concepts support structural integrity management before and during the service-life. The analysis concepts are based on a detailed life-cycle analysis that includes not only costs, but also expected income from the structural system.

3. An overview of SHM and proof loading applications given. These include: operation optimization of structures and portfolios of structures, service life extension, utilization modification, damage progression monitoring, code making and code calibration, early damage warning, structure prototype development / design by testing, and SHM systems prototype development.

4. Conceptual accomplishments are:

   - The introduction of the formal value of information and action analysis (EVSIA). This concept extents the value of information analysis by Raiffa and Schlaifer [RS64], which is limited to the analysis of identical actions, by a probabilistic cost and benefit analysis of actions that are only possible with (pre-) posterior knowledge. An EVSIA analysis will yield at least the same value as an EVSI analysis but can identify more decision actions that are more beneficial.
   - A pre-construction proof load test concept that facilitates the application of proof load tests to structures that are too difficult or too risky to test once they are erected. This could be for example, offshore structures where unlike bridges no controllable method is known to apply sufficiently high loads. By proof load testing sub-elements of the structural part and inferring this test information through a structural model, one can gather information similar to a proof load test of the new structure.

     This way the tests can be conducted under a safe and controlled environment like a factory. A standard test in series application may also reduce the proof load test costs.

     The proof load test parameters have been optimized with regards to extreme loads and deterioration process for the employed system models. For the structure's design phase and the operation phase including its functionality have been considered and modeled.
   - A concept based on the hypothesis that quasi-static hybrid simulations can substitute proof load testing is demonstrated. Hybrid testing uses a combination of physical and numerical models in order to capture interactions with parts of the structure that are not present in the physical model. A hybrid

simulation cannot inquire about properties of the actual structure, but it can provide knowledge about model uncertainties. An important advantage is that no risk is posed to the structure.

The results of the thesis contribute to COST action TU1402: Quantifying the value of structural health monitoring, which in turn will contribute to the probabilistic model code of the Joint Committee of Structural Safety.

Improved and benefit optimized designs facilitated by EVSIA analysis can be of great importance for the offshore wind energy industry. Here, the structures are produced in series and posterior information could help to optimize designs. Current studies on the energy production costs consider only scale effects; for example Hobohm et al. [Hob+13] included in their forecasts savings in the support structure realized by increasing the nominal turbine power from for example 4 MW to 6 MW.

The decision framework, and hypothesis on a quasi-static hybrid simulation as complement or substitution to proof load testing, can be useful for research and planning associated to the condition assessment and load rating increases as it is for example a challenge in Denmark and Germany [TF11; And16b]. For certain structures, e.g. short span bridges it can be difficult or impossible to reach an informative test load during a static proof load test with dead weights [OŁC14]. In such a case, hybrid simulation could be considered as an alternative experimental method.

10.2 Limitations

The introduction of the expected value of sample information and action analysis (EVSIA), which is an extension to the expected value of sample information analysis (EVSI), includes a demonstration of the concept. The cost and benefit model therein has two parts. Part (1), the economic elements that pertain to EVSI and EVSIA are supported by figures obtained from current literature about wind park economics and design. However, the expected cost and risk reduction due to actions that the information facilitate need to be substantiated by studies providing figures or a methodology to compute expenses depending on structural reliability.

The hypothesis that quasi-static hybrid simulations can replace experiments like SHM or proof load testing for of obtaining structural reliability information is currently not supported by experiments that demonstrated this. However, hybrid simulations are well established as dynamic simulations for research and design of earthquake resistance structures [SS08].

The employed structural models are based on logical or Daniels systems. These sys-

tem models are highly relevant for and efficient at modeling the reliability performance, knowledge inference, and thus for value of information analyses. However, these models should be clearly connected to more sophisticated structural and mechanical models representing real structures.

The thesis' focus is on value of information assessments using models associated to the ultimate limit states of structures. Proof loading and a structural health monitoring system may also be able to provide information pertaining to for example serviceability and deterioration limit states.

10.3 Outlook

The results cover only a small area related to the vast field of structural test design. A decision maker may have many more experiment options to choose from than discussed herein. The research could be extended by including other sources of knowledge. Such sources could be permanent monitoring techniques, for example strain gauges or corrosion rate monitoring, and inspections. With an increasing degree of automation, inspection can take on characteristics of monitoring. Depending on the inspection or monitoring demand and environmental conditions, the inspection may be carried out by human staff or robotic devices like unmanned aerial vehicles. These factors influence the costs, accuracy, and temporal availability of posterior knowledge. These are important aspects, which should be considered in an extension of the work leading to a value of information-based inspection and monitoring concept.

The increasing computational cost of complex mechanical models may be counter-acted by using surrogate models like the response surface or space mapping method.

APPENDIX A

Notational conventions

Random events are denoted by capital letters, e.g. $F, \bar{F}, Z_{PL,\uparrow}, Z_{PL,\downarrow}$.
$\bar{}$ indicates a negation, e.g. $\bar{F}$ is the complementary event of F.
Random variables are written in capital letters e.g. R, S. A vector of random variables is written with $\vec{}$ over it, e.g. $\vec{R}$.

A continues random variable X has a probability density function (PDF) like $f_X(x)$. The small x is the value X takes on for the evaluation. The cumulative distribution function (CDF) e.g. $F_X(x)$ is generated by integrating the PDF, $F_X(x) = \int f_X(x)\,dx$.

Realizations of random variables are denoted with ($\hat{}$). $\hat{R}$ is the realization of R.
Conditional probabilities are written like $P(A|B)$, where A is the conditioned, and B is the conditioning variable.

APPENDIX B

List of figures from external sources

Cover page figure: The Skjeggestad Bridge (a.k.a. Mofjellbekken bridge) on the national highway E18 in Holmestrand, Vestfold, Norway after its collapse on february 2nd, 2015. The reason for the collapse was a landslide in the quick clay surrounding a support pillar. `https://commons.wikimedia.org/wiki/File:Skjeggestadbrua_fra_s%C3%B8rvest_2_crop.jpg`. Creative Commons Attribution-Share Alike 4.0 International license. Accessd: 15.11.2018. The image is blended with a self produced graph.

Figure 1.1: Jacket sub-structure for the Norwegian Ivar Aasen field on a barge. Photos by Kess Torn, cc-by-sa-2.0. `https://commons.wikimedia.org/wiki/File:Franklin_offshore_,_Heysehaven_26-4-2015._(17276821035).jpg`. Creative Commons Attribution-Share Alike 2.0 Generic. Accessed: 23.01.2018

Figure 1.2: Examples of tension leg platforms. A hydrocarbon production platform on the left-hand side and a wind energy converter on the right-hand side. Adapted from the National Renewable Energy Laboratory.

Figure 1.3: Example of a conical grouted connection of monopile and transition piece. Adapted from DNV-GL.

Figure 1.4a: The Draugen gravity base platform. Courtesy of Norwegian Contractors.

Figure 1.4b: Schematic of a monopile. Adapted from 4C Offshore. `http://www.4coffshore.com/windfarms/monopiles-support-structures-aid4.html`. Accessed: 23.01.2018

Figure 1.5a: Akashi Kaikyo Ohashi bridge. https://commons.wikimedia.org/wiki/File:Akashi_Kaikyo_Ohashi_01.jpg. Public domain. Accessed: 23.01.2018

Figure 1.5b: Suspension cable cross-section of Akashi Kaikyo Ohashi bridge. https://commons.wikimedia.org/wiki/File:Akashi_Kaiky%C5%8D_Bridge_Cable_Cut_Model.JPG. WeiHsiang Wang. Creative Commons Attribution-Share Alike 4.0 International. Accessed: 23.01.2018

Figure 1.6: Schematic example of a truss bridge with denoted structural elements. Adapted from Wikimedia. https://commons.wikimedia.org/wiki/File:Parts_of_a_truss_bridge.svg. Public domain. Accessed: 23.01.2018

APPENDIX C

Cost & benefit examples

		Denmark		Germany (pre 2017 model)	
t year	Costs €	Benefits €	Total €	Benefits €	Total €
1	390,476.19	2,721,857.14	2,331,380.95	2,890,800.00	2,500,323.81
2	371,882.09	2,592,244.90	2,220,362.81	2,753,142.86	2,381,260.77
3	354,173.42	2,468,804.66	2,114,631.25	2,622,040.82	2,267,867.40
⋮	⋮	⋮	⋮	⋮	⋮
9	264,289.66	1,842,260.05	1,577,970.40	1,956,607.23	1,692,317.57
10	251,704.43	1,754,533.38	1,502,828.95	1,863,435.46	1,611,731.02
11	239,718.51	1,670,984.17	1,431,265.67	1,774,700.43	1,534,981.92
12	228,303.34	1,591,413.50	1,363,110.16	1,690,190.89	1,461,887.55
13	217,431.75	1,515,631.90	1,298,200.15	407,652.72	190,220.97
14	207,077.86	248,872.23	41,794.37	388,240.68	181,162.82
15	197,217.01	237,021.18	39,804.16	369,753.03	172,536.02
16	187,825.72	225,734.45	37,908.73	352,145.75	164,320.02
17	178,881.64	214,985.19	36,103.55	335,376.90	156,495.26
18	170,363.47	204,747.80	34,384.33	319,406.57	149,043.10
19	162,250.92	194,997.91	32,746.98	304,196.74	141,945.81
20	154,524.69	185,712.29	31,187.60	289,711.18	135,186.49
21	147,166.37	176,868.85	29,702.48	176,868.85	29,702.48
⋮	⋮	⋮	⋮	⋮	⋮
25	121,074.14	145,510.44	24,436.30	145,510.44	24,436.30
⋮	⋮	⋮	⋮	⋮	⋮
30	94,864.75	114,011.24	19,146.48	114,011.24	19,146.48
Σ 20 years	5,109,506.24	28,358,432.98	23,248,926.73	29,669,465.79	24,559,959.55
Σ 30 years	6,302,704.92	29,792,454.07	23,489,749.15	31,103,486.89	24,800,781.97

Table C.1: Cost and benefit analyses examples for a feed in tariff of 25 € / MWh

		Denmark		Germany (pre 2017 model)	
t year	Costs €	Benefits €	Total €	Benefits €	Total €
1	390,476.19	2,721,857.14	2,331,380.95	2,890,800.00	2,500,323.81
2	371,882.09	2,592,244.90	2,220,362.81	2,753,142.86	2,381,260.77
3	354,173.42	2,468,804.66	2,114,631.25	2,622,040.82	2,267,867.40
⋮	⋮	⋮	⋮	⋮	⋮
9	264,289.66	1,842,260.05	1,577,970.40	1,956,607.23	1,692,317.57
10	251,704.43	1,754,533.38	1,502,828.95	1,863,435.46	1,611,731.02
11	239,718.51	1,670,984.17	1,431,265.67	1,774,700.43	1,534,981.92
12	228,303.34	1,591,413.50	1,363,110.16	1,690,190.89	1,461,887.55
13	217,431.75	1,515,631.90	1,298,200.15	407,652.72	190,220.97
14	207,077.86	248,872.23	41,794.37	388,240.68	181,162.82
15	197,217.01	237,021.18	39,804.16	369,753.03	172,536.02
16	187,825.72	225,734.45	37,908.73	352,145.75	164,320.02
17	178,881.64	214,985.19	36,103.55	335,376.90	156,495.26
18	170,363.47	204,747.80	34,384.33	319,406.57	149,043.10
19	162,250.92	194,997.91	32,746.98	304,196.74	141,945.81
20	154,524.69	185,712.29	31,187.60	289,711.18	135,186.49
21	147,166.37	176,868.85	29,702.48	176,868.85	29,702.48
⋮	⋮	⋮	⋮	⋮	⋮
25	121,074.14	145,510.44	24,436.30	145,510.44	24,436.30
⋮	⋮	⋮	⋮	⋮	⋮
30	94,864.75	114,011.24	19,146.48	114,011.24	19,146.48
Σ 20 years	5,109,506.24	28,358,432.98	23,248,926.73	29,669,465.79	24,559,959.55
Σ 30 years	6,302,704.92	29,792,454.07	23,489,749.15	31,103,486.89	24,800,781.97

Table C.2: Cost and benefit analyses examples for a feed in tariff of 39 € / MWh

		Denmark		Germany (pre 2017 model)	
t year	Costs €	Benefits €	Total €	Benefits €	Total €
1	390,476.19	2,721,857.14	2,331,380.95	2,890,800.00	2,500,323.81
2	371,882.09	2,592,244.90	2,220,362.81	2,753,142.86	2,381,260.77
3	354,173.42	2,468,804.66	2,114,631.25	2,622,040.82	2,267,867.40
⋮	⋮	⋮	⋮	⋮	⋮
9	264,289.66	1,842,260.05	1,577,970.40	1,956,607.23	1,692,317.57
10	251,704.43	1,754,533.38	1,502,828.95	1,863,435.46	1,611,731.02
11	239,718.51	1,670,984.17	1,431,265.67	1,774,700.43	1,534,981.92
12	228,303.34	1,591,413.50	1,363,110.16	1,690,190.89	1,461,887.55
13	217,431.75	1,515,631.90	1,298,200.15	407,652.72	190,220.97
14	207,077.86	248,872.23	41,794.37	388,240.68	181,162.82
15	197,217.01	237,021.18	39,804.16	369,753.03	172,536.02
16	187,825.72	225,734.45	37,908.73	352,145.75	164,320.02
17	178,881.64	214,985.19	36,103.55	335,376.90	156,495.26
18	170,363.47	204,747.80	34,384.33	319,406.57	149,043.10
19	162,250.92	194,997.91	32,746.98	304,196.74	141,945.81
20	154,524.69	185,712.29	31,187.60	289,711.18	135,186.49
21	147,166.37	176,868.85	29,702.48	176,868.85	29,702.48
⋮	⋮	⋮	⋮	⋮	⋮
25	121,074.14	145,510.44	24,436.30	145,510.44	24,436.30
⋮	⋮	⋮	⋮	⋮	⋮
30	94,864.75	114,011.24	19,146.48	114,011.24	19,146.48
Σ 20 years	5,109,506.24	28,358,432.98	23,248,926.73	29,669,465.79	24,559,959.55
Σ 30 years	6,302,704.92	29,792,454.07	23,489,749.15	31,103,486.89	24,800,781.97

Table C.3: Cost and benefit analyses examples for a feed in tariff of 67.5 € / MWh

Bibliography

[AAK08] Martin Achmus, Khalid Abdel-Rahman, and Yu-Shu Kuo. "Design of monopile foundations for offshore wind energy converters". In: *Geotechnics in Maritime Engineering. 11th Baltic Sea Geotechnical Conference*. 2008, pages 463–470.

[AB12] S. Adhikari and S. Bhattacharya. "Dynamic analysis of wind turbine towers on flexible foundations". In: *Shock and Vibration* 19.1 (2012), pages 37–56. ISSN: 10709622. DOI: 10.3233/SAV-2012-0615.

[And16a] Allan Bødskov Andersen. *2015 Annual report*. Technical report. DONG Energy A/S Kraftværksvej 53 7000 Fredericia Denmark: DONG Energy A/S, 2016. URL: https://assets.dongenergy.com/DONGEnergyDocuments/com/Investor/Annual%7B%5C_%7DReport/2015/dong%7B%5C_%7Denergy%7B%5C_%7Dannual%7B%5C_%7Dreport%7B%5C_%7Den.pdf.

[And16b] Ulrik Andersen. *Nye bæreevneberegninger Vejbroer kan bære meget mere, end man troede*. Copenhagen, Denmark, 2016. URL: https://ing.dk/artikel/vejbroer-kan-baere-meget-mere-end-man-troede-198412.

[ATL17] Arifian Agusta, Sebastian Thöns, and Bernt J Leira. "Value of Information-based Inspection Planning for Offshore Structures". In: *36th International Conference on Ocean, Offshore and Arctic Engineering*. Trondheim, Norway, 2017.

[Bag+13] S. Bagavathiappan et al. "Infrared thermography for condition monitoring - A review". In: *Infrared Physics and Technology* 60 (2013), pages 35–55. ISSN: 13504495. DOI: 10.1016/j.infrared.2013.03.006. URL: http://dx.doi.org/10.1016/j.infrared.2013.03.006.

[BaS17] BaSt. *Brücken an Bundesfernstraßen: Zustandsnoten der Brücken*. 2017. URL: http://www.bast.de/DE/Ingenieurbau/Statistik/statistik-node.html;jsessionid=EDD52EFC65385437996A4DBA876E526B.live11291 (visited on November 21, 2017).

[BB14a] Niklas Bagge and Thomas Blanksvärd. "Instrumentation and Full - Scale Test of a Post - Tensioned Concrete Bridge". In: *Nordic Concrete Research* 51 (2014), pages 63–83.

[BB14b] Stefan Bauer and Henning Brüske. "Detection and Sizing of Subcritical Cracks Using Ultrasonic In-Line Inspection Methods". In: *10th International Pipeline Conference Volume 2: Pipeline Integrity Management*. Calgary, Alberta, Canada: American Society of Mechanical Engineers, 2014. DOI: 10.1115/IPC2014-33395.

[BC14] Jack Ralph Benjamin and C Allin Cornell. *Probability, statistics, and decision for civil engineers*. Courier Corporation, Mineola, New York, 2014. ISBN: 978-0-486-78072-6.

[Ben08] Benson Shing, P. "Real-Time Hybrid Testing Techniques". In: *Modern Testing Techniques for Structural Systems: Dynamics and Control*. Edited by Oreste S. Bursi and David Wagg. Springer Vienna, 2008. Chapter 6, pages 259–292. ISBN: 978-3-211-09445-7. DOI: 10.1007/978-3-211-09445-7_6. URL: http://link.springer.com/10.1007/978-3-211-09445-7%7B%5C_%7D6.

[BH08] Frada Burstein and Clyde W Holsapple. *Handbook on Decision Support Systems 1*. Edited by Frada Burstein and Clyde W Holsapple. Springer, 2008. ISBN: 9783540487128, 9783540487135. DOI: 10.1007/978-3-540-48713-5.

[Bïl90] Ömer G Bïlïr. "The relationship between the parameters C and n of Paris' law for fatigue crack growth in a SAE 1010 steel". In: *Engineering Fracture Mechanics* 36.2 (1990), pages 361–364. ISSN: 0013-7944. DOI: http://dx.doi.org/10.1016/0013-7944(90)90015-9. URL: http://www.sciencedirect.com/science/article/pii/0013794490900159.

[BM12] Erin E. Bachynski and Torgeir Moan. "Design considerations for tension leg platform wind turbines". In: *Marine Structures* 29.1 (2012), pages 89–114.

ISSN: 09518339. DOI: 10.1016/j.marstruc.2012.09.001. URL: http://dx.doi.org/10.1016/j.marstruc.2012.09.001.

[BMW16] BMWI. *EEG-Vergütung und Kapazitätszuweisung*. website. 2016. URL: http://www.erneuerbare-energien.de/EE/Navigation/DE/Technologien/Windenergie-auf-See/Finanzierung/EEG-Verguetung/eeg-verguetung.html.

[BP01] Rebecca J Barthelmie and Sara C Pryor. "A review of the economics of offshore wind farms". In: *Wind Engineering* 25 (2001), pages 203–213. ISSN: 2048402x, 0309524x.

[BP98] Robert Bushman and Andrew J. Pratt. "Weigh in Motion Technology - Economics and Performance". In: *Proceeding of National Travel Monitoring Exposition and Conference*. Charlotte, North Carolina: Raleigh, 1998, page 7. URL: https://www.fhwa.dot.gov/ohim/tvtw/natmec/00024.pdf.

[Bro+00] M. P. H. Brongers et al. "Effect of Hydrostatic Testing on Ductile Tearing of X-65 Line Pipe Steel with Stress Corrosion Cracks". In: *Corrosion Engineering* 56.10 (2000), pages 1050–1058. DOI: 10.5006/1.3294382. URL: http://www.corrosionjournal.org/doi/abs/10.5006/1.3294382?code=nace-prem-site.

[Brü16] Henning Brüske. *Examples of cost and benefit analyses for offshore wind turbines*. COST Action TU1402 Factsheet WG1-7. COST, 2016.

[Bry+75] R. H. Bryan et al. *Test of 6-inch-thick pressure vessels. Series 2: Intermediate test vessels V-3, V-4, and V-6*. Technical report. Oak Ridge, Tennesse, USA: Oak Ridge National Laboratory, 1975. URL: http://www.iaea.org/inis/collection/NCLCollectionStore/%7B%5C_%7DPublic/07/240/7240861.pdf.

[BT16] Henning Brüske and Sebastian Thöns. "Value of Information by updating of model uncertainties utilising proof loading in the context of series and Daniels systems". In: *Proceedings of the International RILEM Conference Materials, Systems and Structures in Civil Engineering*. International RILEM Conference (August 2016). Edited by Sebastian Thöns, pages 52–61. URL: http://3-files.conferencemanager.dk/medialibrary/91444302-169C-4C82-9C9D-DEBF36B57338/images/Hjemmeside.pdf.

[BT17] Henning Brüske and Sebastian Thöns. “On decision analysis about proof loading with inference to untested components”. In: *International Conference on Structural Safety & Reliability* (2017), pages 3030–3039.

[Bur+11] Tony Burton et al. *Wind Energy Handbook*. 2. John Wiley & Sons, Ltd, 2011. ISBN: 78-0-470-69975-1, 978-1-119-99272-1, 978-1-119-99271-4, 978-1-119-99392-6, 978-1-119-99393-3.

[CAF16] S Chala, F Ansari, and M Fathi. “A data warehousing system for knowledge-based structural health monitoring of wind power plant”. In: *IEEE International Conference on Electro Information Technology* 2016-Augus (2016), pages 605–609. DOI: 10.1109/EIT.2016.7535307. URL: https://www.scopus.com/inward/record.uri?eid=2-s2.0-84984596176%7B%5C&%7Ddoi=10.1109%7B%5C%%7D2FEIT.2016.7535307%7B%5C&%7DpartnerID=40%7B%5C&%7Dmd5=.

[Car+14] Rami Carmi et al. “Acoustic Emission and Digital Image Correlation as Complementary Techniques for Laboratory and Field Research”. In: *Advances in Acoustic Emission Technology: Proceedings of the World Conference on Acoustic Emission*. Edited by Gongtian Shen, Zhanwen Wu, and Junjiao Zhang. Volume 158. Beijing, China, 2014, pages 605–622.

[CG13] Joan Ramon Casas and Juan D. Gómez. “Load rating of highway bridges by proof-loading”. In: *KSCE Journal of Civil Engineering* 17.3 (2013), pages 556–567. ISSN: 1976-3808. DOI: 10.1007/s12205-013-0007-8. URL: http://dx.doi.org/10.1007/s12205-013-0007-8.

[Cor67] C Allin Cornell. “Bounds on the reliability of structural systems”. In: *Journal of the Structural Division* 93.1 (1967), pages 171–200.

[Dan45] H E Daniels. “The statistical theory of the strength of bundles of threads. I”. In: *Proceedings of the Royal Society of London. Series A. Mathematical and Physical Sciences* 183.995 (1945), pages 405–435.

[DC05] De Stefano A. and P Clemente. “SHM on Historical Heritage: Robust Methods to Face Large Uncertainties”. In: *Proceedings of the 1 st International Conference on Structural Condition Assessment, Monitoring and Improvement*. SAMCO. December 2005.

[DDS16] R. Damiani, K. Dykes, and G. Scott. "A comparison study of offshore wind support structures with monopiles and jackets for U.S. waters". In: *Journal of Physics: Conference Series* 753 (2016). DOI: 10.1088/1742-6596/753/9/092003. URL: http://stacks.iop.org/1742-6596/753/i=9/a=092003.

[Dia87] D Diamantidis. "Reliability assessment of existing structures". In: *Engineering Structures* 9.3 (1987), pages 177–182. ISSN: 0141-0296. DOI: 10.1016/0141-0296(87)90013-7. URL: http://www.sciencedirect.com/science/article/pii/0141029687900137.

[Dit86] Ove Ditlevsen. "Reliability updating of existing structures". In: *Application of Probabilistic Methods in the design of structures*. Gothenburg, Sweden, 1986, page 14.

[Don99] John J. III Donohue. "Why We Should Discount the Views of Those Who Discount Discounting". In: *Yale Law Journal* 108.January (1999). ISSN: 00440094. DOI: 10.2307/797455.

[DR01] G. Degenkamp and R. Ruinen. "Installation of Vertical Loaded Anchors Using a Subsea Tensioning Device in Ultra-Deepwaters in the Gulf of Mexico". In: *Proceedings of Offshore Technology Conference*. Houston, Texas, 2001.

[DWA07] G. Drummond, J. F. Watson, and P. P. Acarnley. "Acoustic emission from wire ropes during proof load and fatigue testing". In: *NDT and E International* 40.1 (2007), pages 94–101. ISSN: 09638695. DOI: 10.1016/j.ndteint.2006.07.005.

[EEX16] EEX. *Auction | EPEX SPOT*. website. 2016. URL: https://www.eex.com/en/market-data/power/spot-market/auction?%7B%5C_%7Descaped%7B%5C_%7Dfragment%7B%5C_%7D=/2016/08/01%7B%5C#%7D!/2016/08/01.

[EL15] Matthias Ehrhart and Werner Lienhart. "Development and evaluation of a long range image-based monitoring system for civil engineering structures". In: (2015), 94370K. DOI: 10.1117/12.2084221. URL: http://proceedings.spiedigitallibrary.org/proceeding.aspx?doi=10.1117/12.2084221.

[ESL03] Gerhard Ersdal, John Dalsgaard Sørensen, and Ivar Langen. "Updating of Structural Failure Probability Based on Experienced Wave Loading". In: *International Offshore and Polar Engineering Conference* 5 (2003), pages 461–468.

[Eur02] European Standard. *Basis of structural design*. April 2002.

[Eur05] European Standard. "Part 2: Bridges". In: *Eurocode 8: Design of structures for earthquake resistance*. Volume 1998-2:200. 2005.

[Eur17] Euribor. *No Title*. 2017. URL: http://www.emmi-benchmarks.eu/euribor-org/euribor-history.html (visited on September 26, 2017).

[FH11] Yusuke Fujita and Yoshihiko Hamamoto. "A robust automatic crack detection method from noisy concrete surfaces". In: *Machine Vision and Applications* 22.2 (2011), pages 245–254. ISSN: 09328092. DOI: 10.1007/s00138-009-0244-5.

[FHT11] S Faulstich, B Hahn, and P J Tavner. "Wind turbine downtime and its importance for offshore deployment". In: *Wind Energy* 14.3 (2011), pages 327–337. ISSN: 1099-1824. DOI: 10.1002/we.421. URL: http://dx.doi.org/10.1002/we.421.

[FHW03] FHWA. "Recommendations for Bridge and Tunnel Security The American Association of State Highway and Transportation Officials (AASHTO) Transportation Security Task Force". In: September (2003). URL: https://www.fhwa.dot.gov/bridge/security/brp.pdf.

[FKG15] J. Fernandez Galarreta, N. Kerle, and M. Gerke. "UAV-based urban structural damage assessment using object-based image analysis and semantic reasoning". In: *Natural Hazards and Earth System Sciences* 15.6 (2015), pages 1087–1101. ISSN: 16849981. DOI: 10.5194/nhess-15-1087-2015.

[FOM17] FOMC. *Discount and advance rates*. 2017. URL: https://www.federalreserve.gov/newsevents/pressreleases/files/monetary20170711a1.pdf (visited on September 26, 2017).

[FQM17] Michael Havbro Faber, J. Qin, and Simona Miraglia. "On Decision Support for Sustainability and Resilience of Infrastructure Systems". In: *12th International Conference on Structural Safety & Reliability*. Edited by Christian Bucher, Bruce R. Ellingwood, and Dan M. Frangopol. August. Vienna: TU Verlag, 2017, pages 6–10. ISBN: 9783903024281.

[FT10] E B Flynn and M D Todd. “A Bayesian Experimental Design Approach to Structural Health Monitoring”. In: *5th European Workshop on Structural Health Monitoring* (2010), pages 414–419. URL: http://permalink.lanl.gov/object/tr?what=info:lanl-repo/lareport/LA-UR-10-02681.

[FT13] Michael Havbro Faber and Sebastian Thöns. “On the value of structural health monitoring”. In: *22nd Annual Conference on European Safety and Reliability*. Edited by Raphaël D J M Steenbergen. Safety, Reliability and Risk Analysis: Beyond the Horizon. Taylor & Francis Group, London, 2013, pages 2535–2544. ISBN: 978-1-138-00123-7.

[FT95] Gongkang Fu and Jianguo Tang. “Risk-based proof-load requirements for bridge evaluation”. In: *Journal of Structural Engineering* 121.3 (1995), pages 542–556. ISSN: 0733-9445. DOI: 10.1061/(ASCE)0733-9445(1995)121:3(542).

[FVS00] Michael Havbro Faber, Dimitri V. Val, and Mark G. Stewart. “Proof load testing for bridge assessment and upgrading”. In: *Engineering Structures* 22.12 (2000), pages 1677–1689. ISSN: 0141-0296. DOI: 10.1016/S0141-0296(99)00111-X. URL: http://www.sciencedirect.com/science/article/pii/S014102969900111X.

[FVT15] Michael Havbro Faber, Dimitri V. Val, and Sebastian Thöns. “Value of Information in SHM – Considerations on the Theoretical Framework”. In: *Proceedings of the 1st Workshop on Quantifying the Value of Structural Health Monitoring COST Action TU1402*. Edited by Sebastian Thöns. September 2015, pages 5–16. ISBN: 978-8-77-877426-2.

[GH84] Mircea Grigoriu and W. Brent Hall. “Probabilistic models for proof load testing”. In: *Journal of Structural Engineering* 110.2 (1984), pages 260–274. ISSN: 07339445. DOI: 10.1061/(ASCE)0733-9445(1984)110:2(260).

[GJ14] Rongsheng Geng and Peng Jing. “Acoustic Emission: An Indispensable Structural Health Monitoring Means for Aircraft”. In: *Advances in Acoustic Emission Technology: Proceedings of the World Conference on Acoustic Emission*. Edited by Gongtian Shen, Zhanwen Wu, and Junjiao Zhang. Beijing, China: Springer Science+Business Media New York, 2014, pages 503–512. DOI: 10.1007/978-1-4939-1239-1_47.

[GMF10] Michel Ghosn, Fred Moses, and Dan M Frangopol. "Redundancy and robustness of highway bridge superstructures and substructures". In: *Structure and Infrastructure Engineering* 6.1-2 (2010), pages 257–278. ISSN: 15732479. DOI: 10.1080/15732470802664498.

[GR90] S Gollwitzer and Rüdiger Rackwitz. "On the reliability of Daniels systems". In: *Structural Safety* 7.2 (1990), pages 229–243.

[Gre69] A. T. Green. *Stress wave emission and fracture of prestressed concrete reactor vessel materials*. Technical report. Oak Ridge, Tennessee, USA: Qak Ridge National Laboratory, 1969.

[GS15] Marc Gutermann and Carsten Schröder. "Loading vehicle BELFA development and experience gained in 10 years of practice". In: *Bridge Structures* 11 (2015), pages 19–31. DOI: 10.3233/BRS-150081.

[GWS93] Ove Tobias Gudmestad, T.A. Warland, and B.L. Stead. "Concrete Structures for Development of Offshore Fields". In: *Journal of Petroleum Technology* 45.8 (1993). DOI: 10.2118/22376-PA. URL: https://www-onepetro-org.proxy.findit.dtu.dk/journal-paper/SPE-22376-PA.

[Häg+17] Jens Häggström et al. "Full-scale testing to failure of a steel truss railway bridge". In: *Proceedings of the Institution of Civil Engineers - Bridge Engineering* 170.2 (2017), pages 93–101. DOI: 10.1680/jbren.15.00025. URL: http://www.icevirtuallibrary.com/doi/10.1680/jbren.15.00025.

[Hau13] Erich Hau. "Wind Turbines - Fundamentals, Technologies, Application, Economics". In: *Wind Turbines: Fundamentals, Technologies, Application, Economics*. Berlin, Heidelberg: Springer Berlin Heidelberg, 2013. Chapter Wind Turbi, pages 789–843. ISBN: 978-3-642-27151-9. DOI: 10.1007/978-3-642-27151-9_19. URL: http://dx.doi.org/10.1007/978-3-642-27151-9%7B%5C_%7D19.

[HB12] Zainul Huda and Robert Bulpett. *Materials Science and Design for Engineers*. Trans Tech Publications Ltd., 2012. ISBN: 978-3037859988.

[Hed16] Marie Louise Hede. *Betingelser for udbud af etablering af 350 MW havvindkapacitet i kystnære områder*. Tender document. 2016. URL: http://www.ens.dk/sites/ens.dk/files/dokumenter/side/endelige%7B%5C_

%7Dudbudsbetingelser%7B%5C_%7D29%7B%5C_%7Dapril%7B%5C_%7D2016%7B%5C_%7Dversion%7B%5C_%7D2.3.pdf.

[HH12] C Tony Hunley and Issam E Harik. "Structural Redundancy Evaluation of Steel Tub Girder Bridges". In: *Journal of Bridge Engineering* 17.3 (2012), pages 481–489. ISSN: 1084-0702. DOI: 10.1061/(ASCE)BE.1943-5592.0000266. URL: http://ascelibrary.org/doi/10.1061/%7B%5C%%7D28ASCE%7B%5C%%7D29BE.1943-5592.0000266.

[Hir+07] Toshihiko Hirama et al. "Seismic proof test of a reinforced concrete containment vessel (RCCV). Part 3. Evaluation of seismic safety margin". In: *Nuclear Engineering and Design* 237.11 (2007), pages 1128–1139. ISSN: 00295493. DOI: 10.1016/j.nucengdes.2007.01.009.

[HL15] Dániel Honfi and David Lange. "Structural health monitoring, a tool for improving critical infrastructure resilience". In: *Proceedings of the 1st Workshop on Quantifying the Value of Structural Health Monitoring COST Action TU1402*. Edited by Sebastian Thöns. September 2015, pages 17–26. ISBN: 978-8-77-877426-2.

[HMC16] Andrew Ho, Ariola Mbistrova, and Giorgio Corbetta. *The European offshore wind industry - key trends and statistics 2015*. Technical report. European Wind Energy Association, 2016. URL: https://windeurope.org/wp-content/uploads/files/about-wind/statistics/EWEA-European-Offshore-Statistics-2015.pdf.

[Hob+13] Jens Hobohm et al. *Kostensenkungspotenziale der Offshore-Windenergie in Deutschland*. Technical report. Berlin, Germany: Stiftung OFFSHORE-WINDENERGIE, 2013. URL: https://www.prognos.com/uploads/tx%7B%5C_%7Datwpubdb/130822%7B%5C_%7DPrognos%7B%5C_%7DFichtner%7B%5C_%7DStudie%7B%5C_%7DOffshore-Wind%7B%5C_%7DLang%7B%5C_%7Dde.pdf.

[HPS93] G Hayward, J Pearson, and G Stirling. "An intelligent ultrasonic inspection system for flooded member detection in offshore structures". In: *Ultrasonics, Ferroelectrics and Frequency Control, IEEE Transactions on* 40.5 (1993), pages 512–521.

[HT12] Colin Haynes and Michael Todd. “Bayesian probabilistic modeling for damage assessment in a bolted frame”. In: *Proceedings of the SPIE - the International Society for Optical Engineering* 8348 (2012), page 83480D. ISSN: 0277786x, 1996756x.

[HW04] Mark Hallenbeck and Herbert Weinblatt. *Equipment for collecting traffic load data*. Technical report. Washington DC, USA: Transportation Research Board, 2004. URL: http://www.is-wim.org/doc/nchrp%7B%5C_%7Drpt%7B%5C_%7D509.pdf.

[JCG08] JCGM. *Evaluation of measurement data — Guide to the expression of uncertainty in measurement*. Technical report September. Joint Working Group 1 of the Metrology Committee for Guides in Metrology, 2008.

[JCS02] JCSS. *Probabilistic Model Code, Part 3 : Material Properties*. Edited by Michael Havbro Faber and Ton Vrouwenvelder. Kongens Lyngby, Denmark, 2002. URL: http://www.jcss.byg.dtu.dk/-/media/Subsites/jcss/english/publications/probabilistic%7B%5C_%7Dmodel%7B%5C_%7Dcode/part%7B%5C_%7Diii.ashx?la=da.

[JCS08] JCSS. *Risk Assessment in Engineering: Principles , System Representation Example*. Edited by Michael Havbro Faber. Zürich, Switzerland, 2008, pages 1–16. ISBN: 9783909386789. URL: http://www.jcss.byg.dtu.dk/Publications/Risk%7B%5C_%7DAssessment%7B%5C_%7Din%7B%5C_%7DEngineering.

[JCS99] JCSS. *Probabilistic Model Code Part 1 - Basis of Design*. Kongens Lyngby, Denmark, 1999. URL: http://www.jcss.byg.dtu.dk/-/media/Subsites/jcss/english/publications/probabilistic%7B%5C_%7Dmodel%7B%5C_%7Dcode/part%7B%5C_%7Di.ashx?la=da.

[Jia+14] Yu Jiang et al. “Acoustic Emission Tomography to Improve Source Location in Concrete Material Using SART”. In: *Advances in Acoustic Emission Technology: Proceedings of the World Conference on Acoustic Emission*. Edited by Gongtian Shen, Zhanwen Wu, and Junjiao Zhang. Beijing, China: Springer, New York, 2014, pages 323–335. DOI: 10.1007/978-1-4939-1239-1_30.

[Kal+17] Hamed Kalhori et al. “Non-intrusive schemes for speed and axle identification in bridge-weigh-in-motion systems”. In: *Measurement Science and Technology* 28.2 (2017). ISSN: 0957-0233. DOI: 10.1088/1361-6501/aa52ec.

[KC00] Mike Kirkwood and Andrew Cosham. “Can the Pre-service Hydrotest be Eliminated?” In: *Pipes & Pipelines International* 45.4 (2000). ISSN: 0032020X. URL: www.penspenintegrity.com.

[KG10] Hossam A. Kishawy and Hossam A. Gabbar. “Review of pipeline integrity management practices”. In: *International Journal of Pressure Vessels and Piping* 87.7 (2010), pages 373–380. ISSN: 03080161. DOI: 10.1016/j.ijpvp.2010.04.003. URL: http://dx.doi.org/10.1016/j.ijpvp.2010.04.003.

[Kib+94] S E Kibbee et al. “The Seastar Tension-Leg Platform”. In: *Offshore Technology Conference* (1994), 243–256, OTC 7235.

[Kra59] J Krautkrämer. “Determination of the size of defects by the ultrasonic impulse echo method”. In: *British Journal of Applied Physics* 10.6 (1959), pages 240–245. ISSN: 0508-3443. DOI: 10.1088/0508-3443/10/6/302.

[KSF16] Katerina Konakli, Bruno Sudret, and Michael H. Faber. “Numerical Investigations into the Value of Information in Lifecycle Analysis of Structural Systems”. In: *ASCE-ASME Journal of Risk and Uncertainty in Engineering Systems, Part A: Civil Engineering* 2.3 (September 2016), B4015007. ISSN: 2376-7642. DOI: 10.1061/AJRUA6.0000850. URL: http://ascelibrary.org/doi/10.1061/AJRUA6.0000850.

[Kyl+14] Angeliki Kylili et al. “Infrared thermography (IRT) applications for building diagnostics : A review”. In: *Applied Energy* 134 (2014), pages 531–549. ISSN: 0306-2619. DOI: 10.1016/j.apenergy.2014.08.005. URL: http://dx.doi.org/10.1016/j.apenergy.2014.08.005.

[Lan+16] Eva O.L. Lantsoght et al. “Stop criteria for proof loading”. In: *Life-Cycle of Engineering Systems: Emphasis on Sustainable Civil Infrastructure* October (2016), pages 1064–1071.

[Lan+17] Eva O.L. Lantsoght et al. “Proof Load Testing of Reinforced Concrete Slab Bridges in the Netherlands”. In: *Transportation Research Board Annual Meeting* January (2017).

[Lan+18] Eva Olivia Leontien Lantsoght et al. “Towards standardisation of proof load testing: pilot test on viaduct Zijlweg”. In: *Structure and Infrastructure Engineering* 14.3 (2018), pages 365–380. ISSN: 17448980. DOI: 10.1080/15732479.2017.1354032. URL: http://doi.org/10.1080/15732479.2017.1354032.

[LB92] B.N. Leis and F.W. Brust. *Hydrotest strategies for gas transmission pipelines based on ductile-flaw-growth considerations*. Technical report. Arlington, VA: American Gas Association, Inc., 1992.

[LBS91] B.N. Leis, F.W. Brust, and P.M. Scott. *Development and validation of a ductile flaw growth analysis for gas transmission line pipe. [Hydrotesting]*. Technical report. Arlington, VA: American Gas Association, Inc., 1991.

[LN84] Tzyy Shan Lin and Andrzej S. Nowak. “Proof loading and structural reliability”. In: *Reliability Engineering* 8.2 (1984), pages 85–100. ISSN: 0143-8174. DOI: http://dx.doi.org/10.1016/0143-8174(84)90057-X. URL: http://www.sciencedirect.com/science/article/pii/014381748490057X.

[Lot+12] Inge Lotsberg et al. “Design of grouted connections for monopile offshore structures”. In: *Stahlbau* 81.9 (2012), pages 695–704. ISSN: 1437-1049. DOI: 10.1002/stab.201201598. URL: http://dx.doi.org/10.1002/stab.201201598.

[Lub16] Samantha Lubkin. *Deficient Bridges by Year Built 2016*. 2016. URL: https://www.fhwa.dot.gov/bridge/nbi/no10/yrblt16.cfm (visited on November 21, 2017).

[LW05] K Lesny and J Wiemann. “Design aspects of monopiles in German offshore wind farms”. In: *Proceedings of the International Symposium on Frontiers in Offshore Geotechnics*. AA Balkema Publishing. 2005, pages 383–389.

[LWM92] Brenda Little, Patricia Wagner, and Florian Mansfeld. “An overview of microbiologically influenced corrosion”. In: *Electrochimica Acta* 37.12 (1992), pages 2185–2194. DOI: 10.1016/0013-4686(92)85110-7. URL: http://www.sciencedirect.com/science/article/pii/0013468692851107.

[McD67] D. McD. Eadie. "The behaviour of the oldbury No. 1 reactor pressure vessel during prestressing and proof pressure test". In: *Nuclear Engineering and Design* 5.3 (1967), pages 295–310. ISSN: 0029-5493. DOI: 10.1016/0029-5493(67)90067-2. URL: http://www.sciencedirect.com/science/article/pii/0029549367900672%7B%5C%%7D5Cnhttp://pdn.sciencedirect.com/science?%7B%5C_%7Dob=MiamiImageURL%7B%5C&%7D%7B%5C_%7Dcid=271381%7B%5C&%7D%7B%5C_%7Duser=4633001%7B%5C&%7D%7B%5C_%7Dpii=0029549367900672%7B%5C&%7D%7B%5C_%7Dcheck=y%7B%5C&%7D%7B%5C_%7Dorigin=article%7B%5C&%7D%7B%5C_%7Dzone=toolbar%7B%5C&%7D%7B%5C_%7DcoverDate=31-May-1967%7B%5C&%7Dview=c%7B%5C&%7DoriginContentF.

[McS+05] D. McStay et al. "A new tool for the rapid remote detection of leaks from subsea pipelines during remotely operated vehicle inspections". In: *Journal of Optics A: Pure and Applied Optics* 7.6 (2005), S346. ISSN: 1464-4258. DOI: 10.1088/1464-4258/7/6/014. URL: http://stacks.iop.org/1464-4258/7/i=6/a=014.

[MCV11] Graeme Mccann, Andrew Cordle, and Wybren de Vries. "Design drivers for offshore wind turbine jacket support structures". In: *Proceedings of ASME 30th International Conference on Ocean, Offshore and Artic Engineering OMAE*. Volume 5: Ocean S. June. Rotterdam, The Netherlands: American Society of Mechanical Engineers, 2011, pages 419–428. ISBN: 9780791844373. DOI: 10.1115/OMAE2011-49338. URL: http://proceedings.asmedigitalcollection.asme.org/proceeding.aspx?articleid=1624911%7B%5C&%7DresultClick=3.

[MG13] Rito Mijarez and Patrick Gaydecki. "Automatic guided wave PPM communication system for potential SHM of flooding members in sub-sea oilrigs". In: *Smart Materials and Structures* 22.5 (2013), page 55031. URL: http://stacks.iop.org/0964-1726/22/i=5/a=055031.

[MG16] Mira Mitra and S Gopalakrishnan. "Guided wave based structural health monitoring: A review". In: *Smart Materials and Structures* 25.5 (2016), page 053001. ISSN: 0964-1726. DOI: 10.1088/0964-1726/25/5/053001. URL: http://stacks.iop.org/0964-1726/25/i=5/a=053001?key=crossref.1995c0a0922c790beecffd917804bf06.

[MGB05a] Rito Mijarez, Patrick Gaydecki, and Michael Burdekin. "Continuous Monitoring Guided Wave Encoded Sensor for Flood". In: *Insight- Non-destructive Testing and Condition Monitoring* 47.12 (2005), pages 748–751. DOI: 10.1784/insi.2005.47.12.748. URL: http://www.ndt.net/article/wcndt2004/pdf/petrochemical%7B%5C_%7Dindustry/511%7B%5C_%7Dmijarez.pdf.

[MGB05b] Rito Mijarez, Patrick Gaydecki, and Michael Burdekin. "Permanently attached single PZT guided wave encoded sensor for flood detection of oil rig crossbeams". In: *AIP Conference Proceedings* 760 (2005), pages 1795–1801. ISSN: 0094243X. DOI: 10.1063/1.1916888.

[MGB07] Rito Mijarez, Patrick Gaydecki, and Michael Burdekin. "Flood member detection for real-time structural health monitoring of sub-sea structures of offshore steel oilrigs". In: *Smart Materials and Structures* 16.5 (2007), page 1857. URL: http://stacks.iop.org/0964-1726/16/i=5/a=042.

[Min45] M. A. Miner. "Cumulative Damage in Fatigue". In: *Journal of Applied Mechanics-Transactions* 12.3 (1945), pages 159–164.

[Mir+17] Simona Miraglia et al. "Resilience of systems by value of information and SHM". In: *12th International Conference on Structural Safety and Reliability*. Edited by Christian Bucher, Bruce R. Ellingwood, and Dan M. Frangopol. August. Vienna: TU Verlag, 2017, pages 6–10. ISBN: 9783903024281.

[MKW16] Maria Martinez-Luengo, Athanasios Kolios, and Lin Wang. "Structural health monitoring of offshore wind turbines: A review through the Statistical Pattern Recognition Paradigm". In: *Renewable and Sustainable Energy Reviews* 64 (2016), pages 91–105. ISSN: 18790690. DOI: 10.1016/j.rser.2016.05.085. URL: http://dx.doi.org/10.1016/j.rser.2016.05.085.

[ML82] Peter Hauge Madsen and Niels C. Lind. "Bayesian Approach to Prototype Testing". In: *Journal of the Structural Division* 108.April (1982).

[MLB94] Fred Moses, Jean Paul Lebet, and Rolf Bez. "Applications of Field Testing to Bridge Evaluation". In: *Journal of Structural Engineering* 120.6 (1994).

[MM06] Wesley J. Merkle and John J. Myers. “Load Testing and Load Distribution Response of Missouri Bridges Retrofitted with Various FRP Systems Using a Non-Contact Optical Measurement System”. In: *Transportation Research Board 85th Annual Meeting*. 06. 2006.

[MMN11] Anders Myhr, K J Maus, and Tor A Nygaard. “Experimental and computational comparisons of the OC3-HYWIND and Tension-Leg-Buoy (TLB) floating wind turbine conceptual designs”. In: *Proceedings of the 21st International Offshore and Polar Engineering Conference* 8 (2011), pages 353–360. ISSN: 10986189.

[Moa94] Torgeir Moan. “Reliability and risk analysis for design and operations planning of offshore structures”. In: *Structural Safety and Reliability* 1 (August 1994), pages 21–43.

[MP16] Carl Malings and Matteo Pozzi. “Value of information for spatially distributed systems: Application to sensor placement”. In: *Reliability Engineering & System Safety* 154 (October 2016), pages 219–233. ISSN: 09518320. DOI: 10.1016/j.ress.2016.05.010. URL: http://dx.doi.org/10.1016/j.ress.2016.05.010%20http://linkinghub.elsevier.com/retrieve/pii/S0951832016300564.

[MS79] Fred Moses and B. Stahl. “Reliability analysis format for offshore structures”. In: *Journal of Petroleum Technology* 31.03 (1979), pages 347–354.

[NB15] Jonny Nilimaa and Thomas Blanksva. “Assessment of concrete double-trough bridges”. In: *Journal of Structural Health Monitoring* 5 (2015), pages 29–36. DOI: 10.1007/s13349-015-0102-2.

[Nel13] Roger B Nelsen. *An Introduction to Copulas*. Volume 53. 9. 2013, page 276. ISBN: 9788578110796. DOI: 10.1017/CBO9781107415324.004. arXiv: arXiv:1011.1669v3.

[NF07] Kazuyoshi Nishijima and Michael Havbro Faber. “Bayesian approach to proof loading of quasi-identical multi-components structural systems”. In: *Civil Engineering and Environmental Systems* 24.2 (2007), pages 111–121. DOI: 10.1080/10286600601159172.

[NGD05] Hani H. Nassif, Mayrai Gindy, and Joe Davis. "Comparison of laser Doppler vibrometer with contact sensors for monitoring bridge deflection and vibration". In: *NDT and E International* 38.3 (2005), pages 213–218. ISSN: 09638695. DOI: 10.1016/j.ndteint.2004.06.012.

[Nie16] Lisbeth Nielsen. *Tender conditions for Kriegers Flak Offshore Wind Farm*. tender document. 2016. URL: http://www.ens.dk/sites/ens.dk/files/dokumenter/side/kriegers%7B%5C_%7Dflak%7B%5C_%7D-%7B%5C_%7Dfinal%7B%5C_%7Dtender%7B%5C_%7Dconditions%7B%5C_%7Ddraft.pdf.

[Nil+12] Jonny Nilimaa et al. "Transversal Post Tensioning of RC Trough Bridges – Laboratory Test". In: *Nordic Concrete Research* 46.2 (2012).

[Nil+14] Jonny Nilimaa et al. "Unbonded Transverse Posttensioning of a Railway Bridge". In: 19.3 (2014), pages 1–11. DOI: 10.1061/(ASCE)BE.1943-5592.0000527..

[OC13] Henrique Oliveira and Paulo Lobato Correia. "Automatic road crack detection and characterization". In: *IEEE Transactions on Intelligent Transportation Systems* 14.1 (2013), pages 155–168. ISSN: 15249050. DOI: 10.1109/TITS.2012.2208630.

[Oji+16] T Ojio et al. "Contactless Bridge Weigh-in-Motion". In: *Journal of Bridge Engineering* 21.7 (2016), page 4016032. ISSN: 1084-0702. DOI: 10.1061/(ASCE)BE.1943-5592.0000776. URL: http://dx.doi.org/10.1061/(ASCE)BE.1943-5592.0000776.

[OŁC14] Piotr Olaszek, Marek Łagoda, and Joan Ramon Casas. "Diagnostic load testing and assessment of existing bridges: examples of application". In: *Structure and Infrastructure Engineering* 10.6 (2014), pages 834–842. ISSN: 17448980. DOI: 10.1080/15732479.2013.772212.

[OSC10] P. Olaszek, G. Swit, and Joan Ramon Casas. "Proof load testing supported by acoustic emission. An example of application". In: *Bridge Maintenance, Safety, Management and Life-Cycle Optimization: Proceedings of the Fifth International IABMAS Conference*. Edited by Dan Frangopol, Richard Sause, and Chad Kusko. Philadelphia, USA: CRC Press, 2010.

[OWM15] Tor Ole Olsen, Olav Weider, and Anders Myhr. “Large Marine Concrete Structures: The Norwegian Design Experience”. In: *Large Floating Structures*. Edited by C. M. Wang and B. T. Wang. Volume 3. Singapore: Springer, 2015. Chapter 7, pages 157–195. ISBN: 978-981-287-136-7. DOI: 10.1007/978-981-287-137-4_7. URL: http://link.springer.com/10.1007/978-981-287-137-4.

[OŽ01] Eugene O’Brien and Aleš Žnidarič. *Weighing-in-motion of axles and vehicles for Europe (WAVE). Report of work package 1.2*. Technical report. Paris: Laboratoire Central des Ponts et Chausse´ es, 2001. URL: http://wim.zag.si/wave/download/wp12%7B%5C_%7Dfinal.pdf.

[PA08] Theodore P. Philippidis and Theoni T. Assimakopoulou. “Using acoustic emission to assess shear strength degradation in FRP composites due to constant and variable amplitude fatigue loading”. In: *Composites Science and Technology* 68.3-4 (2008), pages 840–847. ISSN: 02663538. DOI: 10.1016/j.compscitech.2007.08.012.

[Pal24] A. Palmgren. “The Lifespan of Swivel Heads”. In: *Zeitschrift Des Vereines Deutscher Ingenieure* 68 (1924), pages 339–341.

[Par+14] K. Paradowski et al. “Research into the Possibilities for Monitoring Technical Conditions of Underground Pipelines Using Acoustic Emission”. In: *Advances in Acoustic Emission Technology: Proceedings of the World Conference on Acoustic Emission*. Edited by Gongtian Shen, Zhanwen Wu, and Junjiao Zhang. Beijing, China: Springer, New York, 2014, pages 435–444. DOI: 10.1007/978-1-4939-1239-1_40.

[Pat+13] Andrew Patterson et al. “Developing Prioritised and Targeted Excavation Strategies for Critical Pipelines”. In: *Proceeding of the Rio Pipeline Conference 2013*. Rio de Janeiro, Brazil, 2013.

[PD11] Matteo Pozzi and Armen Der Kiureghian. “Assessing the Value of Information for long-term structural health monitoring”. In: *Health Monitoring of Structural and Biological Systems 2011* 7984 (2011). DOI: 10.1117/12.881918. URL: http://faculty.ce.cmu.edu/pozzi/files/2015/09/SPIE%7B%5C_%7DSS11.pdf.

[PD12] Matteo Pozzi and Armen Der Kiureghian. "Assessing the value of alternative bridge health monitoring systems". In: *6th International Conference on Bridge Maintenance, Safety and Management, IABMAS*. CRC Press, Como, Italy, 2012. URL: http://faculty.ce.cmu.edu/pozzi/files/2015/09/MP%7B%5C_%7DADK%7B%5C_%7DIABMAS2012.pdf.

[Pea95] Karl Pearson. "Notes on the History of Correlation". In: *Royal Society Proceedings* 58.13 (1895), pages 25–45.

[Poo07] Les. Pook. *Metal fatigue: What it is, why it matters*. Springer, 2007, xvii, 264 s. ISBN: 140205596x, 9781402055966.

[PP15] Fábio Celestino Pereira and Carlos Eduardo Pereira. "Embedded image processing systems for automatic recognition of cracks using UAVs". In: *IFAC-PapersOnLine* 28.10 (2015), pages 16–21. ISSN: 24058963. DOI: 10.1016/j.ifacol.2015.08.101.

[PS07] Panos A Psimoulis and Stathis C Stiros. "Measurement of deflections and of oscillation frequencies of engineering structures using Robotic Theodolites (RTS)". In: *Engineering Structures* 29.12 (2007), pages 3312–3324. ISSN: 01410296. DOI: 10.1016/j.engstruct.2007.09.006.

[PS72] A. A. Pollock and B. Smith. "Stress-wave-emission monitoring of a military bridge". In: *Non-Destructive Testing* 5.6 (1972), pages 348–353. DOI: 10.1016/0029-1021(72)90063-1.

[QTF15] Jianjun Qin, Sebastian Thöns, and Michael Havbro Faber. "On the Value of SHM in the Context of Service Life Integrity Management". In: *12th International Conference on Applications of Statistics and Probability in Civil Engineering, ICASP12*. 2015.

[Rac04] Rüdiger Rackwitz. *Optimal and acceptable technical facilities involving risks*. Volume 24. 3. 2004, pages 675–695. ISBN: 0272-4332. DOI: 10.1111/j.0272-4332.2004.00467.x.

[Rac97] Rüdiger Rackwitz. "Probabilistic Methods for Structural Design". In: edited by C Guedes Soares. Volume 56. Solid Mechanics and its Applications. Springer Science + Business Media B.V, 1997. Chapter Methods of, pages 161–203. ISBN: 978-94-010-6366-1, 978-94-011-5614-1. DOI: 10.1007/978-94-011-5614-1.

[RGF15] Joan Hee Roldsgaard, Christos Thomas Georgakis, and Michael Havbro Faber. "On the Value of Forecasting in Cable Ice Risk Management". In: *Structural Engineering International* 1 (2015), pages 61–70. DOI: 10.2749/101686614X14043795570895.

[Riz14] P Rizzo. "Sensing solutions for assessing and monitoring underwater systems". In: *Sensor Technologies for Civil Infrastructures*. Edited by M L Wang, J P Lynch, and H Sohn. Volume 56. Woodhead Publishing Series in Electronic and Optical Materials. Woodhead Publishing, 2014. Chapter 17, pages 525–549. ISBN: 978-1-78242-242-6. DOI: http://dx.doi.org/10.1533/9781782422433.2.525. URL: http://www.sciencedirect.com/science/article/pii/B978178242242650017X.

[Ron02] Beverley F. Ronalds. "Deepwater Facility Selection". In: *Offshore Technology Conference*. Houston, TX, USA, 2002, pages 1–9.

[RS64] Howard Raiffa and Robert Schlaifer. *Applied Statistical Decision Theory*. 3rd. Graduate School of Business Administration, Havard University, 1964.

[RS85] Rüdiger Rackwitz and K. Schrupp. "Quality Control, Proof Testing and Structural Reliability". In: *Structural Safety* (1985), pages 239–244.

[RU02] Ludger Ruschendorf and Ludger Uckelmann. "Variance minimization and random variables with constant sum". In: *Distributions With Given Marginals and Statistical Modelling*. Edited by Carles M. Cuadras, Josep Fortiana, and José A. Rodriguez-Lallena. Barcelona, Spain: Springer Netherlands, 2002, pages 211–222. DOI: 10.1007/978-94-017-0061-0_22.

[SCG17] Miriam Soriano, Joan Ramon Casas, and Michel Ghosn. "Simplified probabilistic model for maximum traffic load from weigh-in-motion data". In: *Structure and Infrastructure Engineering* 13.4 (2017), pages 454–467. ISSN: 17448980. DOI: 10.1080/15732479.2016.1164728. URL: http://dx.doi.org/10.1080/15732479.2016.1164728.

[SeR12a] SeRoN. *D600: Validation*. Technical report. 2012. URL: http://www.seron-project.eu/download/SeRoN%7B%5C_%7DD600%7B%5C_%7DValidation%7B%5C_%7Dsummary%7B%5C_%7DV1.0.pdf.

[SeR12b] SeRoN. *Deliverable D500: Risk assessment*. Technical report March. 2012. URL: http://www.seron-project.eu/download/SeRoN%7B%5C_%7DD500%7B%5C_%7DRiskAssessment%7B%5C_%7Dsummary%7B%5C_%7DV1.0.pdf.

[SN98] Vijay Saraf and Andrzej S. Nowak. "Proof load testing of deteriorated steel girder bridges". In: *Journal of Bridge Engineering* 3.2 (1998), pages 82–89. ISSN: 10840702. DOI: 10.1061/(ASCE)1084-0702(1998)3:2(82). URL: http://ascelibrary.org/doi/abs/10.1061/(ASCE)1084-0702(1998)3:2(82).

[SPE62] G. C. Sih, P. C. Paris, and F. Erdogan. "Crack-Tip, Stress-Intensity Factors for Plane Extension and Plate Bending Problems". In: *Journal of Applied Mechanics* 29.2 (1962). DOI: 10.1115/1.3640546.

[Spi+12] Martin Spies et al. "Synthetic aperture focusing and time-of-flight diffraction ultrasonic imaging - Past and present". In: *Journal of Nondestructive Evaluation* 31.4 (2012), pages 310–323. ISSN: 01959298. DOI: 10.1007/s10921-012-0150-z.

[SRV01] Mark G. Stewart, David V. Rosowsky, and Dimitri V. Val. "Reliability-based bridge assessment using risk-ranking decision analysis". In: *Structural Safety* 23.4 (2001), pages 397–405. ISSN: 01674730. DOI: 10.1016/S0167-4730(02)00010-3.

[SS06] D J Sanderson and Ronald Schneider. *Dedistribution effects on structural reliability of deepwater jackets*. Technical report. Health and Safety Executive, 2006. URL: http://www.hse.gov.uk/research/rrpdf/rr494.pdf.

[SS08] Victor Saouma and M. V. Sivaselvan. *Hybrid Simulation: Theory, Implementation and Applications*. 1st edition. Bristol, Pennsylvania, USA: Taylor & Francis, 2008. ISBN: 9780415465687.

[SSN96] Vijay Saraf, Andrej Sokolik, and Andrzej S. Nowak. "Proof load testing of highway bridges". In: *Transportation Research Record: Journal of the Transportation Research Board* 1541 (1996), pages 51–57.

[ST10] John Dalsgaard Sørensen and H S Toft. "Probabilistic Design of Wind Turbines". In: *Energies* 3.2 (2010), pages 241–257. ISSN: 19961073. DOI: 10.3390/en3020241.

[ST14] John Dalsgaard Sørensen and Henrik Stensgaard Toft. *Safety Factors – IEC 61400-1 ed. 4 - background document*. Technical report November. DTU Wind Energy, 2014, page 16. URL: http://orbit.dtu.dk/files/118222161/Database%7B%5C_%7Dabout%7B%5C_%7Dblade%7B%5C_%7Dfaults.pdf.

[Str+17] Daniel Straub et al. "Value of information: A road to quantifying the benefit of structural health monitoring". In: *12th Int. Conf. on Structural Safety & Reliability*. Edited by Christian Bucher, Bruce R. Ellingwood, and Dan M. Frangopol. Vienna, Austria: TU Verlag, 2017, pages 3018–3029.

[Str14] Daniel Straub. "Value of information analysis with structural reliability methods". In: *STRUCTURAL SAFETY* 49 (2014). Edited by Kok-Kwang Phoon, pages 75–85. ISSN: 01674730, 18793355. DOI: 10.1016/j.strusafe.2013.08.006.

[SV99] Mark G Stewart and Dimitri V Val. "Role of Load History in Reliability-Based Decision Analysis of Aging Bridges". In: *Journal of Structural Engineering* 125.7 (July 1999), pages 776–783. ISSN: 0733-9445. DOI: 10.1061/(ASCE)0733-9445(1999)125:7(776). URL: http://ascelibrary.org/doi/10.1061/%7B%5C%%7D28ASCE%7B%5C%%7D290733-9445%7B%5C%%7D281999%7B%5C%%7D29125%7B%5C%%7D3A7%7B%5C%%7D28776%7B%5C%%7D29.

[SW13] G. Spagnoli and L. Weixler. "Support for offshore monopile installation through the trench cutter technology". In: *Transactions of the Royal Institution of Naval Architects Part A: International Journal of Maritime Engineering* 155.PART A3 (2013), pages 131–140. ISSN: 17400716.

[TF11] Nguyen Viet Tue and Nancy Freitag. *Untersuchungen an Bauwerken aus hochfestem Beton*. Technical report. Bergisch Gladbach, Germany: Bundesanstall für Straßenwesen, 2011. URL: http://bast.opus.hbz-nrw.de/volltexte/2012/583/pdf/B86.pdf.

[TF13] Sebastian Thöns and Michael Havbro Faber. "Assessing the value of structural health monitoring". In: *Safety, Reliability, Risk and Life-Cycle Performance of Structures and Infrastructures - Proceedings of the 11th Inter-*

national Conference on Structural Safety and Reliability, ICOSSAR 2013 (2013), pages 2543–2550.

[TFR11] Sebastian Thöns, Michael Havbro Faber, and Werner Rücker. "On the utilization of monitoring data in an ultimate limit state reliability analysis". In: *11th International Conference on Applications of Statistics and Probability in Civil Engineering (ICASP)*. August 2011.

[TFV17] Sebastian Thöns, Michael Havbro Faber, and Dimitri V Val. "On the Value of Structural Health Monitoring Information for the Operation of Wind Parks". In: *Proceedings of the 12th International Conference on Structural Safety and Reliability*. Edited by Christian Bucher, Bruce R. Ellingwood, and Dan M. Frangopol. August. Vienna, Austria: TU-Verlag, 2017, pages 3008–3017. ISBN: 9783903024281.

[Tho12] Palle Thoft-Christensen. "Infrastructures and life-cycle cost-benefit analysis". In: *Structure and Infrastructure Engineering* 8.5 (May 2012), pages 507–516. ISSN: 1573-2479. DOI: 10.1080/15732479.2010.539070. URL: http://www.tandfonline.com/doi/abs/10.1080/15732479.2010.539070.

[Thö18] Sebastian Thöns. "On the Value of Monitoring Information for the Structural Integrity and Risk Management". In: *Computer-Aided Civil and Infrastructure Engineering* 33.1 (2018), pages 79–94. ISSN: 10939687. DOI: 10.1111/mice.12332. URL: http://doi.wiley.com/10.1111/mice.12332.

[TNB15] Sebastian Thöns, Jakub Niedźwiedź, and Grzergorz Bednarski. *Pressurized Structural Member Damage Detection*. 2015. URL: http://www.cost-tu1402.eu/-/media/Sites/cost-tu1402/Documents/1,-d-,%20Workshop/WG2/5ST-GB-JN-V2.ashx?la=da.

[TSF15] Sebastian Thöns, Ronald Schneider, and Michael Havbro Faber. "Quantification of the Value of Structural Health Monitoring Information for Fatigue Deteriorating Structural Systems". In: *12th International Conference on Applications of Statistics and Probability in Civil Engineering (ICASP12)* (2015).

[Tso+14] Nikolaos K. Tsopelas et al. "Acoustic Emission for Structural Integrity Assessment of Wind Turbine Blades". In: *Advances in Acoustic Emission Technology: Proceedings of the World Conference on Acoustic Emission*.

Edited by Gongtian Shen, Zhanwen Wu, and Junjiao Zhang. Beijing, China: Springer, 2014, pages 369–382. DOI: 10.1007/978-1-4939-1239-1_34.

[Tup+12] Lee L. Tupper et al. "Measuring Sustainability: How Traffic Incident Management through Intelligent Transportation Systems has Greater Energy and Environmental Benefits than Common Construction-Phase Strategies for "Green" Roadways". In: *International Journal of Sustainable Transportation* 6.5 (2012), pages 282–297. ISSN: 15568318. DOI: 10.1080/15568318.2011.597910.

[VBK15] V. P. Vavilov, O. N. Budadin, and A. A. Kulkov. "Infrared thermographic evaluation of large composite grid parts subjected to axial loading". In: *Polymer Testing* 41 (2015), pages 55–62. ISSN: 01429418. DOI: 10.1016/j.polymertesting.2014.10.010. URL: http://dx.doi.org/10.1016/j.polymertesting.2014.10.010.

[VJS16] J A Voormolen, H M Junginger, and W.G.J.H.M. van Sark. "Unravelling historical cost developments of offshore wind energy in Europe". In: *Energy Policy* 88 (2016), pages 435–444. ISSN: 0301-4215. DOI: http://dx.doi.org/10.1016/j.enpol.2015.10.047. URL: http://www.sciencedirect.com/science/article/pii/S0301421515301749.

[VS02] Dimitri V. Val and Mark G. Stewart. "Safety Factors for Assessment of Existing Structures". In: *Journal of Structural Engineering* 128.2 (2002), pages 258–265. DOI: 10.1061/(ASCE)0733-9445(2002)128:2(258).

[Wan15] Baojin Wang. "Estimating economic impacts of transport investments using TREDIS : a case study on a National Highway Upgrade Program". In: *Australasian Transport Research Forum 2015* October (2015), pages 1–15. URL: http://atrf.info/papers/2015/files/ATRF2015%7B%5C_%7DResubmission%7B%5C_%7D180.pdf.

[WEK99] S. A. Will, J. C. Edel, and J Kallaby. "Design of the Baldpate Compliant Tower". In: *Offshore Technology Conference*. Houston, TX, USA, 1999, page 23. DOI: 10.4043/10915-MS. URL: https://www.onepetro.org/conference-paper/OTC-10915-MS.

[WFG14] Jan Winkler, Gregor Fischer, and Christos Thomas Georgakis. “Measurement of Local Deformations in Steel Monostrands Using Digital Image Correlation”. In: *Journal of Bridge Engineering* 19.10 (2014). ISSN: 1084-0702. DOI: 10.1061/(ASCE)BE.1943-5592.0000615. URL: http://ascelibrary.org/doi/10.1061/%7B%5C%%7D28ASCE%7B%5C%%7D29BE.1943-5592.0000615.

[WH10] Pingrang Wang and Hongwei Huang. “Comparison analysis on present image-based crack detection methods in concrete structures”. In: *Proceedings - 2010 3rd International Congress on Image and Signal Processing, CISP 2010* 5 (2010), pages 2530–2533. DOI: 10.1109/CISP.2010.5647496.

[WMS16] Catherine A. Whyte, Kevin R. Mackie, and Bozidar Stojadinovic. “Hybrid Simulation of Thermomechanical Structural Response”. In: *Journal of Structural Engineering* 142.2 (February 2016), page 04015107. ISSN: 0733-9445. DOI: 10.1061/(ASCE)ST.1943-541X.0001346. URL: http://ascelibrary.org/doi/10.1061/%7B%5C%%7D28ASCE%7B%5C%%7D29ST.1943-541X.0001346.

[Wu+14] Zhanwen Wu et al. “Research on the Acoustic Emission and Metal Magnetic Memory Characteristics of the Crane Box Beam During Destructive Testing”. In: *Advances in Acoustic Emission Technology: Proceedings of the World Conference on Acoustic Emission*. Edited by Gongtian Shen, Zhanwen Wu, and Junjiao Zhang. Beijing, China: Springer New York, 2014, pages 425–433. DOI: 10.1007/978-1-4939-1239-1_39.

[Yan76] J.-N. Yang. “Reliability Analysis of Structures under Periodic Proof Tests in Service”. In: *AIAA JOURNAL* 14.September (1976), pages 1225–1234.

[YCD16] Yang Yu, CS Cai, and Lu Deng. “State-of-the-art review on bridge weigh-in-motion”. In: *Advances in Structural Engineering* 19.9 (2016), pages 1514–1530. DOI: 10.1177/1369433216655922.

[YFN04] Seung Ie Yang, Dan M Frangopol, and Luis C. Neves. “Service life prediction of structural systems using lifetime functions with emphasis on bridges”. In: *Reliability Engineering and System Safety* 86.1 (2004), pages 39–51. ISSN: 09518320. DOI: 10.1016/j.ress.2003.12.009.

[ZGA14] Daniele Zonta, Branko Glisic, and Sigrid Adriaenssens. "Value of information: impact of monitoring on decision-making". In: *Structural Control and Health Monitoring* 21.7 (July 2014), pages 1043–1056. ISSN: 15452255. DOI: 10.1002/stc.1631. arXiv: arXiv:1011.1669v3. URL: http://dx.doi.org/10.1002/stc.456%20http://doi.wiley.com/10.1002/stc.1631.

[Zha+15] Dong Zhan et al. "Multi-Camera and Structured-Light Vision System (MSVS) for Dynamic High-Accuracy 3D Measurements of Railway Tunnels". In: *Sensors* 15.4 (2015), pages 8664–8684. DOI: 10.3390/s150408664. URL: http://www.mdpi.com/1424-8220/15/4/8664.

[Žni+16] Aleš Žnidarič et al. "Railway Bridge Weigh-in-Motion System". In: *Transportation Research Procedia* 14 (2016), pages 4010–4019. ISSN: 23521465. DOI: 10.1016/j.trpro.2016.05.498.

{2.7182818284}ϑωερτυθιοπσδφγηξκλ

This thesis investigates structural health tests in terms of the value they may provide for a decision maker. The structural health tests considered are proof load testing and hybrid simulation. Hybrid simulations have not been used for this purpose, but have great potential. Proof load testing is analyzed in two ways, either employed before or after the construction. As part of the analyses, an extension to the well established concept of value of information is formulated that considers also actions which are only possible with new information gained from e.g. structural health tests.

DTU Civil Engineering
Technical University of Denmark

Brovej, Building 118
2800 Kongens Lyngby

www.byg.dtu.dk

ISBN 9788778774989
ISSN 1601-2917